SIV Reactivation from Latency in Virally Suppressed Macaques Using the HDACi Romidepsin and Cyclophosphamide

by

Adam Joseph Kleinman

Bachelor of Science, North Central College, 2015

Submitted to the Graduate Faculty of the

School of Medicine in partial fulfillment

of the requirements for the degree of

Doctor of Philosophy

University of Pittsburgh

2021

UNIVERSITY OF PITTSBURGH

SCHOOL OF MEDICINE

This dissertation was presented

by

Adam Joseph Kleinman

It was defended on

October 27, 2021

and approved by

Charles R. Rinaldo, Ph.D., Professor, Department of Pathology

Bernard J.C. Macatangay, M.D., Associate Professor, Department of Medicine

Robbie B. Mailliard Ph.D., Assistant Professor, Department of Infectious Diseases and Microbiology

Theresa L. Whiteside, Ph.D., Professor, Department of Pathology

Dissertation Director: Cristian Apetrei, M.D., Ph.D., Professor, Department of Medicine

SIV Reactivation from Latency in Virally Suppressed Macaques Using the HDACi Romidepsin and Cyclophosphamide

Adam Joseph Kleinman, PhD

University of Pittsburgh, 2021

HIV persistence in latent reservoirs requires lifelong antiretroviral therapy (ART) but does not eradicate virus nor ameliorate all non-AIDS comorbidities, necessitating a cure. Here, we investigated multiple strategies to curb the reservoir and facilitate a functional cure of HIV. We thus studied the impact of cyclophosphamide (Cy) and romidepsin (RMD) on the SIV reservoir. Cy was used as a regulatory T cell (Treg) depleting agent and cytoreduction agent at low or high doses, respectively, to reduce the size of the latent reservoir in SIV-infected rhesus macaques (RMs). At low doses, Cy did not selectively deplete Tregs, nor result in SIV reactivation. At high doses, Cy resulted in substantial SIV reactivation, but when administered with ART, it did not reactivate virus and had unacceptable toxicity and morbidity. Thus, we showed that Cy is not feasible as an HIV cure therapeutic. We next characterized the effects of RMD in SIV-uninfected and infected RMs for the purpose of understanding the pharmacokinetics, immunological effects, and potential impact on the viral reservoir. We demonstrated that RMD retention was greater in the gut and LNs than in plasma. Further, RMD was associated with transient lymphopenia that was explained by apoptosis, downregulation of lymphocyte surface markers, upregulation of homing markers, and migration to the gut and LNs. We followed this study - with repeated RMD infusions in our RM model of functional cure. Repeated infusions reactivated virus, with reduced reactivation at subsequent infusions. Two animals did not yield detectable viremia after the second and third infusions and were thus administered CD8-depleting antibody. Remaining RMs received "double infusions" which were well tolerated, induced prolonged immune activation, and increased viral reactivation. Decreases in viral reactivation were associated with longitudinal increases in the SIV-specific immune response and decreases in cell-associated viral DNA. Further, one animal did not reactivate after CD8-depletion and viral outgrowth from $CD4^+$ T cells showed a lack of replication-competent provirus at that time. However, tissue $CD4^+$ T

cells still contained replication-competent provirus. Thus, our results show that repeated RMD infusions can safely reduce the size of the latent reservoir in the context of a healthy immune response.

Table of Contents

List of Tables

List of Figures

Preface

I would like to thank my committee members, Dr. Charles Rinaldo, Dr. Bernard Macatangay, Dr. Robbie Mailliard, and Dr. Theresa Whiteside. I appreciate your willingness and patience to serve on my committee through all of the bumps in the road. I would further like to thank Dr. Cristian Apetrei, my dissertation advisor, for the countless opportunities that he has provided me during my time in his laboratory and his mentorship both inside and outside of lab. I would also like to thank Dr. Ivona Pandrea for her assistance throughout my time in her and Cristian's lab. The two of them have been integral in shaping the outcome of my career and making me a better scientist. I would like to thank Drs. JoAnne Flynn, and Simon Barratt-Boyes and Phalguni Gupta for their support through T32 grants Immunology of Infectious Diseases (IID) (AI060525) and Pitt AIDS Research Training (PART) grant (AI065380), respectively. I would also like to thank the current and past members of the Apetrei/Pandrea lab for all their support and assistance throughout the years. Beyond lab, your friendships have been amazing, and I will forever remember our times together. I will sincerely miss hosting Thanksgiving and Christmas for those who could not be with their families for the holidays, especially Dr. Ranjit (RJ) Sivanandham, for whom I would not be as accomplished without. I further would like to thank Drs. Jonathan Visick, Chris O'Connor and Dave Rausch for their support and mentorship while I was entering the scientific field as an undergraduate, as well as Tom Trayser for believing in me and being a wonderful teacher when I needed it most. Most importantly, I thank my phenomenal wife, Brieanna, and my parents for providing me with never ending love, support, and, especially, patience throughout my doctoral candidacy. Thank you all for your support.

1.0 Introduction

1.1 SIV and its usage in nonhuman primates for HIV modeling

1.1.1 Origin of SIV research strains

In 1985, shortly after the first discovery of HIV-1 [1], a group at the New England Regional Primate Research Center (NEPRC) reported the identification of a nonhuman primate (NHP) lentivirus counterpart of HIV-1 (that would later be known as SIVmac), which was responsible for AIDS cases in the rhesus macaques (*Macaca mulatta*, RMs) colony of the NEPRC [2]. Previously, in the early 1970s', an outbreak of lymphomas, resembling Burkitt's lymphoma, was reported in RMs housed at the California National Primate Research Center (CNPRC) [3-6].

However, the origin of these pathogenic lentiviruses in the RMs remained unknown, as studies in the wild macaques from Asia did not identify any circulation of SIV-like viruses in these NHP species [7-9]. Meanwhile, numerous studies reported identification of a plethora of SIVs naturally infecting multiple species of monkeys and apes in Africa [7]. These viruses were highly divergent from each other and showed a diversity profile evocative of host-dependent evolution [10, 11], suggesting a very old origin of SIVs, predating the monkey speciation in Africa [12]. Yet, the fact that no New World monkeys were carrying SIVs, nor did the Old World monkeys in Asia, was pointing to an origin of the AIDS viruses sometime after the speciation of the Asian monkeys [12]. Interestingly, the virus isolated from the macaques in NEPRC and CNPRC was closely related to the SIV naturally infecting sooty mangabeys (*Cercocebus atys*) [13].

As such, the origin of the SIV infection in captive macaques at the NEPRC was perplexing, particularly when applying the criteria of the cross-species transmission that allowed the identification of the sources of HIVs in chimps and gorillas from Cameroon for HIV-1 [14] and in sooty mangabeys from

West Africa for HIV-2, respectively [15]: (a) Genetic, antigenic and phylogenetic similarities between the human and NHP viruses; (b) Coincidence between the species habitat and the HIV-1/HIV-2 epicenters; (c) Favoring factors of transmission. These requirements were largely not fulfilled for the origin of the SIVmac in the macaque colony at the NEPRC, as the NEPRC did not have any sooty mangabeys. Meanwhile, at the CNPRC, both RMs and sooty mangabeys were housed at the same time in the 1960s, yet, reports suggested that the two species did not enter in close direct or indirect contact [5]. In a twist of events, however, virus archeology studies performed at the NEPRC clearly demonstrated that the origin of SIVmac was in fact at the CNPRC, from survivors of the original lymphoma outbreak that were shipped to the NEPRC in the 1970s' (Figure 1) [16, 17]. The virus then went undetected for >10 years in the NEPRC colony. The proofs of the virus transfer are: (i) detection of SIV antibodies in the CRPRC RMs with lymphomas; (ii) pathologies observed were similar to what is now known as pathogenic SIV infection; (iii) detection of SIV antibodies in the SMMs in the CRPRC colony prior to the outbreak RM exposure to sooty mangabey tissues; (iv) detection of SIVmac DNA in the spleen and lymph nodes in one of the RMs sent to NERPRC [17]. More recently, extensive phylogenetic analyses of the SIVs naturally infecting sooty mangabeys from different Primate Centers in the US traced the origin of the SIVmac to sooty mangabeys in the CNPRC [16]. Moreover, the circumstances of the accidental transmission from sooty mangbeys to RMs were established to rely on the kuru experiments carried out extensively at the CNPRC and New Iberia Research Center (NIRC) in the 1960s [13].

Furthermore, studies have shown [16] that the same experiments carried out at the CNPRC were likely responsible for the infection of SIVs of different other species of macaques, such as the pigtailed macaques (*Macaca nemestrina*) [18] and the stumptailed macaque (*Macaca arctoides*) [19, 20] and crab eating macaque (*Macaca fascicularis*) [21].

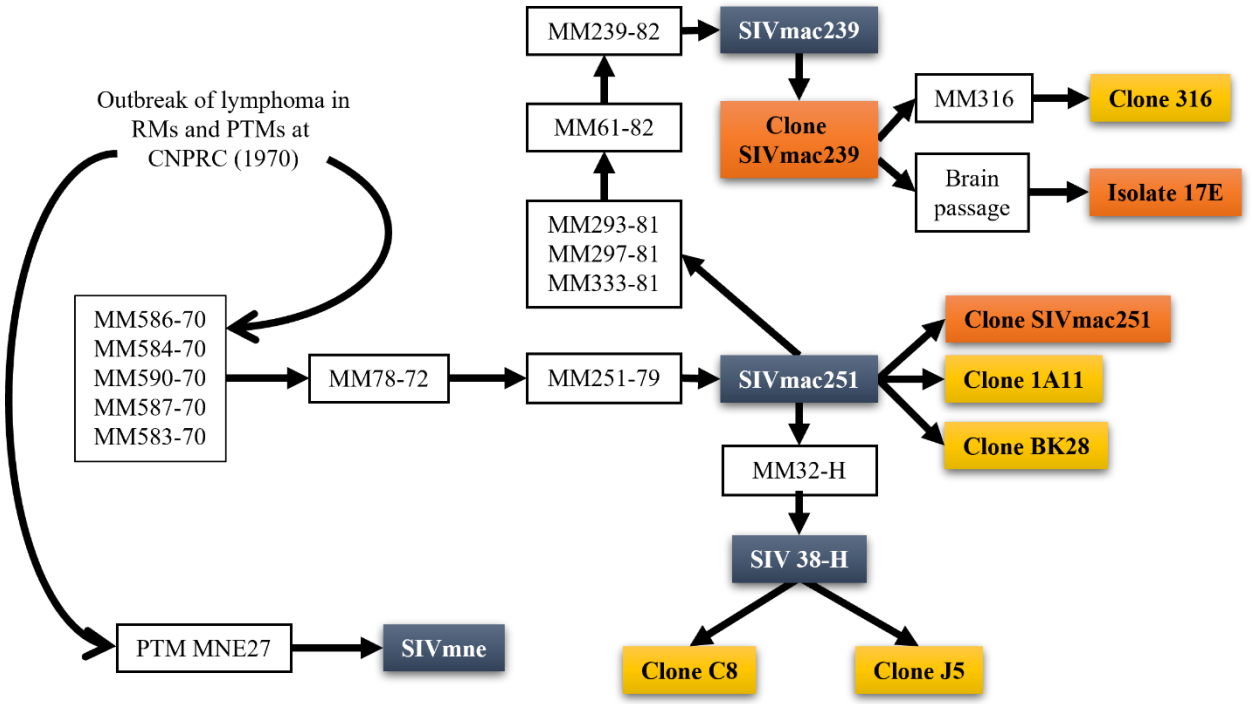

Figure 1. Origin of SIVmac251, SIVmac239, and derivative clones.

SIVmac239 and SIVmac251 originate from rhesus macaques housed at the California National Primate Research Center (CNPRC). The progenitor viruses were from sooty mangabeys at the CNPRC which were used for kuru experiments, allowing for serial passaging and eventual establishment of the SIVmac239 and SIVmac251 isolates.

1.1.2 The animal model for AIDS research

There are multiple advantages of the use of the NHP model for AIDS research: the most important of these is that animal work allows us to perform interventions that would otherwise be impossible to perform in persons living with HIV (PWH): staged infections, invasive sampling, exploratory interruptions of antiretroviral therapies, testing of new therapeutic approaches and vaccines. The model has been extensively characterized over the last three decades, and a wealth of data is available for comparisons. Moreover, multiple virological, immunological and clinical biomarkers have been extensively tested and developed, conferring the model predictability and consistency. It is therefore not surprising that the NHP models for AIDS research, which recapitulate the key features of HIV infection, provided seminal results for HIV prevention, pathogenesis, and treatment.

The early events of HIV transmission and dissemination in the host, with the potential impact on prevention and treatment were obtained in NHPs and showed a very rapid seeding of the reservoirs [22, 23]. Further, the use of NHP models has provided seminal information regarding the persistence of this reservoir and acts as an excellent tool for screening new strategies aimed at inducing cure/functional cure [22, 24-30]. For example, studies showed that the major site of virus replication and $CD4^+$ T-cell depletion is at the mucosal sites, pointing to the mucosa as the major target of vaccine interventions for the prevention of HIV transmission [31-34] and these studies predated those in PWH study participants by a decade.

The comparison between natural hosts of various SIV strains, which do not progress to AIDS, have played a big role in understanding pathogenesis. Studies on the cartography of viral dissemination [35] pointed to major differences between pathogenic and nonpathogenic infections at these early stages of infection, that have the potential to drive these different outcomes [36-38]. Additionally, studies in natural hosts have also established the key role of the immune activation and inflammation for the progression to AIDS and the development of comorbidities [39-43].

1.1.3 SIV/SHIV strains for use in NHPs

While virtually every SIV strain can be used for studies in NHPs, there are several reference SIV strains that have been extensively used for studies in NHPs. In addition to the SIVmac lineage strains and the other strains accidentally generated through the kuru experiments carried out a the CNPRC (SIVmne, SIVstm and SIVmfa), several other SIV strains have been generated and employed over the years for experiments in macaques.

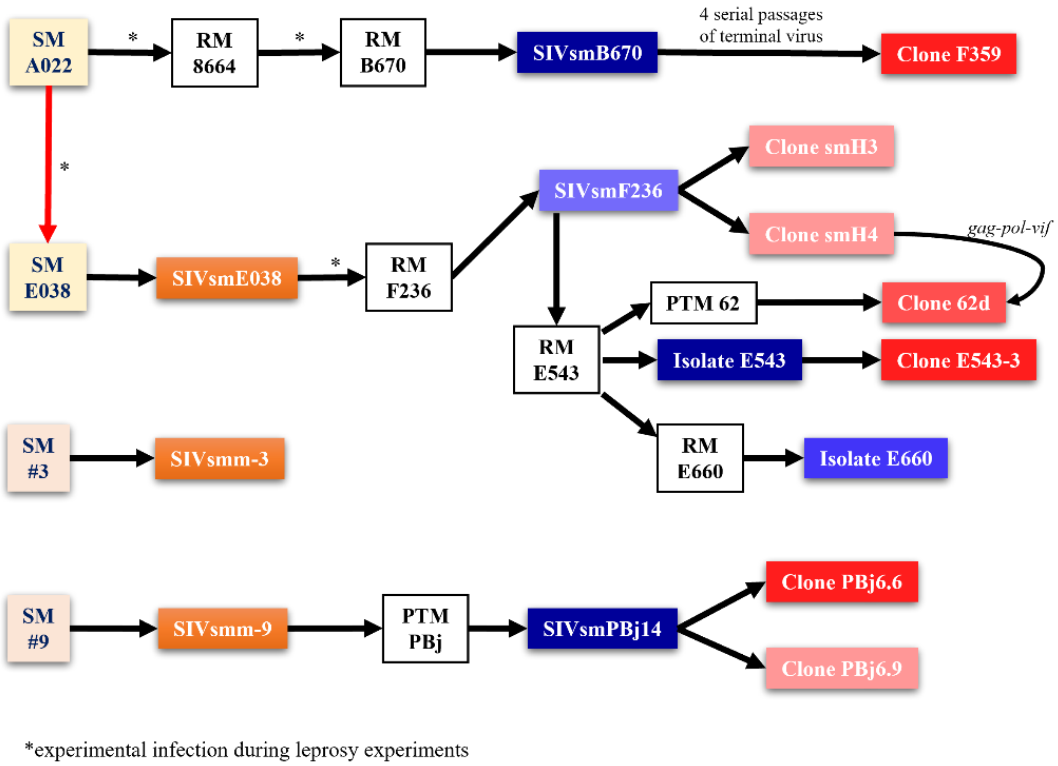

Figure 2. Isolation of various SIV strains used for NHP models.

Different SIV strains vary in their pathogenic features, allowing for different uses by strain and animal species. The origin of different pathogenic isolates from sooty mangabeys at the Tulane National Primate Research Center (TNPRC) and those resulting from leprosy experiments, as designated by asterisk, from a sooty mangabey originally housed at the Gulf South Research Institute (now New Iberia Primate Center).

Virtually concomitantly with the discovery of the SIVmac at the CNPRC, SIVsmB670 was isolated from macaques at the Tulane National Primate Research Center (TNPRC) [44]. There, in 1979, a female SMM from the Gulf South Research Institute (currently New Iberia Primate Center) suspected of having leprosy was used in an extensive experiment involving serial passages of blood and tissues, with the goal of developing an NHP model for leprosy. Due to the very long incubation of leprosy, these experiments were only partially successful. Nevertheless, the passage of *M. leprae* to other SMMs and RMs resulted in cases of full-blown AIDS in several macaques (particularly in the macaque B670) (Figure 2). With each serial passage, the number of AIDS cases increased in the macaque groups and an SIVmac-related, albeit different, SIV could be isolated from both the RMs and SMMs (Figure 2) [5].

After the discovery of SIVsmm in the SMMs-naturally infected at the TNPRC, a new experiment aimed at rederiving a “clean” viral inoculum for the infection of the RMs was performed. Blood from the

SMM A022 was passaged into an uninfected SMM (E038), which was used as a source of virus for the infection of a RM (F236) [45]. The isolate SIVsmmF236 was lambda cloned into two relatively wimpy clones (SIVsmH3 and SIVsmH4) [46]. Meanwhile SIVsmmF236 was passaged into a pigtailed macaque (PTM62) and a RM (E543). The isolate SIVsmmE543 was cloned into a highly pathogenic clone (SIVsmmE543-3) [47] and passaged into another naïve macaque (RM E660) [48]. SIVsmmE660 is currently a reference strain. It has a relatively high pathogenicity [49], and it is a tier 2 strain with regards to the neutralization sensitivity [50, 51].

One of the issues with the SIVsmm family of reference strains is that they are susceptible to the TRIM5α restriction, unlike SIVmac-derived viruses, resulting in a wide range of viral loads (VLs) based on the TRIM5α genotypes [52]. Conversely, the SIVmac group accumulated mutations that conferred resitance to TRIM5a restriction [52].

More recently, both SIVmac and SIVsmm transmitted-founder infectious molecular clones have been derived for use in vaccine studies [53]. Meanwhile, for the purpose of cure studies, in which reservoir diversity and virus reactivation have to be investigated and which require viral diversity, both tagged [54, 55] and barcoded [56, 57] SIVmac clones have been produced, that combine the advantages of both IMCs (uniformity of the pathogenicity of the vial inoculum) and of the viral swarms, thus allowing a proper tracking of the number of viral variants that are reactivated during therapeutic interventions aimed at curbing the reservoir or analytical treatment interruptions (ATIs).

Finally, during a survey of SIVsmm diversity in the Primate Centers in the US, we identified multiple SIVsmm lineages that roughly mirror HIV-1 diversity and selected new potential references strains representative of every lineage [16]. For the vast majority of these new strains transmitted founder IMCs were derived and available.

For the studies of SIV pathogenicity in the African NHP natural hosts, several isolates have been used over the last few decades. Due to the endangered nature of most of the African NHP species, the vast majority of experimental infections in natural hosts are carried in African green monkeys. Of these, the sabaeus monkeys are the model of choice due to the availability of a large wild population in the Caribbean.

The reference strain for the studies in the sabaeus monkeys is SIVsab92018, which was derived from a chronically infected sabaeus monkey from Senegal [58]. Plasma from this animal was directly inoculated into naïve monkeys and collected during the acute infection for further use, without in vitro passage. A transmitted-founder clone has been derived from the acute plasma [59]. Also, SIVsab92018 was also directly passaged into pigtailed macaques and established a model of increased comorbidity prevalence and faster rate of progression while still recapitulating the pathogenic features of HIV infection [60].

Simian-human immunodeficiency viruses (SHIVs) are chimeric SIV-HIV viruses, which are developed as a method to try and mimic HIV-1 infection as best as possible in NHP models, with a large emphasis on vaccine development with the inclusion of the HIV glycoprotein. This is necessary due to the host restriction factors in NHPs that prevent productive infection of HIV-1 and HIV-2 [61]. The first SHIV developed was in 1992 with an SIVmac239 backbone that had its *rev*, *tat,* and *env* genes replaced with HIV-1 *rev*, *tat*, *vpu*, and *env* [62]. Replication was lacking in the first SHIV *in vivo* and thus researchers replaced the *env* with a dual-tropic CCR5/CXCR4 HIV-1 *env*, generating SHIV-89.6. SHIV-89.6 replicated to high levels *in vivo*, but still lacked some pathogenic features, like sustained $CD4^+$ T-cell depletion [63]. Serial passaging and additional modifications created SHIV-KB9, which recapitulated many features [64]. A consequence was that the virus was primarily CXCR4-tropic and resulted in modified (quickened) disease progression and did not properly represent HIV infection [65, 66]. Importantly, the CXCR4-tropic SHIVs were overly sensitive to neutralizing antibodies, thus diminishing their usefulness in vaccine studies [66, 67]. Thus, CCR5-tropic SHIVs became the focus of developing SHIVs [68-72]. In fact, $SHIV_{SF162P3}$ has had great success in vaccine and broadly neutralizing antibody studies [70, 73, 74]. Serial passage of a SHIV using $HIV\text{-}1_{Ada}$ *env* resulted in $SHIV_{AD8}$ and its derivatives, which have also been used in vaccine, antibody, and therapeutics studies with relative success [75-77]. Nonetheless, even the CCR5-tropic SHIVs are not necessarily ideal due to the use of *env* sequences from chronically infected PWH and their passaging in NHPs results in modified *env* sequences [70, 72, 78]. They are therefore not as clinically relevant for vaccine studies as transmitted founder (TF) viruses which have special characteristics that increase fitness, and importantly, will have the relevant Env for targeting in vaccine or antibody studies [79]. Thus, with the

new knowledge it became imperative to design transmitted founder SHIVs that don't require passaging [67], such as *in vivo* competition [80] with rational design and specific residue modifications (Env residue 375) [81-84] to improve binding and subsequent replication. However, issues still occur with spontaneous control and incomplete $CD4^+$ T-cell depletion [83, 84].

1.2 HIV/SIV Replication Cycle and Latency

1.2.1 Viral Entry

On the HIV envelope, the glycoprotein spikes are trimers, being comprised of noncovalently linked gp120 and gp41 heterodimers [85]. Upon HIV/SIV transmission, the virus binds to its $CD4^+$ T target cells through the initial binding of gp120 to the CD4 receptor, which initiates conformational changes allowing for the binding of gp41 to the viral coreceptor, which are either CCR5 or CXCR4 [86-88] for the vast majority of the HIV and SIV strains. Other coreceptors have been described: SIVrcm, the virus that naturally infects red-capped mangabeys uses CCR2 (due to a Δ24 deletion in the CCR5 gene in red capped mangabeys [89] or also, SIVsmm, the virus that infects sooty mangabeys and SIVagm, the viruses from African green monkeys can use CXCR6 [90]. The coreceptor engagement results in the insertion of the gp41 fusion peptide into the cell membrane, followed by folding at the hinge region of gp41 and formation of a six-helix bundle [88, 91]. The six-helix bundle brings the viral envelope and host membrane into close apposition, thus creating a fusion pore, leading to subsequent release of the viral capsid into the host cell [92].

1.2.2 HIV trafficking, uncoating, and reverse transcription from the cytoplasm to nucleus.

Upon entry into the cytoplasm, the viral core engages the cytoskeleton, using the microtubule network of the host cells to translocate to the nucleus [93]. HIV binds to the microtubule network through

binding of microtubule-associated proteins MAP1A and MAP1S to the HIV capsid (CA) [94] and mobilization is driven by dynein and kinesin [95]. During the translocation to the nucleus, the virus begins the uncoating, which is dependent upon the conflicting movements through the interactions of CA with kinesin-1 adaptor protein FEZ1 and dynein adaptor protein BICD2, thereby pulling apart the capsid [95-98]. However, a recent study challenged the extent of uncoating that occurs during translocation to the nucleus, claiming that the majority of uncoating occurs near the integration sites in the nucleus [99].

Once HIV has partially uncoated, reverse transcription begins with the formation of the reverse transcription complex consisting of the HIV viral RNA genome, $tRNA^{Lys3}$ primer (binds to HIV primer binding site) [100], and several viral factors and host factors [101], further substantiating that the capsid is at least partially degraded due to the necessity of host factors such as integrase interactor 1 [102], sin3A-associated protein [103] and histone deacetylase 1 (HDAC1) [103, 104]. Uncoating finishes after nuclear entry through the nuclear pore complex [99], with subsequent completion of reverse transcription resulting in the generation of the complimentary DNA genome [105].

1.2.3 HIV integration into the host genome

In the nucleus, the complementary DNA (cDNA) genome forms the pre-integration complex with integrase, capsid, and host proteins, such as the indispensable LEDGF [106] which tethers the integrase to chromatin. Integrase multimerizes with the cDNA genome to form the intasome as a dimer of integrase subunits [107-110]. Integration is preferentially targeted towards genomic regions of high transcriptional activity [111-113] due to the association of LEDGF with splicing factors [114]. CPSF6 also influences integration sites, but through a different mechanism, as it binds to the capsid [115]. The theorized mechanism is that CPSF6 directs HIV to the actively transcribed chromatin, while LEDGF directs integration to the gene bodies [116]. Once the intasome binds to the host DNA, strand transfer begins, resulting in DNA recombination and successful integration into the host genome, thus forming the provirus [116]. However, not all cDNA is successfully integrated. Some cDNA can form unintegrated

extrachromosomal episomes 1-long terminal repeats (LTR) and 2-LTR circles. These are generally unproductive, but there is a possibility for decircularization and integration, thereby leading to productively infected cells [117].

1.2.4 HIV transcription initiation and production of viral genome

HIV transcription proceeds in multiple steps. Transcriptional regulation is mediated by RNA polymerase II (RNAP II) and cellular transcription factors with promoter elements in the LTR [118]. Early genes, *tat* and *rev* are transcribed first, but during transcription, RNAP II pauses without the elongation complex. After *tat* is transcribed and translated, Tat (trans-activator of transcription) returns to the nucleus and binds to the transactivation response element (TAR) of the HIV LTR [119]. By binding, Tat recruits the host's super elongation complex to TAR, thereby releasing the paused RNAP II and enabling transcription of multiple HIV RNAs using complex splicing to form the singly or partially (Env, Vif, Vpr, Vpu), multiply (Tat, Rev, Nef) [120], and unspliced (full-length) viral RNA [121, 122]. The control of HIV transcription is a major modulator of HIV latency [123] and mechanisms are discussed later.

1.2.5 HIV virion formation and release

The full-length non-spliced RNA is the viral genome and acts as the translation template for Gag and Gag-Pol proteins [124]. Spliced and non-spliced HIV transcripts are then translated and cleaved by the HIV protease to form the accessory and structural proteins [125]. After trafficking to the host membrane, two full-length viral RNA genomes dimerize and associate with HIV Gag, which contains the matrix, capsid, and nucleocapsid domains [126], at the plasma membrane [127]. An immature Gag lattice then forms at the plasma membrane with recruitment of host factors and remaining viral proteins. The viral particle then goes through a membrane fission event mediated by host ESCRT, driven by Gag. After fission

from the host cell, the HIV protease cleaves Gag, thus maturing the Gag lattice to the conical capsid core [126], allowing for new cycles of infection to occur.

1.3 SIV pathogenesis

1.3.1 HIV/SIV transmission and entry

Studies of SIV transmission to RMs allowed us to characterize HIV transmission in great detail, with the goal of identifying windows of opportunity to prevent infection. The mucosal barriers highly hinder infection at the entry site, thereby limiting the infection to a very small, transmitted founder population, which then establishes a productive, disseminating infection in lymphatic tissues [128, 129]. In the vast majority of PWH, a single virus initiates systemic infection [130] and the same is true for intravaginal exposure of RMs to low doses of SIVs [131]. While both CXCR4 and CCR5-tropic viruses can be found in sperm and vaginal secretions [132-134], the viruses that initiate infection (which are baptized TF viruses) are exclusively CCR5-tropic [130]. TF viruses have a specific fitness due to a lower glycosylation [135, 136] and less sensitivity to type I interferons, especially IFN-α [137, 138].

During sexual transmission, the virus migrates across the epithelial barrier at the site of entry via M cell transepithelial transport [139, 140], dendritic cells (DCs) [141, 142], and microtears in the epithelial layer [143]. HIV is then exposed to the local immune cell populations, including lymphocytes and macrophages, and rapidly infects and spreads through the primary target cells: $CCR5^+$ memory $CD4^+$ T cells [144, 145]. The virus undergoes rapid dissemination from the site of entry. Thus, two days after intravaginal inoculation, the virus could be detected in the draining and even in the distant lymph nodes, before becoming detectable in circulation (5 days post-inoculation) [141]. Intrarectal transmission results in an even more rapid viral spread throughout the body [146, 147], with no window of opportunity for potential interventions being observed upon intrarectal challenge [148]. As such, the study of the early events of HIV/SIV transmission showed that the immune response to infection is a double-edged sword: it

helps establish the transmission bottleneck and eliminate virus, but the cellular activation also contributes to infection by increasing the amount of target cells at the site of entry [149].

1.3.2 HIV acute infection

Systemic virus plasma VLs peak at 10^6-10^7 vRNA copies/mL between 12-18 days post-infection (dpi) upon mucosal transmission [150]. The HIV infection in $CD4^+$ T cells results in cell death either by viral cytolysis, bystander effects, or virus-induced apoptosis [151-155], leading to a massive depletion of $CD4^+$ T cells within 3-4 weeks of infection, with an estimated >80% of all memory $CD4^+$ T cells being eliminated from the body [145]. This is especially pronounced at mucosal sites, such as the gut-associated lymphoid tissue (GALT), and particularly the lamina propria [33], where a substantial proportion of $CCR5^+$ effector memory $CD4^+$ T cells are located [149] and the bulk of viral replication occurs [31]. In addition to the memory $CD4^+$ T cells, Th_{17} $CD4^+$ T cells, which play a role in maintaining bacterial defense and mucosal barrier function in the gut and express high levels of CCR5 receptor on their surfaces, are also highly targeted and depleted in the gut mucosa [156-159]. The depletion of $CD4^+$ T cells helps drive bystander death [152] and leads to a massive immunological insult to the mucosa, resulting in multiple breaches through with bacterial content of the intestinal lumen can translocate into the general circulation, a process named microbial translocation [160]. This process represents one of the key triggers of chronic immune activation and inflammation that are staples of HIV pathogenesis [161]. This period of high viral replication and $CD4^+$ T-cell depletion is most often accompanied by clinical manifestations termed acute retroviral syndrome: fever, lymphadenopathy, fatigue, pharyngitis, and headache [162]. Beyond cell death, HIV also reduces the ability of the host to generate new $CD4^+$ T cells and expand existing $CD4^+$ T cell populations [163]. This is not to say that $CD4^+$ T cells are completely helpless against HIV. In fact, there are multiple host restriction factors can modulate HIV/SIV infection.

1.3.3 Host restriction factors and viral counteraction

Human cells are able to express multiple classes of restriction factors that act against HIV: the Apoprotein B editing catalytic subunit-like 3 (APOBEC3) family [164], sterile alpha motif- and HD-domain containing protein 1 (SAMHD1) [165-167], Tetherin [168, 169] and Tripartite motif (TRIM5) family [170]. Other, more minor or more recently discovered restriction factors are: MX-1, endoplasmic reticulum α1,2-mannosidase I (ERManI), translocator protein (TSPO), guanylate-binding protein 5 (GBP5), serine incorporator (SERINC3/5) and zinc-finger antiviral protein (ZAP) [171].

APOBEC3 is a family of cytidine deaminases, of which the most notable is APOBEC3G, which can be incorporated into virions. Therefore, after entry into a new cell, APOBEC3 acts during the reverse transcription phase and converts 2'-deoxycytidine to 2'-deoxyuridine, otherwise known as C-to-U, hypermutating HIV and leading to defective replication [172]. Unlike APOBEC3, which is packaged with the virions, the other restriction factors are not. SAMHD1 is further separated by the others due to the nature of its indirect antagonism of HIV: SAMHD1 reduces intracellular nucleotide concentrations, restricting reverse transcription [166]. Tetherin is a transmembrane protein with glycosylphosphatidylinositol anchors that insert into a variety of enveloped viruses, including HIV. Thus, after HIV undergoes the membrane fission, the transmembrane domains of tetherin dimers are able to remain embedded into the host membrane while the anchor is in the viral envelope, thereby preventing complete release from the host cell envelope [173]. The TRIM5 family disrupts the viral capsid, but the mechanisms are not fully understood. Binding of TRIM5 to the capsid is sufficient to restrict HIV through premature uncoating; nonproductive uncoating also occurs and is dependent on ubiquitination [174, 175].

Given that HIV transmission almost always results in productive infection, it is not surprising that SIV/HIV developed multiple mechanisms to counteract the host restriction factors. The viral protein Vif acts to bind the APOBEC3 proteins, while also recruiting ubiquitin ligase complexes, resulting in polyubiquitination and degradation of APOBEC3 [176]. The HIV-1 viral protein Vpx can antagonize SAMHD1 *via* ubiquitin ligases, leading to degradation [165, 167]. Some SIV strains from the SIVsmm and

SIVrcm lineages can degrade SAMHD1 through the Vpr protein. This is not surprising as Vpx of SIVsmm and HIV-2 originated from a duplication of Vpr [177-179]. Tetherin is counteracted by HIV-1 Vpu by multiple mechanisms: endocytosis, entrapment, and degradation. HIV-2, which lacks Vpu, utilizes Env to promote internalization and sequestration of tetherin, while other SIVs that lack Vpu often utilize Nef to antagonize tetherin [180].

1.3.4 Immune response during acute infection establishes viral set point

During the acute infection, a massive immune response is triggered in response to the viral infection, with two separate waves of cytokines and chemokines. First, IFN-α, IFN-γ, inducible protein 10 (IP-10), interleukin (IL)-12, IL-15, and monocyte chemoattractant protein 1 (MCP-1) all rapidly increase prior to the peak of viremia. This is followed by increases in TNF-α, IL-6, IL-8, IL-18, and IL-12p40 [181-184]. Production of these molecules is mostly by dendritic cells (DCs), with additional production by monocytes, natural killer (NK) cells, and even T cells. Activation of DCs is mediated by toll-like receptor 7 (TLR7) after endocytosis of HIV [185]. DCs are also responsible for cross presentation of antigens [186] and DC produced IFN-α primes T cells [187]. NK cells are direct effectors that are activated during HIV infection and clear infected cells through cytolysis and degranulation. NK cell cytotoxicity and antibody-dependent cell-mediated cytotoxicity (ADCC) result from binding of killer immunoglobulin-like receptors (KIRs), CD16, and the NKG2 protein family [188]. Through degranulation perforin and granzymes are released and induce target cell apoptosis [189]. NK cells produce various cytokines and chemokines, such as IFN-γ and TNFα [190] to limit viral infection and spread and β-chemokines which inhibit HIV entry to $CD4^+$ T cells [191]. The $CD8^+$ T cell response begins prior to the peak of viremia. $CD8^+$ T cells recognize foreign antigens that are presented on the cell surface by major histocompatibility complex (MHC) class I, stimulating the release of perforin, granzymes, and Fas ligand, leading to target cell apoptosis. $CD8^+$ T cells also release IFN-γ and TNF-α into the microenvironment [192]. $CD8^+$ T cells proliferation peaks around 2 weeks after the viral peak, their activation status being inversely correlated with viral set point. This proves

that the post-acute viral control occurs *via* $CD8^+$ T cells [193]. The emergence of the cellular immune responses exerts pressures on the virus at the transition from acute-to-chronic infection, and mutations are selected in the viral genome for $CD8^+$ T-cell escape, leading to a continuous chess game between the $CD8^+$ T cells that can respond to the new epitopes and subsequent viral escape [194, 195]. B cells are also activated during acute infection, generate plasmocytes and initiate antibody production. Initially, the antibody response to HIV is non-neutralizing and does not impact the plasma viremia [196]. However, the antibodies are enriched for IgG3, suggesting that they have not gone through affinity maturation and may be due to the rapid dysregulation of lymphoid tissues where the B cells would interact with T cells for maturation [197].

The viral set point, which occurs around 5-6 weeks post-infection, marks the passage to the chronic infection, when the immune system and HIV have reached a pseudo-equilibrium of steady-state viral replication, immune-mediated clearance, viral escape, and T cell adaptation. It is thus unsurprising that the levels of plasma VLs are predictive for the rate of disease progression to AIDS [198, 199]. Unlike VLs, the immune activation continues to rise into chronic phase, at which point it eventually hits the immune activation set point, in which $CD8^+$ T-cell activation parallels the rate of $CD4^+$ T-cell loss [200]. The immune activation set-point was also negatively correlated with the viral set point. In conjunction with data demonstrating that immune activation rapidly decreases with ART, it is likely that VLs is one of the drivers of the immune activation set-point [201-203].

1.3.5 Progression from chronic infection to AIDS

During the chronic infection, $CD4^+$ T-cell counts remain depleted in the circulation and at the mucosal sites of untreated individuals, with a small recovery with the decrease of plasma viremia at set point [204]. Meanwhile, superficial and mesenteric lymph nodes experience minimal $CD4^+$ T-cell depletion prior to the advanced stages of chronic infection [205, 206]. Nonetheless, in the continuous battle with HIV, the host slowly and inevitably loses the immune cells [207], with an estimated annual rate of decline of -

15.9% of $CD4^+$ T cells [208]. Over time, the continuous $CD4^+$ T-cell depletion associates a decreased immune function. A $CD4^+$ T-cell count below 350 cells/μL (which defines the AIDS-defining complication stage) caries the risk of opportunistic infections. When the counts decrease below 200 cells/μL (which defines AIDS) [209], the risk of opportunistic infections and cancers increases. At this point, VLs increase, as the immune system is no longer fully functional and fail to keep the virus in control; the host becomes increasingly susceptible to infectious diseases, cancers, especially Kaposi sarcoma, genital cancers, neurological disease, and wasting syndrome until the patients eventually die by these complications [210]. This pattern of infection can be observed in the absence of the antiretroviral therapy (ART). With the advent of ART, the clinical landscape of the HIV infection changed dramatically.

1.4 Antiretroviral therapy for HIV

1.4.1 Development of ART has dramatically improved life expectancy of PWH

The first antiretroviral, zidovudine, was approved by the FDA in 1987. Tritherapy, associating nucleozide reverse-transcriptase (RT) inhibitors with either non-nucleoside RT inhibitors or with protease inhibitors was introduced in 1996 and spectacularly impacted the outcome of infection: it completely suppressed viral replication and boosted the $CD4^+$ T-cell counts [211]. Current ART drugs target most of the HIV life cycle: entry inhibitors, prevent virus penetration in the target cells, by blocking CCR5 or CXCR4; fusion inhibitors prevent entry; RT inhibitors (nucleoside and non-nucleoside, NRTI and NNRTI, respectively) abort reverse transcription; integrase inhibitors, or integrase strand transfer inhibitors (INSTI) prevent viral integration; protease inhibitors (PI) prevent virion maturation [210]. The current first line of therapy is two NRTIs and either an NNRTI or INSTI, although new data support a two-drug regimen of dolutegravir and lamivudine for initial treatment [212]. ART thus effectively inhibits viral replication and decreases plasma VLs in PWH. In fact, most individuals will achieve viral suppression below the limits of detection, 50 vRNA copies/mL of plasma, as long as they maintain their regimen, and as long as their VLs

are undetectable, the paradigm (and media slogan) has become “Undetectable = Untransmittable; U=U” [213].

While ART decreases VLs, it reciprocally restores $CD4^+$ T cell counts, although this is highly variable and dependent upon the stage of disease progression and degree of immunodeficiency at treatment initiation. Studies have shown that the earlier ART initiation the better prognosis, with much better although incomplete restoration of $CD4^+$ T cells [214-216], including in the GALT [217]. Studies also show that unsatisfactory $CD4^+$ T cell restoration is correlated with higher mortality [218]. ART administration also contributes to a partial control of the levels of inflammation and immune activation, but cannot restore them to pre-infection levels [159, 219] and similar to $CD4^+$ T cell restoration, late ART initiation results in a more limited control of immune activation [220]. With advances in ART and accessibility, ART has drastically increased the life expectancy of PWH. While in the 2000s’ the life expectancy of a 21-year old PWH was 38 years, by 2016 it had increased to 57 years, a nearly 20 year increase [221]. Thus, ART has changed HIV infection from a life-threatening condition to a manageable chronic disease. Yet, life expectancy is still below uninfected persons (64-year life expectancy for 21-year old) [221] and, as discussed later, ART is not curative, nor does it completely prevent AIDS-related comorbidities.

1.5 Nonhuman primate models for HIV pathogenesis

1.5.1 Similarities and recapitulation of specific pathogenicities

Nonhuman primates (NHPs) are excellent models for the study of HIV-1 due to the variety of pathogenic outcomes that can be induced through various combinations of NHP species and SIV strains. Further, due to their size it is possible to take far more consistent sample volumes (blood and tissues) than with other models, e.g., humanized mice, and their use allows for extensive tissue sampling that would otherwise not be possible in humans. Meanwhile, NHPs are outbred and more genetically close to humans than any other model, which allow a more rigorous modeling in NHPs compared to other inbred species.

Of the several NHP species that can be utilized, cure research primarily uses RMs infected with SIVmac (either the reference swarm SIVmac251 or the infectious molecular clone SIVmac239) as the reference model. Notably, the SIVsmm family is the only one to induce pathogenic infection to RMs upon direct cross-species transmission of the virus from the natural host (sooty mangabeys), and SIVsmm infection yields a pathogenic diversity with a wide range of outcomes of the infection (due to a partial TRIM5α restriction) [52], unlike the SIVmac infection [222-227]. Therefore, the combination of RM and SIVmac strains is the gold standard for HIV modeling because of it reproduces all the major features of HIV-1 infection in a condensed time frame [25]: (i) Integration into host cell genome with similar integration site preference [228-230]; (ii) Conversion to latency in infected cells; (iii) Infected cell distribution to mucosal sites, lymph nodes, and peripheral blood [231-233]; (iv) Depletion of memory $CD4^+$ T cells from the mucosal and lymphoid sites [31-34]; (v) Chronic immune activation and inflammation, associating gut dysfunction and microbial translocation [33, 145, 149, 234, 235]. Although other species/strain combinations are available, they provide targeted usefulness, such as pigtailed macaques infected with SIVsab, which produces a highly pathogenic infection that is perfectly suited for the study of HIV/SIV-associated comorbidities [236-238], but long-term chronic illness is not easily achieved due to the very high pathogenicity of this infection, in which about 40% of SIVsab-infected PTMs progress to AIDS within the 6 months following the SIV challenge [60]. Further, for the study of HIV/SIV effects on the central nervous system (CNS), pigtailed macaques coinfected with SIVDeltaB670 and SIV17E-Fr are used because they quickly progress to immunodeficiency that associates CNS pathologies. This model showed that upon SIV infection, the CNS reservoir is seeded as early as 4 days, and that the macrophages are the major target cells of the virus in the brain [239, 240]. Recently, a new model of RMs infected with a new molecular clone, SIVsmE-CL757, was reported to reproduce the CNS events without the rapid disease induction seen in PTMs [241]. At the opposite spectrum of pathogenic diversity from the SIVmac infection, RM exposure to SIVsab leads to a very robust acute SIV infection followed by a spontaneous complete viral suppression below the limits of detection, allowing for investigation of virus reactivation from the latency without the use of ART [96]. This is particularly helpful for understanding the reactivation potential of "shock and kill" latency reversing agents, as the lack of ART enables *de novo* infection and therefore, larger viral bursts,

allowing for easier detection of viral reactivation after the administration of latency reversal agents. The caveat is the inability to properly compare the reservoir before and after therapy due to the wide spread of the reactivated virus in the absence of ART.

1.5.2 Chronic immune activation and inflammation in HIV/SIV infection

Chronic T-cell immune activation and systemic inflammation are key pathogenic features of HIV/SIV infection [242, 243]. T-cell immune activation and inflammation increase in response to virus early during infection, but they are not resolved after establishment of the viral setpoint, nor after viral suppression with ART [159, 219]. In fact, the immune activation set point is one of the strongest predictors of disease progression [200, 242, 244], better than plasma VLs or $CD4^+$ T-cell counts. This is due to the close association of the immune activation and inflammation with non-AIDS comorbidities and mortality in PWH and SIV-infected NHPs [39-43]. The determinants of chronic immune activation and inflammation in HIV/SIV infection are complex and multiple: (i) Activation of the immune response through viral production and replication [201-203]; (ii) Loss of gastrointestinal tract mucosal barrier integrity through the depletion of Th17 cells, which maintain mucosal barrier integrity [245, 246]; (iii) Microbial translocation from the lumen into systemic circulation and organs results from the damage to the mucosal barrier and epithelial tight junctions [160, 161, 247, 248]; (iv) Coinfections (e.g., hepatitis C virus [249], hepatitis B virus [250], herpes simplex virus type 2 [251], cytomegalovirus [252, 253], and Epstein-Barr virus [254]) contribute to antigen-specific immune activation or pattern recognition receptor (PRR) activation and are increasingly active with progressive immunodeficiency [255]; (v) Toxicity of ART and other risk factors [42, 256].

The chronic immune activation and inflammation impact disease progression through multiple pathways: (i) activated T cells become HIV/SIV target cells through expressing higher levels of coreceptors CCR5 and CXCR4 [257, 258]; (ii) activation of NF-κB results in virus production [259]; (iii) constant activation results in increased T cell turnover and homeostatic proliferation, thereby decreasing the

progenitor pool and inducing immune senescence [260, 261]; (iv) increased expression of immune checkpoint expression (e.g. PD-1 [262-265] and CTLA-4 [266]) which results in decreased functionality (T-cell exhaustion) [267]; (v) collagen deposition and fibrosis (via transforming growth factor beta [TGF-β]) damages the fibroblastic reticular cell network in lymph nodes, resulting in aberrant immune reconstitution [268-271]; (vi) prolonged inflammation facilitates an increased risk of cancers [272, 273]; and (vii) chronic inflammation damages vasculature and induces hypercoagulability, resulting in increased risk for cardiovascular diseases (CVD) [39, 41, 237, 274-276]. In the end, these consequences result in both a higher frequency and earlier onset [277, 278] of AIDS and non-AIDS comorbidities [279]. Comorbidities also include premature aging [280], sarcopenia [281], nonalcoholic fatty liver disease (NAFLD) [282], and HIV-associated neurocognitive disorder (HAND) [283].

Although there are several mechanisms that contribute to the chronic immune activation and inflammation, gut dysfunction and microbial translocation are arguably the largest contributors. Importantly, the onset of microbial translocation results in a vicious cycle of inflammation, mucosal barrier damage, and more microbial translocation; rinse and repeat [161, 284]. Translocated microbial products activate monocytes and macrophages that then produce inflammatory cytokines (IFN-α, TNF-α, IL-1, IL-6, and IL-18), further activating the immune system [238, 285, 286]. This not only results in chronic immune activation and inflammation, but also drives HIV enteropathy, which was described in the earliest stages of the pandemic, when diarrhea, weight loss, malnutrition, malabsorption and villous atrophy were frequently diagnosed in AIDS patients [287].

1.5.3 Gut dysfunction and microbial translocation potentiate immune activation and inflammation

HIV-associated GI pathology is triggered by the early and massive HIV-1 replication, and is characterized by immunological and structural abnormalities, including alterations of both the adaptive and innate mucosal immunity and substantial disruptions of the epithelial barrier [287-289]. These changes lead to increased local inflammation, microbial translocation and dysbiosis, and consequently to generalized

immune activation and inflammation, and comorbidities [42]. This current pathogenic paradigm of AIDS, for which the impact of HIV infection on gut mucosa is the quintessential determinant of HIV infection pathogenesis, was made possible only through extensive use of NHPs. The animal models allowed invasive serial studies of the gut [288, 290], and, as such, the reports on massive rapid depletion of the mucosal $CD4^+$ T cells in NHPs preceded similar observations in humans by a decade [31-34]. Detailed comparative studies facilitated by invasive sampling at key time points of infection in multiple NHP models with different outcomes of SIV infection furthered this major paradigm shift in AIDS pathogenesis [291].

Intestinal mucosal lesions occur early in HIV infection and are rapidly established as part of a vicious circle in which gut damage, microbial translocation and IA/INFL potentiate each other [288]. Virus suppression with ART improves infection outcome, but frequently does not reverse GI dysfunction [42]. As a result, even in study participants in which the virus is suppressed for prolonged periods of time (some PWH received ART for >20 years), residual levels of IA/INFL nonetheless persist, leading to an only partial immune restoration at the mucosal sites, and an increased frequency accelerated aging and HIV-related comorbidities than in the general population.

Two major mechanisms are responsible for the gut dysfunction observed in HIV infection: (i) First, mucosal $CD4^+$ T cell loss [287, 289], the hallmark of HIV/SIV infection [31, 207, 292-294]. The virus infects and kills activated memory and effector CCR5-expressing $CD4^+$ T cells, the major $CD4^+$ T cell subset at the mucosal sites, particularly in the lamina propria of the gut. $CD4^+$ T cell killing occurs in a caspase-1-dependent manner, resulting in a highly inflammatory form of death known as pyroptosis, which drives gut barrier dysfunction through production of inflammatory cytokines [154, 295]. Exposure to microbial products may also divert the mechanism of mucosal cell death toward apoptosis [295]. Increased inflammation induced by microbial products is probably also responsible, at least in part, for enhanced bystander lymphoid and epithelial cell death and gut damage [295]. Similar to HIV-1 infection, $CD4^+$ T cell depletion occurs early in SIV-infected macaques, is substantial, and is one of the correlates of the clinical outcome [289, 296, 297]. Depletion of T-cell subsets that control mucosal defense and homeostasis by limiting bacterial penetration and epithelial barrier integrity and function (i.e., Th-17 and Th-22) has

been correlated with the development of intestinal pathogenesis [245, 298]. Loss of T helper cells may also facilitate proliferation of opportunistic bacteria and damage to the gut [299]. In support of the direct role played by the $CD4^+$ T cell loss in the gut damage is the observation that in patients with idiopathic CD4 lymphopenia, plasma LPS levels are elevated, indicating increased gut permeabilization [300]. (ii) The second mechanism responsible for the gut dysfunction in HIV/SIV infections is through the loss of gut epithelial integrity. In progressive HIV/SIV infection, the excessive gut inflammation induced by virus replication damages the gut epithelium, allowing microbial products to first penetrate the gut mucosa and then translocate into the general circulation [160, 288]. Immune cells exposed to these microbial products are subsequently activated through different PRRs, such as lipopolysaccharide (LPS) binding to toll-like receptor 4 (TLR4) [161], and thus lead to further gut damage by either directly fueling virus replication or indirectly through the release of proinflammatory cytokines and excessive cell death [299, 301]. Conversely, the natural hosts of SIVs, which do not have progressive infection, have low levels of LPS in the periphery, indicating a lack of microbial translocation throughout infection [161, 302]. AGMs were found to rapidly activate and maintain regenerative mechanisms in the gut mucosal tissue, thereby counteracting the vicious cycle [36]. Indeed, intravenous administration of LPS to SIV-infected AGMs resulted in systemic inflammation uncharacteristic of the infection [41, 303]. These data were further supported by direct mucosal damage of SIV-infected AGMs through administration of dextran sulphate with similar results: systemic inflammation, T-cell activation, and increased plasma viremia [235]. Conversely, PTMs were treated with sevelamer, which binds LPS, and transiently reduced immune activation, inflammation, and even plasma viremia in the animals [248]. Thus, mucosal barrier damage, microbial translocation, and inflammation/immune activation are irrefutably intertwined.

1.5.4 Study of natural hosts demonstrates important differences between pathogenic and nonpathogenic infection

The natural reservoir of SIVs is represented by African NHPs. Over 40 species of monkeys in Africa are infected with species-specific SIVs [12]. In their natural hosts, such as African green monkeys (AGMs), sooty mangabeys (SMs) and mandrills (MNDs), SIV infection appears to be nonpathogenic [12, 304, 305]. In these species, disease progression is highly uncommon, only occurring in a handful of animals which had greatly outlived their normal life expectancy [306, 307].

Extensive studies performed over the last three decades, allowed us to thoroughly characterize the pathogenesis of SIV infections in their natural hosts. Through these comparative pathogenesis studies, we identified similarities and differences between the pathogenic and the nonpathogenic infections, thus establishing features that were specifically associated with the progression to AIDS in the pathogenic infections [308]. The most important shared feature of the pathogenic and nonpathogenic HIV/SIV infections is the robust acute viral replication, followed by high steady-state replication that is higher than in the majority of untreated chronically PWH [58, 227, 309-314]. Meanwhile, African natural hosts similarly undergo a severe $CD4^+$ T-cell depletion at the mucosal sites with the same order of magnitude as that observed in PWH and pathogenic SIV infections, in line with the primary target cell of SIV in African NHPs being the $CD4^+$ T cell [31, 33, 145, 149, 302, 315-317]. Furthermore, the humoral and cellular immune responses are similar between the pathogenic and nonpathogenic SIV infections [7, 11, 308, 318-320].

These common features between pathogenic and nonpathogenic infections suggest that the lack of disease progression in natural hosts is not the result of a viral attenuation. Indeed, the rare cases of AIDS documented in African NHPs [306, 307] and the observation that direct SIV cross-species transmission from their natural hosts to macaques results in pathogenic infections that progresses to AIDS [60, 227, 321] confirm that control of disease progression is independent of the virus and instead relies on host adaptations. This likely occurred because of the SIV-African NHP host coevolution occurring over hundreds of

millennia [10, 16, 322-324]. This virus-host coevolution allows natural hosts to counteract the deleterious consequences of the SIV infection and resulted in phenotypic features of natural hosts that contribute to the prevention of disease progression to AIDS [10, 90, 322, 323, 325-329]. In particular, these would be: few target cells ($CCR5^+$ $CD4^+$ T cells) at mucosal sites [16, 316, 330, 331] and downregulation of CD4 on helper T cells when they transition to memory phenotype [330, 332]. The usage of CXCR6 as a coreceptor may also server to further preserve $CD4^+$ cells in AGMs and sooty mangabeys [90, 333].

The main factor behind the lack of disease progression in the natural hosts of SIVs is their ability to actively control chronic immune activation and inflammation [37, 308], the main drivers of disease progression and mortality in PWH [242, 243]. Chronic systemic T-cell immune activation and inflammation are kept at bay through an exquisite ability of the natural hosts of SIVs to maintain the integrity of the mucosal barrier throughout the course of SIV infection [38, 235], due to specific healing mechanisms recently described [36]. This lack of mucosal dysfunction allows the natural hosts to avert microbial translocation [161, 302], in stark contrast to the pathogenic HIV/SIV infections, in which microbial translocation occurs as a result of acute viral replication and proinflammatory responses causing extensive damage to the intestinal mucosa [334].

1.5.5 Nonhuman primate models for HIV-related comorbidities

Although ART is able to curb viremia, there is still a disproportionate risk of non-AIDS comorbidities in PWH, with higher rates of CVD, kidney disease, hepatic disease, and other events [335], replacing opportunistic infections as the leading causes of mortality and morbidity. In fact, from 2000 to 2010, AIDS-related deaths in a French study group decreased from 47% to 25% [336], while a multicohort study showed a decrease from 34% to 22% in 1999-2000 to 2009-2011, respectively [337]. The transition from AIDS-related mortality and morbidity to non-AIDS is associated with an increased lifespan for PWH, yet there is still a life expectancy deficit, averaging 8 years less [221, 338]. Further, as the PWH population

ages, there is an increasing risk of multiple comorbidities arising per individual than in the uninfected population [339].

Due to the differences in natural hosts and pathogenic infections, a method to increasing our understanding of HIV pathogenesis is to compare the two and find differences in host biology. This strategy has allowed for incredible progress in our understanding of HIV transmission, pathogenesis, prevention, and treatment [25, 43, 340, 341]. SIVsab, the SIV that naturally infects AGMs, also infects PTMs. Both infections present with high VLs, but completely opposite disease outcomes. SIVsab-infected AGMs do not progress to AIDS, while SIVsab-infected PTMs present with nearly all pathogenic features of HIV infection and readily progress to simian AIDS [43, 236]. As mentioned earlier, comparisons between the two models were integral to understanding immune activation, inflammation, gut dysfunction, and microbial translocation in HIV infection. Indeed, other comorbidities are also investigated with NHP models. PWH are at an undeniably higher risk for CVD [342], which is recapitulated in both SIVsab-infected PTMs and SIVmac-infected RMs. These models present with hypercoagulation, demonstrated by significant increases in D-dimer and thrombin-antithrombin complex. This is especially prevalent in the SIVsab-infected PTMs, where these biomarkers were increased early after infection and associated with cardiovascular lesions and were greatly indicative of progression to AIDS and mortality [236]. Additionally, thrombotic microangiopathy was present in multiple organs, while myocardial hypertrophy, fibrosis, myocarditis and infarction were also observed [236]. This model has also shown that therapeutic interventions for reducing microbial translocation, immune activation, and inflammation resulted in decreased hypercoagulation, further supporting the role of immune activation and inflammation in hypercoagulation [237, 248].

Liver dysfunction is frequent in PWH and has multiple sources: (i) infection of the Kupffer and stellate cells in the liver [343, 344]; (ii) microbial translocation and the chronic inflammation [344, 345]; (iii) coagulopathy [42, 346]; (iv) cofactors, e.g. hepatitis C virus coinfection [347] and excessive alcohol consumption [348]; and (v) ART toxicity [345]. SIVsab-infected PTMs demonstrated inflammatory

infiltrates and hepatic fibrosis, which together resemble chronic active hepatitis [43], and RMs demonstrated that the liver is highly involved in clearing virus from circulation [349].

Respiratory comorbidities are on the rise with PWH living longer, such as chronic obstructive pulmonary disease (COPD) [350], however the mechanisms are not well elucidated. The SIVsab PTM model was also used to investigate pulmonary lesions that may play a role in the rise of COPD in PWH. In the PTMs, early infection presented with immune infiltrates in the lung parenchyma and near large bronchi. During chronic infection, emphysema and thickened alveolar walls are observed with disruption of the lung architecture and fibrosis, in direct contrast the SIVsab-infected AGMs which presented with no immune infiltration or subsequent lung disruption [43].

Acute renal failure and chronic kidney disease are associated with advanced immunodeficiency and age, therefore greatly increasing the risk in older PWH [351]. HIV-associated nephropathy (HIVAN) can quickly progress to end-stage renal disease and mortality if left untreated [352]. However, like respiratory comorbidities, the mechanisms are not fully known. Although several ART drugs have been associated with kidney damage, they do not explain the full extent of renal disease [353]. It is believed that chronic immune activation and inflammation are likely the main mechanism because early initiation of ART, which allows for better maintenance of immune function, minimizes the risk of kidney disease in PWH [353]. In RMs infected with $SHIV_{KU-1}$, researchers found the equivalent of HIVAN with glomerulosclerosis and collapsing glomerulopathy [354], and another SHIV-infected RM presented with nephrotic syndrome: peripheral edema, hypoalbuminemia, and proteinuria [355]. In our model of SIVsab-infected PTMs, we have shown similar kidney pathologies to HIVAN, including hyperplasia of the bowman capsule epithelial lining, glomerulosclerosis and collapsing glomerulopathy, and interstitial nephritis [43].

The rate of HAND in PWH has drastically decreased after the advent of ART, but less severe neurocognitive issues remain and risk increases with age [356]. HAND is a spectrum that includes asymptomatic neurocognitive impairment (ANI), mild neurocognitive disorder (MND), and HIV-associated dementia (HAD), with HAD being the most severe form. The spectrum is defined by neuropsychological testing and functional status assessments. The biomarkers accessible by blood for

HAND are not very specific: $CD4^+$ T cell count at nadir of depletion, sCD14, sCD163, and viral DNA, all of which can be associated with general progression [356]. Cerebrospinal fluid, however, shows associations with neuronal injury markers, as well as inflammation, demonstrating more specific markers [356]. Further, neuroimaging markers are helpful and functional MRI has demonstrated accelerated aging in the brains of PWH [357]. Animal models allow for invasive approaches and euthanasia further permits investigation into brain pathologies at necropsy. The SIV-infected PTMs again is the model of choice for neurocognitive disorders because of the recapitulation of HIV CNS pathologies, increased proportion of neurocognitive disorders, and quick rate of progression relative to others [358, 359].

1.6 HIV Cure research and current strategies

1.6.1 The need for an HIV cure

An essential step of the HIV replication cycle is integration into the host genome, whereby it can use host cell machinery to produce its viral mRNA products and RNA genome. Once the viral latency is established, the cells cease to produce viral products, and they can no longer be recognized by the immune system, allowing the provirus to persist in these cells indefinitely [360]. The totality of the integrated proviruses forms the latent reservoir; the HIV-infected $CD4^+$ cells that contain integrated HIV and revert to a resting state with altered gene expression, for example reduced NF-κB, which is normally triggered by T cell activation, results in a pool of hidden, activatable provirus [361]. While ART effectively suppresses the circulating virus [362], the reservoir cells are not impacted by ART, and treatment cessation is always followed by a viral rebound with VL levels similar to those observed pretherapy [363-366]. The source of this virus rebound is the latent reservoir, which can be reactivated by multiple stimuli inducing T-cell activation and latency reversal. This is the scientific basis of the need for a life-long adherence to ART. ART was one of the greatest achievements of modern medicine, yet long-term toxicity, viral resistance, stigma, and costs, all call for an effective HIV cure aimed at complete HIV eradication from PWH. ART

does not completely restore the immune system, nor eradicate HIV. Multiple strategies towards an HIV cure are pursued [367-385], but none effectively curbed the reservoir nor induced robust and durable virus control, except the hematopoietic stem-cell transplantation, which is not scalable and has unreasonable limitations [386-389]. The major barriers to a successful HIV eradication are: (i) HIV persistence in latently infected cells invisible to immune responses; (ii) inability of a damaged/exhausted immune system to eliminate HIV-infected cells; and (iii) chronic INFL that persists on ART [390-393].

1.6.2 The latent reservoir currently prevents HIV cure

The existence of the HIV latent reservoir is the primary obstacle for cure HIV eradication from the host. The latent reservoir is established immediately following infection, as early as 3 dpi, and prior to detectable viremia [22-24, 394], in resting $CD4^+$ T cells: [362, 363, 395-398] with different immunophenotypes: central memory [374, 399, 400], transitional memory [374, 400], stem cell memory T cells [401], Tregs [402], and follicular T helper $CD4^+$ cells [403]. In addition to the $CD4^+$ T cells, macrophages and monocytes can be latently infected by HIV/SIV [404]. Dendritic cells are suspected to contribute to the reservoir by carrying SIV/HIV virions on their surface [405]. Latently infected cells lack a specific surface marker which would allow specific targeting of the latently infected cells [406] which is one of the major barriers against an HIV cure.

The prospect for an HIV cure became a reality after the success of the "Berlin patient", a PWH who underwent allogeneic bone marrow stem-cell transplantation to treat acute myeloid leukemia. The donor was chosen specifically for homozygosity for the *CCR5 Δ32* allele, and thus without a functional CCR5 coreceptor and resistance to HIV infection; as a result, after two stem cell transplantations, graft-versus-host disease, irradiation, immunosuppressive therapies and whole body irradiation, the Berlin patient presented with a drug-free HIV remission [407] which lasted for 12 years prior to his death. A second patient that underwent a similar procedure with a *CCR5 Δ32* allele donor (the "London patient") is also reported to be in remission [387]. Yet, while cure research got a tremendous boost leading to major

improvements in our understanding of the nature of viral reservoirs and of the mechanisms of HIV latency in the decade following this remarkable success story, this procedure is not scalable, and, as such, there were not many subsequent cases of success in this field. The "Boston patients," which also went through a similar transplantation (yet with stem cells from donors with intact *CCR5*), rebounded by months 3 and 8 post-ART interruption [408]. As such, these cases demonstrated that standard bone marrow transplantation is not sufficient to cure HIV. Furthermore, while ART can suppress plasma viral RNA to below limits of quantification, cessation of ART results in viral rebound in virtually every situation, including the "Mississippi baby," who was on ART from 30 hours to 18 months of age, and was thought to be functionally cured [409]. In this patient, the virus eventually rebounded 2 years after interruption of ART [410], due to the persistence in the latent reservoir. Additional cases of people believed to have been cured or functionally cured post-cessation of treatment based on conventional measurements of the viral reservoir include the VISCONTI cohort [411] and a South African child [412].

On the other hand, NHP models have demonstrated that early initiation of ART does not prevent the viral rebound post-therapy interruption [22], indicating that the reservoir is established very early in infection, suggesting that interventions aimed at curing HIV infection will need to curb the reservoir rather than prevent its formation. Nevertheless, in the same NHP studies, a delay in virus rebound at the cessation of art was observed in macaques in which therapy was initiated very early, at 3 dpi, prior to detectable viremia. In a case of an PWH treated with allogeneic stem cell transplantation for treatment of acute lymphoblastic leukemia, researchers found that the virus rebounding nearly one year after treatment interruption was phylogenetically distinct from the HIV strain detected in PBMCs prior to transplantation [413]. These rebounds illustrate that not only we do not have an effective cure strategy, but we also have not fully mastered the diagnostic tools necessary for monitoring the effectiveness of various cure strategies, indicating a need for more effective methods and strategies.

1.6.3 Mechanisms of HIV latency establishment

HIV latency was first described with *in vitro* experiments demonstrating that cells that survived infection did not produce virus, but could be induced with 5-iodo-2'-deoxyuridine [414]. Shortly after, studies showed the stimulation of HIV transcription was regulated by the same pathways that induce T-cell activation [415-417], which suggested that activated $CD4^+$ T cells were not likely to support latency. However, resting $CD4^+$ T cells poorly support productive infection [418, 419]. Thus, the paradigm of reservoir formation became the transition of infected, active $CD4^+$ T cells to a resting state, and it was proven in 1995 that resting $CD4^+$ T cells from PWH can harbor replication competent provirus [420]. In fact, multiple *in vitro* studies have since supported that infected, activated $CD4^+$ T cells gradually transition back to the resting state and support latent infection [421-427].

The preferential integration of HIV into transcriptionally active sites [111-113] suggests that HIV expression is at least partially independent of the host gene expression. After integration, two nucleosome structures, Nuc-0 and Nuc-1, are formed at the 5' LTR, blocking transcription initiation by RNAP II [428]. These nucleosomes are associated with epigenetic modifications that contribute to HIV latency: histone deacetylation [429-431] and methylation [432-434], leading to contraction of the chromatin structure and repression of transcription. Further, not only are the modifications observed, but the histone methyltransferases and deacetylases are also associated with the LTR [429, 432, 434, 435] and recruitment is facilitated by various transacting factors [425, 436-438]. These data also help explain the strong reactivation potentials of various HDAC inhibitors.

Transcriptional interference is another mechanism driving HIV latency, depending on the relative orientation of the provirus in the host gene. With same sense polarity, the tendency to integrate into active sites can readily cause elongation of the host gene to displace transcription factors at the HIV LTR, thereby preventing transcription initiation [439, 440]. When the provirus is integrated in the opposite polarity to the host gene, transcriptional interference manifests with collisions between the elongation complexes of the host gene and HIV transcription [441].

Recruitment of the host factor positive transcription elongation factor b (P-TEFb) from the 7SK small nuclear ribonucleoprotein (snRNP) complex is facilitated by competitive binding of HIV Tat to HEXIM1, causing the release of P-TEFb [442, 443]. P-TEFb then mediates the phosphorylation of RNAP II [444, 445] and Spt5 [446], preventing early termination of transcription, which leads to efficient transcription elongation. The bromodomain proteins BRD2 and BRD4 act competitively with HIV Tat for P-TEFb binding, resulting in diminished transcription elongation [447, 448]. Thus, it is not surprising that BRD2/4 binding by bromodomain inhibitor JQ1 results in viral reactivation [449, 450].

1.6.4 Reservoir decay is not curative.

Early reservoir decay modeling suggested that maintaining ART for 7.7 years may be able to completely eradicate the latent reservoir [451], yet this has been clearly debunked, with PWH reaching decades without complete clearance on ART. Newer modeling from PWH on ART indicates that the half-life of total HIV DNA is 42 years, whereas the intact provirus half-life is 7 years [452], thereby negating the theory of eradicating HIV-infected cells solely through sustained ART. The data demonstrate that early ART initiation is beneficial for the rate of reservoir decay [452], but still not enough to eliminate the reservoir.

1.6.5 Technical obstacles towards reservoir quantification

A technical obstacle towards the latent reservoir eradication of the latent reservoir is the lack of a proper quantification of the inducible virus. Initial measurements used cell-associated HIV DNA (caDNA) to quantify the latent reservoir [363, 420, 453], but it soon became clear that only a fraction of these cells were capable of producing infectious virus [395], thus demonstrating an inherent issue with measuring caDNA: not all cells may be relevant for the recrudescence of infection after ART cessation. Full genome

sequencing revealed that the proviruses forming the latent reservoir are both intact and defective [454], further diminishing the significance of caDNA as a measurement of the inducible virus. Reservoir quantification took a step further when a the quantitative viral outgrowth assay (qVOA) was established to be the gold standard for measuring the inducible virus [395]. The qVOA dilutes purified, resting $CD4^+$ T cells from HIV donors and activates them with a stimulant (e.g. phytohemagglutinin [PHA] [395], phorbol 12-myristate 13-acetate [PMA] and ionomycin [455], or anti-CD3/CD28 [365, 456]) in the presence of feeder cells (irradiated PBMCs). The original method of activation (PHA) was shown to induce activation in nearly all resting T cells [457], and minimal differences were seen with the other activation methodologies [458]. However, qVOA is time consuming because it requires that stimulated cells are cultured for 14-21 days so that enough p24 can be generated for quantification via ELISA [395]. An alternative method of using PCR as the end quantification [459] decreases time consumption, but has its own issue of viral RNA being produced from a fraction of defective proviruses, thus artificially increasing the size of the replication competent reservoir [460].

An additional problem with the qVOA is that the *in vitro* stimulation lacked efficacy in reactivating all of the replication-competent viruses from the purified $CD4^+$ T cells, as demonstrated by the observation that multiple rounds of cell activation yielded additional virus [461, 462] and sequencing with subsequent infection of cells *in vitro* confirmed replication capabilities of wells negative for viral outgrowth [461]. Beyond the immediate ramifications towards quantification, this also pointed towards another barrier of HIV cure: HIV-infected T cells can activate and clonally expand without reactivating virus, thereby avoiding the immune response while bolstering the reservoir size [463]. A way to mitigate the problem of incomplete activation, is to perform sequencing for determining the percentage of provirus that has intact provirus.

For full-genome sequencing, researchers extract genomic DNA and use nested PCR with limiting dilutions. The PCR products are then run on agarose gels and extracted for sequencing [464], thus this technique minimizes errors, but it also is highly time consuming and intensive. Unfortunately, reducing the time constraints and labor by using subgenomic sequencing introduces detection and accuracy problems

due to either defects in regions outside of the amplified region or deletions overlapping the amplified region [465]. Utilizing next-generation sequencing is one method to increase efficiency and cost effectiveness [466-468] and has higher sensitivity than Sanger sequencing, allowing for a better detection of mutations [469]. The recently developed intact proviral DNA assay (IPDA) is based on digital droplet PCR (ddPCR) multiplex technology [470]. It uses primers against conserved regions of *env*, the packaging signal (PS) and Rev-response element (RRE), to elucidate defective *versus* intact provirus. The benefit of this assay is that it requires few cells (5 million $CD4^+$ T cells) and does not have the inefficiency of long-distance PCR. The caveat is that by only detecting a small region of the genome (~2%), the IPDA can easily miss other defects that would render the virus replication incompetent [470] and also has issues with polymorphisms affecting detection [471]. To mitigate this issue, a combination of quadruplex qPCR and NGS, termed Q4PCR was developed. Like IPDA, Q4PCR also uses the PS and RRE regions, but also includes primers for *pol* and *gag*. Using Q4PCR with NGS showed that IPDA had high variability between in detection of true intact provirus [472]. Additional head-to-head comparisons between these two methods are warranted.

Nonetheless, the proviral sequencing demonstrated that only a small fraction (~5-7%) of the proviruses are intact, regardless of the timing of ART initiation [454] and accounts for around 60 per million $CD4^+$ T cells [461], a 60-fold increase in the number of replication competent virus estimated by qVOA [473]. These data were initially promising for the eradication of HIV, as it suggested the possibility of eliminating far less infected cells than previously thought. However, studies demonstrated that the ability of defective proviruses to produce viral proteins may be stimulating the immune system, thus contributing to the viral pathogenesis [460, 474, 475].

1.6.6 SIVmac-infected RMs as a model for cure research.

In addition to the general roadblocks to cure, there are specific limitations to cure research in humans [476, 477]: (a) ART cannot be stopped without the risk of emergence of drug-resistant strains; (b) residual viral replication prevents proper characterization of the reservoir; and (c) invasive sampling of

multiple potential reservoir sites is limited. These limitations make use of animal models imperative for the study of the viral reservoir and for testing cure strategies. Although humanized mice have potential for cure research [478-482], size limitations of individual animals prevent detailed reservoir assessment. Therefore, the model of choice is the SIVmac-infected RM on ART.

HIV and SIV share key features of virus persistence: (a) HIV/SIV DNA are similarly integrated in the target cell genome [483-485]; (b) response to interferons results in transcriptional control of long terminal repeat sequences (LTRs) through histone acetylation favoring HIV/SIV DNA persistence [486]; (c) costimulatory signals induce latent HIV/SIV without co-engagement of T cell receptors [487]; and (d) distribution of cells containing HIV/SIV DNA and RNA sequences in blood, LNs, and mucosal sites are similar in humans and RMs [231, 488, 489]. SIVmac infection of RMs reproduces all the stages of HIV infection in a shorter time frame. These characteristics demonstrate similar reservoir dynamics between HIV and SIV infection. Historically, SIVmac was difficult to control with ART, requiring complex and expensive drug combinations [490]. Emergence of new integrase inhibitors and use of coformulated drugs now allow SIVmac suppression with ART regimens that are similar to, or the same as, those used in HIV infection [491], thus further establishing SIVmac-infected RMs as the gold standard model.

1.6.7 Strategies towards an HIV/SIV cure.

Multiple strategies to reduce/eradicate the latent reservoir have been proposed, yet with relatively modest success: (i) ART intensification [492-495]; (ii) permanent transcriptional silencing of HIV [369, 496]; (iii) gene editing of CCR5 [497]; (iv) genetic engineering of anti-HIV chimeric antigen receptor (CAR) T cells [384, 498, 499]; (v) apoptosis promotion [500, 501]; (vi) bone marrow transplantation [408]; (vii) broadly neutralizing antibodies [502, 503]; (viii) vaccines [504]; (ix) regulatory T cell (Treg) manipulation strategies [402, 502, 505]; (x) use of checkpoint inhibitors to enhance HIV-specific immune responses [506-509] (xi) “shock and kill”. This last approach operates on the premise that therapeutic agents named latency reversing agents (LRAs) can be used to reverse the viral latency, which then allows for

immune surveillance to recognize antigens of the reactivated virus and thus clear the infected cells. This strategy is performed in virus-suppressed individuals on ART, which prevents *de novo* infections of susceptible cells [25, 510-512]. Theoretically, repeated cycles of virus reactivation and clearance would result in a significant curbing/clearance of eradicating the HIV reservoir, and this strategy is the focus of the dissertation. The potential interplay between different cure strategies is shown in Figure 3.

In spite of some promising results being reported by previous studies, none of the LRAs tested so far showed enough potency to justify their large-scale use as HIV cure agents [513-515]. In addition to this lack of efficacy resulting in insufficient reservoir reactivation [515], some LRAs were reported to induce a massive, indiscriminate T-cell activation that can be detrimental to the host health or even lethal [516, 517]. Finally, some LRAs, particularly HDACi, were reported to have a negative impact on the cell-mediated immune response [511, 518-520].

Other cure strategies also have issues with efficiency, be it the lack of reducing residual viremia or reservoir size with ART intensification [521], insufficient virus reactivation with Treg manipulation [502] and additional toxicity when combined with ART [505], lack of viral clearance in response to checkpoint inhibitors [506, 507], inherent resistance and escape mutations against broadly neutralizing antibodies [522], lack of great enough efficiency and long-term stability of gene therapies and CAR T cells [384, 523], or safety concerns of bone marrow transplants coupled with the lack of success [408, 524]. As such, after more than a decade of intensive research, the end is still not in sight.

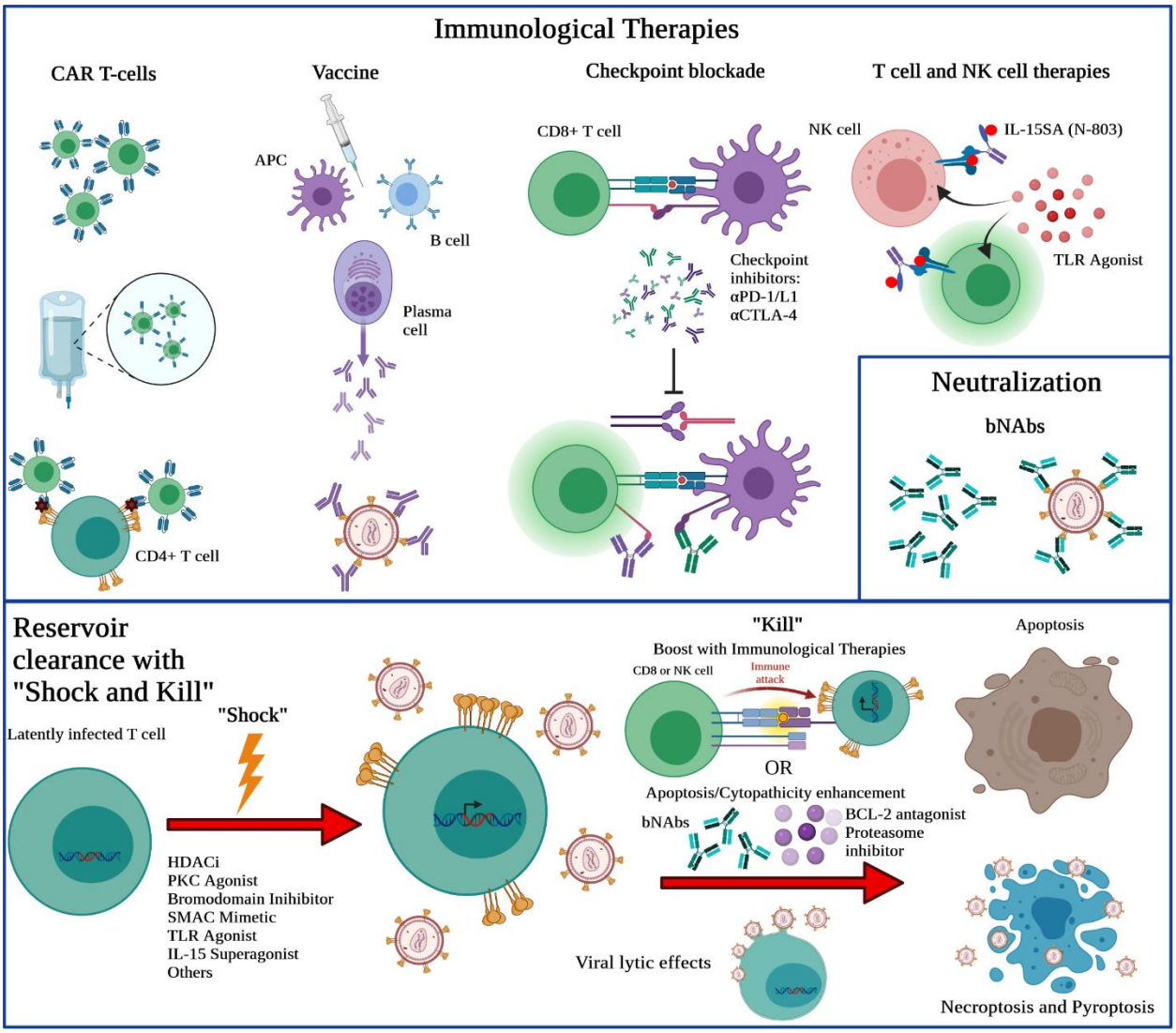

Figure 3. Cure strategies focusing upon clearance of the latent reservoir.

There are many different therapeutics that are being investigated for HIV cure. Of note, eradication of the latent HIV reservoir and establishment of potent immune responses may result in eventual functional or sterilizing cure and will likely require combination approaches as shown in this schematic.

1.6.7.1 ART intensification as a cure strategy

ART intensification was thought to potentially alleviate some of the residual virus replication in patients on ART [525, 526]. However, several studies have demonstrated that ART intensification does not solve the issue of low-level residual replication. In fact, efavirenz, lopinavir/ritonavir, and atazanavir/ritonavir [527], raltegravir [528], dolutegravir [529], and maraviroc [530] were all used to intensify ART, to no avail. Due to the major role of the gut in HIV pathogenesis, another study focused

upon the gut when attempting ART intensification with raltegravir and maraviroc. With this combination, there was no benefit to the immune populations of the gut, decreases in inflammatory markers beyond what was seen in the control group, further demonstrating the futility of ART intensification [531].

1.6.7.2 "Block and lock" – Transcriptional silencing for HIV functional cure

HIV transcription involves both viral and cellular machinery. During viral production, HIV initially transcribes short, completely spliced transcripts that create the transactivator of transcription (Tat) and the regulator of virion expression (Rev). Tat acts as an autoregulator for HIV and binds to the HIV transactivation response element (TAR) of the HIV promoter. This allows for the recruitment of the RNAP II elongation factor, P-TEFb, that results in transcription initiation and elongation [532, 533]. One strategy for an HIV cure is to force the viruses into latency, by blocking viral transcription and locking the viral promoter into a late state, thereby preventing disease progression. This is called the "block-and-lock" strategy, and it utilizes antagonists to viral proteins or host transcription machinery [534]. There are several different targets of "block-and-lock", but the most investigated is the use of Tat inhibitors, due to Tat's role in HIV transcription [532, 533]. NullBasic was the first Tat-inhibitor developed in 2009 and is comprised of a transdominant Tat mutant which is meant to outcompete wild-type Tat [535]. *In vitro*, NullBasic-expressing cells produced significantly fewer virus and reduced the efficacy of viral reactivation after PMA stimulation. However, this protein did not completely inhibit production of full-length mRNA and also had to be stably expressed in the cells to silence transcription [536]. Didehydro-cortistatin A (dCA) [537] is currently the most advanced small molecule inhibitor developed. In cell cultures, dCA was shown to be inhibit viral activation and even inhibit reactivation after stimulation with prostratin [538]. When administered to HIV-infected, ART-treated, humanized bone marrow/liver/thymus (BLT) mice, treatment of dCA significantly decreased the aggregate number of viral RNA copies *vs*. controls and increased the time to viral rebound after analytic treatment interruption. There, all mice rebounded by 10 days post-interruption in the control group and 19 days post-interruption in the dCA group [538]. Unfortunately, other block-and-lock small molecule inhibitors, such as HSP90 inhibitors, Jak-STAT inhibitors, and kinase

inhibitors, are more prone to side effects, due to their roles in host transcription [539]. In fact, characterization of CDK and mTOR inhibitors indicated that due to cellular toxicity, the vast majority these inhibitors had to be discarded [540]. This illustrates the difficulty of developing small molecular inhibitors against host proteins for HIV silencing.

Finally, transcriptional gene silencing was another method of silencing that different groups tested. It is based on the use of short hairpin RNAs and short interfering RNAs that are able to reduce viral burden, but run into issues with delivery methods [534].

1.6.7.3 Gene therapy and engineered CAR T cells for HIV cure

In vitro and *ex vivo* gene therapy with CRISPR/Cas9 has been able to disrupt proviruses [541-543], but the lack of a systemic delivery mechanism and of target effects in humans hinders gene therapy as an HIV intervention [544]. Nonetheless, advancements in gene therapy have allowed for engineered immune cells to be used to combat HIV. For instance, engineered T cells with chimeric antigen receptors (CAR) against HIV have shown promise in eliminating HIV, but are still hindered *in vivo* by lacking sustained activity of the cells for the time period necessary for eradication, off target effects, the threat of CAR immunogenicity, and the possibility of inducing a cytokine storm in the patients [545]. One of the large issues with CAR T cells is protection of the CAR T cells against HIV infection. Thus, researchers developed conjugated coreceptors, C34 conjugated to CCR5 or CXCR4, and tested them *in vitro*. These were found to be able to protect against HIV infection, and the C34-CXCR4 conjugate demonstrated better protection than the C34-CCR5 conjugate [546]. Following these results, new dual CD4-CAR T cells, expressing both 4-1BB/CD3-ζ and CD28/CD3-ζ ectodomains with a co-expressed C34-CXCR4 fusion inhibitor, to protect against HIV infection, were tested in humanized BLT mice. The results demonstrated elimination of infected cells *in vivo*, including memory $CD4^+$ T cells, while also reducing the loss of $CD4^+$ T cells during acute phase, and decreasing plasma viremia and cell-associated HIV DNA (from memory $CD4^+$ T cells). However, the protection from HIV was eventually lost over time, demonstrating the need to develop chimeric cells with complete resistance to HIV [547].

1.6.7.4 Enhancing apoptosis and cytopathic effects as a cure strategy

Due to the production of the HIV protease, infected cells are pushed to a pro-survival state. The HIV protease cleaves procaspase 8 to create Casp8p41, which is capable of binding to BAK and inducing apoptosis [548-551]. However, in cells producing high levels of the antiapoptotic protein BCL-2, such as central memory $CD4^+$ T cells, which form the bulk of the HIV/SIV reservoir, Casp8p41 binds to BCL-2 instead of BAK, thereby neutralizing the proapoptotic ability of Casp8p41 and inducing the pro-survival phenotype. Transcriptional profiling of $CD4^+$ T cells that survived coculture with HIV-specific CTLs demonstrated that BCL-2 is a major overexpressed marker, further substantiating its role in persistence. Venetoclax is a Bcl2 antagonist, which was shown to induce the death of HIV-infected cells *in vitro,* with a strong selectivity towards infected cells [500, 501]. Another proapoptotic drug is Ixazomib, a proteasome inhibitor. Because BCL-2-Casp8p41 complex together and become polyubiquinated and then degraded at the proteasome, the use of a proteasome inhibitor prevented degradation of Casp8p41, allowing for increased activity and binding to BAK. When administered to cells *in vitro,* Ixazomib was able to increase death of HIV-infected cells with the added benefit of reactivating HIV via NF-κB [552]. It thus appeared that the combination of the two drugs is ideal for first increasing viral reactivation, then induce a proapoptotic state, while preventing the decay of the Casp8p41. When this combination was attempted *in vitro*, the reduction of HIV-infected cells surpassed that of either drug alone. However, when used *ex vivo,* the nonspecific toxicity was overwhelming [553]. Meanwhile, when Venetoclax was administered *ex vivo* after bryostatin-1 stimulation, there was insignificant clearance of infected cells, but when venetoclax was combined with HIV-specific CTLs, there was a modest decrease in the amount of HIV-infected cells and when anti-CD3/CD28 was used instead of bryostatin-1, there were significant decreases of the infected cell counts [554]. These data thus support the use of BCL-2 antagonists, but also show that more potent, safe LRAs are needed for this strategy, because anti-CD3/CD28 stimulation cannot be used *in vivo* for safety reasons [555, 556].

1.6.7.5 Bone marrow transplant for HIV cure

The only two cases of cure PWH have been the "Berlin patient" [407] and "London patient" [387], both of which were treated with allogeneic bone marrow stem-cell transplantation with donors homozygous for the *CCR5 Δ32* allele. This resulted in reconstructed immune systems that lacked functional CCR5 coreceptors and thereby conferred resistance to HIV. As much as these two cases bring hope to the world of HIV, they are unfortunately alone. The "Boston patients" tried to recapitulate the results without the *CCR5 Δ32* allele and resulted in viral rebound [408]. Additional follow-up attempts have also not been successful [557], especially with the emergence of non-CCR5 tropic virus negating the use of the *CCR5 Δ32* [558] and rebound regardless of reservoir quantification [559]. The overall safety of hematopoietic stem cell transplantation is also a heavy burden that restricts this strategy [557].

1.6.7.6 Broadly neutralizing antibodies for the HIV cure

The use of broadly neutralizing (bn) antibodies (bnAbs) stem from the study of monoclonal antibodies (mAbs), the first of which being b12, which was isolated from a PWH in the 1990's [560]. bnAbs allow for virus elimination through multiple mechanisms: (i) binding blocks the virus from interacting with host cell receptors and can prevent endocytosis, fusion, or penetration [561]; (ii) aggregation of virions due to antibody binding [561]; (iii) recognition by intracellular TRIM21 and targets to proteosome [562]. Antibodies can also target infected cells for antibody-dependent cellular cytotoxicity, although this is considered a function of non-neutralizing antibodies [563]. About a decade ago, the first bnAbs were isolated from a PWH that displayed potent neutralization specific for the CD4 binding site (CD4bs) of gp120. The primary bnAb studied from this individual, VRC01, neutralized 91% of 190 viral strains representing all major circulating HIV-1 clades; the other two bnAbs from the same individual were not as potent. In comparison, b12 was only able to neutralize 41% of isolates [564]. Other bnAbs have since been identified, with other affinities, e.g. the V3 loop and its glycans, the MPER, and the V1-V2 loop of gp120, and are reviewed in [565]. NHP studies demonstrated efficient protection by various bnAbs against SHIV challenges [566-570]. Phase I clinical trials have reported the safety of bnAbs in humans [571-573] and

follow-up trials have now demonstrated that bnAbs are able to suppress viremia. Additionally, administration of bnAbs 3NBC117 and 10-1074 to PWH during ATI resulted in increased Gag-specific $CD8^+$ and $CD4^+$ T cell responses, as well as lengthened viral suppression [574]. However, there are caveats to the results: (i) suppression is short lived [575-577]; (ii) patients developed anti-bnAb responses [575, 576], although they were left susceptible to bnAbs targeting different epitopes; (iii) lackluster prevention of virus via cell-to-cell transmission [578-580]. Thus, groups are working to develop bnAb cocktails that will cover multiple epitopes for neutralization to potentially enhance efficacy [581, 582], including the development of bispecific [583] and trispecific [503] antibodies. bnAbs have been tested in RMs to either cure or induce functional cure. SHIV-infected RMs were treated with bnAbs 3BNC117 and 10-1074 3 days postinfection. In both groups, viremia was controlled while bnAbs were detectable and rebounded after clearance. Postrebound viral control occurred in half of the RMs [584]. However, treatment at 3 dpi lacks clinical relevancy. Thus, repeated experiments were conducted at 14 dpi and ART-treated RMs were included. Postrebound control was partial, and only one animal controlled below the limit of detection. ART did not result in more postrebound controllers [585]. In both studies, $CD8^+$ T-cell depletion resulted in abrogated viral control [584, 585], supporting the role of $CD8^+$ T cells in viral control. BnAbs have also been combined with other cure agents. bnAb PGT121 was combined with TLR7 agonist GS-9620 and administered to $SHIV_{SF162P3}$-infected RMs on ART (initiated 7 dpi). This resulted in delayed viral rebound, with 45% not rebounding and neither adoptive transfer nor $CD8^+$ T-cell depletion demonstrated replication competent virus in those RMs [586]. A follow-up study started ART at 14 dpi to increase clinical relevancy [587], and received a different TLR7 agonist, GS-986, with both bnAbs PGT121 and N6-LS. However, treatments did not result in the same viral control, while still being associated with a delay in viral rebound [587]. Another recent study utilized different combinations of IL-15 superagonist, N-803, with bnAbs 10-1074 and 3BNC117. The combination of N-803 and 10-1074 had an efficacy of postrebound control of 60%, while N-803 + 10-1074 and 3BNC117 had a postrebound efficacy of 75% [588].

1.6.7.7 HIV vaccines for HIV prevention or therapeutics

An HIV vaccine is still not in our grasp. Of the main roadblocks against the development of an effective HIV vaccine one is that no individual has been known to have established an HIV infection and spontaneously completely cleared the infection. A small fraction of PWH spontaneously control the plasma viremia to below the limits of detection are known as elite controllers, but the mechanisms of their viral control have yet to be elucidated and replicated in viremic individuals [589]. Furthermore, the elite controllers are not eradicating the virus, thus being only useful as models of a functional cure. To date, HIV vaccine clinical trials were not successful: the STEP trial had to be discontinued after the first interim review found non-efficacy and, in fact, increased the risk for HIV acquisition in those that were already Ad5 seropositive [590]. Another vaccine strategy based on the use of the canarypox vector (ALVAC) surpassed the threshold necessary for 50% vaccine efficacy in phase 1-2 trials [591] and continual analysis after a 12-month booster showed increased IgG binding antibody response rates and $CD4^+$ T-cell response rates [592]. Unfortunately, after the advancement to a phase 2b/3 trial, HVTN 702, the interim analysis determined that there was no significant difference between infection rates of those vaccinated and thus determined inefficacious [593]. A third vaccine strategy is the use of mosaic vaccines which are focusing on eliciting a $CD8^+$ T-cell-mediated control [594, 595]. These vaccines use mosaic proteins, polyvalent antigens formed from peptides of natural sequences determined by computer modeling for the optimal coverage of epitopes [596]. A phase I/IIa clinical trial found that the mosaic Ad26 prime with Ad26+gp140 boost vaccine regimen was highly immunogenic, eliciting strong binding antibody responses, antibody-dependent cellular phagocytosis responses, and T-cell responses. Further, in RMs they found it produced 66% protection from six SHIV-SF162P3 challenges [595]. This vaccine regimen is now being tested in two clinical trials, HVTN 705 (HPX2008; Imbokodo) and HVTN 706 (HPX3002; Mosaico). However, the Imbokodo study only provided a 25.2% efficacy estimate against HIV infection and was discontinued after phase 2b [597]. Another vaccine using a recombinant modified vaccinia Ankara-based (MVA-B) vaccine with gp120 and a fused Gag-Pol-Nef polyprotein was found to be well tolerated and increased T cell responses against Gag, but did not change the latent reservoir or time to rebound after ATI [598].

Another vaccine strategy which is based on the use of the RhCMV vector, was reported to induce functional cure in half of the vaccinated monkeys when administered prophylactically; cell-associated DNA was detectable without disease progression [28, 599, 600]. However, given as a therapeutic, the RhCMV/SIV vaccine did not result in control of infection [24]. To try to improve upon their RhCMV vaccine, Hansen *et al* [27] deleted the Rh110 gene to suppress lytic capabilities. This ΔRh110 RhCMV/SIV vaccine enabled viral control and progressive clearance in 59% of vaccinated RMs. Further, 75% of the RMs which cleared viremia were able to control a second challenge 3 years later. An adapted human CMV (HCMV) vaccine was tested in uninfected persons to try to mimic the same unconventional MHC II $CD8^+$ T cell responses seen with the RhCMV vector but were unsuccessful [601]. Peptides-based strategies are also used for HIV vaccines [602, 603]. Early peptide vaccines were moderately immunogenic in humans [604, 605] and lacked protection in most recipients [606]. Currently, the VAC-3S vaccine utilizes a gp41 motif (3S) with the CRM197 carrier protein to induce responses against HIV and increased CD4 restoration and reduced PD-1 expression, suggesting an improvement of T-cell exhaustion [607]. The Vacc-4x is another peptide-based vaccine that uses $p24^{gag}$ domains. Vacc-4x did not result in protection, but viral set point was reduced after ATI [608]. Vaccinations several years later, in the same participants, resulted in decreased viral DNA and maintained a reduced viral set point at ATI, but protection remained elusive [609]. However, not all peptides are used for vaccines and are reviewed in [610]. Enfuvirtide is a synthetic peptide that binds gp41 and blocks fusion with the host membrane and is a current HIV therapeutic [611] and Maraviroc blocks CCR5 binding [612]. More recently, a short HIV fusion inhibitory peptide with a longer half-life was developed, IBP-CP24, to overcome the half-life and resistance issues of Enfuvirtide. IBP-CP24 shows promising results with a half-life 14-fold greater than enfuvirtide while reducing plasma viremia in HIV-infected humanized mice [613]. At the extreme end of vaccination are two vaccination strategies: (i) an engineered herpesvirus that expresses all nine SIV gene products [614]; (ii) vaccine regimen with DNA, modified vaccinia Ankara, VSV, Ad5, RM rhadinovirus, and DNA a second time, to achieve vaccination containing the entirety of the SIV Env [615]. From the herpesvirus vaccine, 4/6 animals were protected through six intravenous challenges within four months, supporting future investigation

[614]. Unfortunately, the sequential proteome-based vaccine method was unable to elicit protective immunity against SIVmac239, demonstrating the difficulty of SIV/HIV vaccines [615].

1.6.7.8 Targeting Tregs as a strategy for cure research

The suppressive function of Tregs during HIV infection has opened the forum to assess the benefit of manipulating Tregs for PWH. Tregs can be latently infected with HIV and represent a potentially important HIV reservoir: (a) they expand in blood and tissues during chronic HIV and SIV infections [616]; (b) The Treg fraction containing HIV/SIV DNA is higher than in non-Tregs in PWH on ART [617] and RMs [618]; (c) Tregs are less susceptible to cell death than conventional T cells [616]. Meanwhile, during acute infection, Tregs may decisively contribute to the rapid seeding of the HIV reservoir by reversing $CD4^+$ T cell immune activation. Finally, during chronic HIV/SIV infection, multiple lines of evidence support a Treg involvement in suppressing protective effector immune responses against HIV: (a) Treg expansion correlates with loss of CTL function [619-621]; (b) ex vivo Treg depletion from blood and LNs enhances T-cell responses to HIV/SIV antigens [616]; (c) HIV nonprogressors have a high perforin/FoxP3 ratio; (d) $HLAB27^+$and $B57^+$ HIV-specific $CD8^+$ T cells from controllers evade Tregs [622, 623]. Treg suppression of virus-specific immune responses may impact the efficacy of the "shock and kill" strategies, which require effective killing of the reactivated virus. Treg targeting was therefore considered to represent an excellent cure strategy, in which, through a single intervention, one could directly reduce the reservoir size, reactivate the virus, and boost cell-mediated immune responses in RMs on ART.

However, this is not without its issues, as Tregs are also beneficial in some ways, particularly in suppressing general immune activation. The major problem with targeting Tregs is that the most typical marker for Tregs, FoxP3, is intracellular and, as such, it cannot be directly targeted *in vivo*. Multiple other targets have however been considered for *in vivo* Treg depletion strategies, such as: targeting CD25 or CCR4, and low dose cyclophosphamide.

1.6.7.8.1 Targeting CD25 for Treg depletion.

Denileukin difitox (ONTAK), IL-2-diphtheria toxin conjugate, has been used to deplete Tregs [624, 625]. IL-2 identifies and binds the $CD25^+$ cells, allowing the diphtheria toxin to enter the cell and cause cell death by ADP-ribosylating host eEF-2 and preventing protein synthesis [626]. In cancer patients Ontak showed some efficacy [627-631] . Ontak administration to SIVsab-infected RMs, a model of spontaneous complete control of HIV infection [632, 633], resulted in the depletion of 75-85% of the peripheral Tregs, an 8 to 10-fold increase in immune activation of the peripheral $CD4^+$ and $CD8^+$ T cells, a boost of SIV-specific T cells, and a relatively robust virus reactivation [634]. A follow-up study in SIVsab-infected RMs with a new anti-human, bivalent IL-2-DT [635, 636] demonstrated similar positive results of depletion of peripheral Tregs, including partial depletion in the lymph nodes (>50%) and intestines (25%), immune activation, viral rebound up-to 10^3 vRNA copies/mL, and bolstered SIV-specific $CD8^+$ T cell responses [505]. However, when IL-2-DT was given to functionally cured RMs on ART, there were severe adverse effects necessitating the suspension of treatment [505]. Further, the specificity of Treg depletion was substantially hindered, with $CD4^+$ and $CD8^+$ T cells being greatly depleted, and there was no viral reactivation despite the immune activation [505].

1.6.7.8.2 Targeting CCR4 for Treg depletion.

Tregs express a high level of CCR4 [637-639], which is the receptor for CC chemokines (MIP-1, RANTES, TARC, and MCP-1), and has been shown to be a coreceptor for HIV-1 [640]. A diphtheria-toxin based anti-human CCR4 immunotoxin was developed, which effectively binds to and cause protein synthesis inhibition in target cells. It depletes 40% of total $FoxP3^+$ $CD4^+$ T cells in the peripheral blood, but only 9-22% of total $FoxP3^+$ $CD4^+$ T cells in the LNs [641]. The anti-CCR4 monoclonal antibody, Mogamulizumab, also showed promise by depleting $CCR4^+$ malignant cells and $CCR4^+$ Tregs [642, 643]. Unfortunately, the use of anti-CCR4 immunotoxin in functionally-cured RMs did not result in viral reactivation, regardless of prominent immune activation and proficient Treg depletion [505].

1.6.7.8.3 Cyclophosphamide (Cy) for Treg depletion.

Cy is a well-established chemotherapeutic agent, which acts as a nonselective cytoreductive agent [644-647]. In low, metronomic dosages, Cy retains its antitumor capabilities, with reduced side effects and improved clinical responses [648] and selective and significant depletion and reduced functionality of Tregs [649-651]. Treg selectivity has been attributed to decreased DNA repair, as demonstrated by the increased and sustained DNA intercross-linking, as well as increased and sustained phosphorylated histone 2AX. A different mechanism for sensitivity, decreased production of glutathione, a detoxifier for Cy and its active metabolites, was also evoked. Indeed, Tregs have decreased ATP levels, which abrogate glutathione production, thereby inducing hypersensitivity to Cy [652]. Interestingly, $CCR2^{+}$ Tregs are preferentially depleted in mice over $CCR2^{neg}$ Tregs. An analysis of the cell cycles demonstrated increased proliferation and activation in $CCR2^{+}$ Tregs [653]. Patients treated with Cy experienced a ~20% Treg decrease sustained for 25 days and a decrease in proliferation marker Ki-67, further substantiating the loss of Treg homeostatic proliferation [654]. When the dose was increased, the selective depletion of Tregs was ablated, underpinning the importance of the low dose for specific Treg targeting [655].

To be an effective therapy for HIV, Cy must deplete Tregs from the LNs, where there is a major viral reservoir and studies have shown that Cy selectively depleted the $CD8^{+}$ lymphoid-resident DCs while sparing the skin-derived migratory DCs and pDCs in the LNs and spleen. This selective depletion in turn boosted antigen presentation and cytokine secretion by the mDCs and pDCs, with a reduction in Treg suppressive capabilities [656]. In an HIV-positive patient with SLE, treatment with Cy induced an enormous burst in viral replication, with plasma viral loads peaking to $>10^{7}$ copies/mL and quickly returned to below detectable levels [657]. Using escalating doses resulted in no significant difference in the HIV DNA burden of LNs and PBMCs *versus* the control group, but, of note, plasma viral loads were not suppressed in these patients, with two study participants out of five admitting to nonadherence to ART [658]. Thus, it is possible that the increase in plasma viral loads and lack of viral DNA clearance may have been due to nonadherence. As such, Tregs are a promising target for HIV cure strategies for improving T-

cell functionality. However, the current treatments are not specific enough and result in insufficient reactivation and clearance, indicating the need for combination therapies to make Treg depletion viable.

1.6.7.9 T-cell exhaustion and targeted therapies

Tackling the immune system dysregulation in PWH is an important goal of any cure approach. During HIV infection, T cells, especially $CD8^+$ T cells, gradually lose their effector functions, in a state known as T cell exhaustion, which was first described in chronic lymphocytic choriomeningitis virus-infected mice [659]. In fact, in HIV progressors, the basal phosphorylation levels of proteins downstream from T cell receptor signaling were increased and correlated with impaired signaling [267]. These cells are marked by expression of immune checkpoint molecules, such as cytotoxic T lymphocyte-associated molecule-4 (CTLA-4) [266], programmed cell death-1 (PD-1) [262-265], T-cell immunoreceptor with immunoglobulin and ITIM domains (TIGIT) [660], and lymphocyte activation gene-3 (LAG-3) [661], as well as glycoprotein T-cell immunoglobulin and mucin domain-containing molecule 3 (Tim-3) [662, 663]. PD-1 and LAG-3 expression levels are even correlated with time to virus rebound after ART cessation [664].

1.6.7.9.1 CTLA-4 Blockade in HIV Cure

$CTLA\text{-}4^+PD\text{-}1^{neg}\,CD4^+$ T cells from multiple tissues are enriched for replication-competent SIV in infected RMs under ART, suggesting a potential therapeutic target for reservoir elimination [266]. During HIV infection, CTLA-4 plays a role in suppression of HIV-specific T cells, with CTLA-4 blockade enhancing $CD4^+$ T cell functionality, i.e., IFN-γ production and cell proliferation [665, 666]. In PWH treated with Ipilimumab (α-CTLA-4 mAb) for melanoma, plasma VLs remained below the limit of detection using standard qPCR methods, whereas a general decline in plasma VLs was seen when using the single copy assay, with an opposing increase in cell-associated unspliced RNA post-treatment, likely due to expansion of infected T cells [506]. Additionally, in animals treated in chronic infection with CTLA-4 blockade, decreases in viral RNA was noted, along with an increase in the SIV-specific immune response

[507]. However, when used in early infection with the pathogenic SIVmac251-infected RM model, CTLA-4 blockade increased immune activation and viral replication, but did not augment responses to vaccination, nor increase SIV-specific responses, a key to reservoir clearance, and abrogated responsiveness to ART [667]. This is contrary to the results previously published during chronic infection [507]. Thus, further studies need to be conducted to determine whether stand-alone CTLA-4 blockade can be used as a latency reversing strategy or as a boost to the HIV-specific immune responses.

1.6.7.9.2 PD-1 Blockade in HIV Cure

PD-1 expressing $CD4^+$ T cells during HIV infection are also enriched for inducible virus and blockade with nivolumab (anti-PD-1) to a patient resulted in increased cell-associated unspliced RNA, yet not plasma viremia, consistent with slight latency reversal [265]. A PWH with advanced nonsmall cell lung cancer was given nivolumab and monitored. The patient had insignificant changes in the plasma viral loads, with an increase in cell-associated DNA which normalized one month later. Overall immune activation markers remained stable, although there were increases in IFN-γ^+ $CD8^+$ cells and cell counts [668]. More promising data emerged from another nivolumab-treated lung cancer PWH. In this individual, plasma viremia demonstrated latency reactivation beginning at D14, while HIV DNA was decreased, and concomitant immune activation increased along with HIV reverse transcriptase and Nef-specific $CD8^+$ T cells as well, thus pointing towards a shock and kill mechanism [669]. Unfortunately, the effects of PD-1 blockade are simply inconsistent between patients, as another study demonstrated divergent data from the others, with no consistency between changes in cell associated DNA, RNA, or plasma viremia, as well as the HIV-specific immune responses [670]. However, *ex vivo* treatment of pembrolizumab (monoclonal anti-PD-1 antibody) with the latency reversing agent bryostatin was able to drastically, and significantly increase the amount of virus induction [671]. The ectonucleotidase CD39, which converts ATP to AMP (subsequently converted to the immunosuppressive adenosine by CD73) [672], is used to identify terminally exhausted $CD8^+$ T cells, which are often coexpressing PD-1 [673]. In $CD39^+$ $CD8^+$ T cells, the adenosine receptor, A2aR is expressed at higher levels in PWH, especially in the treatment naïve. Further,

i*n vitro* combination inhibition of PD-1 and A2aR was synergistically more effective than either inhibition standalone in rescuing $CD8^+$ T cell function [674]. Thus, CTLA-4 and PD-1 blockades are likely to be most helpful when used in combination with other therapies and/or more potent LRAs.

1.6.7.9.3 IL-15 for HIV cure

IL-15 is associated with the generation and survival of $CD8^+$ T cells [675, 676], including HIV-specific $CD8^+$ T cells and is investigated as an ART alternative or enhancement [677]. IL-15 enhances NK cell activation and function [678]. In RMs, IL-15 induced proliferation of SIV-specific $CD8^+$ T cells but did not increase functionality [679, 680]. The combination treatment of IL-15 after latency reversal with vorinostat resulted in increased clearance of infected cells [678]. However, free IL-15 administration can be very toxic [681], leading to the development of safer and more effective IL-15 superagonists. The heterodimeric IL-15/IL-15Rα increased $CD8^+$ T cells and NK cells activity and decreased viral RNA in the plasma and LN [682]. Different IL-15 modifications have been made, but only N-803 [683] (previously ALT-803), has been tested beyond *in vitro* due to having the greatest efficacy thus far. N-803 has shown reactivation potential *in vitro* and primed $CD4^+$ T cells for recognition by immune effectors [684]. N-803 has shown improved NK cell activation and functionality *in vitro* and in HIV-infected humanized mice and protected against HIV challenge when given up-to 3 days after challenge [381]. In ART-naive, SIV-infected RMs, N-803 transiently decreased VLs by 1-2 logs [685] while in two studies, latency reversal occurred in ART-treated RMs, but only with CD8 depletion, which reactivates virus on its own [686, 687]. Indeed, in ART-treated SHIV-infected RMs, N-803 did not reactivate latent virus on its own and there was no change in viral DNA, even with immune activation [688]. Thus, N-803 would benefit from combinatorial treatments with a latency reversing agent for reservoir clearance.

1.6.7.9.4 IL-21 in HIV cure

Similar to IL-15, IL-21 expression in SIV/HIV is associated with maintaining the NK, B, and T cell responses [689] and enhances effector functions when given *in vitro* and *ex vivo* without large increases

in general immune activation [690, 691]. Administered to SIV-infected RMs, IL-21 increased CD8 and NK cell activity and increased SIV-specific antibodies in the serum, without inducing $CD4^+$ T cell activation nor viral reactivation [692]. In SIV-infected RMs on ART, IL-21 improved intestinal $CD4^+$ T cell restoration, with reduced immune activation in both the gut and circulation. After ART cessation, immune activation and plasma VLs remained lower than control animals demonstrating a greatly positive effect of IL-21 treatment [693]. IL-21 in conjunction with IFNα in ART-treated, SIV-infected RMs drastically improved NK cell functionality and Env-specific activity. Further, the treatments resulted in reduced replication competent virus in LNs and increased time to rebound after analytical treatment interruption [694] supporting further investigation of IL-21 treatments.

1.6.7.10 "Shock and Kill" – Latency reactivation for HIV cure.

Over the last 10 years, the shock and kill approach was one of the most widely pursued avenues for an HIV cure, with multiple classes of agents being tested as potential LRAs: histone deacetylase inhibitors (HDACis) [695-697], protein kinase C (PKC) agonists [698, 699], bromodomain inhibitors (JQ1) [700], second mitochondrial activator of caspases (SMAC) mimetics [701], stimulator of interferon genes (STING) agonists [702], Toll-like receptor (TLR) agonists [703-708], and ingenol derivatives [709-712] alone or in combinations [713, 714].

1.6.7.10.1 HDAC Inhibitors for "Shock and Kill"

Theoretically, HDACi are strong candidates for latency reversal. Nucleosomes are a basic structural unit of DNA that contain chromosomal DNA wrapped around two of each core histone, H2A, H2B, H3, and H4, forming an octameric core. As the DNA wraps around the cores, it can be modified with acetylation, methylation, and phosphorylation, which changes the binding tightness through charge, thereby affecting the function [715]. In the case of acetylation, histone acetyl transferases (HATS) acetylate the positively charged lysine residues of the histone N termini. This epigenetic change decreases the electrostatic affinity

between the histone proteins and DNA and as a result, the DNA becomes more accessible to transcription factors [716-718].

Among genome modifications, deacetylation of the integrated HIV proviral structure around the long-terminal repeats has been shown to inhibit transcription of the provirus by tightening the DNA around the histone, thereby driving the provirus towards latency [425, 719-722]. Disruption of deacetylation has been shown to reactivate latent HIV-1 *in vitro* [695] and *in vivo* [697, 723-727], however, long lasting changes in the reservoir have yet to be achieved.

Of the HDACi, Romidepsin (RMD), a bicyclic class I HDACi (targets HDACs 1, 2, 3, and 8) [728-730], produces the most potent HIV reactivation *ex vivo* [368]. RMD (1S,4S,7Z,10S,16E,21R)-7-ethylidene-4,21-bis (1-methyletheyl)-2-oxa-12,13-dithia-5,8,20,23-tetraazabicyclo[8.7.6] tricos-16-ene-3,6,9,19,22-pentone) is a cyclic depsipeptide naturally made by *Chromobacterium violaceum* [731-733] and is FDA approved for treatment of cutaneous T cell lymphomas [730]. RMD initially garnered attention when it was demonstrated to revert Ha-ras-transformed NIH 3T3 cells [728, 734]. Unlike most therapeutics, RMD is a prodrug, with a disulfide bond that is reduced intracellularly to form the active form [729]. This generates a thiol moiety which is then able to bind the zinc ion (Zn^{2+}, a necessary ion for the catalytic reaction of HDACs [735]) in the binding pocket of HDACs, thereby inhibiting HDAC function [733]. Beyond the inhibition of HDACs, the mechanism of action for RMD is not completely elucidated. In fact, multiple pathways are affected in leukemia and lymphoma cell lines and cells, respectively [736]. Thus, RMD promotes apoptosis through upregulation of cell cycle arrest proteins, activation of the unfolded protein response, and DNA hypomethylation [736]. In the leukemia cell line HL-60, RMD induced apoptosis through generation of reactive oxygen species (H_2O_2 and O_2^-) from the redox cycle of RMD and is dependent on glutathione [737]. In lung cancer cell line A549, RMD induces cell cycle arrest at the G2-M transition with increased expression of p21 and hypophosphorylated retinoblastoma proteins (pRb) and induced apoptosis, which was confirmed by caspase-3 activity [738]. RMD also downregulates expression of BCL-2 and BCL-XL and activated both caspase-3 and caspase-9 in the small cell lung cancer cell lines. The activation of caspase-3, caspase-9 and lack of caspase-8, indicates that RMD acts through the

mitochondrial apoptosis pathway [739], contradicting that seen in chronic lymphocytic leukemia which had apoptosis mediated by caspase-8 [740]. Further, in lung, prostate, and colorectal cancer cell lines, RMD was found to inhibit the phosphatidylinositol 3-kinase (PI3K)/protein kinase B (Akt) pathway to induce apoptosis [741, 742].

In the treatment of cutaneous T-cell lymphoma (CTCL), RMD has a maximum tolerated dose of 14 or 17.8 mg/m^2 depending on the dosing schedule of days 1, 8, and 15 on a 28-day cycle or days 1 and 5 on a 21-day cycle, respectively, with repeated rounds recommended [743, 744]. Unfortunately, side effects are not uncommon and the more common ones were grade 1-2 gastrointestinal symptoms and fatigue [727] when administered to PWH at the dose of 5 mg/m^2 to disrupt latency [368, 745, 746] while maintaining tolerability.

Romidepsin can reactivate HIV from CD4$^+$ T cells *in vitro*, and, when compared to other HDAC inhibitors, it exuded the strongest reactivation potency [368] even at plasma concentrations that are lower than what is used for chemotherapy. These data were reproducible in cells from ART treated PWH *ex vivo* [368]. In RMS, *in vivo* administration of RMD resulted in a massive increases in T-cell activation and viral rebound in post-treatment controllers [519]. RMD administration to PWH and RMs on ART also demonstrated T-cell activation and viral reactivation [727, 747]. Yet, neither of these studies were able to demonstrate a statistically significant decrease in the SIV/HIV reservoir. *Ex vivo*, RMD (as well as Panobinostat and SAHA) was shown to have a negative effect on the HIV-specific immune response, i.e., suppression of cytokine production and decreased cellular viability [518], as well as reduced proliferation and viability and also restriction of *de novo* infections after stimulation with IL-2 and PHA [748]. Unlike the Jones *et al*. [518], Jønsson *et al*. showed that RMD treatment differentially changed expression patterns of interferon-stimulated genes, such as increases in IFIT1, ISG15, and STAT1, but decreases in APOBEC3G, MX2, and TRIM22 [748]. In RMs, the SIV-specific immune response was not significantly altered [519], nor were the HIV-specific immune responses altered in PWH *in vivo* [727]. In the BCN02 clinical trial (NCT02616874), PWH received MVA.HIVconsv vaccination and weekly infusions of RMD,

and, while RMD administration reduced the total number of vaccine-elicited T cells secreting multiple cytokines, the $CD8^+$ T cells retained their HIV suppressive functionality [746].

1.6.7.10.2 Protein kinase C (PKC) agonists for "shock and kill"

PKC agonists work through the canonical NF-κB pathway to enable HIV reactivation [749, 750]. Many of the agents: phorbol esters (prostratin) [751]; bryostatin-1 [752] and its analogs [753, 754]; have demonstrated HIV reactivation potential *in vitro* and *ex vivo* [755], but the common problem when moving to *in vivo* models was generalized immune activation and its resulting toxicity/tolerability due to higher doses required for *in vivo* reactivation [516, 756]. To combat this issue, combinatorial LRA treatments, such as bryostatin-1 or prostratin with an HDAC inhibitor (e.g., Romidepsin, SAHA, and largazole) or bromodomain inhibitor JQ1, allow for lower LRA doses with similar or increased potency and decreased toxicity *ex vivo* [757, 758]. Similarly, prodrugs for prostratin, ingenol, and bryostatin-1 were developed to improve tolerability and reduce bolus toxicity, and maintained immune activation and HIV reactivation *in vitro* and *ex vivo* [759]. However, these combinations and prodrugs have yet to be tested *in vivo* and further testing is warranted.

1.6.7.10.3 Ingenol derivatives for "shock and kill"

Ingenol 3-angelate is an inflammatory substance extracted from the sap of the *Euphorbia peplus* plant [760]. Ingenol 3-angelate and its derivatives are structurally analogous to phorbol esters and mechanistically act through the PKC and NF-κB pathway [761, 762]. By activating the NF-κB pathway, ingenol derivatives reactivate latent HIV *in vitro* and *ex vivo* [710, 711, 762, 763]. Initially, ingenol derivatives were investigated for HIV inhibition and CD4 downregulation through PKC activation and data from the same study showed some derivatives reactivated HIV [764]. With data demonstrating that PKC agonists have anti-latency properties, renewed focus was placed upon new ingenol derivatives that can promote HIV reactivation, while reducing the toxicity associated with early ingenol derivatives, PMA, and prostratin [763, 765]. The derivative ingenol-B reactivated HIV *in vitro* [766], but in ART-treated, SIV-

infected RMs, ingenol-B did not reactivate virus in the circulation, but did have a viral blip in the cerebrospinal fluid (CSF). In combination with the HDACi vorinostat, reactivation was achieved in circulation and CSF [240]. In PWH treated with ingenol mebutate gel on the skin, HIV was reactivated locally in skin biopsies without plasma viremia, nor systemic immune activation [767]. The intravenous version of ingenol mebutate, PEP005, was found to have a synergistic reactivation when combined with JQ1, while also downregulating surface receptors CD4, CCR5, and CXCR4 *ex vivo* [710]. Thus, further research is warranted.

1.6.7.10.4 Bromodomain inhibitors for "shock and kill"

JQ1, a small molecule bromodomain inhibitor developed in 2010, was shown to bind to BRD4 [768]. BRD4 competes with Tat for P-TEFb binding, restricting HIV replication [769]. JQ1 treatment of HIV-infected $CD4^+$ T cells modestly reactivated virus, while suppressing T cell proliferation and downregulating CD3, CD28, and CXCR4 *in vitro* and *ex vivo* with minimal toxicity [700]. The combination of JQ1 with prostratin produced synergistic increases in reactivation *in vitro* [449]. Due to the modest reactivation potential of JQ1, new bromodomain inhibitors have been tested, with OTX015 [770], UMB-136 [771], apabetalone [772], and CPI-203 [773] showing greater reactivation potential, while also maintaining minimal toxicity and the synergistic activity with PKC agonists (e.g. prostratin and bryostatin-1) *in vitro*. Additionally, 8-methoxy-6-methylquinolin-4-ol (MMQO) [774], a quinolone based bromodomain inhibitor, reactivates HIV *ex vivo* and maintains immunosuppression similar to JQ1, without acting through the Tat transactivator [775]. Thus, these different bromodomain inhibitors are promising LRAs, but require *in vivo* studies to further elucidate their potential.

1.6.7.10.5 Second mitochondrial activator of caspases (SMAC) mimetics for "shock and kill"

SMAC mimetics are of high interest as LRAs because: (i) BIRC2 acts as a repressor of the NF-κB pathway and is antagonized by SMAC mimetics [776, 777]; (ii) less generalized immune activation through the noncanonical NF-κB pathway *versus* canonical pathway [778]; (iii) reactivates HIV *in vitro* and

synergizes with HDACis [779]. The SMAC mimetics AZD5582 [701] and birinapant [780] have both shown reactivation potential *in vitro* and *ex vivo*. AZD5582 was also shown to induce viral reactivation in BLT humanized mice and RMs with minimal systemic immune activation, no reduction in CD8 immune responses, and low toxicity [781]. AZD5582 also has greater reactivation potency when combined with CD8 depleting antibody M-T807R1 [782]. The SMAC mimetic Ciapavir demonstrated similar functionality in humanized mice and synergized with bromodomain inhibitors JQ1 and I-BET151, but when used with bryostatin-1 or ingenol-3-angelate induced greater toxicity [783]. SMAC mimetics are also showing efficacy against infected macrophages, but this is discussed later. Overall, SMAC mimetics warrant additional exploration *in vivo*.

1.6.7.10.6 Stimulator of interferon genes (STING) agonists for "shock and kill"

STING agonists were of initial interest as boosters for the innate immune response and antigen-specific immune responses [784]. Indeed, one STING agonist, 3'3'-cGAMP primed HIV-1-specific $CD8^+$ T cells [785] and cGAMP delivered with nanoparticle PC7A induced protection against HIV through type I IFN and inhibited HIV-1 replication [786]. However, cyclic GMP-AMP (cGAMP) and c-di-AMP are also capable of latency reactivation *ex vivo* while also increasing the frequency of SIV-specific $CD8^+$ T cells [702]. In an *ex vivo* combinatorial study, the STING agonist cGAMP and HDACi, resminostat, had additive, but not synergistic reactivation potential [787]. In a pilot study of ART-treated, infected RMs, the STING agonist reactivated SIV in a third of RMs [788]. Thus, STING agonists are promising LRAs, but will be much more effective in combinatorial regimens.

1.6.7.10.7 Toll-like receptor (TLR) agonists for "shock and kill"

TLR agonists are similar to STING agonists in that they were initially looked at for HIV inhibition [789], yet are now investigated as both LRAs and immunomodulatory agents. Because TLRs are pattern recognition receptors they react to signals indicating the necessity for an immune response [790]. TLR2 and TLR9 agonists reactivated HIV from transgenic mouse spleen cells *ex vivo* [791]. Although that was

the first major study to demonstrate and explain the reactivation, a previous clinical trial for the antisense oligodeoxynucleotide phosphorothioate GEM91 [792] had noted increased HIV-1 [793], contradictory to the *ex vivo* data with GEM91 [789], and it is hypothesized that this was through TLR9 activation [793]. Further investigation into a TLR9 agonist, CPG7909, as a pneumococcal vaccine adjuvant in PWH showed increased immunogenicity, a boost in HIV-specific $CD8^+$ T cells and a reduction in caDNA, but also increased adverse effects [794]. MGN1703 was thus developed to decrease the toxicity of existing TLR9 agonists [795] and was tested *ex vivo* [796] and then in PWH with 4 weeks [797], followed up with a second study of 24 weeks of treatment [798]. Although MG1703 resulted in increased innate immune responses and HIV reactivation, overall viral burden was not significantly reduced, nor was a there difference in time to rebound [798]. TLR7 agonist GS-9620 reactivated HIV *ex vivo* and enhanced HIV-specific $CD8^+$ T cells [707]. These results were seconded in SIV-infected RMs, with reduced caDNA and inducible virus after TLR7 agonist GS-986 treatment [29]. However, GS-9620 was unable to reproduce any of the virological effects of GS-986 in RMs [799] nor PWH [800]. Combinatorial TLR2 (Pam2CSK4) and TLR7 (GS-9620) agonists were tested *ex vivo* and enhanced reactivation potency by acting through separate mechanisms, thus suggesting this strategy should be tested further *in vivo* to improve outcomes *versus* single TLR agonist administration [708].

1.6.8 Role of Immunometabolism in HIV Pathogenesis and Cure

1.6.8.1 Immunometabolism and HIV Pathogenesis

Immunometabolism refers to the interface between the previously distinct fields of metabolism and immunology. With time, researchers have clearly shown that these are in fact linked, with specific metabolites being required for a proper function of macrophages, neutrophils and T cells, such as glucose, glutamine, fatty acids, and amino acids [801]. As for the pathways involved, there are six utilized in immune cells: glycolysis (the main pathway metabolic pathway for T cell effector functions [802]), tricarboxylic acid (TCA) cycle, pentose phosphate pathway (PPP), fatty acid oxidation (FAO), fatty acid synthesis (FAS),

and amino acid metabolism. Additionally, the mammalian target of rapamycin (mTOR) is an important regulator in the adaptive immunity, especially for the $CD8^+$ T cell response [803]. However, immunometabolism differs between acute, chronic, and latent viral infections. During acute infection, when the $CD8^+$ T cells are developing they upregulate mTORC1 and aerobic glycolysis to support their energy demands. However, during this time, HIV-specific T cells are beginning their metabolic dysregulation with extensive proliferation and activation, promoting an altered mitochondria that is burnt out to sustain the hyperproliferative state [804]. With chronic infection, T cell exhaustion and T cell metabolism become highly correlated, such as PD-1 ligation which results in diminished glucose and amino acid metabolism and mTOR activity [805-807]. Differently from PD-1, CTLA-4 modulates glycolysis and amino acid metabolism, but does not enhance FAO as seen with PD-1 ligation [805], a mechanism which is thought to promote survival during PD-1 ligation when the other metabolites are not being utilized. During chronic viral infections $CD8^+$ T cells were profiled with glycolysis dependency, dysfunctional mitochondria, and abrogated oxidative phosphorylation (OXPHOS), which is involved in the TCA cycle [808]. Interestingly, the same study demonstrated that CMV-specific T cells were more functional and able to utilize OXPHOS, but the glycolysis pathway was inhibited. This points towards differences in the metabolism of not only chronic *versus* latent infections, but also of functional CD8 responses [808]. In HIV controllers, $CD8^+$ T cells were found to be metabolically separate from progressor $CD8^+$ T cells. HIV controller $CD8^+$ T cells were characterized by the upregulation of survival genes pathways and metabolic plasticity, (with functional mitochondria and OXPHOS) and is supported by the mTORC2 pathway [809].

1.6.8.2 Modulation of Immunometabolic Programming for HIV Cure/Therapeutics

With the complex relationship between HIV/SIV pathogenesis, immunometabolism, and T-cell exhaustion, there is growing interest in targeted metabolic therapies. Another effect of metabolism is the susceptibility to HIV. The accepted paradigm is that CD4 susceptibility to HIV increases with differentiation, but what was recently described is the propensity for HIV to selectively infect $CD4^+$ T cells that are utilizing high levels of OXPHOS and glycolysis. Partial *in vitro i*nhibition of glycolysis with 2-

deoxy glucose (2-DG) demonstrated that the glycolytic environment is required to complete reverse transcription and had a greater effect in further differentiated cells. Further, limiting glycolysis with 2-DG also showed a selective toxicity towards infected cells and 2-DG was also able to greatly reduce HIV replication after phytohemagglutinin (PHA) stimulation [810], thereby showcasing an additional metabolic regulation of HIV that can potentially be exploited. Regarding dysfunctional mitochondria, IL-12 administration was able to reverse the dependence on glycolysis and restore mitochondrial changes and metabolic pathways [808]. IL-15 is also known to promote FAO and mitochondrial biogenesis [811]. *Ex vivo*, $CD8^+$ T cells from noncontrollers were shown to be enhanced after IL-15 treatment, with increased fatty acid uptake and enhanced mitochondrial respiratory capacity. Further, IL-15 pretreatment enhanced the SIV-specific $CD8^+$ T-cell response of SIV-infected macaques and restored metabolic plasticity [809]. These two studies thus point towards potential therapeutics for HIV *via* metabolic restoration.

1.6.9 Macrophages and the HIV/SIV Reservoir

1.6.9.1 Macrophages Contribution to the HIV/SIV reservoir.

In addition to the $CD4^+$ T cells, macrophages also harbor provirus and are capable of producing replication competent virus. In macaques infected with $SHIV_{DH12R}$ (highly pathogenic SHIV containing envelope glycoproteins from HIV-1 strain DH12 [812]), following the characteristic extensive depletion of the $CD4^+$ T cells, the remaining virus-producing cells were 95% macrophages with less than 2% expressing the CD4 receptor [813]. Although studies have not been able to concretely agree on the presence of replication competent virus in peripheral blood monocytes, the presence of HIV in tissue macrophages is undeniable [374, 814-817]. HIV studies utilizing humanized myeloid-only-mice (MoM) demonstrated the ability of macrophages to maintain infection without CD4 cells [480]. Further, ART administration to infected MoM after infection resulted in two-thirds of the MoM from developing persistent infection with one third of the treated mice developing persistent infection that allowed for viral rebound after ART cessation, thus demonstrating the ability of HIV to persist in macrophages and reconstitute infection after

ART [818]. Unfortunately, HIV infection of macrophages does not lead to viral cytolysis or apoptosis, with macrophages resistant to Vpr-mediated apoptosis [819].

HIV-infected macrophages are particularly present in the brain and central nervous system (CNS) [815]. During acute infection, infiltration of CD4 cells and monocytes from the blood to the brain allows for infection of the microglia and perivascular macrophages, causing neurological disorders, such as asymptomatic neurocognitive impairment, mild neurocognitive disorder, and HIV-associated dementia [820]. Fortunately, ART reduces neurological disorders. In brains of ART-treated and untreated PLWH with HIV-associated neurocognitive disorders, genome-wide microarray analysis found that ART reduced the dysregulation of the brain transcriptome relative to untreated individuals, but regardless of ART, there was still a portion of adaptive and innate immune response genes that were upregulated in both treated and untreated.

1.6.9.2 Crosstalk Between Macrophages and Exhausted T Cells

The exhaustion of T lymphocytes during HIV infection may provide further detriment to the host than lack of reservoir clearance. During infection, killing of HIV-infected $CD4^+$ T lymphocytes by CTLs is a major mechanism of viral suppression. However, the elimination of macrophages is a harder task to accomplish. In SIV-infected macaques, $CD8^+$ T cells *ex vivo* were unable to eliminate infected macrophages to the same extent as they could $CD4^+$ T cells [821]. Although they are not the primary reservoir for HIV/SIV, the interaction between CTLs and infected macrophages yields a new dilemma: the extended formation of the synapse induces further secretion of IFN-γ and other pro-inflammatory cytokines [822], thereby potentially increasing the chronic inflammation during HIV infection. Similarities to this are seen in dendritic cell:T cell interactions [823], and the priming of naïve $CD8^+$ T cells is demonstrated to alleviate the lack of killing [824, 825].

1.6.9.3 Targeting Macrophages with "shock and kill"

Although most of the "shock and kill" therapeutics are aimed at $CD4^+$ T cells, recent research shows that SMAC mimetics LCL-161, AT-406 (also known as Debio-1143), and birinapant, can also play a role in the direct elimination of HIV-infected macrophages. With an upregulation of BIRC2 and XIAP in HIV_{BA-L}-infected macrophages, similar to HIV-infected $CD4^+$ T cells, the infected macrophages are 10-100x more susceptible to cell death via SMAC mimetic than uninfected macrophages [826]. Of the three mimetics tested, only AT-406 resulted in viral reactivation in the macrophages [826], supporting previous findings that AT-406 induces viral reactivation in resting $CD4^+$ T cells from PLWH and humanized mouse models with ART [827]. Thus, SMAC mimetics are looking to be a promising new LRAs.

2.0 Hypothesis and Specific Aims

The advent of ART is one of the most prominent accomplishments of modern medicine, yet life expectancy is not fully restored in PWH. Further, ART (i) requires life-long adherence; (ii) is associated with short- and long-term toxicity, (iii) does not completely restore immune integrity, and (iv) is not curative. Additionally, replication-competent virus persists indefinitely in latent reservoirs which are invisible to HIV-specific immune responses and cessation of ART results in recrudescent infection within 2 to 8 weeks. Of the multiple eradication strategies, only stem-cell transplantation has resulted in documented cure with the "Berlin patient" and "London patient," but this is not scalable and has unreasonable morbidity. Regardless, there is hope in other strategies. The "shock and kill" cure strategy relies on reservoir reactivation with latency reactivation agents (i.e., romidepsin [RMD]), with subsequent elimination of infected cells through the cell-mediated immune response and viral cytopathic effects. Regulatory T cell (Treg) depletion is a similar concept to "shock and kill," in that it relies upon depleting a suppressive cellular population (Tregs), resulting in immune activation and viral reactivation. Further, the lack of suppressive signaling will allow for an enhanced cell-mediated immune response to antigen. The goal of this dissertation study was to characterize the potential uses of two strategies for the reduction of the viral reservoir and boosting SIV-specific immune responses, with a goal of advancing the field towards a cure/functional cure for HIV research: cyclophosphamide (Cy) and romidepsin (RMD). Cyclophosphamide is an alkylating agent that has been shown to selectively deplete regulatory T cells (Tregs) at low doses and to act as a cytoreduction agent at high doses (in stem-cell transplantation conditioning regimens). Due to the presence of HIV in numerous cell types and the success of the "Berlin" and "London" patients, we believed that cytoreduction with Cy would result in a reduction of the latent reservoir through direct clearance of infected cells with subsequent clearance by the cell-mediated immune response due to immune activation during immune restoration. RMD is an HDACi that has been previously shown to reactivate latent SIV, but there were also conflicting results on its impact on the SIV/HIV-specific immune responses. As such, we hypothesized that Cy and RMD can be used to reduce the size of the latent

reservoir in SIV-infected rhesus macaques and increase the SIV-specific cell-mediated immune response. To test this hypothesis, we proposed the following specific aims:

SA1. Determine the effects of Cy as a low dose Treg depleting agent or high dose cytoreduction agent on the latent reservoir in our rhesus macaque model of SIV functional cure and SIVmac239 model of pathogenic infection.

SA2. Characterize the pharmacokinetics and immunological effects of RMD in uninfected rhesus macaques

SA3. Assess the effects of repeated RMD infusions on viral reactivation, SIV-specific immune responses, and reservoir size in our rhesus macaque model of SIV functional cure.

3.0 Lack of Specific Regulatory T Cell Depletion and Cytoreduction Associated with Extensive Toxicity After Administration of Low and High Doses of Cyclophosphamide

Results from this study were partially presented as an oral presentation titled, "Evaluation of Different Treg Depletion Approaches as Strategies for Improved SIV Reactivation and Clearance" at the 9th IAS Conference on HIV Science (IAS 2017) in Paris, France by Dr. Ranjit Sivanandham. This work has been adapted from a published manuscript in AIDS Research and Human Retroviruses: Kleinman AJ, Sivanandham R, Sette P, *et al*, AIDS Research and Human Retroviruses 2021 June, doi:10.1089/aid.2021.0036. Adam J Kleinman contributed through the design and oversight of the study, processing samples, analyzing blood chemistries, performing and analyzing flow cytometry experiments, conducting viral quantifications, constructing figures, and writing the manuscript. Ranjit Sivanandham and Colin McAndrews contributed to sample processing. Ranjit Sivanandham also contributed to blood chemistry analysis and flow cytometry analysis. Egidio Brocca-Cofano also contributed to flow cytometry analysis. Paola Sette contributed to viral quantifications. Brandon F. Keele supplied the SIVmac239M and contributed to the design of the study and editing of the manuscript.

3.1 Chapter 3 Synopsis

Up to 93% of the human immunodeficiency virus (HIV) latent reservoir comprised defective proviruses, suggesting that a functional cure is possible through the elimination of a small population of cells containing intact virus, instead of the entire reservoir. Cyclophosphamide (Cy) is an established chemotherapeutic agent for immune cell cancers. In high doses, Cy is a nonselective cytoreductor, used in allogeneic stem-cell transplantation, while in a low dose, metronomic schedule, Cy selectively depletes regulatory T cells (Tregs). We administered low and high doses to simian immunodeficiency virus (SIV)-infected rhesus macaques (RM) to assess their effects on the SIV reservoirs. As a Treg-depleting agent, Cy

unselectively depleted Treg and total lymphocytes, resulting in minimal immune activation and no viral reactivation. As a cytoreductive agent, Cy induced massive viral reactivation in elite controller RMs without ART. However, when administered with antiretroviral therapy (ART), Cy had substantial adverse effects, including mortality. Our study thus dissuades further investigation of Cy as an HIV cure agent.

3.2 Introduction

Testing novel strategies for HIV eradication is a priority of AIDS research. Here, we assessed the utility of cyclophosphamide (Cy) for different cure strategies, by using two different regimens, with two different goals: Treg depletion and nonmyeloablative cytoreduction. We hypothesized that: (i) low doses of Cy (LDC) administered metronomically over one month would selectively deplete Tregs, as in humans [655], allowing for increased immune activation and viral reactivation with the added benefit of bolstering the cell-mediated immune response by reducing suppressive signaling from Tregs [505, 828]; and (ii) extensive nonselective depletion of lymphocytes with high doses of Cy (HDC) may be a valid HIV cure intervention through direct elimination of reservoir cells [657, 658, 829]; and subsequent restriction of reservoir diversity (through depletion, followed by the clonal expansion of the integrated genomes during cell restoration).

3.3 Materials and Methods

3.3.1 Ethics statement

Both strategies were tested in SIV-infected rhesus macaques (RMs) housed and handled at the University of Pittsburgh following the guidelines of the Association for Assessment and Accreditation of

Laboratory Animal Care (AAALAC) and the Animal Welfare Act. The University of Pittsburgh approved these studies in the Institutional Animal Care and Use Committee (IACUC) protocol 16027641.

3.3.2 Sample processing, whole blood counts and chemistries, flow cytometry, and viral quantification

Whole blood was serially collected and tested for complete blood counts and chemistries (Marshfield Laboratories, Cleveland, OH), and for staining immune cells, as described [505, 830]. Plasma viral loads (pVLs) were quantified by real-time PCR [313, 315, 831].

3.4 Results and Discussion

3.4.1 Low dose cyclophosphamide does not result in selective depletion of Tregs

To selectively deplete Tregs, we administered a low dose Cy (25 mg/day for 7 days, every two weeks for 1 month) to two SIV-infected, ART-naïve RMs at 337 days postinfection (dpi) and monitored the lymphocyte populations. LDC doses achieved a mild Treg depletion as demonstrated by a 42% reduction of the $CD4^+$ $FoxP3^+$ T cell fraction (Figure 4A). However, Treg depletion was not specific, as 40% of the overall $CD3^+$ T cell population were also depleted by 7-days post-treatment (dpt) (Figure 4B). Similar trends were also observed for $CD4^+$ and $CD8^+$ T cells, and for $CD20^+$ lymphocytes (data not shown). Treg depletion was short-lived, which contrasts with the overall $CD3^+$ cell depletion, which did not recover between treatments. Both LDC treatments decreased the baseline levels of Tregs with a near full recovery occurring within a week (Figure 4A and B).

As expected with Treg depletion, LDC administration was associated with increased CD69 expression on $CD8^+$ T cells, which occurred gradually through 14 dpt, reaching a level nearly two-fold over

pretreatment (Figure 4C). Immune activation did not significantly change with the second treatment, remaining elevated through 29 dpt. Conversely, CD69 expression on $CD4^+$ T cells remained level across both treatment phases (Figure 4D). Changes in HLA-DR/CD38 coexpression and Ki-67 expression were small and only noted in RM99 (data not shown). These results support a failure to specifically deplete Treg cells during LDC administration.

Since the primary endpoint of Treg depletion in these ART-naïve animals was viral reactivation [505, 828], we also monitored pVLs (Figure 4E). Prior to LDC administration, the two SIV-infected, ART-naïve RMs receiving LDC were either viremic (RM99, at 1,457 vRNA copies/mL), or below the limit of quantification (RM101, <30 vRNA copies/mL). Upon LDC treatment, pVLs decreased by an order of magnitude in RM99, were maintained low throughout the follow-up (up-to 26 dpt), and returned to baseline by 29 dpt. In RM101, however, no change in pVL was observed throughout the follow-up (Figure 4E). Because these animals are elite controllers [832, 833] and RM99 was viremic, it is possible that Treg depletion resulted in a reduction of the suppressive signaling on already active SIV-specific $CD8^+$ T cells, bolstering the anti-SIV response without drastic increases in immune activation. However, since LDC lacked Treg specificity, it is possible that the overall loss of peripheral lymphocytes drove the decreases in pVLs. Overall, these results are lackluster and do not support the use of LDC as a Treg depleting agent for latency reversal.

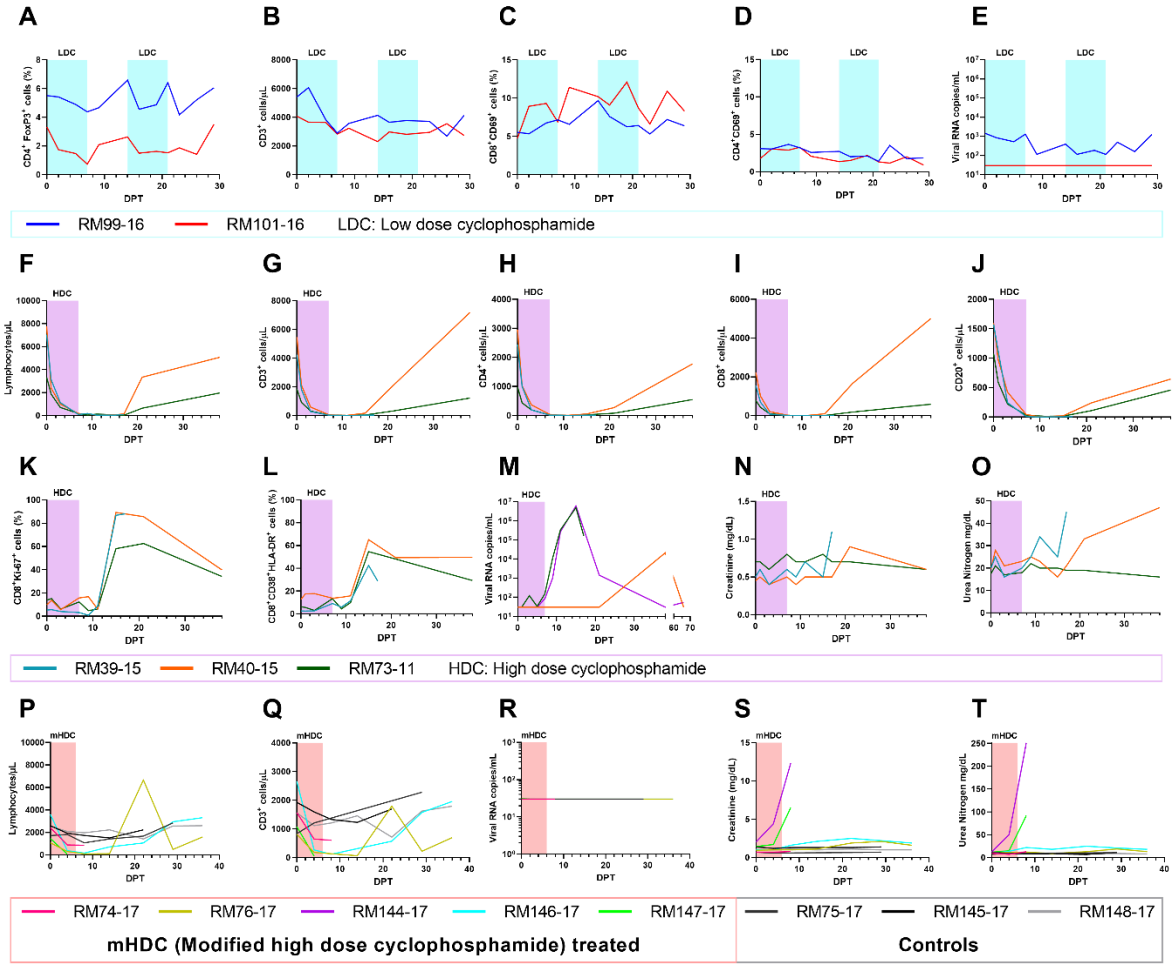

Figure 4. Comparison of different regimens of cyclophosphamide administration in SIV infection for regulatory T cell depletion and cytoreduction.

Parameters of low-dose cyclophosphamide administration for Treg depletion are shown in **A-E**. The percentage of $CD4^+$ T cells expressing FoxP3 (Tregs) (**A**) decreased at each treatment, while $CD3^+$ T cells (**B**) remained depleted through both treatments. LDC was marked with minimal immune activation as shown with CD69 expression on $CD8^+$ T cells (**C**) and $CD4^+$ T cells (**D**), with a reduction in plasma viral load in one animal and no reactivation in the other (**E**). Figures **F-O** show the parameters of high dose cyclophosphamide administration to elite controllers for cytoreduction. Total lymphocytes (**F**), $CD3^+$ T cells (**G**), $CD4^+$ T cells (**H**), $CD8^+$ T cells (**I**), and $CD20^+$ cells (**J**) were all massively depleted with treatment. Recovery was accompanied by reciprocal immune activation as demonstrated by expression of Ki-67 (**K**) and HLA-DR/CD38 coexpression (**L**) on $CD8^+$ T cells. Complimentary viral reactivation (**M**) occurred during the immune activation, resulting in pVLs reaching the levels of acute infection. Slight increases in kidney biomarkers creatinine (**N**) and urea nitrogen (**O**) were observed. Figures **P-T** show the parameters of modified high dose cyclophosphamide administration in RMs infected with the pathogenic SIVmac treated with ART. Total lymphocytes (**P**) and $CD3^+$ T cells (**Q**) were depleted to a lesser extent with the modified regimen and did not result in an observable increase in pVLs (**R**). However, Cy with ART became highly toxic as demonstrated by creatinine (**S**) and urea nitrogen (**T**). Treatment durations are marked by highlighted areas on graphs, DPT: day post-treatment; LDC: low dose cyclophosphamide; HDC: high dose cyclophosphamide; mHDC: modified high dose cyclophosphamide.

3.4.2 High dose Cy does not reactivate SIV on ART and induces unacceptable toxicity and morbidity

Three additional SIV-infected, ART-naïve RMs were utilized for initial testing of high dose Cy (HDC) as a cytoreductive agent. Without ART, 7 days of HDC (50 mg/kg/day) beginning at 456 dpi resulted in a pan depletion of peripheral blood cells (Figure 4F), with $CD3^+$ T cells being depleted from a baseline level of 3,852 cells/μL to 9 cells/μL at 11 dpt (Figure 4G). Complete recovery did not occur before 38 dpt, when $CD3^+$ T-cell counts reached an average of 4,195 cells/μL. $CD4^+$, $CD8^+$, and $CD20^+$ lymphocytes, and even NK cells decreased and recovered in a similar manner to $CD3^+$ T cells (Figure 4H-J).

Due to this massive cytoreduction, the immune activation levels could not be properly assessed at the nadir of lymphocyte depletion. Yet, with the lymphocyte restoration, high levels of cells expressing Ki-67 (Figure 4K) and HLA-DR/CD38 (Figure 4L) were expressed in $CD8^+$ T cells.

Prior to HDC treatment, in all of these ART-naïve SIV-infected RM controllers, the virus was undetectable. HDC administration resulted in massive viral reactivation in two of three RMs (Figure 4M), with detectable pVLs at 3 and 7 dpt in RM39 and RM73, respectively. In both these RMs, viral replication peaked at 15 dpt at $4.9x10^6$ (RM39) and $6.2x10^6$ (RM73) vRNA copies/mL. Plasma viremia again was undetectable at 38 dpt in RM73 and partially controlled (at 164,490 copies/mL) by 17 dpt in RM39 which then required euthanasia due to treatment-induced severe anemia. In the remaining RM, virus reactivation occurred late and was transient (21,257 copies/mL at 38 dpt), followed by undetectable levels in the next time point. Because the immune activation was decreasing leading up-to 38 dpt and other immune populations had returned to baseline, it is unlikely that the belated reactivation was due to HDC. Interestingly, after HDC administration, two of the RMs demonstrated slightly increased serum creatinine (Figure 4N) and urea nitrogen (Figure 4O), beyond the normal range in RMs [834, 835], indicating some nephrotoxicity.

With the promising observation of massive viral reactivation and significant cytoreduction observed after HDC administration to SIV-infected ART naïve RMs, we next designed a study aimed at

reducing/eliminating the viral reservoir in PWH who were chronically infected and on ART at the time of interventions. Eight RMs were infected with barcoded SIVmac239M [836] intravenously and received daily subcutaneous injections of a coformulated ART regimen (tenofovir, emtricitabine, and dolutegravir) [491] starting from 12 dpi for a duration of 8 months to achieve a durable viral suppression. At 252 dpi, while still on ART, a modified HDC treatment (50 mg/kg, 4 days and 25 mg/kg, 2 days) was administered to five RMs with the remaining three RMs used as controls (RM75, RM145, and RM148) and did not receive HDC. We hypothesized that this modified dose of HDC would be less toxic to SIV-infected, ART-treated RMs. The new regimen was less effective in inducing cytoreduction than the original one, with 15% residual lymphocytes persisting at the nadir (Figure 4P) *versus* <0.1% remaining in the first HDC group. The same was true for the $CD3^+$ T cells (Figure 4Q). Remarkably, no virus reactivation was observed in these SIV-infected, ART-treated RMs after the modified HDC administration (Figure 4R), suggesting that the high pVLs observed in the ART-naïve RMs likely stemmed from a small reactivation event that was highly exacerbated by *de novo* infections in the absence of ART. Unfortunately, after Cy administration, 2 SIV-infected, ART-treated RMs required euthanasia at 8 dpt due to subcutaneous hemorrhaging on limbs, chest, and oral mucosa; these RMs also presented with diarrhea, lethargy and RM144 developed hemorrhagic cystitis. At necropsy, we observed additional intestinal hemorrhages. Serum creatinine (Figure 4S) and blood urea nitrogen (Figure 4T) demonstrated severe nephrotoxicity in these two RMs, although the mechanism of increased toxicity is not understood. These very severe adverse effects prompted study discontinuation.

In conclusion, our study assessing the usefulness of two Cy dosing regimens as different strategies towards an HIV cure did not yield acceptable results. When used for Treg depletion, LDC was not specific, failed to induce viral reactivation, and only increased immune activation by a small amount relative to other Treg depletion agents [505, 828]. When the HDC was used, a substantial cytoreduction was achieved, but when given with ART, as necessary if used as an HIV therapeutic, generated unacceptable toxicity and

morbidity with virtually no viral reactivation. Therefore, further studies of Cy in PWH are not advised based upon these findings.

4.0 Pharmacokinetics and Immunological Effects of Romidepsin in Rhesus Macaques

This work was presented as a poster titled, “Pharmacokinetics and immunological effects of Romidepsin in rhesus macaques” at Strategies for an HIV Cure 2018 in Bethesda, MD. This work has been adapted from a published manuscript in Frontiers in Immunology: Kleinman AJ, Cottrell ML, Sivanandham R, *et al*, Frontiers in Immunology, 2020, December, doi:10.3389/fimmu.2020.579158. Adam J. Kleinman contributed through the design and oversight of the study, processing samples, analyzing blood chemistries, performing and analyzing flow cytometry experiments, immunofluorescence quantifications, constructing figures, and writing the manuscript. Cuiling Xu and Ranjit Sivanandham contributed to sample processing. Cuiling Xu, Ranjit Sivanandham, and Egidio Brocca-Cofano contributed to flow cytometry and functional study experiments and analyses. Egidio Brocca-Cofano performed and analyzed the histone acetylation assay. Ranjit Sivanandham and William McFadden performed histologies and stainings. Ivona Pandrea assisted in immunofluorescence image acquisition. Mackenzie Cottrell performed pharmalogic experiments and analyses and interpretation. Tammy Dunsmore provided veterinary care, administered RMD, and collected samples.

4.1 Chapter 4 Synopsis

HIV/SIV persistence in latent reservoirs requires lifelong antiretroviral treatment and calls for effective cure strategies. Romidepsin (RMD), a histone deacetylase inhibitor, was reported to reactivate HIV/SIV from reservoirs in virus-suppressed individuals. We characterized in detail the pharmacokinetics and safety profile of RMD in three SIV-naïve rhesus macaques which received two rounds of treatment. In plasma, RMD mean terminal half-life was 15.3 h. In comparison, RMD mean terminal half-life was much longer in tissues: 110 h in the lymph nodes (LNs) and 28 h in gastrointestinal tract. RMD administration was accompanied by transient liver and systemic toxicity. Isoflurane anesthesia induced near-immediate

transient lymphopenia, which was further exacerbated and extended with the extensive immune modifications by RMD. The effect of RMD on circulating immune cells was complex: (i) slight increase in lymphocyte death rates; (ii) transient, robust increase in neutrophils; (iii) massive downregulation of lymphocyte surface markers CD3, CD4, and CD8; (iv) migration of $CD3^+$ T cells to the gut and LNs; and (v) hindrance to CD8+ T cell functionality, yet without reaching significance. Our results show that, in contrast to transient plasma concentrations, RMD has a long-term presence in tissues, with multiple immunomodulatory effects and minimal to moderate kidney, liver, and lymphocyte toxicities. As such, we concluded that RMD can be used for "shock and kill" approaches, preferentially in combination with other latency reversal agents or cytotoxic T lymphocyte boosting strategies with consideration taken for adverse effects.

4.2 Introduction

The advent of antiretroviral therapy (ART) has been a tremendous success in extending the life expectancy of persons living with HIV [837]. However, ART is virostatic and does not target the integrated virus, which persists in latent reservoirs. As such, an HIV cure is needed [398]. The proof of concept that HIV cure is possible was provided by the "Berlin patient," who received an allogeneic stem cell transplantation using donors homozygous for the *CCR5* Δ*32* allele [386] and was in remission off ART for over 10 years [838]. A second patient that underwent a similar procedure (the "London patient") is also reported to be in remission [387]. However, attempts to reproduce this clinical outcome via stem cell transplantation from donors with functional CCR5 genes, or very early ART initiation have been unsuccessful and resulted in viral rebound 3-48 months after ART cessation [408-410]. These failures are due to the persistence of the latent HIV reservoirs which, upon ART cessation, can reactivate and drive a productive infection [363, 395, 839, 840]. Studies of the early dynamics of the SIV reservoir in nonhuman primates (NHPs) showed that ART initiation as early as 3 days postinfection, i.e., prior to detectable viremia, did not prevent reservoir seeding [22].

Not only is the reservoir very rapidly established, but it is also proteiform. Numerous cellular types are able to host latent HIV/SIV and contribute to the reservoirs: central memory [374, 399, 400], transitional memory [374, 400], follicular T helper $CD4^+$ cells [403], stem cell memory T cells [401], and regulatory T cells [402, 617]. The common feature of these cells is that they are of resting phenotype [363, 395-398, 841, 842], and that no marker can clearly identify the latently infected cells [406], which makes interventions towards reservoir eradication and HIV cure extremely difficult [402].

One of the most popular HIV cure strategies is the "shock and kill," the goal of which is to induce viral transcription from the latent reservoir using latency reversing agents (LRAs), followed by immune-mediated clearance of infected cells, thus depleting the viral reservoir, in the presence of ART to prevent *de novo* infections of uninfected cells [25, 510-512]. Histone modifications around the integrated proviral HIV long-terminal repeats (LTRs), stemming from histone deacetylase activity, inhibit transcription and lead to viral latency [425, 719-721]. Thus, histone deacetylase inhibitors (HDACi) loosen the DNA around histones and free the provirus for transcription and viral production [722]. This mechanism makes HDACi one of the most studied classes of drugs for the "shock and kill" approach [695-697].

Of the HDACi tested for HIV latency reversal, the depsipeptide romidepsin (RMD) [728, 729] has been extensively studied. It has been shown to be the most potent HDACi in terms of HIV reactivation, both *in vitro* and *ex vivo* [368]. RMD reactivates latent SIV with subsequent boosts in T cell activation [519, 747] in rhesus macaques (RMs) and induces reactivation of latent HIV in humans [727, 843]. There is debate as to whether RMD has an impact on the cytotoxic T lymphocyte (CTL) response to viral antigens, with some studies finding little change [519, 727], and another demonstrating inhibition of the CTL response [518]. This is of particular importance, as the cell-mediated immune response is a major player in controlling virus. In view of this relatively moderate success, we performed a detailed assessment of RMD pharmacokinetics in plasma and tissues, its toxicity and tolerability, and its impact on the counts and function of immune cell populations from circulation, lymph nodes (LNs), and intestines in SIV-naïve RMs to determine whether the immunological effects of RMD are appropriate for use as an HIV therapeutic.

4.3 Materials and Methods

4.3.1 Ethics statement

All the RMs included in this study were housed and handled at the University of Pittsburgh following the standards of the Association for Assessment and Accreditation of Laboratory Animal Care (AAALAC) and the Animal Welfare Act [844]. The University of Pittsburgh approved these experiments under the Institutional Animal Care and Use Committee (IACUC) protocol 15045866.

4.3.2 Study design

6 RMs (*Macaca mulatta*) were included in this study. Three SIV-naïve RMs were treated twice with 7 mg/m^2 of RMD administered over a 4-hour IV infusion and separated by a 70-day washout period to allow for complete clearance of RMD. Two rounds were utilized to gather additional cells which were limited by the extensive sampling conducted at each treatment. 3 additional RMs received infusions with saline solution in the same conditions of sedation and restraint as RMs in the RMD group (control group). Sampling was performed as shown (Figure 5). Both superficial and mesenteric LNs were biopsied along with intestinal resections. Tissues were not collected from the control RMs.

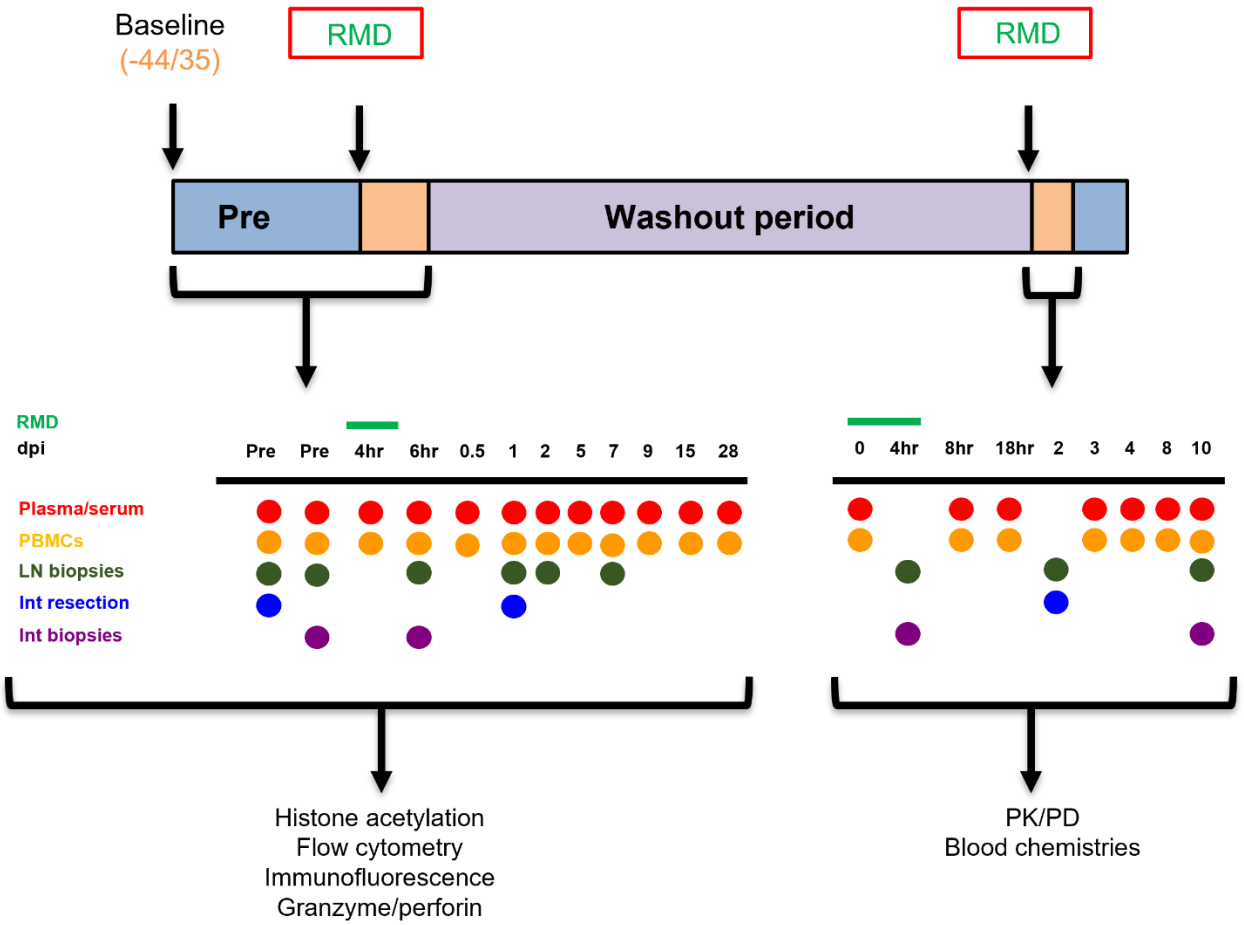

Figure 5. Experimental design of RMD pharmacokinetic and immunological effects study.

The timeline denotes the days at which baseline measurements began, romidepsin (RMD) was administered, and the washout period, in days postinfusion. The sampling schedules for both the first and second rounds of RMD treatment are shown. Blood chemistries, flow cytometry, immunohistochemistry, histone acetylation, and granzyme/perforin assays were completed with the samples taken from the first round of RMD treatment. PK/PD of RMD in blood and tissues was assessed for the second round of RMD treatment. dpi, days postinfusion; PBMCs, peripheral blood mononuclear cells; LN, lymph node; Int, intestinal.

4.3.3 Animals, treatments, and sampling.

Two male and one female SIV-naïve RMs ages 2 to 5 years and weighing between 5.6 and 8.9 kg, received RMD (Istodax, Celgene Corporation, Summit, NJ) at a dose of 7 mg/m^2. RMD was administered by slow infusion via catheter for 4 hours. The animals were sedated with ketamine (10-20 mg/kg). An IV catheter was placed in a saphenous or cephalic vein. An endotracheal tube was inserted and maintained until the animals were ready to be placed back into their cage, with 1-2% isoflurane to keep them

anesthetized. Blood pressure, oxygen, heart and respiratory rates were measured every 15 minutes. Animals were maintained in the surgical plane until after the 6- or 8-hr postinfusion bleeds to reduce sedation events.

To assess the impact of this prolonged anesthesia procedure on the tested immune and toxicity parameter, two additional male and one female RMs, aged 17-18 years and weighing between 11.7 and 13.3 kg, were included as controls and were subjected to the same anesthesia and infusion procedures as the RMD treated RMs, but RMD was replaced with a 0.85% saline solution. These animals were bled immediately prior to infusion and then at timepoints of 6 hours (hrs), and 1, 2, 5, and 7 days postinfusion.

RMD was given in two separate rounds with a 70-day interval to allow for complete washout. The dose was established based on previous studies in humans [743, 744] and our previous experience with RMD [519], which showed efficacy of RMD in RMs with relatively limited biological side effects.

Figure 5 illustrates the sampling schedule. Briefly, during the first RMD treatment, sampling included two bleeds at 35 and 13 days prior to treatment, four blood draws within 1 days postinfusion (4, 8, 16, and 24 hrs postinfusion), and then at 2, 5, 7, 9, 15, and 28 days postinfusion. Intestinal biopsies were taken at 13 days prior to infusion; intestinal resections were taken at 30 days before infusion and 1 day postinfusion; LNs were collected at 30 and 13 days prior to infusion, 6 hrs postinfusion, and 1 and 7 days postinfusion. The samples collected during the first round of RMD treatment were used for immune population dynamics and functionality.

During the second round of RMD treatment, blood was taken at 0, 2, 4, 6, and 18 hrs postinfusion, and at 3, 4, 8, and 10 days postinfusion. Intestinal resections from the jejunum were taken at 2 days postinfusion. Intestinal biopsies were taken at 4 hrs postinfusion and 10 days postinfusion. Superficial LNs were taken at 4 hrs postinfusion and 10 days postinfusion. Mesenteric LNs were collected at 2 days postinfusion. The samples collected during the second round were utilized for the pharmacokinetic assays and toxicity assessment.

Blood was collected intravenously from the femoral vein. Animals were sedated with 10-20 mg/kg ketamine IM with assistance from a squeeze cage. The site of collection was wiped with alcohol and after retraction of the collection needle, the site of collection was compressed until the vein clotted.

Complete blood counts (CBCs) and serum chemistries were monitored in the collected samples from both the RMD-treated RMs and control RMs by either the Marshfield Laboratories (Cleveland, OH), IDEXX Reference Laboratories (IDEXX Laboratories, Inc, Westbrook, ME) or in house, using a ProCyte Hematology Analyzer (IDEXX Laboratories, Inc).

Endoscope-guided intestinal biopsies were collected at the timepoints outlined in Figure 5. Animals were sedated with 10 mg/kg ketamine for this procedure. To collect adequate numbers of intestinal lymphocytes for analyses, between 12 and 15 pinch biopsies (approximately 1 mm^3 each) of intestinal mucosa (duodenum and upper jejunum) were obtained at each timepoint using an endoscope and small biopsy forceps.

Superficial LNs were collected from each RM at the times indicated in Figure 5. The animals were prepared aseptically using standard procedures (i.e. hair shaved from surgical site and site cleaned with alcohol and betadine) and draped using sterile drapes. The superficial LNs were located by palpation and the overlying skin incised. The LN was freed and removed by blunt dissection and ligation of attached vessels. Soft tissue was sutured with 3-0 Vicryl. Skin was sutured with a subcuticular pattern using 3-0 Vicryl and/or skin glue.

Jejunal resection, anastomoses and mesenteric LN biopsies were conducted at the times indicated in Figure 5. Each animal was prepared for surgery using standard procedures and draped using sterile drapes. An intravenous catheter was placed in the saphenous or cephalic veins and animals were intubated and maintained at a surgical plane of anesthesia using medical grade oxygen and isoflurane. A ventral midline incision was made and the jejunum isolated and packed off from the rest of the abdominal contents. After clamping the jejunum, a 20 cm section of jejunum was resected, and the anastomoses performed using 4-0 PDS in a simple-interrupted pattern. The rent in the mesentery was closed with 3-0 Vicryl in a simple continuous pattern. Mesenteric LNs were removed following isolation and ligation of any connected blood

vessels. The incision was closed using 3-0 Vicryl in a simple continuous pattern in the muscle layer and the skin closed with a subcuticular pattern using 3-0 Vicryl followed by application of tissue glue along the incision line.

4.3.4 Cell separation from whole blood

Peripheral blood mononuclear cells (PBMCs) were separated from whole blood as described [237, 845], and either used in an assay immediately or frozen. Briefly, whole blood was centrifuged at 2,200 rpm for 20 min and plasma was collected. The blood was then layered over lymphocyte separation media (LSM, MPBIO, Solon, OH) and separated by centrifugation at 2,200 rpm for 20 min. The buffy coat containing PBMCs was collected, washed with 1X phosphate-buffered saline (1X PBS, Lonza, Basel, Switzerland), and counted. PBMCs were frozen at 5 million cells/mL with freezing media consisting of 95% fetal bovine serum (FBS, VWR, Radnor, PA, USA) and 5% DMSO (Thermo Fisher Scientific, Walthead, MA).

4.3.5 RMD pharmacokinetics

RMD was quantified in both plasma and tissues using LC-MS/MS. Tissue biopsies were weighed then homogenized in Precellys® hard tissue grinding kit tubes (Cayman Chemicak, MI, USA) with 1 mL of methanol. Plasma and tissue homogenates were then extracted by protein precipitation with isotopically labeled internal standards (atazanavir-d5 and darunavir-d9 for tissue and plasma, respectively). Analytes were separated by reverse phase chromatography on an Atlantis T3 (50x2.1 mm, 3 μm) analytical column (Waters, Milford, MA, USA) prior to detection on an API-5000 triple quadrupole mass spectrometer (AB SCIEX, Foster City, CA, USA). Calibration standards and quality control samples were within 20% of nominal values with a dynamic range of 0.02-50 ng/mL of tissue homogenate and 0.2-200 ng/mL of plasma. Tissue homogenate concentrations were normalized for sample weight assuming a tissue density of 1 g/mL.

Noncompartmental analysis was performed using Phoenix WinNonlin v8.1 software (Pharsight Cooperation, Cary, NC, USA) to calculate the area under the concentration time curve ($AUC_{0\text{-}10days}$) using the linear trapezoidal rule. To calculate the half-life of RMD in plasma, the terminal elimination rate constant (kel) was estimated by fitting a linear regression line on a semi-log plot to the individual plasma concentration vs time data. All plasma observations after 96 hours were below the limit of quantification and omitted from the fitting. Given the relatively sparse sampling strategy in tissues, the mean concentration time profile was used to estimate kel as described above.

4.3.6 Flow cytometry

Whole blood was stained to monitor the impact of RMD on the immune cell populations. TruCount was used to determine absolute counts of $CD3^+$, $CD4^+$, $CD8^+$ T cells and $CD20^+$ B cells as described [238, 846, 847]. Fifty μL of whole blood were stained with antibodies against CD3-V450, CD4-APC, CD20-APC-H7, and CD45-PerCP in TruCount tubes (BD Biosciences, Franklin Lakes, NJ, USA) with a set number of fluorescent beads as internal standards. $CD8^+$ T cell counts were assessed through the ratio of $CD8^+$ to $CD3^+$ T cells. Whole blood was also stained with combinations of the following fluorescently labeled antibodies: CD3-V450 (SP34-2), CD4-APC (L200), CD8-PE-CF594 (RPA-T8), CD14-PE-Cy7 (M5E2), CD38-FITC (AT-1) (Stemcell, Vancouver, BC, CA), CD20-APC-H7 (2H7), CD69-APC-Cy7 (FN50), CD95-FITC (DX2), CCR5-PE (3A9), Annexin V-FITC, HLA-DR-PE-Cy7 (L243), NKG2A-PE (Z199) (Beckman Coulter, Pasadena, CA), Strepavidin-Alexa Fluor 750 (Life Technologies, Carlsbad, CA), Biotin-CCR7 (eBioscience, San Diego, CA), LIVE/DEAD Fixable Blue Dead Cell Stain Kit (Thermo Fisher Scientific); all antibodies were from BD Biosciences unless otherwise noted. For Ki-67-PE (B56) intracellular staining, cells were fixed and permeabilized prior to Ki-67 staining. Data were acquired with a LSR-II flow cytometer (BD Biosciences) or Fortessa flow cytometer (BD Biosciences) and analyzed with FlowJo software 10.7.0 (Treestar, Ashland, OR), as described [238, 634].

4.3.7 T lymphocyte functional assay

To simplify the complication of RMD treatment and SIV infection, it was vital to assess the impact of RMD administration on the T-cell function, particularly on the cellular immune responses on uninfected RMs. Due to the incapability to assess the SIV-specific immune responses, the overall cytotoxic capacity of lymphocytes in the blood was assessed as follows. Frozen PBMCs were thawed, counted, and were either unstimulated or stimulated with PMA and ionomycin (Sigma, St. Louis, MO). PBMCs were stained with the following antibodies: CD3-V500 (SP34-2), CD4-APC (L200)), CD8-PE-CF594 (RPA-T8), CD107a-APC-Cy7 (H4A3), Granzyme A-PerCP/Cy5.5 (CB9) (BioLegend), Granzyme B-Alexa Flour 700 (GB11), Granzyme K-FITC (GM6C3) (Santa Cruz Biotechnology, Dallas, TX), IFN-γ-FITC (4S.B3), and Perforin-PE (B-D48) (BioLegend); antibodies were from BD Biosciences unless otherwise noted. Stained PBMCs were then acquired on an LSR-II flow cytometer. Data were analyzed using FlowJo software (Treestar).

4.3.8 Histone acetylation assay

The efficacy of RMD treatment was assessed by monitoring histone acetylation of frozen PBMCs: at the baseline, 6 hrs postinfusion, and 1, 2, and 5 days postinfusion, using a flow-cytometrical method, as described [519]. Briefly, separated PBMCs were stained for surface markers for 20 min with: CD3-APC-Cy7 (SP34-2), CD4-V500 (L200), CD8-PE (SK1), CD14-BV570 (M5E2) (BioLegend, San Diego, CA), CD28-PE-CF594 (CD28.2), CD69-BV421 (FN50), CD95-PE-Cy5 (DX2), PD-1-PE-Cy7 (EH12.2H7) (BioLegend); all antibodies were from BD Biosciences, unless otherwise stated. PBMCs were then lysed with PhosFlow Lyse/Fix buffer (BD Biosciences) for 30 min and permeabilized with Perm Buffer (0.4% Triton X-100 in PBA [Sigma]) for 10 min, followed by washing. Permeabilized PBMCs were stained with the following antibodies for intracellular markers: Ac-H4 (3HH4-2C2) (Active Motif, Carlsbad, CA, USA) and Ki-67- Alexa Flour 647 (BD Biosciences). Ac-H4 recognizes motifs on histones H3 and H4 and was conjugated to FITC using Zenon reagent kit (Invitrogen, Carlsbad, CA). Stained PBMCs were then washed,

fixed with BD Stabilizing Fixative (BD Biosciences), and acquired with a LSR-II flow cytometer. Data were analyzed with FlowJo software.

4.3.9 In vitro assessment of RMD impact on immune cells and homing markers

To assess the RMD impact on the expression of cellular and homing markers, fresh PBMCs collected from 3 SIV-naïve RMs were subjected to either no RMD treatment or escalating doses of RMD (2, 10, and 20 ng/mL). The PBMCs were incubated with RMD in RPMI1640 supplemented with 1% Penicillin/Streptomycin, 1% HEPES buffer, 1% L-glutamine, and 5% heat-inactivated bovine calf serum for 0, 1, 2, or 5 days. PBMCs were then stained with CD3-V500, CD4-Alexa Flour 700 (L200), CD8-PE-CF594, CCR4-PE-Cy7 (1G1), CCR5-APC (3AP), CCR7-PE (3D12), CCR9-FITC (112509) (R&D Systems, Minneapolis, MN, USA), β7-PE-Cy5 (FIB504), and LIVE/DEAD Fixable Blue Dead Cell Stain Kit (Thermo Fisher Scientific); all antibodies were from BD Biosciences unless otherwise noted. Stained PBMCs were acquired on a LSR-II and data were analyzed with FlowJo software (TreeStar).

4.3.10 Immunofluorescence

$CD3^+$ T cell frequency in the intestine and LNs was assessed through immunofluorescence, as described [848]. Fixed, paraffin-embedded tissues from the 3 RMs were cut and placed onto microscope slides. The slides were treated 3 times with xylene (Thermo Fisher Scientific), run through an ethanol battery, washed with dH_2O, and placed into 1X PBS (Thermo Fisher Scientific). Slides were microwaved with Antigen Unmasking Solution (Vector Labs, Burlingame, CA) for antigen retrieval. Once slides had cooled, they were washed 3 times in 1 X PBS and the tissues were circled with Immedge Pen (Vector Labs) to create a hydrophobic barrier. Dako Serum-Free Protein Block (Agilent, Santa Clara, CA) was added to the tissues. The Dako Protein Block was dumped off and the slides incubated with mouse α-CD3 (Agilent).

The primary antibody was dumped off and slides washed in 1 X PBS as previously noted. The remaining steps were completed in the dark. The slides were incubated with the secondary antibody, goat α-mouse (Alexa Fluor 488) (Invitrogen) followed by a subsequent 1 X PBS wash. The slides were incubated with DAPI (Millipore Sigma, Burlington, MA), and then dumped off and washed with 1 X PBS, followed by dH_2O, and dried. Coverslips were then mounted to the slides with fluorescent mounting media (Agilent). Slides were visualized and imaged with Zeiss Imager M1 microscope and Axiovision software (V4.8.2.0 [Carl Zeiss AG, Oberkochen, Germany]). Image quantifications were performed using the FIJI distribution [849] of ImageJ 1.52c [850], where positive fluorescent signals were isolated by setting color thresholds and the percent positive area was calculated.

4.3.11 Cortisol ELISA

To assess the levels of stress associated with the different animal procedures used, frozen plasma was thawed, and dilutions of either 1:16 to 1:50 were used to measure the circulating cortisol levels with a cortisol ELISA kit (ENZO, Farmingdale, NY, USA), as per manufacturer instructions. The results were read at 405 nm on a Ultrospec 2100 Pro (Amersham Biosciences, Little Chalfont, UK) and results interpolated by Prism 8.4.3 (GraphPad Software, Inc., San Diego, CA) using 4 parameter logistic curve fitting.

4.3.12 Statistics and data analysis

Graphing and statistical analyses were completed with Prism 8.4.3. Data were expressed as individual values in Figures 5-11, 14, and 15. Data for Figures 12, 13, and S1 were expressed as means ± standard errors of the means (SEM). To compare differences in toxicities and lymphocyte dynamics, a Friedman test with Dunn's multiple comparisons test was utilized. To analyze cell surface marker

expression and homing marker expression, Mixed-effects model with Geisser-Greenhouse correction and Tukey's multiple comparisons test was used. $CD3^+$ cell migration to tissue sites and CTL functionality with RMD treatment utilized Wilcoxon paired non-parametric (two-tails) test was used. For all statistical tests $p<0.05$ was considered significant.

4.4 Results

4.4.1 RMD distributes extensively into the mucosal tissues and persists for at least 10 days

RMD was quantified in plasma, LNs, and the intestine after the second IV infusion. As expected, concentrations were the highest in the plasma at the first sampling time (2 hrs postinfusion: 4.7, 7.7, and 47 ng/mL). The mean terminal half-life of RMD in the plasma was 15.3 hours with quantifiable concentrations for up to 3 to 4 days postinfusion (Figure 6A). Assuming a tissue density conversion of 1.0 g/mL according to previous publications [851-853], the concentrations in LNs were the highest (70, 75, and 101 ng/mL) at 4 hours postinfusion and the mean terminal half-life (110 hours) was 7-fold longer than plasma with quantifiable concentrations for 10 days postinfusion (Figure 6B). In the GI tract, RMD concentrations were the highest [median (range) of 3,665 (354-3,932) ng/g)] at 4 hours postinfusion, and the mean terminal half-life (28 hours) was 1.8-fold longer than plasma with quantifiable concentrations for 10 days postinfusion (Figure 6C). RMD exposure (i.e., area under the concentration vs time curve; $AUC_{0\text{-}10days}$) was 27-153-fold higher in LNs and 426-2,860-fold higher in intestine than in plasma.

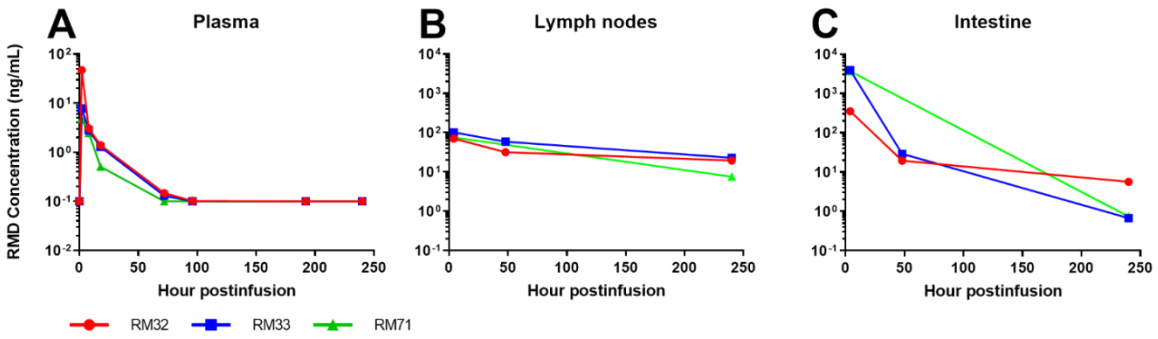

Figure 6. Romidepsin retention is greater in tissues than plasma.

RMD concentrations were measured in plasma (A), lymph node (B), and intestinal tissue (C) post 4-hour infusion of 7 mg/m^2 RMD.

To assess the functional impact of RMD, we monitored the levels of H3 and H4 histone acetylation within CD4$^+$ and CD8$^+$ T cells from blood. Histone acetylation increased rapidly in RMs upon RMD administration (Figure 7), peaking at 6 hrs postinfusion in two of three RMs and 1 day postinfusion in the third RM (RM33). The histone acetylation returned to near baseline level by 5 days postinfusion in both CD4$^+$ and CD8$^+$ T cells in all of the RMs (Figure 7), similar to previous findings at the same dosage [519], and agreeing with the drug concentrations in plasma (Figure 6A).

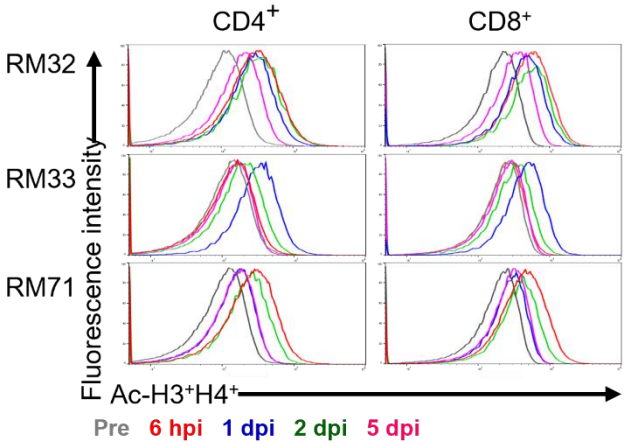

Figure 7. Histone acetylation is rapidly increased in peripheral CD4$^+$ and CD8$^+$ T cells with RMD treatment.

The levels of histone acetylation (H3 and H4) were measured in peripheral CD4$^+$ and CD8$^+$ T cells by flow cytometry prior to RMD treatment at 6 hours postinfusion (hpi), 1, 2, and 5 days postinfusion (dpi).

4.4.2 Transient toxicity with RMD treatment

We next assessed RMD toxicity by monitoring multiple serum biomarkers. Potential hepatotoxicity was documented by postinfusion increases of aspartate aminotransferase (AST) (186 U/L at 18 hrs postinfusion) and alanine aminotransferase (ALT) (98 U/L at 18 hrs postinfusion) (Figure 8A), both of which surpassed the normal ranges of AST (31-108 U/L) and ALT (14-94 U/L). The increase in AST was significant relative to pretreatment baseline levels (39 U/L) ($p<0.05$) while the ALT increase from the baseline (22 U/L) was not. At 3 days postinfusion, the AST and ALT levels (101 U/L and 89 U/L, respectively) were still higher than the baseline, indicating acute toxicity, although no longer statistically significant. The levels of AST and ALT then decreased to the high end of their respective normal ranges: 91 U/L and 80 U/L, respectively, at 4 days postinfusion. Comparing the peak of AST and ALT between the RMD treated and control groups demonstrated a significantly higher level AST ($p<0.05$), whereas ALT was substantially, although insignificantly ($p=0.07$) greater (Figures 8A).

Kidney biomarkers, urea nitrogen and creatinine, were scantily affected by RMD administration (Figure 8B). Prior to treatment, urea nitrogen and creatinine were 22 and 0.60 mg/dL, respectively. After RMD administration, the markers peaked at 35 and 0.77 mg/dL at 18 hrs postinfusion, respectively. Urea nitrogen increased above the normal range determined during our previous studies with RMs (8-25 mg/dL), while the level of creatinine remained within the normal range (0.5-1.2 mg/dL) and neither reached statistical significance. At 3 days postinfusion, creatinine returned to the baseline of 0.63 mg/dL, while urea nitrogen was still slightly elevated at 29 mg/dL and returned closer to the baseline level at 4 days postinfusion (25 mg/dL) (Figure 8B). The controls were also minimally impacted by anesthesia and saline administration (Figure 8B).

We assessed general toxicity by testing the levels of lactate dehydrogenase (LDH) and creatinine kinase (CK). Both LDH and CK increased after RMD infusion and neither returned to the baseline at 4 days postinfusion (Figure 8C). LDH increased from 702 to 1,562 U/L at 3 days postinfusion, while CK peaked

at 7,445 U/L at 18 hrs postinfusion, from 367 U/L. These increases were substantially higher than the normal ranges of LDH (514±187 U/L [834]) and CK (132-505 U/L, based on previous experiments). At 4 days postinfusion, CK (1,740 U/L) and LDH (1,323 U/L) declined, indicating a likely return to normal levels of both enzymes shortly thereafter. Although the only statistically significant change was CK at 18 hrs postinfusion ($p<0.05$), these increases cannot be ignored. Similar to the liver markers, a significantly greater peak was observed in the LDH of the RMD treated RMs compared to the control group ($p<0.05$), and yet a substantially, but insignificantly, higher peak was observed in the CK of the RMD treated RMs than control groups (Figures 8C).

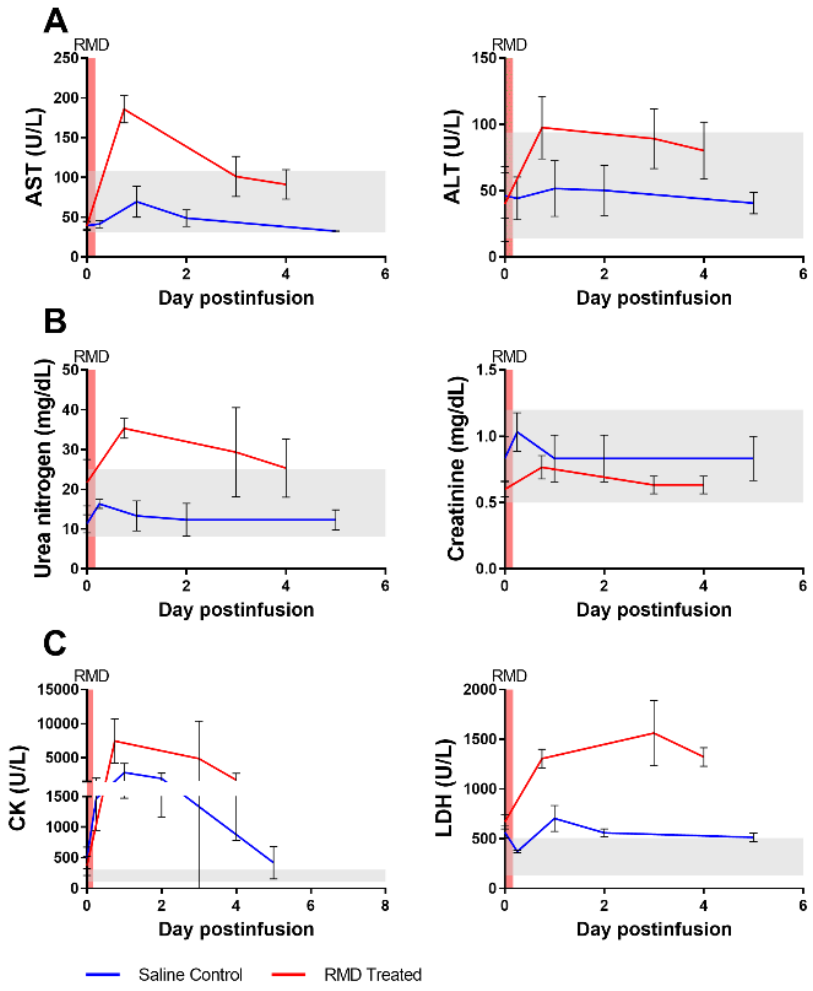

Figure 8. RMD is associated with mild acute nephrotoxicity and general toxicity.

Blood chemistries of markers for hepato- and nephrotoxicity and general markers of cell death of three SIV-naïve rhesus macaques after second round of RMD. (A) Hepatotoxicity markers, aspartate aminotransferase (AST) and alanine transaminase (ALT). (B) Nephrotoxicity markers, urea nitrogen and creatinine. (C) General markers of cell death, creatinine kinase (CK) and lactate dehydrogenase (LDH). The grey area represents the average reference values for the markers in three SIV-naïve, untreated RMs.

To further investigate the differences in biomarker changes between the RMD treated and saline controls, we assessed the concentration of cortisol in plasma as a surrogate of stress. The cortisol levels increased in both groups after the infusion. However, whereas cortisol levels peaked in the saline control group at 6 hours postinfusion and decreased towards the baseline levels from day 1 on, they remained elevated through 2 dpi in the RMs infused with RMD (Figure 9).

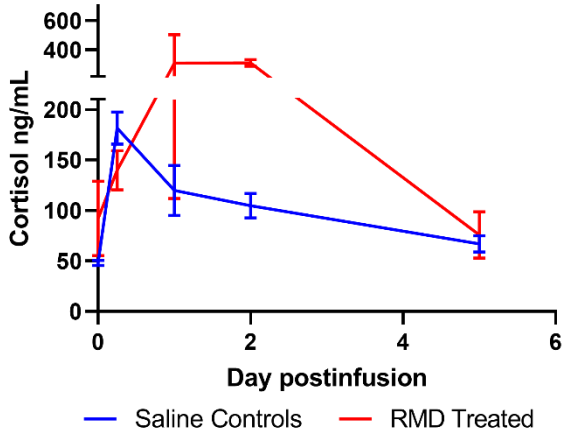

Figure 9. Cortisol concentrations in plasma after RMD and saline infusions.

Cortisol ELISA was performed with plasma at timepoints pre, 6 hpi, 1, 2, and 5 dpi from both RMD treated and saline control groups. Data is shown as mean ± SEM, n=3 per group.

4.4.3 Immune cell dynamics in blood

Following RMD administration, total circulating lymphocytes experienced a transient, but significant decrease from 5,050 cells/μL at the baseline to 1,463 and 1,753 cells/μL at 12 hrs and 2 days postinfusion, respectively, $p<0.05$ (Figure 10A). $CD4^+$ T cells, including $CD4^+CD8^+$ T cells, decreased from 2,518 cells/μL prior to treatment, to 402 cells/μL at 12 hrs postinfusion ($p<0.05$), 496 cells/μL at 1 day postinfusion ($p<0.05$) and were still decreased at 366 cells/μL ($p<0.05$) through 2 days postinfusion, with a fast, strong recovery to 1,305 cells/μL at 5 days postinfusion (Figure 10B). Similarly, $CD8^+$ T cells showed a substantial, significant decrease from 1,047 cells/μL at the baseline, to 204 cells/μL at 12 hrs postinfusion ($p<0.05$), 178 cells/μL at 1 day postinfusion ($p<0.05$) and 204 cells/μL at 2 days postinfusion ($p<0.05$). $CD8^+$ T cells started to recover back to 634 cells/μL at 5 days postinfusion, with near full recovery by 7 days postinfusion (741 cells/μL) (Figure 10C). B cells ($CD3^-CD20^+$) followed the same pattern as $CD4^+$ and $CD8^+$ T cells (Figure 10D). Conversely, neutrophils transiently increased from 3,273 cells/μL to 14,287 cells/μL at 12 hrs postinfusion, well above the normal range of $6.2 \pm 2.4x10^3$ cells/μL [834], followed by a rapid decline to 9,123 cell/μL at 1 day postinfusion and 2,427 cells/μL at 5 days

postinfusion (Figure 10E). At no time point did the acute increase in neutrophils reach statistical significance.

Interestingly, the saline-infusion control group decreased in total lymphocytes after infusion, but the impact was subdued relative to RMD treated RM. In fact, both $CD4^+$ (Figure 10B) and $CD8^+$ T cells (Figure 10C) decreased to lower cell counts, while having higher baseline values, and took longer to recover in the RMD treated RMs. B cells declined in RMD treated RMs while there was no change in the control group (Figure 10D). Furthermore, the neutrophil dynamics of the saline-infusion control group had a much smaller increase compared to that of the RMD treated RMs and returned to baseline three days prior to the RMD treated group (Figure 10E).

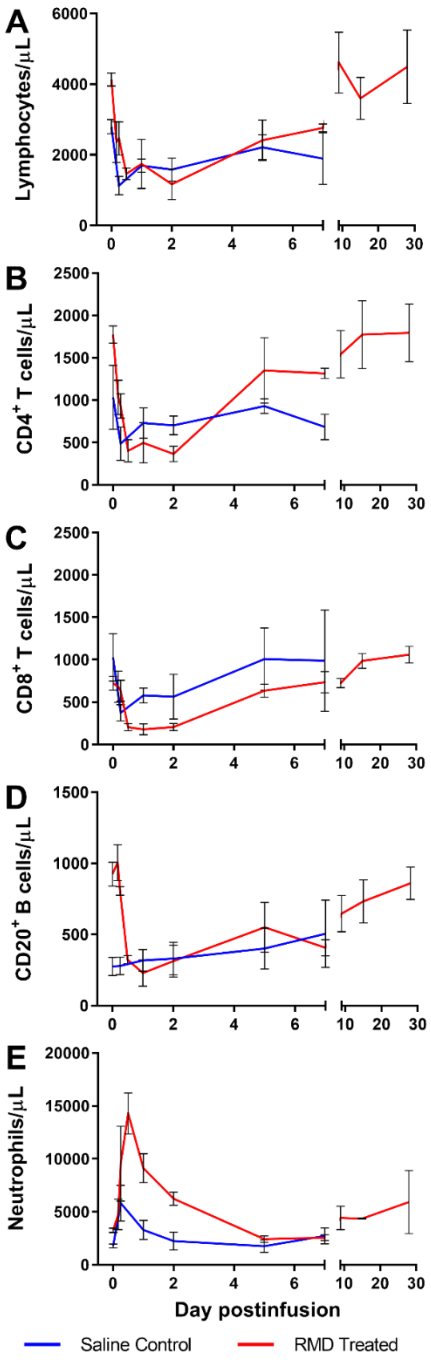

Figure 10. RMD induces rapid transient lymphopenia.

Immune cell populations in 3 SIV-naïve RMs treated with 7 mg/m2 RMD via 4-h infusion vs. 3 saline-treated controls. Total lymphocyte counts (A), absolute counts of CD4+ (B) and CD8+ (C) T cells, CD3−CD20+ B cells (D), and segmented neutrophils (E) from circulation.

To define the mechanism(s) of the $CD4^+$ and $CD8^+$ T cells decline after the RMD infusion, we first monitored the levels of apoptotic T cells by flow cytometry. The frequency of apoptotic $CD4^+$ T cells decreased from 3.7% at the baseline to 1.8% after RMD administration (Figure 11A). In contrast, the frequency of apoptotic $CD8^+$ T cells slightly increased from 2.1% at the baseline to 4.6% at 2 days postinfusion) (Figure 11B). The initial decrease in apoptosis was also observed in the saline control group, but the increased frequency of the apoptotic $CD8^+$ T cells did not occur in controls (Figures 11A and 11B). Furthermore, the expression of T cell activation markers of CD69 and Ki-67 increased on both $CD4^+$ and $CD8^+$ T cells isolated from circulation from the RMD treated RMs by 1 day postinfusion (Figure 12), although none of the increases reached significance. This increase was in stark contrast to the saline controls which experienced no significant increase in the T cell immune activation levels (Figure 12).

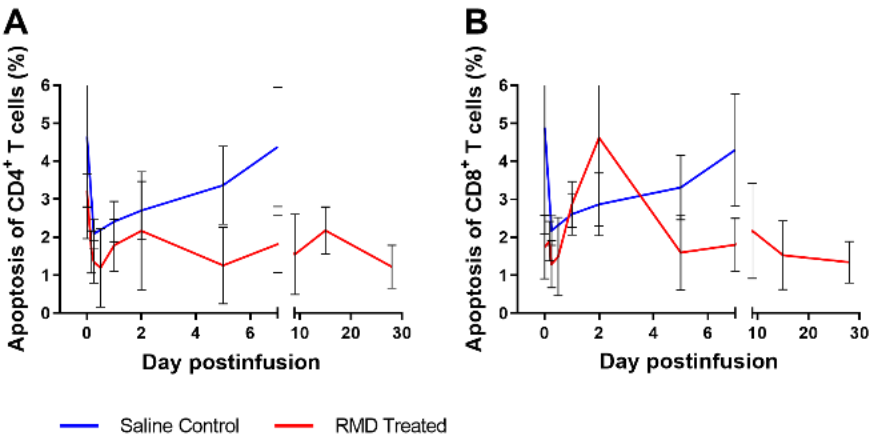

Figure 11. RMD is not associated with large increases in apoptotic T cells.

Whole blood was stained with Annexin V and Live/Dead stain to determine apoptosis of CD4+ (A) and CD8+ (B) T cells; animal number, n = 3 per group.

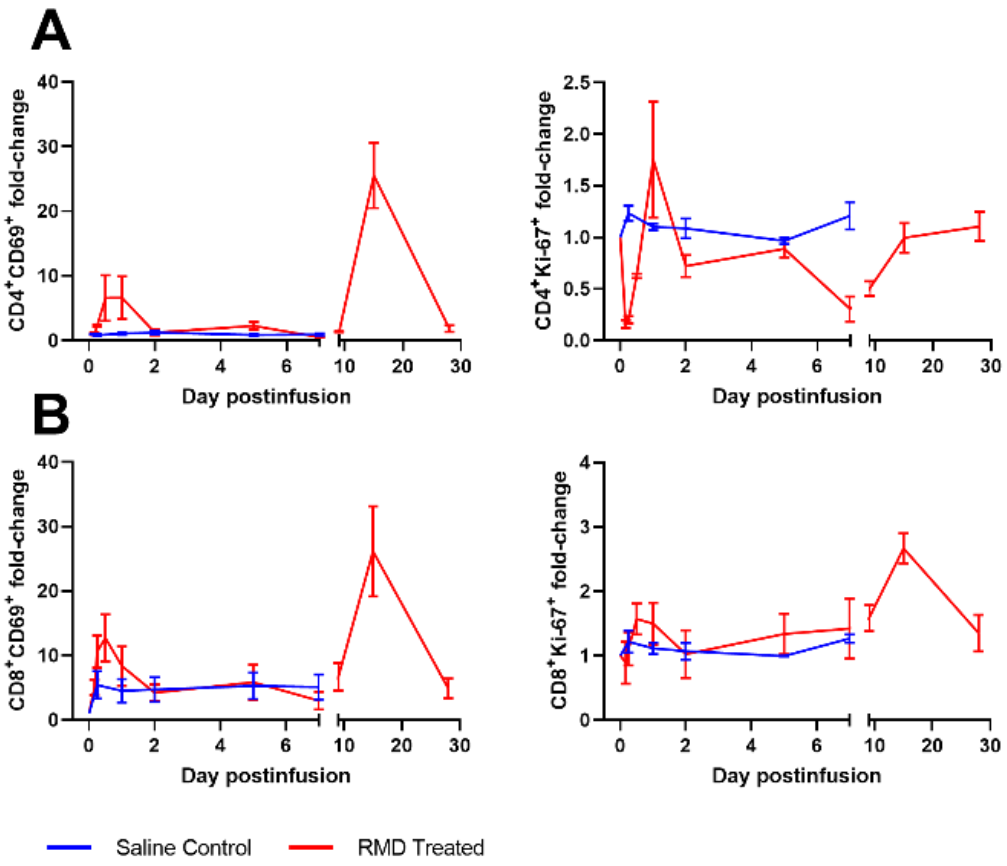

Figure 12. Lymphocyte activation is increased with RMD treatment.

Whole blood was stained for (A) CD4+ and (B) CD8+ lymphocyte markers: CD69 and Ki-67; animal number, n = 3 per group.

4.4.4 Downregulation of surface receptors of CD3, CD4, and CD8 after RMD infusion

Due to the massive, transient decrease in total counts of cells expressing CD3, including both $CD4^+$ and $CD8^+$ T cells, and the lack of corresponding increase in apoptosis, we conducted *ex vivo* RMD stimulation experiments on PBMCs and monitored changes in the expression of surface and homing markers on lymphocytes. Fresh PBMCs were incubated with various RMD doses (2, 10, and 20 ng/mL) for 1, 2, or 5 days. We observed a decrease trend of the expression of CD3, CD4 and CD8 surface markers, as measured by both individual cell expression (as mean fluorescence intensity) and total cells positive for the markers (% of cells). This decreased expression corresponded with the RMD dose and the

duration in days of cell incubation with RMD (Figure 13). In the absence of RMD, CD3 expression increased from the baseline of 50% of cells to 56% at day 1, 66% at day 2 and 61% at day 5. In the presence of RMD, minimal changes occurred at day 1 for all dosage treatments. Then, CD3 expression decreased to 48%, 30% and 32% at day 2 and decreased further to 20%, 16%, and 19% at day 5 for 2, 10 and 20 ng/mL, respectively (Figure 13A). Importantly, these changes both with and without RMD occurred while maintaining lymphocyte counts, suggesting these changes are due to modifications in surface expression. Although these changes are staggering, they did not reach statistical significance. Similar decrease trends of $CD4^+$ (Figure 13B) and $CD8^+$ (Figure 13C) expression were observed in time and dose dependent manners. Further, we noted complementary increased proportions of $CD4^-$ $CD8^-$ $CD3^+$ T cells with increasing dosages of RMD (Figure 13D). However, the dependence on RMD concentration did not reach statistical significance for $CD3^+$, $CD4^+$, and $CD8^+$ ($p>0.05$), but the increase in $CD4^-$ $CD8^-$ $CD3^+$ T cells did ($p<0.05$). Our results thus suggest that the decreased expression of surface markers was due to extended RMD treatment rather than solely the amount of time in media.

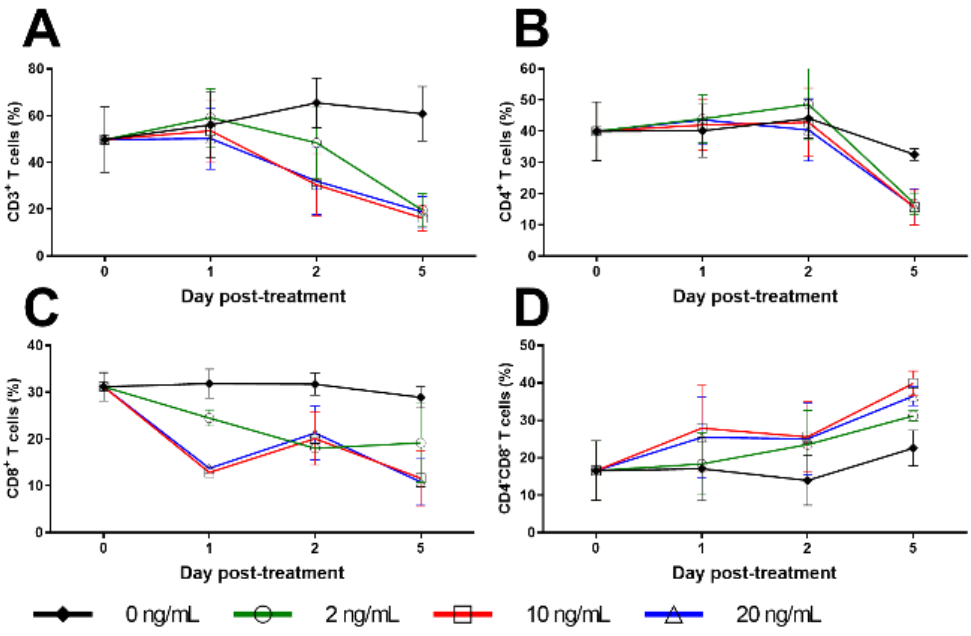

Figure 13. RMD treatment in vivo results in downregulation of cell surface marker expression.
Percentage of freshly separated PBMCs expressing CD3 (A), CD4 (B), and CD8 (C), and CD4−CD8− double negative PBMCs (D) treated with increasing RMD doses of (0, 2, 10, and 20 ng/ml); animal number: n = 3.

4.4.5 Homing receptor induction suggests migration of lymphocytes to the gut and LNs

To assess if the loss of the lymphocytes may be due to their migration to tissues, we measured the expression of various homing markers (α4β7, CCR4, CCR5, CCR7 and CCR9) on $CD3^+$, $CD4^+$, and $CD8^+$ T cells in the same RMD stimulation experiments. α4β7 expression on $CD4^+$ T cells at baseline was 8% and remained virtually unchanged without treatment, averaging 8% through day 2 (Figure 14A), and 7.5% at day 5. Under RMD treatment, α4β7 expression on $CD4^+$ T cells increased to 9% (10 ng/mL) and 10% (20 ng/mL) at day 1 and to 16% (10 ng/mL) and 15% (20 ng/mL) at day 2, but surprisingly decreased to 2% (10 ng/mL) and 3% (20 ng/mL) at day 5, with no changes at any timepoint reaching significance. Contrary to $CD4^+$ T cells, α4β7 expression on $CD8^+$ T cells continuously increased with treatment (Figure 14B) from 7% of the baseline to 59% (2 ng/mL) ($p>0.05$), 95% (10 ng/mL) ($p<0.05$), and 91% (20 ng/mL) ($p<0.05$) at day 5. In the absence of RMD, α4β7 expression on $CD8^+$ T cells remained virtually unchanged regardless of incubation time. This demonstrates that the effect of RMD on α4β7 expression of on $CD8^+$ T cells was due to both the incubation time and RMD concentration, $p<0.05$.

CCR4 expression on $CD4^+$ T cells was mostly unchanged (Figure 14C). CCR4 expression on $CD8^+$ T cells dramatically increased from 6% of the baseline to 73% (2 ng/mL) ($p>0.05$), 93% (10 ng/mL) ($p<0.05$) and 90% (20 ng/mL) ($p<0.05$) at day 5, which were much higher than 29% of untreated $CD8^+$ T cells ($p>0.05$) (Figure 14D). We found no statistical significance with CCR4 expression on $CD4^+$ T cells, but did observe significance in the effects of incubation time ($p<0.05$), yet not in RMD dosage on CCR4 expression on $CD8^+$ T cells.

The changes in the expression of the gut homing marker CCR5 were the most discordant between $CD4^+$ and $CD8^+$ T cells. Regardless of RMD treatment, CCR5 expression on $CD4^+$ T cells followed the similar decrease trend from 3% of the baseline to 2% (0 ng/mL) ($p>0.05$), 1% (2 ng/mL) ($p>0.05$), <1% (10 ng/mL) ($p>0.05$) and <1% (20 ng/mL) ($p>0.05$) at day 5 (Figure 14E). Conversely, on the untreated $CD8^+$ T cells, CCR5 expression increased from 4% of baseline to 7% in the absence of RMD ($p>0.05$),

59% with 2 ng/mL ($p>0.05$), 93% with 10 ng/mL ($p<0.05$), and 90% with 20 ng/mL ($p<0.05$) at day 5, respectively (Figure 14F). The effect of incubation time was significant for CCR5 expression on both $CD4^+$ ($p<0.05$) and $CD8^+$ T cells ($p<0.05$), whereas only $CD8^+$ T cell changes were significant for the effect of RMD concentration ($p<0.05$).

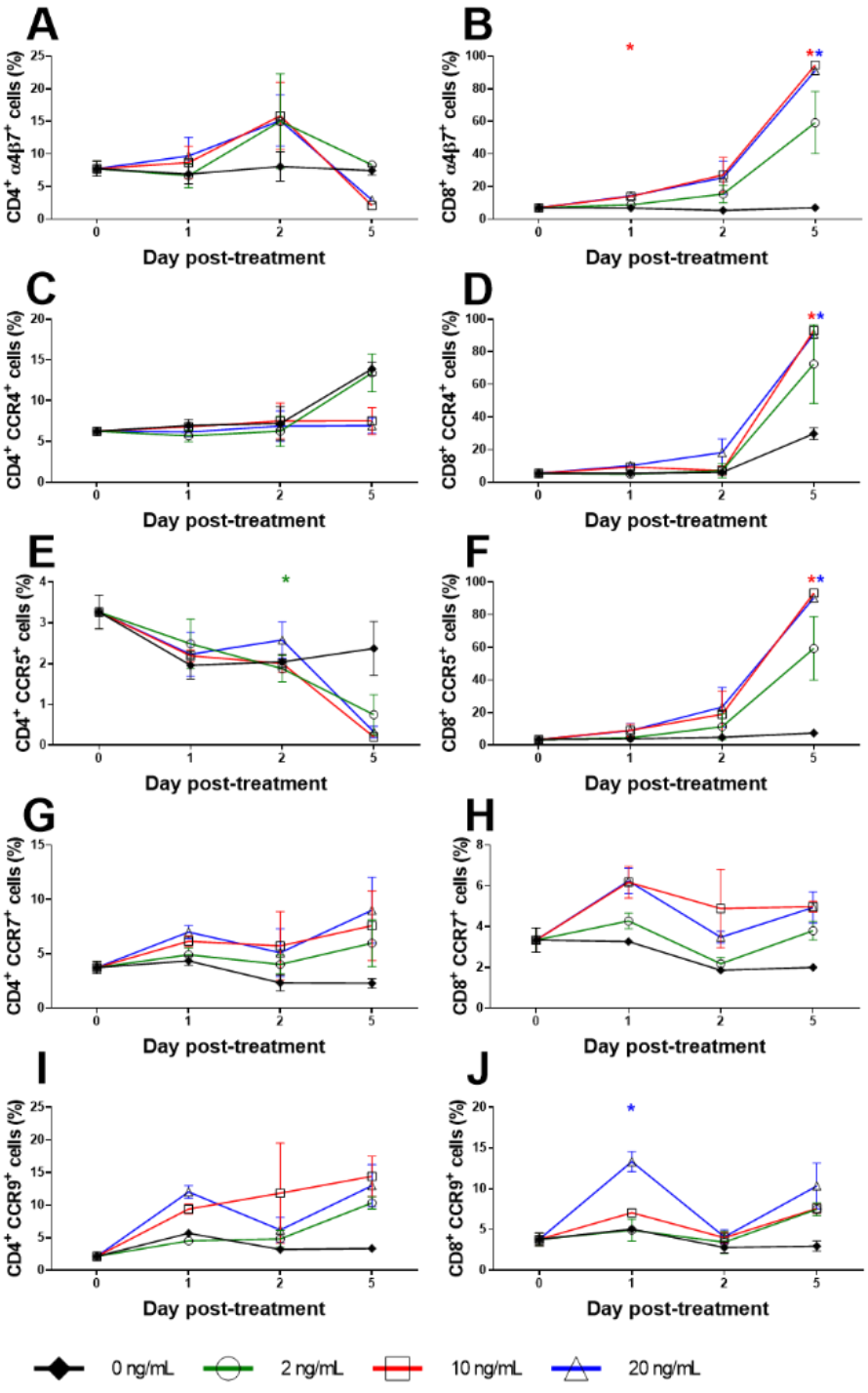

Figure 14. RMD treatment results in increases in homing marker expression in vitro.

The expression percentage of α4β7+ on (A) CD4+ and (B) CD8+, CCR4+ on (C) CD4+ and (D) CD8+, CCR5+ on (E) CD4+ and (F) CD8+, CCR7+ on (G) CD4+ and (H) CD8+, and CCR9+ on (I) CD4+ and (J) CD8+ with increasing dosages of RMD (0, 2, 10, and 20 ng/ml); animal number: n = 3. Asterisks indicate statistical significance of means to baseline as shown with concentration color ($p < 0.05$).

In the absence of RMD, CCR7 expression decreased from 4% at the baseline to 2% at day 5 on $CD4^+$ T cells and from 3% at the baseline to 2% at day 5 on $CD8^+$ T cells. In comparison, CCR7 (LN homing [854]) and CCR9 (gut homing [855]) expression increased in both $CD4^+$ and $CD8^+$ T cells with RMD (Figure 14). CCR7 expression on $CD4^+$ T cells peaked at day 5 after incubation with 20 ng/mL RMD (9%), $p>0.05$ (Figure 14G). CCR7 expression on $CD8^+$ T cells increased to a lesser extent (Figure 14H) but peaked at day 1 with 6% and 6.2% at 10 ng/mL and 20 ng/mL, respectively. At day 5, CCR7 expression on $CD8^+$ T cells (5%) with 20 ng/mL RMD was still more than that observed at the same timepoint with no treatment (2%). Although there is a trend towards increased CCR7 expression on $CD4^+$ and $CD8^+$ T cells with RMD treatment, neither the individual timepoint nor the effects of incubation time, nor RMD concentration, reached statistical significance.

The gut homing marker CCR9 [855] expression increased on both $CD4^+$ and $CD8^+$ T cells. CCR9 expression peaked at day 5 at 14% (10 ng/mL) and 13% (20 ng/mL) on $CD4^+$ T cells. In the absence of RMD, CCR9 expression increased from 2% at the baseline, to 3% at day 5 (Figure 14I). These changes did not reach significance ($p>0.05$). CCR9 expression on $CD8^+$ T cells mirrored that on $CD4^+$ T cells, with 4% of the baseline increasing to 8% (10 ng/mL) ($p>0.05$) and 10% (20 ng/mL) ($p>0.05$) at day 5. Meanwhile, CCR9 expression on untreated cells was of 3%, at day 5 ($p>0.05$) (Figure 14J), further substantiating the increases observed after incubation with RMD. Statistical analysis of CCR9 expression with a mixed effects model demonstrated statistical significance with regards to incubation time in $CD8^+$ T cells, $p<0.05$, while RMD concentration was not statically significant ($p=0.0641$). Such a statistical finding was not demonstrated with $CD4^+$ T cells.

4.4.6 CD3 signal increases in the gut and LNs after RMD administration

We further investigated the frequency of $CD3^+$ T cells in the intestine and mesenteric and superficial LNs in the RMD treated RMs by immunofluorescence (IF) on paraffin-embedded tissues.

Using color thresholds to determine the area fraction positive for signal of stained CD3, we assessed changes in the relative amount of $CD3^+$ T cells in tissues. In the superficial LNs, the amount of $CD3^+$ T cells showed modest increases over 7 days, from an average of 30% of pretreatment to 40% and 41% area fraction, at 6 hrs and 7 days postinfusion, respectively (Figures 15A-D). Of note, we did not have tissue for IF from RM32 pretreatment, and the RM showed a decrease from 6 hrs to 7 days postinfusion, in contrast to the increases seen in the other two RMs. The mesenteric LNs were analyzed pretreatment and 1 day postinfusion, with only one animal (RM71) showing a moderate increase in $CD3^+$ T cells by an area fraction change from 31% to 43%, respectively (Figures 15E-G). In the other two animals (RM32 and RM33) the $CD3^+$ T cells area fraction remained virtually unchanged ($p>0.05$). In the intestine, we observed an increase trend of $CD3^+$ T cells in all three RMs from pretreatment to 1 day postinfusion (5.8% vs. 7.6%, respectively) (Figures 15H-J), yet this increase did not reach statistical significance.

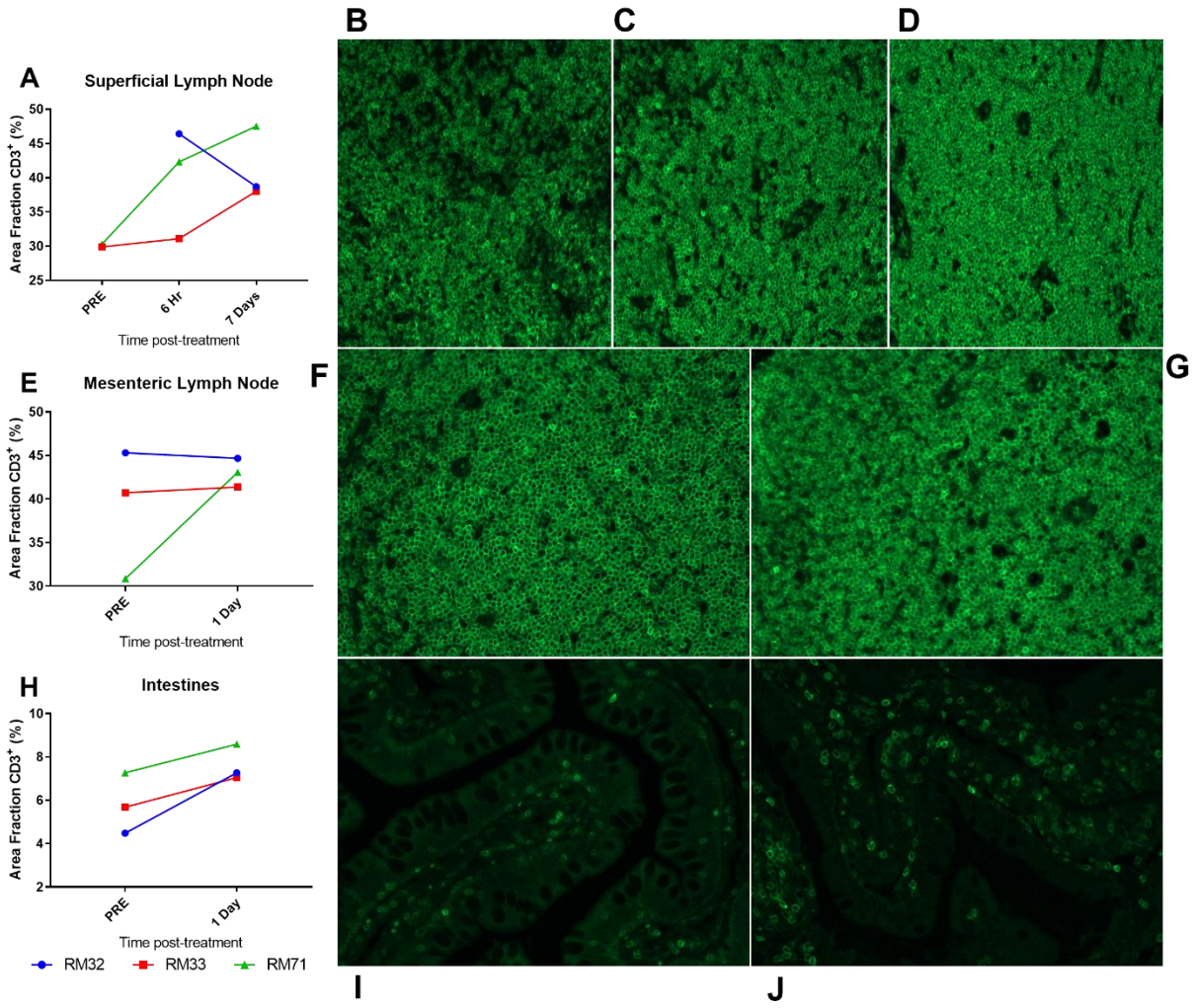

Figure 15. RMD infusion in RMs induces migration of CD3$^+$ T cells from the periphery to tissues.

Superficial LNs (A–D), mesenteric LNs (E–G), and intestinal resections (H–J) were embedded in paraffin and subsequently stained for CD3. Threshold quantification of total positive area for CD3 fluorescence for superficial LNs (A), mesenteric LNs (E), and intestinal resections (H). Representative images from superficial LNs are shown at pre (B, 6 hpi (C), and 7 dpi (D); mesenteric LNs at pre (F), 1 dpi (G); intestinal resections at pre (I) and 1 dpi (J).

4.4.7 RMD administration diminishes cytotoxic T lymphocyte functionality

Previous studies reported conflicting data as to whether the functionality of CTLs is diminished by RMD administration [519, 856]. Therefore, we performed functional assays on lymphocytes collected from superficial and mesenteric LNs and intestinal resections, focusing on the overall expression of the

surrogate killing marker CD107a, along with granzymes A, B, and K, IFN-γ, and perforin with PMA and ionomycin stimulation (Figure 16).

All the markers of T cell functionality diminished upon RMD treatment, apparently confirming the results of previous studies [856]. The CD107a expression decreased in the superficial LN from 1% at pretreatment to <1% at 2 days postinfusion. Similar changes were observed in the mesenteric LN (1% *vs* <1% at 1 day postinfusion) and intestine (2% *vs* 1% at 2 days postinfusion) (Figure 16A). Granzyme A decreased from 1% to <1% at 2 days postinfusion, 1% to <1% at 1 day postinfusion, and 2% to <1% at 2 days postinfusion in the superficial LNs, mesenteric LNs, and intestine, respectively (Figure 16B). Granzyme B decreased from 4% in the superficial LN to 1% at 2 days postinfusion, with similar changes in the mesenteric LN (5% *vs* 2% at 2 days postinfusion) and intestines (11% *vs* 3% at 2 days postinfusion) (Figure 16C). Granzyme K had similar decreases of 1% to <1% in the superficial LN at 2 days postinfusion, 2% to <1% in the mesenteric LN at 1 day postinfusion, and 1% to <1% in the intestine at 2 days postinfusion (Figure 16D). IFN-γ had moderate changes in its expression after RMD treatment. IFN-γ decreased in the superficial LN (4% *vs* 1%) at 2 days postinfusion, mesenteric LN (5% *vs* 3%) at 1 day postinfusion, and intestines (2% *vs* 1%) at 2 days postinfusion (Figure 16E). Perforin also decreased in expression after RMD treatment. The superficial LN $CD8^+$ T cells decreased perforin expression from 1% pretreatment to <1% at 2 days postinfusion, and the mesenteric LN and intestines mirrored these changes, decreased from 2% in the mesenteric LN to <1% at 1 day postinfusion and 1% in the intestines to <1% at 2 days postinfusion (Figure 16F). Thus, we found that RMD treatment resulted in a trend towards decreased cytotoxic functionality of $CD8^+$ T cells in all three tissues assayed, indicated by decreases in the proportion of $CD8^+$ T cells expressing these cytokines in response to PMA/ionomycin stimulation postinfusion (Figure 16). Further investigation into the multifunctionality of the $CD8^+$ T cells demonstrated that there were substantial reductions in the percentage of $CD8^+$ T cells expressing any combination of the cytokines in all

three tissues as well as decreased proportions of cells producing higher combinations of cytokines (Figure 17).

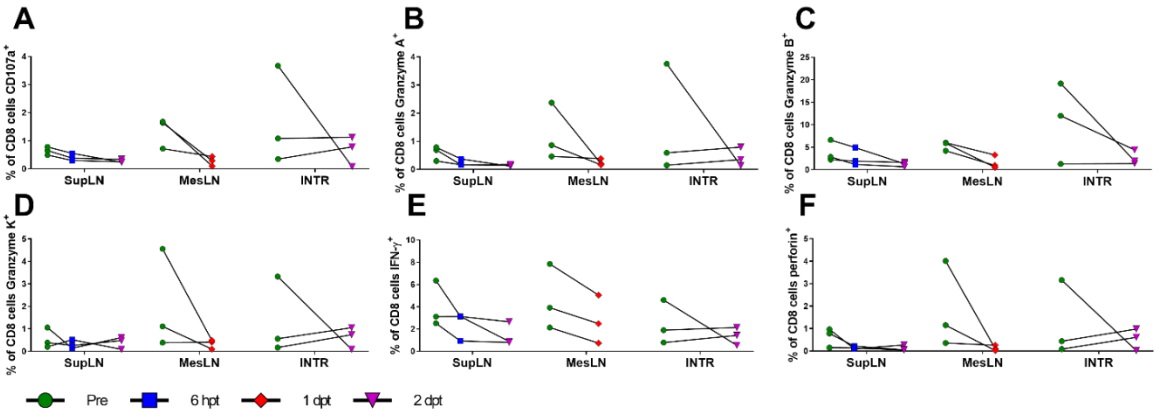

Figure 16. Cytotoxic T lymphocyte activity is decreased with RMD treatment.

Functional assays were performed for cytotoxic T lymphocyte markers of functionality, CD107a (A), Granzyme A (B), Granzyme B (C), Granzyme K (D), IFN-γ (E), and perforin (F) in CD8+ T cells stimulated with PMA and ionomycin. SupLN, Superficial LN; MesLN, Mesenteric LN; INTR, Intestinal resections.

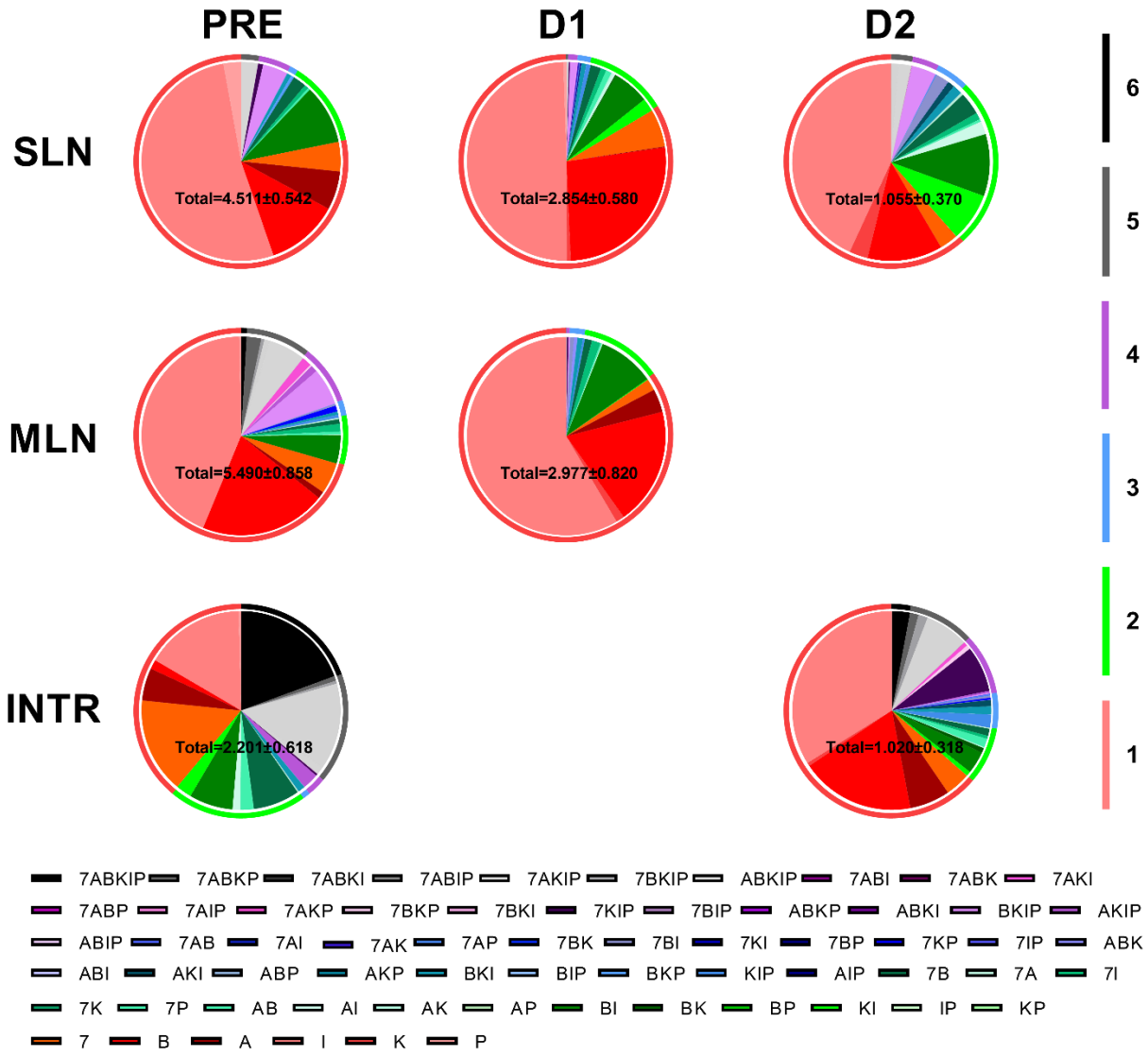

Figure 17. Multifunctional CD8$^+$ T cells from tissues have decreased activity after RMD administration.

Functional assays were performed for cytotoxic T lymphocyte markers of functionality, CD107a (7), Granzymes A (A), B (B), and K (K), IFN-γ (I), and perforin (P) in PMA and ionomycin stimulated CD8+ T cells from: SLN at pre 6 hours postinfusion and 2 days postinfusion, MLN at pre and 1 day postinfusion, and INTR at pre and 2 days postinfusion. Inner circle is colored by individual combinations as shown in the lower legend and the number denotes total percentage of CD8+ T cells expressing any combination of the stated cytokines ± SEM, n=3 per group. The ring shows the proportion of cells presenting combinations of 1, 2, 3, 4, 5, or all 6 cytokines tested as designated by the side legend. SLN: Superficial LN; MLN: Mesenteric LN; INTR: Intestinal resections.

4.5 Discussion

RMD is a drug used in chemotherapy of cutaneous T cell lymphomas [857], which has garnered interest as a LRA, being considered as potentially one of the most potent HIV reactivators of the HDACi [368]. We have previously reported that RMD is capable of reactivating latent SIV in post-treatment controllers [519]. Here, we assessed the pharmacokinetics and safety profile of RMD by treating three SIV-naïve RMs with a 7 mg/m^2 IV infusion over 4 hours.

We report extensive tissue distribution of RMD from the blood in RMs with tissue: blood penetration ratios of ≥27 and ≥426 in the LNs and GI tract, respectively. Polyexponential clearance from the plasma that is typically indicative of extensive tissue distribution has been previously described for RMD in humans [744, 858]. Consistent with these observations, we also observed biphasic plasma elimination. Our estimated terminal elimination half-lives are longer than those reported in humans (~3.5 hours) [858], and rhesus macaques [859]. However, both of these studies appear to calculate their terminal elimination half-lives based on the early distribution phase, which limits the accuracy of the terminal clearance of RMD in those studies. Similarly, in our study, RMD exhibited an early distribution half-life of approximately 3-6 hours. In fact, clinical studies providing estimates of RMD's terminal elimination half-life (6.6-19 hours) [744] are consistent with our findings of ~15.3 hours. This is likely due to the extended timepoints that were measured and give a better depiction of the terminal elimination half-lives.

We also report that, in contrast to the relatively rapid RMD clearance from circulation, RMD persists in the LNs and intestine significantly longer, and is still detectable 10 days postinfusion in these tissues. However, we currently do not understand the mechanism of persistence. Because we measured the prodrug form of RMD, it is possible that the maintained concentrations are due to either greater distribution to the tissue compartments, reduced conversion of the RMD to the active, reduced form, trapping of RMD between the extracellular and interstitial spaces, or a combination of these. As it is, the prolonged RMD half-life and the ability to quantify RMD at 10 days postinfusion in tissues compared to plasma is of interest,

as the HIV reservoir is known to persist in the LNs and GALT [149, 400, 860] and viral diversity during recrudescence of infection post-ART interruption suggests multiple sources of reactivation [861]. Thus, the sustained concentration of prodrug RMD in the intestinal and lymphoid tissues addresses this issue and suggests that RMD is a viable drug for reactivation studies. In fact, the plasma concentrations of RMD given at 7 mg/m^2 were greater than that found to readily reactivate HIV *in vitro* (5 nM) [727] through 8 hours postinfusion (5.16 nM [2.79 ng/mL]).

The brain is also a key HIV reservoir [862-864]. However, we did not collect central nervous system (CNS) tissue, nor cerebral spinal fluid (CSF), an established surrogate for testing drug penetration of the blood-brain barrier [865], to test potential penetration of RMD into the brain. Our rationale was that previous studies have demonstrated that RMD has poor penetration into the CSF, with only 2% the AUC of CSF/plasma, therefore suggesting poor penetration into the brain [859]. At 2 hrs postinfusion, the plasma concentration was 19.9 ng/mL (37.6nM). Assuming a 2% penetration, this would have equate to 0.73nM in the CSF, which is not a strong enough concentration to reactivate HIV *in vitro* [727]. Further compounding the lack of penetration is that HIV strains isolated from the CNS were shown to contain polymorphisms in the LTR which resulted in reduced abilities to reactivate, including when treated with RMD [866]. Thus, we reasoned that it is unlikely that RMD would reactivate HIV/SIV in the CNS at the given dose of 7 mg/m^2 and we did not focus on the brain in this study.

Interestingly, we observed an increased concentration of RMD in the plasma of RM32 *vs*. the other two RMs, which was accompanied by a lower intestinal concentration at 4 hrs and 48 hrs. These are strikingly different concentrations: 47 ng/mL vs 8 and 5 ng/mL at 2 hrs postinfusion in the plasma and 354 ng/g vs 3,932 and 3,666 ng/g at 4 hours postinfusion in the intestines of RM32, RM33, and RM71, respectively. Upon further investigation, we noted that RM32 had the greatest lymphopenia and subsequently the least immune activation with a slight delay in immune rebound. However, blood chemistries did not show a significant difference in enzyme changes. We also noted a more reduced histone acetylation in RM33 relative to the other two RMs, whereby 1 dpi was the most notable increase. Plasma

and tissue RMD concentrations were not lower relative to the other RMs, however, suggesting a different unknown mechanism for the reduced acetylation.

We next assessed the RMD toxicity in the SIV-naïve RMs. By performing blood chemistries, we assessed the levels of markers for hepatotoxicity (AST and ALT), nephrotoxicity (urea nitrogen and creatinine), and general toxicity (LDH and CK). The levels of urea nitrogen and creatinine were the least changed within the three categories, with a minimal increase that was still within the normal range for RMs [834], indicating that RMD has little to no nephrotoxicity in RMs. It is likely that the minimal elevations seen in urea nitrogen and creatinine are due increased protein turnover rate resulting from biopsy procedures. This is further supported by the results in the control group which did not have biopsy procedures conducted and had even fewer increases in urea nitrogen and creatinine than the RMD group. AST and ALT increased to levels that were well above the normal range and returned to normal by 4 days postinfusion, suggesting moderate liver toxicity which was not observed in the saline-infusion group. The increases seen in CK and LDH were transient, both biomarkers returning to baseline by 4 days postinfusion, indicating transient systemic toxicity in line with the observed loss of lymphocytes from the periphery. Another explanation for the increases in AST, ALT, CK and LDH could also be musculoskeletal damage. With the long sedation events and biopsies at the beginning of experimentation, it is possible that we are observing damage from these procedures, ketamine-induced rhabdomyolysis [867], or stress. The increase in CK and the lack of LDH increase in the control group is in line with previous studies indicating that isoflurane can increase serum CK, while having no significant effect on LDH [868]. Although the elevated cortisol corresponds to the increase in CK, we did not observe a corresponding increase in AST, ALT, and LDH that we would have expected if stress were a major contributing factor to the toxicity [869]. Therefore, the substantially raised liver enzymes, CK, and LDH relative to the saline control group is best explained by a mixture of toxicity as a result of RMD treatment, biopsy-mediated rhabdomyolysis, and a small contribution from stress, with some of the CK changes due to isoflurane anesthesia. Overall, we report that

RMD administration should be carefully monitored if given and using a dosage of 7 mg/m^2 or greater risks liver damage in RMs.

Previous studies have reported an immediate and brutal lymphopenia after RMD treatment [747]. In contrast to what is seen in a traditional bone marrow transfer, where regeneration of T cells occurs in approximately 60 days [870], the T-cell rebound after RMD administration was very rapid, starting by 2 days postinfusion, and resulting in a near-full restoration as early as 5 days postinfusion for CD8$^+$ T cells and 7 days postinfusion for CD4$^+$ T cells. However, the saline control group had less drastic, transient lymphopenia that recovered days earlier, in line with previous studies demonstrating immune suppression after isoflurane anesthesia with increased cortisol [871, 872]. These results thus suggest that the isoflurane anesthesia used played a small role in the initial loss of lymphocytes from the periphery. Moreover, the fractions of apoptotic CD4$^+$ and CD8$^+$ T cells were scantily affected by RMD treatment and the Ki-67 expression, a marker of lymphocyte proliferation, on CD4$^+$ and CD8$^+$ T cells was not massively increased during the time of lymphocyte recovery. Interestingly, immune cell fluctuations after recovery, e.g. day 15, were concomitant with a secondary increase in CD69 and Ki-67 expression and also seen in other studies [519, 727], although the exact mechanism of the delayed response is not known. Further, upon *in vitro* treatment with RMD, we observed the decrease in surface expression of CD3, CD4, and CD8 with complementary increases in double negative CD3$^+$ T cells. This suggested that the lymphocyte populations were not decreasing only by cell death, but also by a combination of downregulation of T cell surface markers, upregulation of homing markers, and subsequent migration from the periphery to the intestines and lymphatics along with retention in lymphatics. This does not necessarily imply the lack of cell death. In fact, the massive increase in segmented neutrophils immediately after treatment concomitant with the loss of lymphocytes is indicative of an immune response to damage-associated molecular patterns. However, changes in the expression of cell surface markers may occur as a result of activation, as previously demonstrated with T-cell stimulation by the phorbol ester PMA [873]; meanwhile, increased CD69 expression follows lymphocyte retention in lymphoid organs [874]. Both of these mechanisms may explain

the changes observed after RMD infusion. In line with this theory, we observed an immediate, transient increase in CD69 after infusion. When RMD was administered *in vitro*, CD3, CD4, and CD8 expression decreased while homing markers responded differently from each other between $CD4^+$ and $CD8^+$ T cells. Increases of CCR7 (LN homing marker) and CCR9 (gut homing marker) expression were observed for both $CD4^+$ and $CD8^+$ T cells, although only the RMD effect on CCR7 expression on $CD8^+$ T cells reached significance. Additionally, we found that the $CD8^+$ T cells expressed massive, significant increases of CCR4, CCR5, and α4β7 expression with RMD treatment. Thus, the changes in expression of CD69 and homing markers, together with the increase in $CD3^+$ T cells in the gut and LNs, further suggest an additional mechanism in which peripheral lymphocyte reduction was achieved through a combination of retention and migration to the gut and LNs. Together, these data suggest that the cause of the transient loss of $CD4^+$ and $CD8^+$ T cells in the periphery is due to a combination of isoflurane anesthesia causing stress that leads to the initial loss, with the major contribution from subsequent effects of RMD treatment: (i) downregulation of lymphocyte surface markers, (ii) retention of lymphocytes in the lymphatics, (iii) upregulation of specific homing markers, and (iv)subsequent migration of peripheral lymphocytes to the intestines and LNs, and minimal apoptosis, in agreement with the postulated reasoning in our previous report [519].

RMD has been reported to have a negative effect on the cytotoxic lymphocyte response [856], but this finding has been contradicted [519]. We found that with RMD treatment, $CD8^+$ T cells expressed fewer markers of cytotoxic functionality and lost some of the multifunctionality (CD107a, Granzymes A, B, and K, IFN-γ, and perforin). Importantly, the expression of these markers was also hindered by the RMD treatment when the cells were stimulated with PMA and ionomycin. Although these data seem to be in agreement with RMD having a negative effect on the CTL responses, they did not reach significance. However, our results must be taken with caution, as the PMA and ionomycin treatment is not an exact replica of antigen response. Nonetheless, our data suggest that RMD may work the best as an HIV therapeutic in combination with an immune activator, such as a PD-1 or CTLA-4 blockade, or a Treg

depletion agent [402], to supplement the cell-mediated immune response for eliminating infected, reactivated cells.

Although the "shock and kill" approaches for the HIV cure are moving away from HDACi and towards novel agents, such as STING agonists [702] and SMAC mimetics [701, 702, 781], our results suggest that RMD may still hold a place within HIV cure. We demonstrated that the observed lymphopenia postinfusion is due to a combined RMD effect, consisting of (i) apoptosis; (ii) downregulation of cell surface markers CD3, CD4, and CD8; (iii) upregulation of homing markers α4β7, CCR7, and CCR9; and (iv) migration from the periphery to the gut and LNs. As such, our results show that, despite RMD's acute toxicity and hindrance of T lymphocyte functionality, RMD's potent HDAC inhibition, coupled with its prolonged pharmacokinetics in tissue, makes it a drug that would benefit from being used in combination with another therapeutic agent, particularly one with minimal liver toxicity that enhances the cell-mediated immune response, as an effective LRA, in HIV cure.

5.0 Functional Cure of SIV is Predicted by Size of Inducible Virus Reservoir in Tissues, but Not in Circulating Cells

Results from this study have been presented in part as an oral presentation titled, "Different regimens of Romidepsin administration for reversion of SIV latency in a rhesus macaque model of complete viral control" at the 10th IAS Conference on HIV Science (IAS 2019) in Mexico City, Mexico and as a poster titled, "Repeated doses of romidepsin reactivates SIV and bolsters SIV-specific immune responses in a rhesus macaque model of complete viral control" at the 2019 HIV & HBV Cure Forum in Mexico City, Mexico. The results presented here are adapted from a submitted manuscript (Adam J Kleinman, Sindhuja Murali Kilapandal Venkatraman, Paola Sette, Ranjit Sivanandham, Benjamin B Policicchio, Cuiling Xu, Ellen Penn, Egidio Brocca-Cofano, Quentin Le Hingrat, Dongzhu Ma, Ivona Pandrea, and Cristian Apetrei). Adam Kleinman contributed to the design and oversight of the study, blood and tissue processing, flow cytometry staining and analyses, T-cell functional studies and analyses, viral outgrowth assay and analyses, and writing of the manuscript. Ranjit Sivanandham contributed to sample processing and performance and analyses of functional studies. Sindhuja Murali Kilapandal Venkatraman assisted in oversight, processed samples and performed and analyzed flow cytometry experiments. Ellen Penn assisted with study oversight, sample processing, flow cytometry and flow analyses. Paola Sette performed viral load quantifications and Dongzhu Ma performed cell-associated viral DNA quantifications. Egidio Brocca-Cofano performed T-cell functional studies and analyses. Quentin Le Hingrat assisted with T-cell functional studies and viral outgrowth assays.

5.1 Chapter 5 Synopsis

HIV persistence requires lifelong antiretroviral therapy (ART), calling for a cure. Latency reversing agents (LRAs), such as the histone deacetylase inhibitor romidepsin, reactivate and clear HIV/SIV through cell-mediated immune responses. We tested serial and "double infusions" of romidepsin in a rhesus macaque (RM) model of SIV functional cure. Off ART, romidepsin reactivated SIV in all RMs. Subsequent infusions diminished reactivation; some infusions did not yield detectable reactivation, these monkeys receiving a CD8-depleting antibody. In the monkeys that reactivated the virus after every romidepsin administration, we administered double infusions, which were well tolerated, induced immune activation, and effectively reactivated SIV. Minimal changes in the levels of cell-associated viral DNA occurred, but viral outgrowth from $CD4^+$ cells was decreased in RMs lacking reactivation after receiving a $CD8^+$-depleting antibody, or after the fifth romidepsin treatment. The frequency of SIV-specific $CD8^+$ T cells increased after romidepsin infusions, mirroring lack of reactivation. Sequential decreases in viral reactivation with repeated romidepsin administrations and absence of viral reactivation after $CD8^+$ T-cell depletion suggest that, in the context of healthy immune responses, romidepsin decreased the inducible viral reservoir, and gradually increased immune-mediated viral control, suggesting that improving immune function should be the start point of HIV cure strategies.

5.2 Introduction

Antiretroviral therapy (ART) is one of the most effective therapeutic strategies of the twentieth century, with a remarkable ability to suppress HIV replication and an exquisite impact on extending the life expectancy of persons living with HIV [837]. However, ART is only virostatic, i.e. does not actively eradicate proviruses from infected individuals, which persist in the latent reservoirs, calling for new therapeutic approaches aiming for an HIV cure [398]. Over 10 years of intensive research, only two cases

of HIV cure, defined as prolonged, complete viral remission and absence of detectable HIV proviruses in tissues after cessation of ART, were documented: the Berlin patient and the London patient [386, 387]. Both occurred after allogeneic stem cell transplantations using donors homozygous for the *CCR5* Δ*32* allele [386, 387]. Conversely, when allogeneic stem cell transplantation with intact *CCR5* was performed, remission was only transient, as reported for the Boston patients [408], pointing to the importance of the use of a nonfunctional *CCR5*, although this is still not sufficient to guarantee viral remission [875]. Furthermore, a case of very early and aggressive ART in a newborn (the "Mississippi baby"), also had some impact on the viral reservoir (illustrated by a significant delay in virus rebound after cessation of ART), but in the meantime demonstrated that ART alone cannot cure HIV [409, 410]. Importantly, circulating $CD4^+$ T cells from both the Boston patients and Mississippi baby were negative for viral DNA at the time of treatment interruptions, yet recrudescence of infection occurred in all these study participants. The reason for these failures is that HIV has the ability to persist in rapidly established latent reservoirs which, upon ART cessation, reactivate and produce recrudescent infection [363, 395, 839, 840]. Studies of early reservoir dynamics in rhesus macaques (RMs) reported that even initiation of ART as early as 3 days postinfection (dpi), i.e. prior to detectable viremia, does not prevent reservoir seeding [22, 24, 394]. Further, proviruses are found in resting $CD4^+$ T cells [363, 395-398, 841]: central memory [374, 399, 400], transitional memory [374, 400], stem cell memory T cells [401], Tregs [402], and follicular T helper $CD4^+$ cells [403]. Corroborated with the early reservoir establishment and the lack of a specific surface marker for latently infected cells [406], this explains why interventions to eliminate the latent reservoir are astonishingly onerous.

Multiple strategies to reduce/eradicate the latent reservoir have been proposed, yet with relatively modest success: (i) ART intensification [492-495]; (ii) permanent transcriptional silencing of HIV [496]; (iii) use of checkpoint inhibitors to enhance HIV-specific immune responses [506-509]; (iv) gene editing of CCR5 [497]; (v) genetic engineering of anti-HIV chimeric antigen receptor (CAR) T cells [384, 498, 499]; (vi) bone marrow transplantation [408]; (vii) broadly neutralizing antibodies [502, 503]; (viii) Treg manipulation strategies [402]; (ix) "shock and kill". However, these strategies have all experienced issues

with efficacy or additional problems. For example, ART intensification does not reduce the reservoir size [521], nor do checkpoint inhibitors [506, 507] and Treg manipulation results in insufficient viral reactivation [502]. Broadly neutralizing antibodies are susceptible to resistance and immune escape [522], while CAR T cells and gene therapies do not have long-term stability and lack sufficient efficacy [384, 523]. Bone marrow transplantation has unacceptable toxicity and morbidity combined with no success beyond the "Berlin" and "London" patients [408, 524]. Even "shock and kill" has had issues with lack of reservoir reactivation and clearance [513-515] as well as the potential for detrimental immune activation [516, 517].

Over the last 10 years, the shock and kill approach was one of the most pursued avenues for an HIV cure, with multiple agents being tested as potential latency reversing agents (LRAs): histone deacetylase inhibitors (HDACis) [695-697], protein kinase C (PKC) agonists [698, 699], bromodomain inhibitors (JQ1) [700], second mitochondrial activator of caspases (SMAC) mimetics [701], stimulator of interferon genes (STING) agonists [702], Toll-like receptor (TLR) agonists [703-708], and ingenol derivatives [709-712] alone or in combinations [713, 714]. Shock and kill operates on the premise that LRAs reverse viral latency, which allows for immune surveillance to recognize antigens of the reactivated virus and subsequently clear the infected cells. This strategy is performed in virus-suppressed individuals on ART, which prevents *de novo* infections of susceptible cells [25, 510-512]. The premise is that repeated cycles of virus reactivation and clearance would significantly curb/clear the HIV reservoir.

Theoretically, HDACi are strong candidates for latency reversal. Among genome modifications, deacetylation of histones at the integrated HIV proviral structure around the long-terminal repeats has been shown to inhibit transcription of the provirus by tightening the DNA around the histone, thereby driving the provirus towards latency [425, 719-722].

The depsipeptide romidepsin (RMD) is a potent HDACi [728, 729] that has been extensively studied in "shock and kill" approaches and has been shown to be the most potent, both *in vitro* and *ex vivo* [368]. In rhesus macaques (RMs), RMD reactivates latent SIV, with subsequent boosts in T cell activation [519, 747]; in humans, RMD reactivates latent HIV [727, 843]. However, reports of the RMD impact on

the cytotoxic T lymphocyte response to viral antigens yielded conflicting results [518, 519, 830]. As such, RMD-induced CTL suppression may have detrimental effects on the important "kill" step of this cure strategy [519, 727].

Here, we investigated the use of RMD as a latency reversing agent in RMs infected with SIVsab, an NHP model of functional cure [96, 633]. We utilized repeated rounds of RMD infusion with the hypothesis that repeated infusions will progressively dwindle the reservoir and enhance the SIV-specific immune response with each subsequent reactivation round.

5.3 Materials and Methods

5.3.1 Ethics statement.

All animals were housed and manipulated at the Plum Borough Research Facility of the University of Pittsburgh, following the guidelines of the Association for Assessment and Accreditation of Laboratory Animal Care (AAALAC) and the Animal Welfare Act [844]. The University of Pittsburgh approved these experiments with the Institutional Animal Care and Use Committee (IACUC) protocols 15045866 and 18042404.

5.3.2 Animals and treatments.

Five RMs (*Macaca mulatta*) were IV-infected with 100 tissue culture infectious infusion of SIVsab92018 and allowed time to control infection. The ages, weights, and sexes of the animals are included in Table 1. Two of these RMs received 3 rounds of RMD (7 mg/m^2) through slow intravenous perfusion over 4 hours. These animals then received a CD8+ cell-depleting antibody (M-T807R1; 50 μg/kg)

due to lack of viral reactivation upon the RMD treatments. The remaining three RMs received three rounds of RMD in the same conditions as the first group, followed by two rounds of "double infusions," RMD, i.e., two infusions (7 mg/m^2) through slow intravenous perfusion over 4 hours separated by 48 hours, and a final single infusion due to an animal requiring euthanasia due to clinical signs of severe allergic reaction one dpt.

Table 1. Sex, age and weight of RMs included in the study of repeated RMD administrations.

Animal number	Sex	Age	Weight
RM85	**Male**	**8 years**	**10kg**
RM89	**Male**	**8 years**	**11kg**
RM94	**Male**	**6 years**	**11kg**
RM95	**Male**	**6 years**	**11.5kg**
RM100	**Male**	**12 years**	**10kg**

5.3.3 Cell separation from whole blood and tissues.

PBMCs were separated from whole blood as described previously [237, 519]. Briefly, blood was centrifuged for 20 minutes at 2,200 rpm to separate the plasma, which was subsequently removed and frozen. Blood was layered over lymphocyte separation media (LSM, MPBIO, Solon, OH) and layer separation was achieved by centrifugation for 20 minutes at 2,200 rpm. The PBMC layer was pipetted off and washed with 1X phosphate-buffered saline (1X PBS, Lonza, Basel, Switzerland). Washed PBMCs were then counted and frozen at 5 million cells/mL using freezing media (95% fetal bovine serum [FBS, VWR, Radnor, PA, USA], 5% DMSO [Thermo Fisher Scientific]), with 2 million cells dry frozen.

Lymphocytes were separated from LNs and spleen by extensive mincing of the tissue, followed by pushing through a 70μm cell strainer, as previously described [144]. Cells were frozen the same as PBMCs.

Lymphocytes were separated from intestinal sections at necropsy as previously described [876]. Briefly, tissues were trimmed of fat and cut open longitudinally. The blunt, plastic safety covering of the safety scalpel was used to gently remove excess mucus and waste from the tissues. The gut sections were then cut into 1 cm^2 pieces and incubated twice in 8 mM EDTA solution (Fisher Scientific, Pittsburgh, PA) with HBSS (Lonza) for 30 minutes at 37°C on an orbital shaker at 300rpm. Tissue pieces were then cut to one half to one quarter size and incubated with the same conditions in an RPMI 1640-collagenase solution (0.75%; Sigma-Aldrich, St. Louis, MO). The resulting cell suspension was layered over percoll (Sigma-Aldrich) gradients of 60% and 35% and spun at 2,200 rpm for 20 minutes. Cells were frozen as with PBMCs.

5.3.4 Flow cytometry.

Whole blood or cells separated from LNs or intestinal tissue were stained with antibodies for flow cytometry, as described [315]. BD Trucount (BD Biosciences) was utilized to quantify absolute cell counts for $CD3^+$ T cells as described [315]. $CD4^+$ and $CD8^+$ T cell absolute counts were determined by acquired percentages of $CD3^+$ T cells from other flow cytometry panels. Antibodies used for staining are listed in Table 2. Intracellular staining for Ki-67 was completed as previously described [54]. Acquisition was completed on the LSR-II flow cytometer (BD Biosciences) and data were analyzed with FlowJo software (Treestar, Ashland, OR).

Table 2. Antibodies used in the study of repeated RMD administrations.

Antibody	Clone	Fluorophore	Manufacturer
CD3	SP34-2	V450	BD Biosciences
CD4	L200	APC	BD Biosciences
CD8	RPA-T8	PE-CF594	BD Biosciences
CD14	M5E2	PE-Cy7	BD Biosciences
CD20	2H7	APC-H7	BD Biosciences
CD25	2A3	PE	BD Biosciences
CD28	CD28.2	PE-Cy7	BD Biosciences
CD38	AT-1	FITC	Stemcell
CD39	eBioA1	PE	Invitrogen
CD45	D058-1283	PerCP	BD Biosciences
CD69	FN50	APC-Cy7	BD Biosciences
CD73	AD2	PerCP-Cy5.5	BD Biosciences
CD95	DX2	PE-Cy5	BD Biosciences
CCR4	1G1	PE-Cy7	BD Biosciences
Ki-67	B56	PE	BD Biosciences
HLA-DR	L243	PE-Cy7	BD Biosciences
Annexin V	-	FITC	BD Biosciences
NKG2a	Z199	PE	Beckman Coulter
FoxP3	259D	AF488	BioLegend
LIVE/DEAD	-	UV	Life Technologies

5.3.5 SIV-specific immune response assay.

The SIV-specific immune responses were assayed as previously described [505, 828, 877]. Briefly, frozen PBMCs were thawed, counted, and were either unstimulated or stimulated with the ENV, Gag1 (peptides 1-68), or Gag2 (69-136) peptide pools (NIH Reagent Program). After 2 hours, cells were treated with monensin and brefeldin A to prevent acidification of endocytic vesicles and exocytosis of cytokine containing vesicles, respectively. PBMCs were then stained and acquired on a LSR Fortessa flow cytometer (Becton Dickinson, NJ, USA). Flow cytometry data were analyzed with FlowJo version 10.6.1 (Treestar, OR, USA).

5.3.6 Viral quantification.

SIV plasma VLs were measured using quantitative reverse-transcription PCR, as described [313, 315, 505]. Briefly, RNA was extracted from plasma with the RNeasy Mini Kit as per manufacturer's instructions (Qiagen, Valencia, CA, USA). RNA was then reverse transcribed with Superscript III First-strand synthesis Supermix for qRT-PCR kit (Invitrogen, Carlsbad, CA, USA) and ran on SimpliAmp Thermal Cycler (Applied Biosystems, Foster City, CA, USA). TaqMan Gene Expression Master Mix (Applied Biosystems) was added to the resulting cDNA with primers and probes as previously described and ran on either a ABI 7900HT (Applied Biosystems) or QuantStudio 7 (Applied Biosystems).

5.3.7 Viral outgrowth assay.

Inducible, replication-competent virus was detected by intracellular staining of SIV p27 in MOLT-4 clone 8 cells (obtained through the NIH HIV Reagent Program, Division of AIDS, NIAID, NIH: MOLT-4 Cells, Clone 8, ARP-175, contributed by Dr. Ronald Desrosiers [878]) cocultured with PBMCs, as described [24, 879, 880]. Briefly, $CD4^+$ T cells were negatively selected from PBMCs according to manufacturer's instructions ($CD4^+$ T cell isolation kit, Miltenyi Biotec, Auburn, CA). $CD4^+$ T cells were then stimulated with PMA (50 ng/mL) and ionomycin (1 μg/mL) for 6 hours, washed and plated at 100,000-250,000 cells per well, depending on cell availability, with 100,000 MOLT-4 clone 8 cells. Cocultures were followed for 17-19 days, upon which time the cells were harvested, washed, and stained for CD3-V450, CD4-APC, and intracellular SIV p27-FITC (ARP-2321) conjugated to FITC using the FluoReporter FITC Protein Labeling Kit according to manufacturer's instructions (Life Technologies) at 100 ng/replicate. ARP-2321 was obtained through the NIH HIV Reagent Program, Division of AIDS, NIAID, NIH and Centre for AIDS Reagents, NIBSC, UK, supported by EURIPRED (EC FP7 INFRASTRUCTURES-2012 - INFRA-2012-1.1.5.: Grant Number 31266). www.euripred.eu/: Anti-Simian Immunodeficiency Virus

(SIV) SIVmac gp41 Monoclonal (KK41), ARP-2321 (CFAR# 3005), contributed by Dr. Karen Kent and Caroline Powell. Cultures positive for SIV p27 were designated as having ≥0.1% SIV p27 in the MOLT-4 populations.

5.3.8 Statistics.

Graphical and statistical analyses were completed with Prism 9.1.2 (GraphPad Software, Inc., San Diego, CA, USA). To analyze immune cell dynamics and phenotypes and toxicities, a mixed-effects model with Geisser-Greenhouse correction and Tukey's multiple comparisons test was used due to the difference in timepoints between some of the animals. To compare differences between the percentage and total SIV-specific responses producing one or more cytokines at a time we utilized the Friedman test with Dunn's multiple comparisons. To compare the cell-associated DNA and viral outgrowth between rounds of treatment, we utilized the Kruskal-Wallis ANOVA with Dunn's multiple comparisons.

5.4 Results

5.4.1 Study design.

To assess RMD efficacy in reactivating the latent SIV, we used RMs that are infected with SIVsab (virus that naturally infects African green monkeys), our RM model of functional cure of a replication competent SIV, which is achieved in 100% of RMs [96, 633]. The ages, weights, and sexes of the animals are detailed in Table 1. The study design was as follows: all RMs received three rounds of RMD (7 mg/m^2) through slow intravenous perfusion over 4 hours. As no viral reactivation was observed after the second and third round of RMD administration in two RMs, the group was split and the RMs showing no virus

reactivation received $CD8^+$ cell depleting antibody (M-T807R1; 50 μg/kg). For the remaining three RMs, the first three rounds of RMD administration were followed by two rounds of "double dosing," consisting of two RMD administrations (7 mg/m^2) at 48 hours interval, and finally, a single infusion due to an animal requiring euthanasia due to clinical signs of severe allergic reaction one day post-infusion. Since SIVsab is spontaneously completely controlled (< 1 copy/ml of plasma) in 100% of RMs [96, 633], the model can be employed to study virus reactivation without ART. In this study design, with the animals not receiving ART, the reactivated virus can complete cycles of replication, which results in robust virus rebounds detectable with conventional viral load (VL) assays.

5.4.2 RMD administration is associated with acute toxicity that is not increased by a second administration 48 hours later.

We have previously shown that RMD infusion is associated with moderate acute toxicity. Similar to our previous study [830], markers of liver toxicity (alanine aminotransferase [ALT] and aspartate aminotransferase [AST]), kidney toxicity (urea nitrogen and creatinine), and general toxicity (lactate dehydrogenase [LDH] and creatine kinase [CK]) transiently increased post-RMD infusion. ALT and AST increased rapidly after each infusion, peaking within two days of infusion (at approximately 3 and 5 times the baseline levels for ALT and AST, respectively) and returning to near pretreatment levels by 7 dpt (Figure 18A and 18B). Interestingly, when switching to double infusions, we did not observe an additive effect on RMD toxicity (Figure 18A and 18B).

Nephrotoxicity was minimal, as demonstrated by minimal increases in urea nitrogen (Figure 18C), while creatinine remained virtually unchanged (Figure 18D). When regimens were switched to double infusions, we did not observe a larger increase in urea nitrogen compared to single infusions but did see a prolonged elevation.

General toxicity markers LDH and CK increased post-infusion. LDH levels increased from baseline up to 2-fold (Figure 18E). Switching to double RMD infusions did not result in further increases in the LDH levels (Figure 18E). CK increased more dramatically (up to 20-fold compared to baseline levels) (Figure 18F). Switching to double infusions did not result in more prominent increases compared to single infusion.

Although one animal required euthanasia during the sixth round of treatment due to a severe allergic reaction, the increases in toxicity markers are in line with what we've seen in uninfected animals previously [830], validating the safety of RMD in SIV-infected *versus* uninfected RMs.

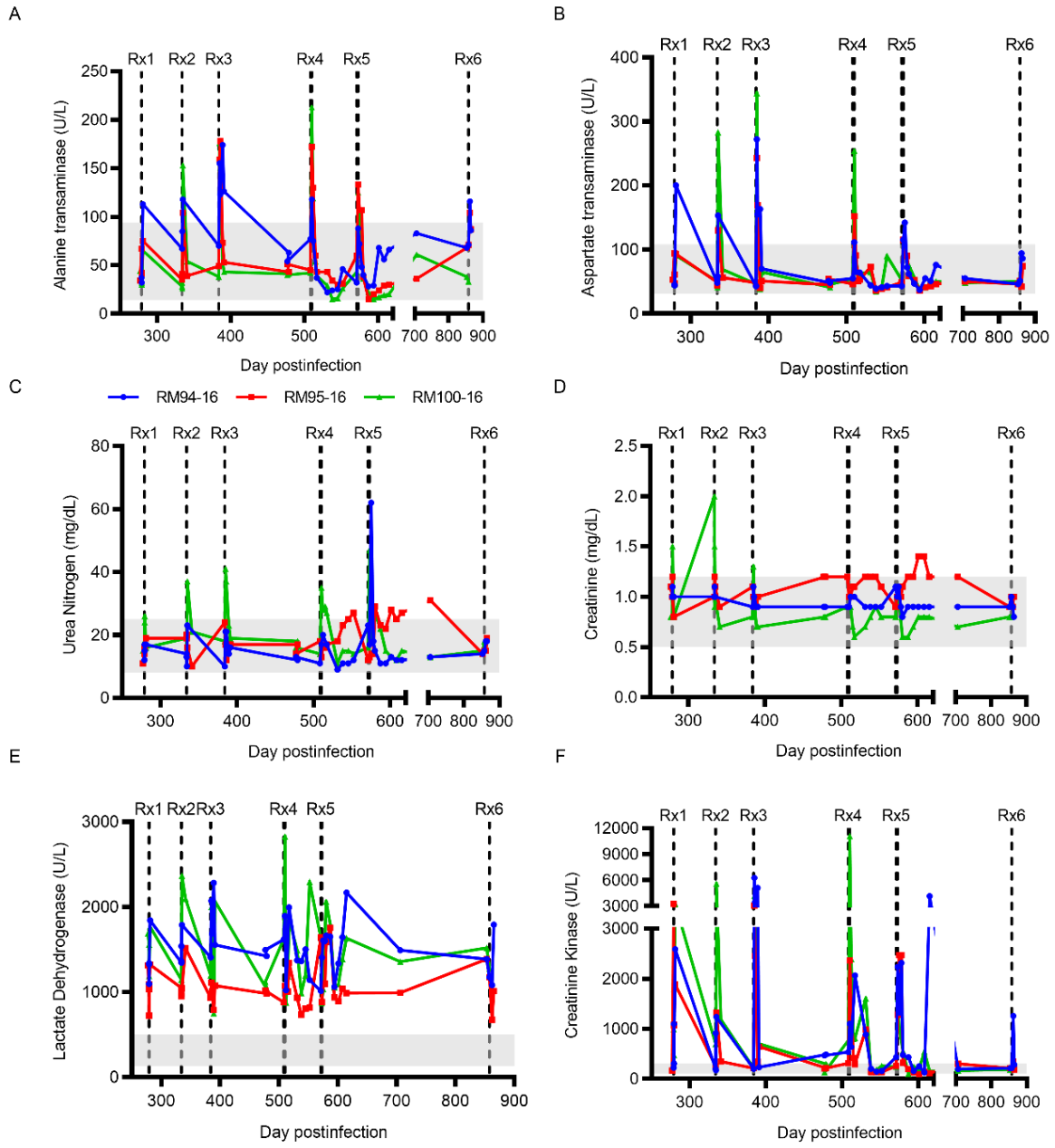

Figure 18. Romidepsin treatment is associated with acute toxicity, but double infusions do not exacerbate.

Serum from animals was used to determine levels of liver markers alanine aminotransferase (ALT) (A) and aspartate aminotransferase (AST) (B), kidney markers urea nitrogen (C) and creatinine (D), and general toxicity markers lactate dehydrogenase (LDH) (E) and creatinine kinase (CK) (F). Grey shaded area represents a reference range from uninfected rhesus macaques.

5.4.3 RMD induces transient loss of circulating lymphocytes.

Following the RMD treatments, the circulating $CD3^+$ (Figure 19A), $CD4^+$ (Figure 19B), and $CD8^+$ (Figure 19C) T cell populations experienced substantial, yet transient, decreases, in line with our previously reported studies [519, 881]. These decreases were rapid, occurring as early as 1 dpt (Figure 19), and were significant after rounds 1 and 2. RMD administration in double infusions resulted in slightly more pronounced reductions of the lymphocyte counts, but these differences did not reach statistical significance (Figure 19). Circulating lymphocytes were then rapidly restored close to pretreatment levels. In some animals (i.e., RM100) the rebounds of the circulating lymphocytes even largely exceeded the pretreatment levels (Figure 19).

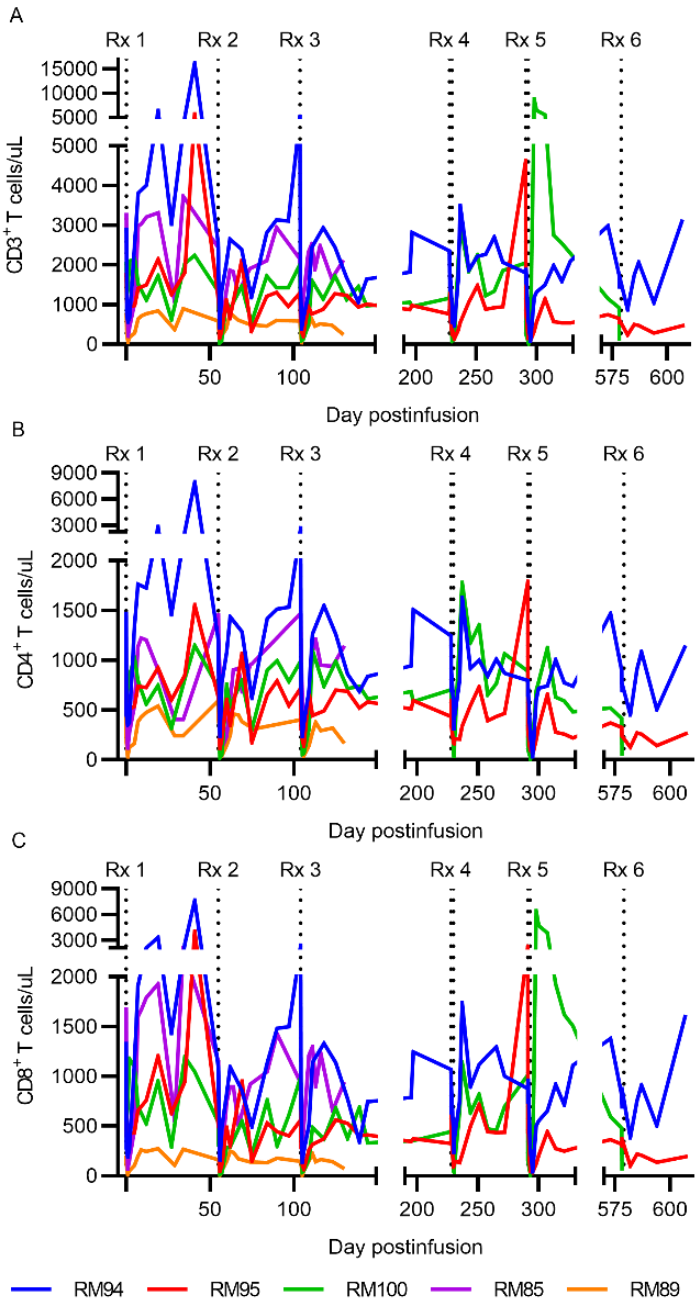

Figure 19. Romidepsin treatment induces transient but pronounced loss of peripheral T lymphocytes.

RMs consistently experienced a transient loss of peripheral CD3+ (A), CD4+ (B), and CD8+ T lymphocytes (C) after romidepsin infusions.

5.4.4 RMD administration induces significant increases of the activated T-cell fraction.

Because T-cell immune activation is related to both SIV reactivation and generating the cell-mediated immune responses, we used multiple flow cytometry biomarkers to assess the levels of T-cell activation. Both $CD4^+$ T cell and $CD8^+$ T cell fractions expressing the general immune activation marker CD69 mildly increased after each RMD infusion (Figure 20A-B). There was a general trend towards an increase in the $CD4^+$ T-cell fraction expressing CD69 within 1 dpt, followed by a rapid return to baseline (Figure 20A). Yet, starting with round 3, we observed statistically significant increases in the CD69 expression by $CD4^+$ T cells between 2 dpt to 40 dpt ($p<0.05$). The fraction of circulating $CD8^+$ T cells expressing CD69 was greater than that of $CD4^+$ T cells (Figure 20B), and the increases in immune activation tended to last longer for $CD8^+$ T cells than $CD4^+$ T cells (Figures 20A and 20B). After switching to the double infusions, we did not observe an additive increase in CD69 expression on $CD4^+$ or $CD8^+$ T cells when compared to single infusions.

Unlike the CD69 expression, consistent increases of the HLA-DR and CD38 co-expression on both $CD4^+$ and $CD8^+$ T cells were observed, albeit smaller for the $CD4^+$ T cells (Figures 20C and D). The increases in the T-cell fractions expressing HLA-DR and CD38 occurred later than those for CD69 and lasted longer (between 5 dpt and 19 dpt), peaking at 19 dpt. Similar increases were seen for rounds 2 and 3 (Figures 20C and D). Yet, when RMD administration was switched to the double infusions, marked increases ($p<0.05$) in the T-cell fractions co-expressing HLA-DR and CD38 occurred, which were more dramatic for the $CD8^+$ T cells.

Finally, we monitored the fractions of the circulating T cells expressing the proliferation marker Ki-67. Ki-67 expression dramatically increased on both $CD4^+$ and $CD8^+$ T cells, peaked between 9-14 dpt and returned to pretreatment levels after 19 dpt (Figures 20E and F). These increases were statistically significant ($p<0.05$). The switch to double infusions resulted in a prolonged increase in Ki-67 expression, with similar trends being observed for both $CD4^+$ T cells and $CD8^+$ T cells (Figure 20E-F).

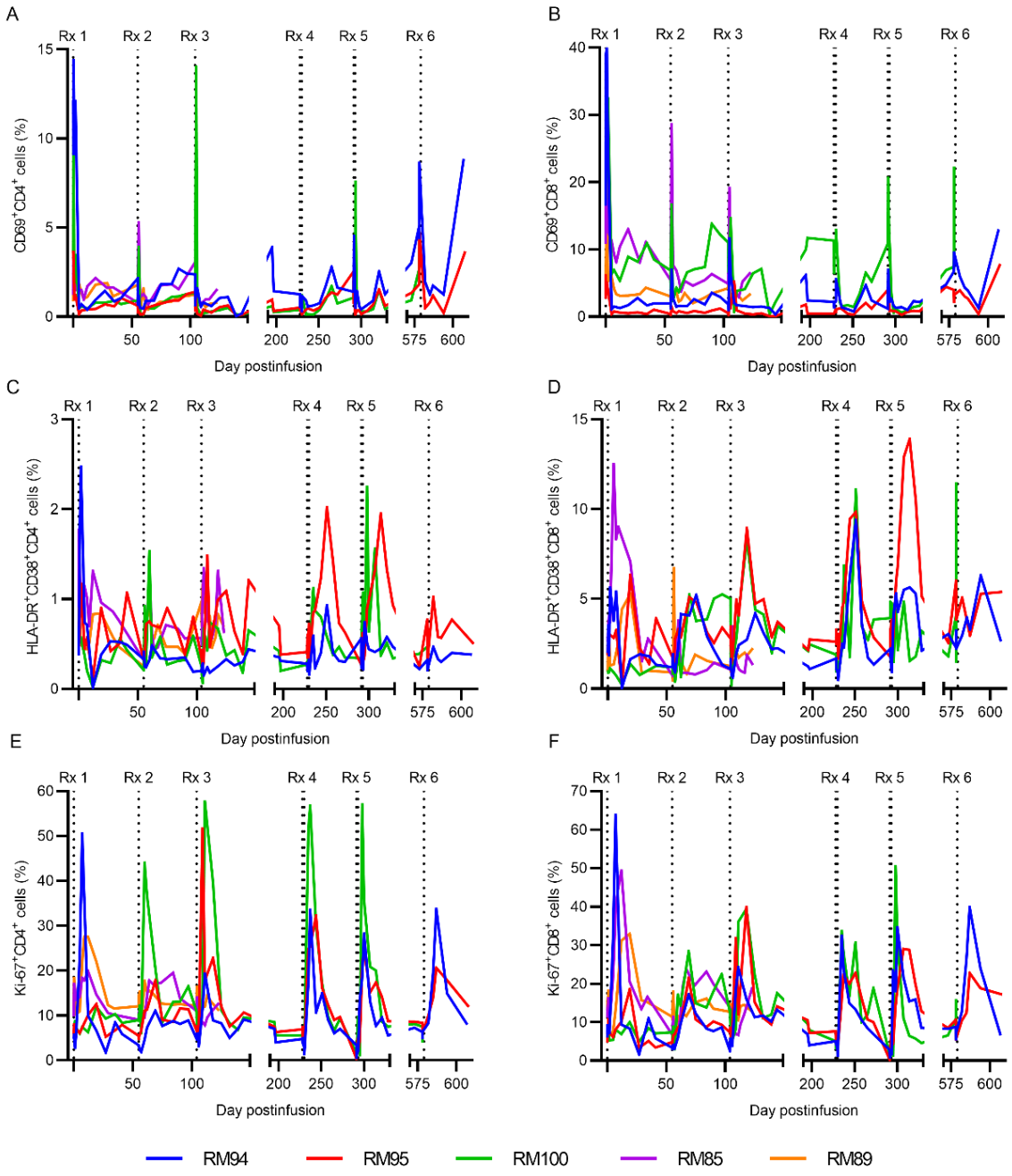

Figure 20. Romidepsin treatment induces immune activation in peripheral T lymphocytes.

RMs consistently experienced increases in three separate markers of immune activation: CD69 expression on CD4+ (A) and CD8+ T cells (B), HLA-DR+CD38+ coexpression on CD4+ (C) and CD8+ T cells (D), and Ki-67 intracellular expression on CD4+ (E) and CD8+ T cells (F).

5.4.5 RMD administration decreases short-term SIV-specific immune responses

RM85 and RM89 were assayed for acute changes in $CD8^+$ T cell activity before and after the second round of RMD treatment with SIV Env and Gag peptide pools, as both animals did not present viral reactivation after two consecutive rounds of RMD treatment. After RMD administration, both animals experienced decreases in the total cytotoxicity of their $CD8^+$ T cells, as illustrated by the total fraction of $CD8^+$ T cells expressing cytokines (e.g., IFN-γ, MIP-1β, IL-2, TNF-α, and the surrogate killing marker CD107a [LAMP-1]) (Figure 21). Between the two animals, there were differences in the initial cytokine production by $CD8^+$ T cells, such that the pretreatment expressing cytotoxic cytokines decreased from 1.09% at 0 dpt to 0.68% at 7 dpt for RM85 and 1.90% at 0 dpt to 0.93% at 7 dpt for RM89 when stimulating with the Gag2 pool. Further decreases were seen at 9 dpt, when the frequency of SIV-specific $CD8^+$ T cells decreased to roughly half of the baseline levels: 0.47% in RM85, and to 0.81% in RM89. At 29 and 34 dpt, functionality varied between the two RMs. The frequency of SIV-specific $CD8^+$ T cells further decreased in RM85 to 0.35% at 29 dpt, with subsequent recovery to 1.02% at 34 dpt. In RM89, the frequency of SIV-specific $CD8^+$ T cells increased at 29 dpt (1.21%), but then decreased at 34 dpt (to 0.26%). Similar trends were seen with the Env and Gag1 peptide pools, with decreases at 7 and 9 dpt followed by recovery to near the pretreatment levels at later time points (Figure 22).

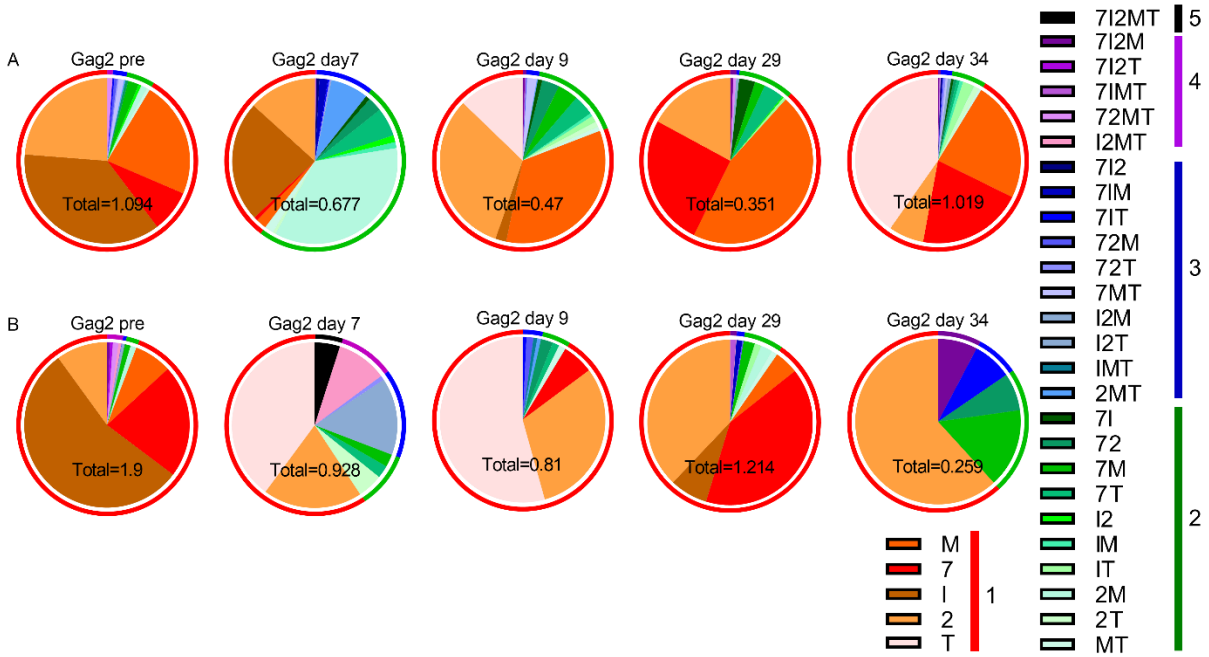

Figure 21. Romidepsin treatment is associated with acute loss of CD8$^+$ T-cell functionality.

After the second round of treatment PBMCs from RM85 (A) and RM89 (B) were stimulated with Gag peptide pools (peptides 69-136) and assayed for IFN-γ (I), MIP-1β (M), IL-2 (2), TNF-α (T), and CD107a (LAMP-1) (7). Total percentages are presented inside of the circles, while color coding of the rings indicate whether 1, 2, 3, 4, or 5 cytokines are being produced. N=2

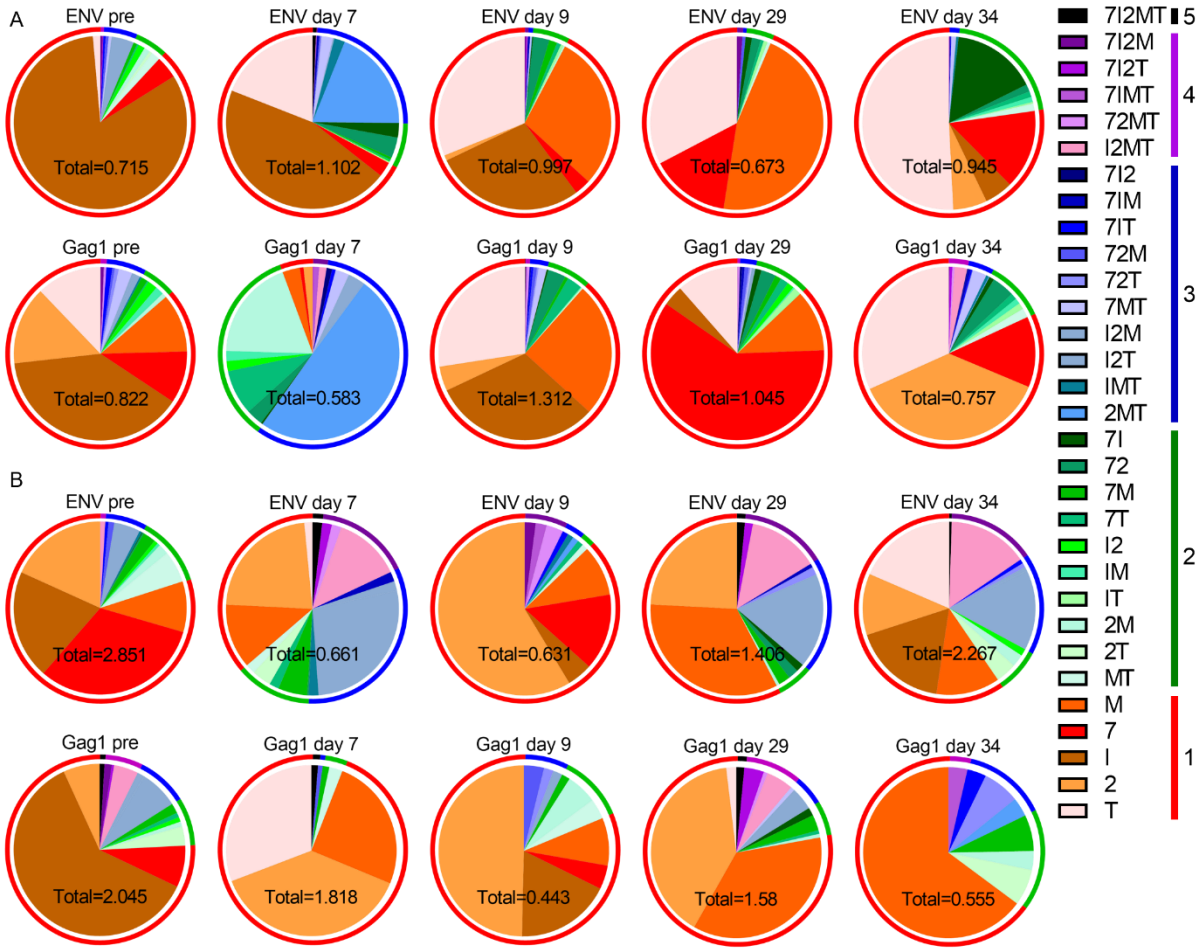

Figure 22. Romidepsin treatment is associated with acute loss of CD8$^+$ T-cell functionality.

After the second round of treatment, RM85 (A) and RM89 (B) were stimulated with Env and Gag1 (peptides 1-68) peptide pools and assayed for IFN-γ (I), MIP-1β (M), IL-2 (2), TNF-α (T), and CD107a (LAMP-1) (7). Total percentages are presented inside of the circles, while color coding of the rings indicate whether 1, 2, 3, 4, or 5 cytokines are being produced.

5.4.6 Repeated RMD treatments boost SIV-specific immune responses.

Because RMD was administered serially, we believed that subsequent infusions with viral reactivation would result in enhanced SIV-specific immune responses, contrary to the short-term changes. We have previously shown that repeated RMD administration does not decrease histone acetylation [519]. Therefore, we stimulated PBMCs taken prior the first infusion and one month after the first, second, and

third infusions with Env, Gag1, and Gag2 peptide pools to assess the cell-mediated immune response against SIV (Figure 23). We found that after treatment with the Env peptide pool (Figure 23), the percentage of $CD8^+$ T cells expressing cytokines related to the cell-mediated response (e.g. IFN-γ, MIP-1β, IL-2, TNF-α, and CD107a) increased from preinfusion at each round tested. At baseline, the average percentage of $CD8^+$ expressing cytokines after stimulation was 0.21±0.08%. After round 1, it was 0.90±0.28%, which then increased to 0.93±0.26% and 1.78±0.54% after rounds 2 and 3, respectively. Similar to Env stimulation, with Gag1 and Gag2 stimulation we observed an increase from baseline after rounds 1 and 3 (Figure 23). In fact, cytokine expression increased from 0.60±0.24% at preinfusion to 0.89±0.23%, 0.54±0.21% and 1.84±0.44% after rounds 1, 2, and 3, respectively with the Gag1 peptide pool. $CD8^+$ T cells stimulation with the Gag2 peptide pool increased their expression of functional cytokines from 0.87±0.37% at preinfusion, to 1.41±0.35%, 0.56±0.18%, and 1.79±0.48% following infusions 1, 2, and 3, respectively (Figure 23). However, these increases in SIV-specific immune responses did not reach significance.

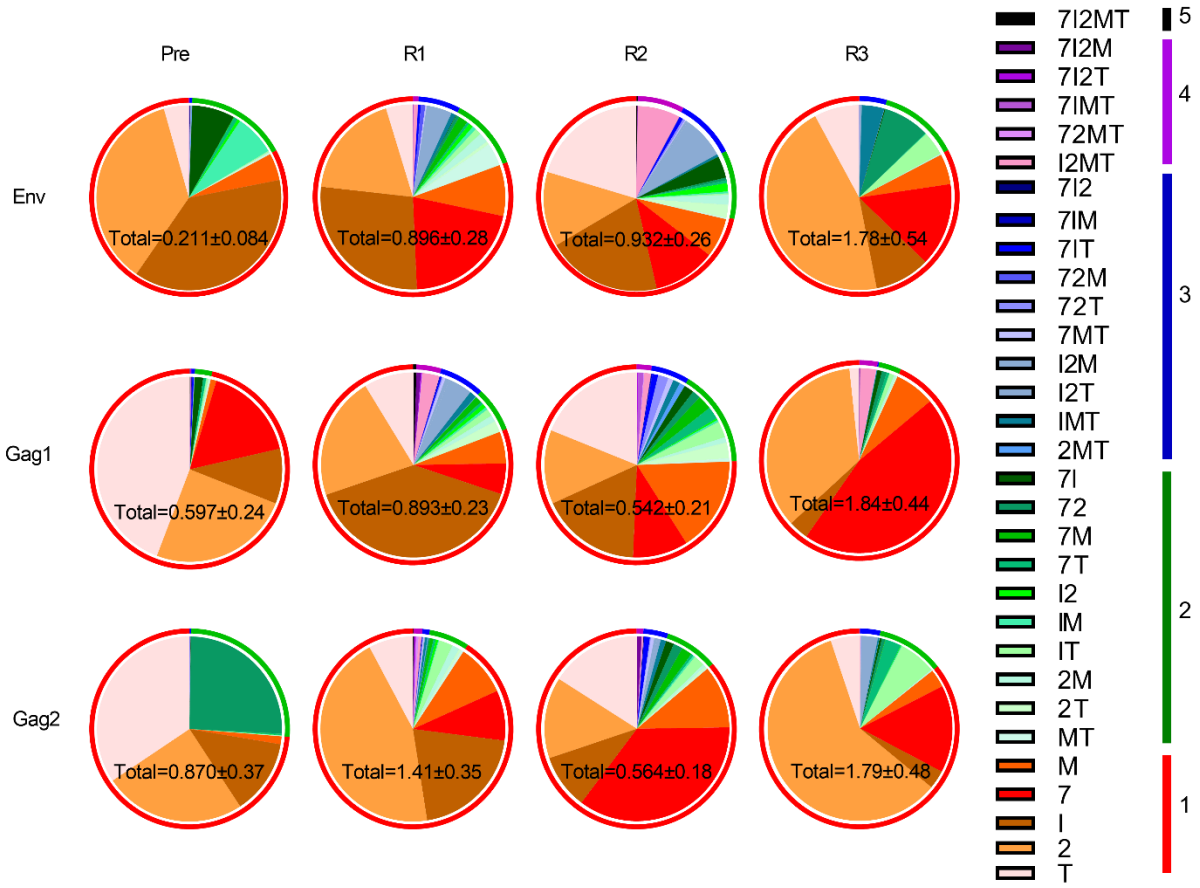

Figure 23. Repeated romidepsin treatments bolsters CD8⁺ T-cell functionality.

Prior to treatment and around 30 days after each round, PBMCs from the RMs were stimulated with peptides pools of Env, Gag1 (peptides 1-68), and Gag2 (peptides 69-136) and stained for IFN-γ (I), MIP-1β (M), IL-2 (2), TNF-α (T), and CD107a (LAMP-1) (7). Total percentages of CD8+ T cells producing cytokines are presented inside of the circles ± the SEM, while color coding of the rings indicate whether 1, 2, 3, 4, or 5 cytokines are being produced. N=5

5.4.7 RMD reactivates latent SIV in RMs.

At each round of RMD administration, relatively robust virus rebounds occurred in RMs in the absence of ART (Figure 24A). After the first round, SIV rebounded in all of the five RMs receiving RMD. The average rebound of virus reached 1,130 copies/mL, and occurred between 7 and 28 days post-treatment (dpt), with the highest peak of 3,342 copies/mL occurring in RM89 at 26 dpt.

After the second round of RMD administration SIV rebounded in three of five animals; no detectable virus was observed in RM85 and RM89 at any time point after the second RMD administration.

The average zenith of viral rebound was 504 vRNA copies/mL of plasma, and occurred between 5 and 29 dpt, with the highest peak occurring in RM94 at 29 dpt (700 vRNA copies/mL).

After the third treatment, SIV rebounded in the same three of five animals; again, no detectable viremia was observed in RM85 and RM89. The average of the virus rebound peaks was 4,304 copies/mL, and occurred between 5 and 21 dpt, with the highest peak occurring in RM100 at 29 dpt (12,194 vRNA copies/mL).

Since no detectable virus rebound was observed in RM85 and RM89 after two consecutive rounds of RMD administration, these RMs were excluded from rounds four and five. The remaining three RMs received "double infusions," i.e., two administrations of 7 mg/m^2 RMD at 48 hours interval. The conversion to double infusions slightly increased peak viral reactivation in all three RMs at the fourth round of treatment, but these increases did not reach statistical significance ($p>0.05$). We observed a similar trend to the single infusions whereby subsequent treatments yielded lower levels of viral reactivation at the fifth round of treatment. The peak viral rebound was 6,356 copies/mL for RM100, while RM95 rebounded up to 139 copies/mL, both drastic decreases from the round 4 peaks of 30,730 and 1,260 copies/mL, respectively. Interestingly, RM94 did not reactivate after the fifth round, but did have a viral blip of 52 copies/mL after the sixth round of RMD administration, while RM95 did not reactivate after the sixth round. However, the sixth RMD treatment was discontinued after the first infusion due to a fatal allergic reaction that resulted in the euthanasia of RM100 at 1 dpt.

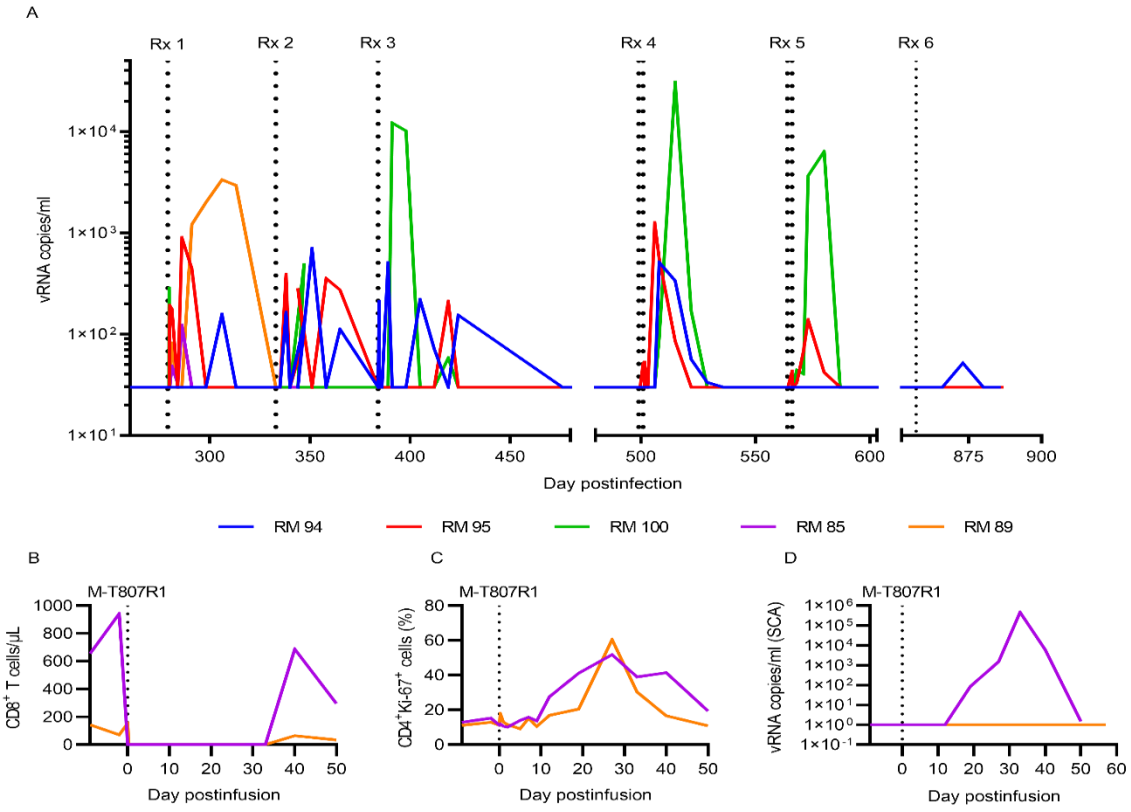

Figure 24. Romidepsin treatment induces reactivation of latent SIV.

Five rhesus macaques were treated with RMD and experienced viral reactivation postinfusion. Subsequent infusions decreased reactivation potency, whereas the addition of a second infusion 48 hours postinfusion ("double infusion") increased viral reactivation (A). After no reactivation in RM85 and RM89, CD8-depleting antibody M-T807R1 was administered. CD8+ T-cell depletion (B) and CD4+ T-cell activation (C) in the M-T807R1 treated animals were confirmed, and plasma viral loads were measured (D).

For RM85 and RM89, instead of continuing with RMD treatments after two rounds without detectable viremia, we proceeded to administer a $CD8^+$ cell-depleting antibody (M-T807R1) as a surrogate method for analytic treatment interruption in these functional cured RMs, in which the virus is controlled in the absence of ART [882]. After infusion of M-T807R1, $CD8^+$ T cells were depleted by >99% (Figure 24B) and a massive increase in the fraction of $CD4^+$ T cells expressing Ki-67, a marker of cell proliferation, occurred (Figure 24C). Plasma virus in RM85 rebounded up to 459,918 copies/mL at 33 dpt (Figure 24D), mirroring the expression of Ki-67 in the $CD4^+$ T cells. Surprisingly, RM89 did not reactivate virus above

our limit of quantification (1 copy/mL) (Figure 24D), even with the drastic increase of Ki-67 expression in $CD4^+$ T cells.

5.4.8 SIV-specific immune responses are associated with decreased viral rebound.

Interestingly, the two animals that did not reactivate after two consecutive rounds of single infusion RMD (RM85 and RM89) had greatly increased $CD8^+$ T cell reactivity compared to RM94, RM95, and RM100, such that even the preinfusion timepoints were at 0.42±0.23%, 1.25±0.88%, and 2.05±1.5% for the Env, Gag1, and Gag2 peptide pools, respectively (Figure 25).

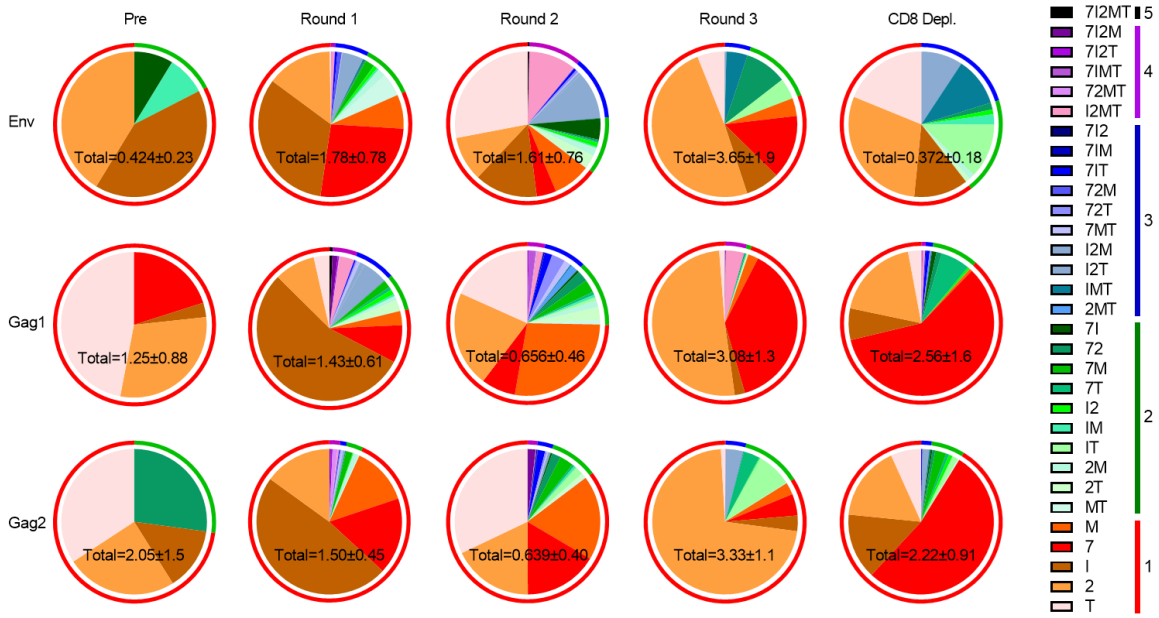

Figure 25. Repeated romidepsin treatments increase $CD8^+$ T-cell functionality.

RM85 and RM89 were stimulated with Env, Gag1 (peptides 1-68), and Gag2 (peptides 69-136) peptide pools and assayed for IFN-γ (I), MIP-1β (M), IL-2 (2), TNF-α (T), and CD107a (LAMP-1) (7). Total percentages are presented inside of the circles, while color coding of the rings indicate whether 1, 2, 3, 4, or 5 cytokines are being produced. N=2

Meanwhile, RM94, RM95, and RM100 were at 0.069±0.03%, 0.17±0.08%, and 0.086±0.05% for the Env, Gag1, and Gag2 peptide pools, respectively (Figure 26). Further, the percentages of reactive SIV-

specific cells after infusions were also higher in RM85 and RM89, providing a potential explanation for the viral control in these two animals. Of RM94, RM95, and RM100, RM94 had the greatest increases: from 0.15% to 0.78% and 1.9% for pretreatment, round 3 and round 5, respectively, as an average of the three peptide pools. Interestingly, RM95 after round 6 also had a large increase to 1.3% of $CD8^+$ T cells expressing cytokines and did not reactivate virus. However, RM100 had their highest CD8 values after round 3, 0.95%, and reactivated virus nonetheless.

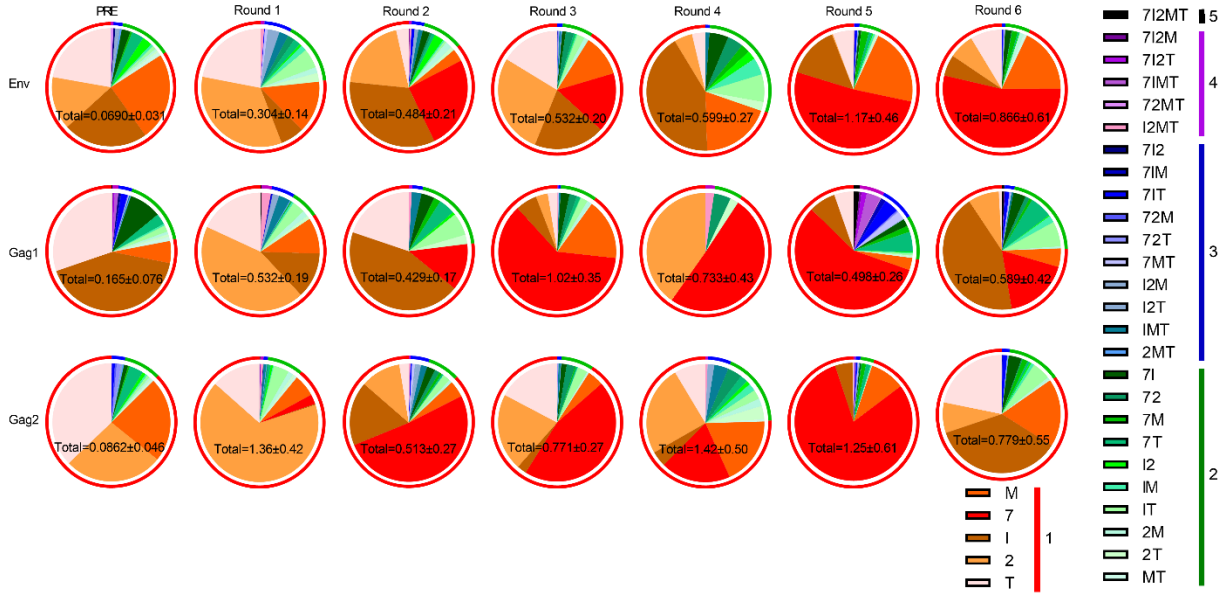

Figure 26. Repeated romidepsin treatments increases and maintains $CD8^+$ T-cell functionality after six rounds of treatment.

RM94, RM95, and RM100 were stimulated with Env, Gag1 (peptides 1-68), and Gag2 (peptides 69-136) peptide pools and assayed for IFN-γ (I), MIP-1β (M), IL-2 (2), TNF-α (T), and CD107a (LAMP-1) (7). Total percentages are presented inside of the circles, while color coding of the rings indicate whether 1, 2, 3, 4, or 5 cytokines are being produced. N=3; round 6 n=2

5.4.9 RMD treatment transiently diminishes the replication competent reservoir.

Using longitudinal sampling after each round of RMD administration, we tracked changes in cell-associated SIV DNA (CA-vDNA). Samples were taken from timepoints closest to 30 days postinfusion to avoid potential interference from active viremia. Although, in average, there was a small decrease in CA-vDNA over time in RMs receiving RMD, individual animals had variable responses to treatment (Figure

27A). Thus, in three RMs (RM85, RM89 and RM95) an average decrease of 77% in the CA-vDNA levels occurred over the course of RMD treatments, in RM94 the CA-vDNA levels increased, and, finally, in RM100 the CA-vDNA levels remained virtually unchanged during the follow-up. After the first RMD treatment, a decrease in the viral burden was observed in three out of five RMs, with the viral reservoir decreasing below the detection threshold for RM89. However, RM89 did contain detectable viral DNA after the other rounds of treatment, nonetheless remaining below its baseline level of 170 copies/10^6 cells. Further, RM85 had a large increase in viral DNA after the CD8 depletion, most likely due to reseeding of the reservoir as a result of the massive viral reactivation. After the switch to double infusions, increased CA-vDNA copies were observed for all three RMs (RMs 94, 95, and 100), with a subsequent decrease after round 5. CA-vDNA decreased again after round 6 in RM95, but not in RM94 (Figure 27A). These changes in CA-vDNA were not statistically significant.

Due to the inherent limitations of using CA-vDNA to measure the reservoir [473], we further characterized the dynamics of the reservoir in RMs treated with RMD in an outgrowth assay. $CD4^+$ T cells isolated from PBMCs through negative selection were cocultured with MOLT-4 clone 8 cells, which are susceptible to SIVsab infection, after stimulation with PMA and ionomycin. The PBMCs were taken at timepoints closest to the start of the following RMD administration when no viremia was detected to allow for normalization after potential reactivation and immune activation. After 17-19 days in coculture, the presence of intracellular p27 in MOLT-4 cells was used as the determining marker of viral outgrowth. While viral reactivation decreased during the latter rounds of RMD treatment, the presence of replication-competent virus did not complementarily decrease as expected. Instead, only two RMs (RM89 and RM94) demonstrated a marked decrease in the levels of replication-competent virus (Figure 27B). RM89 did not reactivate virus after the second or third RMD rounds, nor following $CD8^+$ cell depletion. However, only after $CD8^+$ T-cell depletion did the amount of replication competent virus significantly decrease, with 0/10 $CD4^+$ T cell cocultures staining positive for intracellular p27 ($p<0.01$). Similarly, RM94 displayed viral outgrowth in only 2/7 $CD4^+$ T cell cocultures after the fifth round of treatment ($p<0.05$), indicating a decrease in the levels of replication competent proviruses. However, after round six, 5/5 $CD4^+$ T cell

cocultures presented with viral outgrowth. Given the changes in viral reactivation, we further investigated necropsy-collected tissues for RM89, RM94, and RM95. RM89 and RM95 did not reactivate prior to necropsy, yet, in the necropsy samples, virus outgrowth occurred in both animals, as well as in RM94, which had a viral spike of 52 copies/mL at 16 dpt of round 6, pointing to the presence of replication-competent proviruses within the superficial and mesenteric lymph nodes, jejunum, and spleen (Figure 27C) with only the jejunum of RM95 showing potentially diminished viral reservoir at 3/5 wells positive for p27.

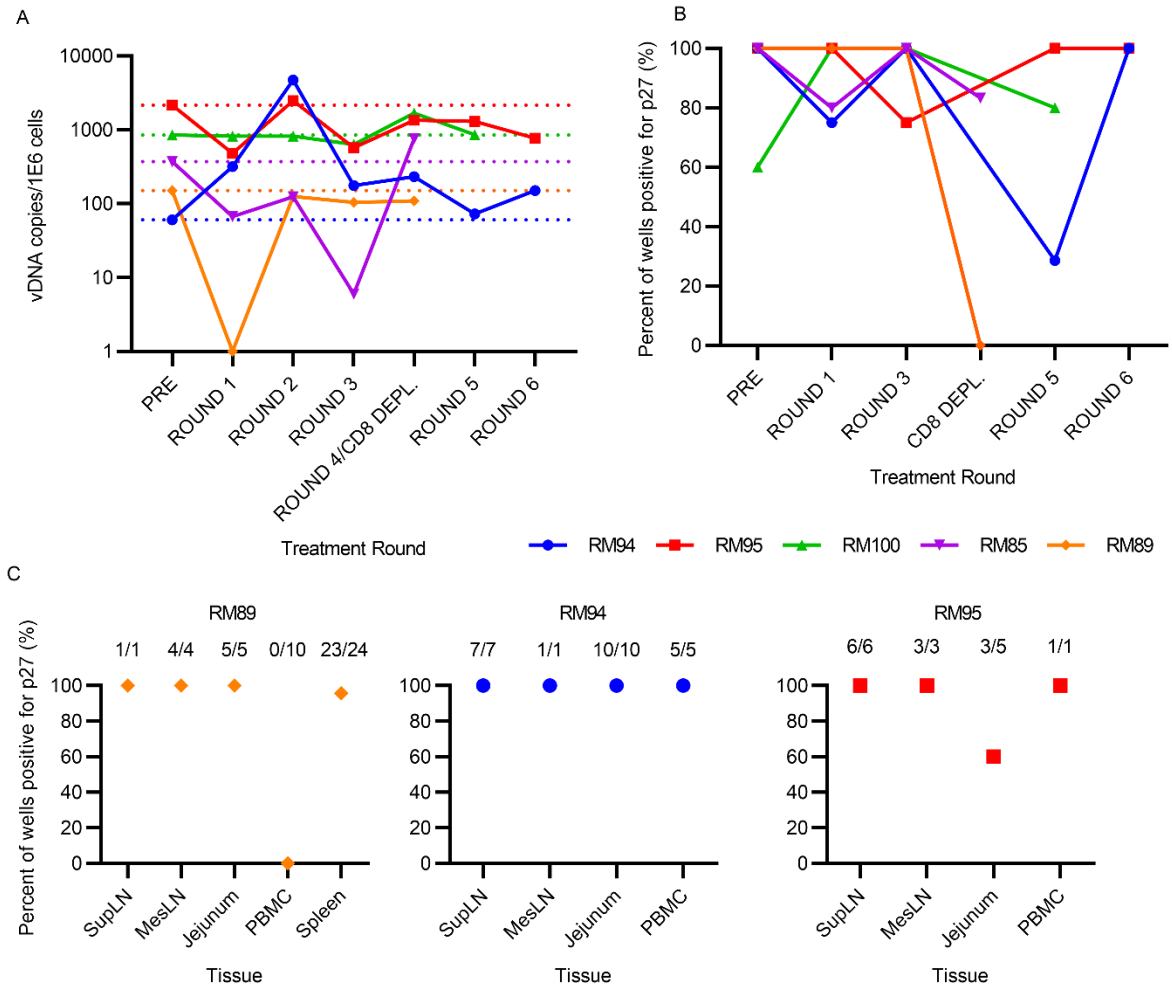

Figure 27. Romidepsin infusion in a rhesus macaque model of SIV functional cure does not yield consistent decreases in cell-associated viral DNA or replication competent virus.

Cell-associated vDNA was quantified by qPCR (A). Viral outgrowth was measured by p27 intracellular staining after co-culture of negatively selected CD4+ T cells with MOLT-4 cells at each round of treatment (B) and in tissues at necropsy (C). Dashed lines in (A) are baseline CA-vDNA levels for each animal.

5.5 Discussion

In this study, by using a SIV/RM model of spontaneous functional cure and healthy immune responses, we found that multiple rounds of RMD administration bolstered the immune responses, gradually decreased viral reactivation, and in one animal, diminished the circulating reservoir of replication competent virus. Our results also show that RMD administration has the capacity to alter the reservoir resulting in a discrepancy in the levels of replication competent proviruses between blood and tissues.

In this model, in which functional cure is achieved spontaneously, without ART, the viral rebound observed after RMD administration was not solely due to viral reactivation, but also to *de novo* infections, which had an additional effect of boosting the healthy immune response against SIV. Though the data are variable, the SIV-specific immune response was slightly hindered in the days immediately following treatment, yet not significantly, in agreement with previous data demonstrating a nonsignificant decrease in $CD8^+$ T-cell functionality directly after RMD administration [881]. Nonetheless, the longitudinally bolstered SIV-specific immune responses post-RMD infusion were likely due to the virus reactivation, allowing for an additional strong immune response to potentially activate new naïve $CD8^+$ T cells or to induce additional expansion of SIV-specific $CD8^+$ T cells. The concept of improved viral control with repeated reactivation events is supported by increased viral control of HIV after structured analytic treatment interruptions which allowed for plasma viremia to become detectable prior to reinitiating ART [883]. Further, the increase in T-cell activation after each treatment, despite undetectable viremia, points to another possible reason for the observed decreased viral reactivation after RMD; whereby CD8 cells were better primed to react to any virus-producing cell. In fact, HLA-DR and CD38 co-expression on $CD8^+$ T cells correlates with increased HIV-specific responses in PWH [884]. It is thus not surprising that every subsequent round of RMD administration did not elicit the same reactivation as the preceding rounds. This points to the critical role of the cellular immune responses for virus control, off and on ART [885], or after viral reactivation. This conclusion is further supported by the case of one animal (RM85), in which repeated

RMD administrations gradually abolished virus reactivation, yet, $CD8^+$ cell depletion led to a massive virus rebound, in the range of the viral levels observed during the acute infection.

Upon investigation into the cell-associated viral DNA, we found that the CA-vDNA copies per million PBMCs changed in three different manners. RM100 was virtually unchanged throughout the infusions, with only a small increase in CA-vDNA after a large reactivation event at the fourth infusion. RM94 initially increased after the first two infusions of RMD, but then decreased at each round towards baseline, concomitant with decreases in viral reactivation events after infusions. Finally, three of the five RMs maintained decreased CA-vDNA through round 3 for RM85 and RM89 and round 6 for RM95. RM85 and RM89 showed discrepant responses after $CD8^+$ T-cell depletion: RM85 greatly reactivated virus and CA-vDNA increased past baseline after depletion, while RM89 had minimal changes in CA-vDNA after $CD8^+$ T-cell depletion. The increase for RM85 is unsurprising due to the nature of the study in which the animals are ART-naïve, thus the viral reactivation after $CD8^+$ T-cell depletion for RM85 likely initiated *de novo* infections, thereby expanding the reservoir and increasing the CA-vDNA. Although the CA-vDNA is not a perfect marker, there are associations between the changes in CA-vDNA and viral replication: massive or prolonged virus reactivation resulted in increased levels of CA-vDNA (e.g. RM100 after the fourth round of infusions and RM94 after the second round of infusions). Further, when subsequent reactivation events were diminished, particularly beginning after the second infusion, CA-vDNA was decreased in RM94 and RM95. Finally, RM85 and RM89 did not reactivate after the second and third infusions, and their CA-vDNA was diminished relative to baseline. Interestingly, RM89 had a large and prolonged reactivation after the first RMD infusion and resulted in undetectable CA-vDNA, which matched the massive increase in SIV-specific $CD8^+$ T-cell functionality and polyfunctionality measured after the first infusion.

While the CA-vDNA indicated small changes in the size of the viral reservoirs in functionally cured SIVsab-infected RMs treated with RMD, the PCR-based assays do not take into consideration the replication competency of the viral sequences amplified. To address this issue and assess the replication competence of the virus in the reservoirs, we utilized a flow cytometry-based viral outgrowth assay [24, 879, 880]. This assay showed a loss of replication competent proviruses in the peripheral blood of both

RM94 and RM89 after round 5 and CD8 depletion, respectively. By comparing viral loads and outgrowth with the SIV-specific $CD8^+$ T cells, our data strongly implicate $CD8^+$ T cells in the viral control: (i) The functionality of the SIV-specific $CD8^+$ T cells greatly increased in both these RMs in later rounds of RMD administration; (ii) after round 6, RM95 produced more cytokines and did not reactivate, but still had viral outgrowth; (iii) after round 6 RM94 had a much lower percentage of SIV-specific $CD8^+$ T cells and reactivated after RMD treatment; (iv) RM85 did not reactivate after the second or third infusion, but reactivated after $CD8^+$ T-cell depletion. Thus, these results support the conclusion that $CD8^+$ T cells are playing a large role in the control of virus and may have cleared a portion of the circulating reservoir.

An alternative explanation is that NK cells play a substantial role in the functional cure. M-T807R1A does not discriminate between $CD8^+$ T cells and NK cells, due to the presence of CD8α on NK cells [885], resulting in partial depletion.

Meanwhile, after experimental depletion, recovering $CD8^+$ cells yielded a significantly greater fraction that were MHC/Gag tetramer positive [886]. As a result, they may provide greater suppression, establishing a stranglehold on infected cells and preventing viral expansion or eliminating cells that may have escaped previous detection by the NK cells. Yet, this also puts a damper on the SIV-specific $CD8^+$ T cell response assays for after CD8 depletion, as these cells may be artificially boosted through this mechanism, and the true reactivity to the antigens may be lower if given more time for the cells to stabilize MHC/Gag.

In both animals, $CD8^+$ cell depletion was associated with increases in B cells with proliferating potential (Figure 28). Thus, noncytolytic control through B cells is another possible explanation for the lack of reactivation in RM89, with the caveat that we did not test antibody affinities.

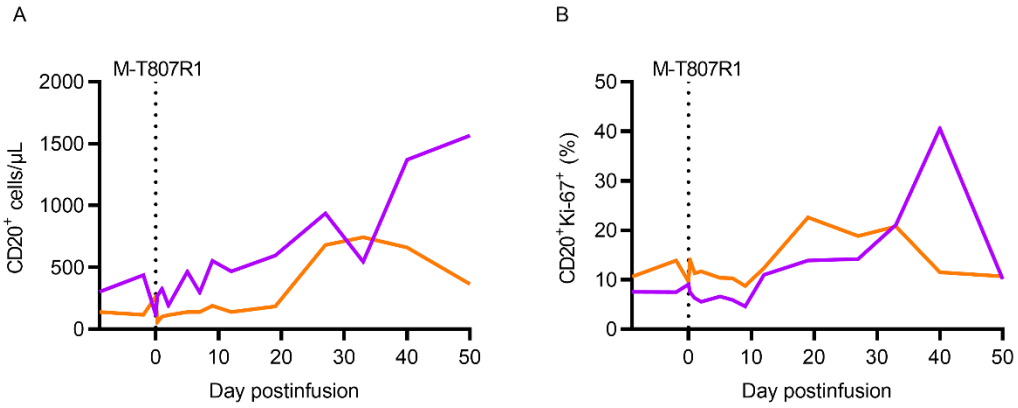

Figure 28. CD8$^+$ T-cell depletion is associated with increased B-cell activation.

RM85 and RM89 received CD8 depleting antibody M-T807R1. B cells (CD3-CD20+) (A) and B cell Ki-67 expression (B), a marker of proliferation, were increased postinfusion.

Viral outgrowth was observed from the gut and LN samples from RM89, RM94, and RM95 at necropsy. The observed discrepancies between the lack of inducible proviruses in CD4$^+$ T cells and outgrowth from tissues in RM89 and RM94 may be due to the different immunophenotypes of the CD4$^+$ T cells in blood (where the pool is comprised of more naïve cells) and the intestine (where the pool is comprised of more effector and memory cells). Note also that the gut comprises 60% of the T lymphocytes in the body [887, 888]. Additionally, it has a higher viral burden, both DNA and RNA, than the blood [473, 860, 889, 890], contributing up to 83-95% of the HIV-infected cells in humans, with different mechanisms driving latency in the gut *versus* the blood [891]. We also reported that RMD drives CD3$^+$ T cell homing to the gut and LNs in RMs [830], which could further diminish the peripheral SIV reservoir if tissue-homed infected cells do not reenter circulation. Altogether, these rationales may explain the presence of replication competent virus in the gut and LNs, while no viral outgrowth can be detected peripherally. It also can explain how RM94 decreased in viral reactivation and outgrowth after the fifth round of infusions, yet still reactivated the virus after the sixth RMD round, as there was likely reentry of reservoir cells into the circulation from tissues. The mechanism by which tissue sites harbor replication competent virus, but do not reactivate after RMD nor M-T807R1 is currently not known. We have previously demonstrated that RMD half-life in the intestine and LNs is longer than in blood [830]. However, in patients with cutaneous

T cell lymphoma the compartmental response of the LNs to RMD is not as strong as the blood or skin responses [892]. Thus, the overall effects of RMD may be diminished in the gut and LN, supporting the presence of replication competent virus at these sites.

Nonetheless, the discrepancy between blood and tissue that we document here is an essential piece of data, which is also supported by previous case studies. The two famous cases of the Mississippi baby [409] and the Boston patients [408] focused upon measurements of the levels of virus in PBMCs and plasma to determine whether the patients were functionally cured. However, as demonstrated in these cases [893-895], the lack of viremia and cell-associated DNA/RNA from plasma and PBMCs at the cessation of ART, and even months later, were not predictive of virus rebound. In our cases the obvious explanation is the presence of replication competent virus in tissues. Note, however, that the post-treatment controllers in the Visconti study, which is one of the largest cohort of functionally cured patients, had detectable HIV DNA in PBMCs, yet achieved sustained viral remission [411]. As such, our results suggest that the functional cure should be predicted by testing tissue samples, in addition to circulating cells and plasma.

Another novelty of our study is the use of the double infusion regimen in RMs 94, 95, and 100. We demonstrated that the double infusions did not extend the delay for immune recovery and there was no significant increase in toxicity. Although one animal was euthanized, this was due to a severe allergic reaction and not specific toxicity from RMD. Importantly, we identified a prolonged, increased $CD8^+$ T-cell activation after double infusions, which resulted in the greatest increase in SIV-specific $CD8^+$ T-cell functionality for these three animals. This is not surprising as the enhanced $CD8^+$ T-cell activation likely bolstered responsiveness to antigen.

In conclusion, we report that repeated RMD administrations resulted in a gradual diminishment of viral reactivation in a model of spontaneous functional cure of HIV infection. Further, the switch to RMD "double infusions" also increased viral reactivation with the same pattern of subsequent diminishment, and surprisingly, further boosted the SIV-specific immune responses. Remarkably, no viral reactivation was observed in an animal in which $CD8^+$ cells were experimentally depleted *in vivo*. Compounded with the lack of viral outgrowth from PBMCs, this feature provides evidence for a successful reduction of replication

competent SIV in circulation. Further testing in tissues, however, presented viral outgrowth, suggesting that the correlates of the HIV remission must be investigated beyond blood in order to conclude a cure/functional cure. Nevertheless, these data provide a glimpse of potential viral control through the cell-mediated immune response when in an environment of a healthy immune response and thereby suggests that before deploying HIV cure strategies, the first aspect to tackle should be the restoration of the immune system and reversion of T-cell exhaustion in chronically infected PWH.

6.0 Conclusions

ART has an exquisite ability to suppress HIV replication, thus extending life expectancies of PWH to nearly that of uninfected persons. However, ART neither eradicates the HIV proviruses from infected cells nor completely ameliorates the chronic immune activation and inflammation that result from infection. This fuels the growing issue of non-AIDS comorbidities in the aging PWH population [339] and points to the need of new therapeutic paradigms for an HIV cure. Although two cases of HIV cure, the "Berlin patient" [386] and the "London patient" [387] demonstrated that a cure is feasible, the approach leading to a cure in these two patients is not scalable, the procedures are very risky and expensive and, as such, no other instances of stem-cell transplantation, nor other therapeutic interventions have resulted in complete viral remission and absence of detectable viral DNA from the PWH.

Thus, the goals of this dissertation were to investigate two different approaches with potential to help progress towards a cure/functional cure of HIV: the use of cyclophosphamide, as either a Treg depleting agent or a cytoreductive agent, and the use of Romidepsin as an LRA in HIV cure strategies.

In chapter 3, we tested the hypotheses that cyclophosphamide could be used as a regulatory T-cell depleting agent in low doses or a cytoreduction agent in high doses in a rhesus macaque model of SIV infection. However, with low dose Cy, we did not induce viral reactivation as achieved with other Treg depletion agents [505, 828]. It was not through a complete absence of effect of the drug. Treg depletion occurred, as did a significant increase in immune activation in the aviremic RM; yet, our intervention did not lead to any virological effect. In the RM with active viremia, Cy decreased viral loads, a surprising result given the very mild Treg depletion and immune activation. Granted, an increase in CD69 expression on $CD8^+$ T cells, which was observed in the animals receiving Cy would be indicative of low immune activation, but this did not reach levels seen with other depletion agents which could otherwise explain potential viral suppression. The observed effect could be explained by a reduced suppression exerted by the depleted Treg population on already active SIV-specific $CD8^+$ cells, bolstering the anti-SIV response without drastic increases in immune activation. However, Cy treatment also depleted $CD3^+$ T cells by 40%,

demonstrating a lack of Treg specificity and, therefore, an alternative explanation is that the overall loss of cells from the periphery may be the driving factor in the decreased viral loads.

We next used high dose Cy with our RM model of functional cure and depleted nearly all immune cells from the periphery. This depletion event resulted in massive viral reactivation to the extent of acute infection, as is normally seen with $CD8^+$ T-cell depletion in this model [96, 633]. However, because these RMs were not on ART, there is no way to know whether this is due to true reactivation events or *de novo* cell infection from a small population of reactivated cells. Thus, we repeated the experiments in ART-treated SIVmac239M-infected RMs using a modified, decreased dosage of Cy for safety. Unfortunately, two animals required euthanasia at 8 dpt with unexpected adverse effects from ART and Cy coadministration and an additional animal was lost to surgical complications. Additionally, there was no viral reactivation on ART, suggesting that the majority of viral reactivation without ART was indeed from *de novo* infections. In conclusion, our studies to examine the use of different dosing regimens of cyclophosphamide for HIV therapeutic strategies failed to achieve their goals. With Treg depletion, we failed to induce viral reactivation and only increased immune activation by a small amount relative to other Treg depletion agents [505, 828]. Utilizing high dose cyclophosphamide, we were able to achieve substantial cytoreduction, but when cytoreduction was performed on ART, as would be necessary if used as an HIV therapeutic, unacceptable toxicity and morbidity occurred. Therefore, we unfortunately cannot recommend pursuing the use of cyclophosphamide as a Treg depleting agent nor cytoreductive agent for the purpose of HIV therapeutics.

In the next set of experiments, we switched to a classical LRA-based "shock and kill" approach and investigated the use of RMD in SIV-uninfected rhesus macaques. We have previously reported that RMD can reactivate latent SIV [519, 747], but we also observed transient loss of $CD4^+$ and $CD8^+$ T cells at levels that exceeded those explained by apoptosis. Thus, our RMD infusions were conducted to establish a baseline understanding of RMD pharmacokinetics and its effects on immune populations. We reported that, unlike circulation, which has a quick clearance and a half-life of 15.3 hours, the tissue compartments retain RMD for significantly longer. In fact, RMD was still present in the intestine and LNs at 10 days post-

infusion, although the mechanism of retention has not been elucidated. RMD infusions resulted in moderate liver toxicity as demonstrated by increases in AST and ALT well beyond the normal range for rhesus macaques. The transient increases observed in the general toxicity markers CK (which we have shown that might be partially increased by isoflurane anesthesia) and LDH further support a transient systemic toxicity with rhabdomyolysis, which match the loss of lymphocytes from the periphery. However, apoptosis did not fully explain the changes because of: (i) the rapid recovery of lymphocytes in the circulation, with full $CD4^+$ T cell recovery as early as 7 dpi; (ii) minimal changes in the proportion of apoptotic $CD4^+$ and $CD8^+$ T cells by flow cytometry; (iii) lack of extensive Ki-67 expression indicates that a massive proliferation event is not the source of cells. Additionally, the extensive use of isoflurane anesthesia due to our sampling schedule can also be a cause of lymphopenia [871, 872]. We utilized *in vitro* assays to investigate the potential causes of the lymphopenia beyond apoptosis or medical interventions, such as isoflurane anesthesia. We found that *in vitro* administration of RMD resulted in decreased surface expression of CD3, CD4, and CD8, complementary to increases in double negative CD3 T cells, which has been shown to occur with PMA stimulation as well [873]. Further, surface expressions of homing markers CCR7 and CCR9 were substantially increased on both $CD4^+$ and $CD8^+$ T cells, with CCR4, CCR5, and $\alpha4\beta7$ increasing on only $CD8^+$ T cells. Thus, with our data showing an increase in $CD3^+$ T cells in the lymph nodes and gut after RMD treatment, we postulated that RMD induces the lymphopenia in the circulation through multiple mechanisms, including: (i) apoptosis; (ii) downregulation of surface markers CD3, CD4, and CD8; (iii) upregulation of LN and gut homing markers and migration of peripheral lymphocytes to the LN and gut. We finished this study by showing that, upon RMD administration to the RMs, there is a decrease in the levels of cytotoxic molecules in $CD8^+$ T cells after nonspecific stimulation with PMA and ionomycin, although these changes did not reach significance. We thus demonstrated that RMD is safe to use for HIV cure strategies, but would benefit from being combined with other therapeutic agents that could boost the cell-mediated immune response to complement RMD's negative impact on the cellular immune responses.

We further expanded upon our previous RMD study and administered repeated RMD infusions to SIVsab-infected rhesus macaques, our model of SIV functional cure [96, 633]. This model reproduces many

viral features of acute infection, including early reservoir seeding, but is followed by complete control of SIV replication and a healthy immune response, where functional cure can be temporarily reverted with $CD8^+$ T-cell depletion [96, 633]. As RMD has been demonstrated to have the ability to reactivate SIV [519, 747], we hypothesized that with a healthy immune system, repeated infusions will progressively enhance the SIV-specific immune responses and decrease the size of the SIV reservoir. Indeed, we observed that repeated infusions yielded decreased reactivation at each subsequent infusion, which was boosted by changing to "double infusions", two infusions separated by 48 hours. Further, as two animals (RM85 and RM89) did not reactivate SIV after the second and third round of RMD infusion, we treated the two animals with a CD8-depleting antibody instead of double infusions to investigate the presence of replication competent virus as a surrogate for analytical treatment interruption [633, 882]. However, in our animals after repeated reactivations with RMD, $CD8^+$ T-cell depletion reactivated SIVsab in RM85, but not RM89, suggesting a lack of replication-competent virus in this animal. We followed up with measuring the cell-associated viral DNA as a marker of the viral reservoir and found that both RM85 and RM89 had decreases in CA-vDNA after RMD infusions but CA-vDNA was not completely cleared in any of these animals. Given the inherent impossibility of CA-vDNA measurement to distinguish between replication-competent proviruses and defective proviruses, we measured viral outgrowth by coculture of negatively selected $CD4^+$ T cells from PBMCs. We found that after $CD8^+$ T-cell depletion, RM89 yielded no viral outgrowth from 2.5 million $CD4^+$ T cells, while RM85 had viral outgrowth. Of the three animals that proceeded to double infusions, RM94 and RM95 did not reactivate at rounds 5 and 6, respectively and CA-vDNA similarly decreased from the previous rounds. Additionally, RM94 had substantially decreased outgrowth at round 5, but returned at round 6, and RM95 nevertheless still had inducible virus, as demonstrated by the viral outgrowth. We subsequently tested viral outgrowth from tissues at necropsy from RM89, RM94, and RM95, where we found an abundance of replication competent virus in the tissues, although RM95 had reduced replication-competent provirus in jejunal $CD4^+$ T cells. These results thus support at least a partial reduction in the replication competent reservoir. Further, they also identify an important discrepancy between blood and tissues, which has also been reported for the cases of suspected, and later debunked, cure [409, 893-895]. We completed our study by investigating the impact of RMD on both short-term and

long-term longitudinal SIV-specific immune responses. Although our previous study showed decreased $CD8^+$ T-cell activity with general (PMA/ionomycin) stimulation, we believed that because these animals present with a healthy immune system, the viral reactivation combined with immune activation by RMD would result in an increase of SIV-specific immune response over time. In fact, RMD infusions bolstered the SIV-specific $CD8^+$ T cells in all animals, demonstrated by substantially increased percentages of $CD8^+$ T cells expressing cytotoxic molecules and polyfunctionality after stimulation by Env and Gag peptide pools. Additionally, our data strongly implicated $CD8^+$ T cells as a major mechanism of viral control in our animals: where SIV-specific $CD8^+$ T-cell responsiveness was increased, viral reactivation was decreased or absent. In the cases of RM89 and RM94, even the levels of inducible virus, as determined by the viral outgrowth assay were diminished. Thus, the important takeaways from our study are three-fold: (i) The presence of replication competent proviruses in the tissues when no viral reactivation occurred after $CD8^+$ T-cell depletion demonstrates a clear necessity for cure strategies to quantify tissue proviruses before concluding cure. (ii) Nevertheless, the data presented in this specific aim provide support to our hypothesis that repeated administrations of Romidepsin can decrease the viral reservoir and bolster the SIV-specific immune responses in the context of a healthy immune system. (iii) Finally, these data therefore suggest that restoration of immune function and reversion of T-cell exhaustion in chronically infected PWH should be included in cure strategies aimed to clear the reservoir.

In summary, we have disproven our first specific aim by showing in rhesus macaque models of HIV infection that Cy does not act as a strongly specific Treg-depleting agent, nor does Cy safely cytoreduce the immune system when concomitant with ART. However, we have supported our hypotheses relating to RMD by demonstrating that infusion in SIV-naïve RMs results in lymphopenia stemming from downregulation of surface markers, expression of homing markers, and subsequent migration to lymph nodes and intestine. Further, in our SIVsab model of function cure in RMs, repeated infusions of RMD greatly increased the SIV-specific $CD8^+$ T-cell response and decreased subsequent viral reactivation. Importantly, in the case of RM89, repeated RMD infusions and a $CD8^+$ T-cell depletion resulted in a significant reduction of the levels of inducible virus in the periphery, but not tissues. These data will

contribute to further HIV cure strategies by demonstrating the importance of a healthy immune response for cure strategy success and the necessity for examining tissue reservoirs.

7.0 Future Directions

The results presented here show that administration of an HDAC inhibitor (Romidepsin) in a RM model of functional cure (i.e., of *in vivo* latency), under the pretense of a healthy immune response, can decrease the viral reservoir. During progressive HIV infection, this healthy immune response is not present, and agents aimed at improving the immune system have not recapitulated viral control in PWH when used alone. Additionally, LRAs were shown to only reactivate a small portion of reservoir [461, 515, 896], regardless of cellular activation status [897] and have yet to demonstrate substantial reductions in the latent reservoir. As such, these results further diminish the usefulness of single therapy regimens, as the vast majority of the reservoir will remain untouched because the lack of viral production will prevent recognition by the immune system, let alone the lack of clearance by viral cytopathic effects. Nonetheless, the silver lining in current HIV cure research is that recent combinatorial studies have resulted in much better efficacy than the single treatment studies [588, 678, 710, 787]. However, these studies have been completed during acute infection, and are thus not applicable to the vast majority of PWH who are chronically infected. Regardless, those studies, along with our data, point towards the eventual development of a functional cure being possible through bolstering the immune response while limiting extensive viremia. Moving forward, the field will need to continue to rely heavily upon nonhuman primate models for HIV cure due to the intricacy of combinatorial studies and, more importantly, the potential for unexpected adverse effects. For example, the use of IL2-DT for Treg depletion had a positive impact on the spontaneously functionally cured SIV infection in RMs [828], but when combined with ART, resulted in unacceptable toxicity [505], although not to the extent of Cy + ART. Further, the venetoclax + ixazomib combination had synergistic *in vitro* efficacy, but didn't make it to *in vivo* testing because *ex vivo* toxicity with PBMCs was too great [553]. Nevertheless, new combinations must still be tested, and our results indicate that the HIV cure field should work more closely with the cancer immunotherapy field, given the role of immune dysfunction in both disease paradigms. In addition, the field should take note from its own research on ART and try to find combinations that target different mechanisms of HIV latency persistence or immune dysfunction, similar

to how there is an antiretroviral for each step of the HIV life cycle. This is because, as demonstrated in every study, what works for one animal or patient may not work for another and this needs to be taken into consideration. By trying different combinations, we may end up with separate treatments for separate phenotypes or stages of infection, e.g., PWH that initiated ART late during chronic infection may respond better with the inclusion of a PD-1/PD-L1 or CTLA-4 blockade due to the further extent of T-cell exhaustion. Meanwhile, during acute infection, a combination of IL-15/21 or TLR agonist with bnAbs may be more efficient in boosting the innate and adaptive immune responses while decreasing excessive viremia and immune depletion, allowing for the cell-mediated immune response to have a better response to virus.

Although RMD reactivated virus in our RMs, a recent clinical trial did not observe any virological effects in ART-treated PWH [898]. In fact, immune activation was observed, yet plasma viremia and CA-vRNA were unchanged and undetectable in both single dose and multi-dose cohorts [898]. Thus, the only future for RMD is in combination with another drug or molecule that would synergize with it and allow for lower doses without negatively affecting efficacy: potentially a SMAC mimetic [779] or PKC agonist [240, 757, 758]. One strategy worth investigating is combining TLR2 and TLR7 agonists. Dual TLR2/TLR7 agonists resulted in increased efficacy through separate immune activation mechanisms [708], and may work better than single TLR7 agonists for viral reactivation and immune stimulation. Combining TLR2/7 agonists with bnAbs [586, 587] may be a valid strategy for clearance after reactivation and maintaining immune control, similar to the GS-9620 + bnAb PGT121 [586] or IL-15 superagonist (N-803) + bnAbs 10-1074 and 3BNC117 [588] studies. Interestingly, a cancer study showed that HDACis (including RMD) increase production of human endogenous retroviral elements in cancer cells and that concomitant treatment of TLR7/8 agonists allows for the cells to induce intrinsic apoptosis when they otherwise wouldn't have enough stimuli to do so, while also at doses that are individually subcytotoxic [899]. This therapy can readily be applied to HIV research, but will first require *ex vivo* testing to ensure cell viability of uninfected cells is maintained and bystander death isn't prolific. Should toxicity prove acceptable, additional inclusion of bnAbs could assist by providing another mechanism of reservoir clearance and wouldn't modulate immune activation, thereby avoiding an increase in the chance of cytokine storm. However, as HDACi do

not reactivate a substantial portion of the reservoir [461, 515, 896], repeated treatments would likely be necessary with advancement to *in vivo*, as done in section 5.

Other combinations for improving the immune function should also be considered. IL-15 and IL-21 have both shown efficacy for improving viral control [381, 692, 693] but have yet to be tested in combination for HIV cure. In mice, IL-15 and IL-21 both act on B, T, and NK cells, but IL-15 is essential for T cells, whereas IL-21 is more important for NK cells. Indeed, there is still overlap between the two and they act synergistically to boost $CD8^+$ T cells and function [900, 901] and, importantly, improve antigen-specific T-cell responses [902]. Thus, a study of the combination of IL-15/21 as an HIV therapeutic is warranted *ex vivo* and *in vivo*, although this combination would likely require decreased doses relative to single treatments to prevent cytokine storms. IL-15/21 would likely also not be feasible as a combination with a LRA, due to too much immune stimulation, but could work very well with bnAbs during acute or early chronic infection. One downside to IL-15 therapy is the induction of PD-1 and PD-L1 expression [903] and unsurprisingly, IL-15 superagonist N-803 is currently being tested with PD-1 monoclonal antibodies to reduce the increased PD-1/PD-L1 expression while also inherently decreasing T-cell exhaustion for cancer treatments [904-906]. Another method of combination IL-15 or IL-21 and αPD-1 is the use of fusion proteins. By placing IL-15 [907] or IL-21 [908] on a PD-L1 or PD-1 antibody, IL-15/21 are targeted to PD-1 expressing cells, which will be enriched for tumor reactive $CD8^+$ T cells. This can also apply to HIV-specific $CD8^+$ T cells which are likewise enriched for PD-(L)1 [262-265] and may reduce the risk of inducing systemic immune activation with combination therapy. Both of these concepts should be tested for HIV *in vivo* to determine the more efficacious method for HIV. Further, as neither IL-15, IL-21, nor PD-1 therapies have strong latency reversal potency, *in vitro* experiments should be carried out with the addition of a stronger LRA. In fact, the combination of a SMAC mimetic (i.e., Ciapavir) with a bromodomain (i.e. JQ1 or a newer molecule) could be a strong contender, as these two drugs have been shown to be synergistic for latency reversal [783]. This particular combination is preferable for a combination with IL-15 or 21 because both CIapavir and JQ1 induce viral reactivation with minimal

immune activation, and thus this should limit the potential adverse effects from systemic immune activation.

Overall, there are many developing combinatorial strategies that are increasing our hope for an HIV cure. Although RMD alone is not one of them, our results demonstrating the importance of a healthy immune response support ameliorating the immune dysfunction in PWH as an important aspect to cure strategies.

Bibliography

1. Barré-Sinoussi F, et al. Isolation of a T-lymphotropic retrovirus from a patient at risk for acquired immune deficiency syndrome (AIDS). *Science (New York, NY).* 1983;220(4599):868-71.

2. Daniel M, et al. Isolation of T-cell tropic HTLV-III-like retrovirus from macaques. *Science (New York, NY).* 1985;228(4704):1201-4.

3. Stowell RE, et al. Outbreak of malignant lymphoma in rhesus monkeys. *Laboratory investigation; a journal of technical methods and pathology.* 1971;25(5):476-9.

4. Terrell TG, et al. Malignant lymphoma in macaques: a clinicopathologic study of 45 cases. *Journal of the National Cancer Institute.* 1980;64(3):561-8.

5. Gardner MB. The history of simian AIDS. *Journal of medical primatology.* 1996;25(3):148-57.

6. Letvin NL, et al. Induction of AIDS-like disease in macaque monkeys with T-cell tropic retrovirus STLV-III. *Science (New York, NY).* 1985;230(4721):71-3.

7. Ansari AA, and Silvestri G. *Natural hosts of SIV: implication in AIDS.* Newnes; 2014.

8. Lowenstine LJ, et al. Seroepidemiologic survey of captive Old-World primates for antibodies to human and simian retroviruses, and isolation of a lentivirus from sooty mangabeys (Cercocebus atys). *International journal of cancer.* 1986;38(4):563-74.

9. Ohta Y, et al. Isolation of simian immunodeficiency virus from African green monkeys and seroepidemiologic survey of the virus in various non-human primates. *International journal of cancer.* 1988;41(1):115-22.

10. Ma D, et al. SIVagm infection in wild African green monkeys from South Africa: epidemiology, natural history, and evolutionary considerations. *PLoS pathogens.* 2013;9(1):e1003011.

11. Raehtz K, et al. The well-tempered SIV infection: Pathogenesis of SIV infection in natural hosts in the wild, with emphasis on virus transmission and early events post-infection that may contribute to protection from disease progression. *Infect Genet Evol.* 2016;46(308-23.

12. VandeWoude S, and Apetrei C. Going wild: lessons from naturally occurring T-lymphotropic lentiviruses. *Clinical microbiology reviews.* 2006;19(4):728-62.

13. Apetrei C, et al. Kuru experiments triggered the emergence of pathogenic SIVmac. *AIDS (London, England).* 2006;20(3):317-21.

14. Corbet S, et al. env sequences of simian immunodeficiency viruses from chimpanzees in Cameroon are strongly related to those of human immunodeficiency virus group N from the same geographic area. *J Virol.* 2000;74(1):529-34.

15. Chen Z, et al. Genetic characterization of new West African simian immunodeficiency virus SIVsm: geographic clustering of household-derived SIV strains with human immunodeficiency

virus type 2 subtypes and genetically diverse viruses from a single feral sooty mangabey troop. *J Virol.* 1996;70(6):3617-27.

16. Apetrei C, et al. Molecular epidemiology of simian immunodeficiency virus SIVsm in U.S. primate centers unravels the origin of SIVmac and SIVstm. *J Virol.* 2005;79(14):8991-9005.

17. Mansfield KG, et al. Origins of simian immunodeficiency virus infection in macaques at the New England Regional Primate Research Center. *Journal of medical primatology.* 1995;24(3):116-22.

18. Benveniste RE, et al. Inoculation of baboons and macaques with simian immunodeficiency virus/Mne, a primate lentivirus closely related to human immunodeficiency virus type 2. *J Virol.* 1988;62(6):2091-101.

19. Khan AS, et al. SIV of stump-tailed macaque (SIVstm) is a divergent Asian isolate. *Journal of medical primatology.* 1991;20(4):167-71.

20. Novembre FJ, et al. SIV from stump-tailed macaques: Molecular characterization of a highly transmissible primate lentivirus. *Virology.* 1992;186(2):783-7.

21. McCarthy KR, et al. Phylogeny and History of the Lost SIV from Crab-Eating Macaques: SIVmfa. *PLoS One.* 2016;11(7):e0159281.

22. Whitney JB, et al. Rapid seeding of the viral reservoir prior to SIV viraemia in rhesus monkeys. *Nature.* 2014;512(7512):74-7.

23. Henrich TJ, et al. HIV-1 persistence following extremely early initiation of antiretroviral therapy (ART) during acute HIV-1 infection: An observational study. *PLOS Medicine.* 2017;14(11):e1002417.

24. Okoye AA, et al. Early antiretroviral therapy limits SIV reservoir establishment to delay or prevent post-treatment viral rebound. *Nature Medicine.* 2018;24(9):1430-40.

25. Policicchio BB, et al. Animal Models for HIV Cure Research. *Frontiers in Immunology.* 2016;7(12.

26. Deleage C, et al. Defining HIV and SIV Reservoirs in Lymphoid Tissues. *Pathogens & immunity.* 2016;1(1):68-106.

27. Hansen Scott G, et al. A live-attenuated RhCMV/SIV vaccine shows long-term efficacy against heterologous SIV challenge. *Science Translational Medicine.* 2019;11(501):eaaw2607.

28. Hansen SG, et al. Profound early control of highly pathogenic SIV by an effector memory T-cell vaccine. *Nature.* 2011;473(7348):523-7.

29. Lim S-Y, et al. TLR7 agonists induce transient viremia and reduce the viral reservoir in SIV-infected rhesus macaques on antiretroviral therapy. *Science translational medicine.* 2018;10(439):eaao4521.

30. Siddiqui S, et al. Persistent Viral Reservoirs in Lymphoid Tissues in SIV-Infected Rhesus Macaques of Chinese-Origin on Suppressive Antiretroviral Therapy. *Viruses.* 2019;11(2):105.

31. Veazey RS, et al. Gastrointestinal tract as a major site of CD4+ T cell depletion and viral replication in SIV infection. *Science (New York, NY).* 1998;280(5362):427-31.

32. Smit-McBride Z, et al. Gastrointestinal T lymphocytes retain high potential for cytokine responses but have severe CD4(+) T-cell depletion at all stages of simian immunodeficiency virus infection compared to peripheral lymphocytes. *J Virol.* 1998;72(8):6646-56.

33. Brenchley JM, et al. CD4+ T cell depletion during all stages of HIV disease occurs predominantly in the gastrointestinal tract. *The Journal of experimental medicine.* 2004;200(6):749-59.

34. Mehandru S, et al. Primary HIV-1 infection is associated with preferential depletion of CD4+ T lymphocytes from effector sites in the gastrointestinal tract. *The Journal of experimental medicine.* 2004;200(6):761-70.

35. Deleage C, et al. Defining early SIV replication and dissemination dynamics following vaginal transmission. *Science Advances.* 2019;5(5):eaav7116.

36. Barrenas F, et al. Macrophage-associated wound healing contributes to African green monkey SIV pathogenesis control. *Nature Communications.* 2019;10(1):5101.

37. Kornfeld C, et al. Antiinflammatory profiles during primary SIV infection in African green monkeys are associated with protection against AIDS. *The Journal of clinical investigation.* 2005;115(4):1082-91.

38. Raehtz KD, et al. African green monkeys avoid SIV disease progression by preventing intestinal dysfunction and maintaining mucosal barrier integrity. *PLoS pathogens.* 2020;16(3):e1008333.

39. Kuller LH, et al. Inflammatory and coagulation biomarkers and mortality in patients with HIV infection. *PLoS Med.* 2008;5(10):e203.

40. Pandrea I, and Apetrei C. Where the wild things are: pathogenesis of SIV infection in African nonhuman primate hosts. *Current HIV/AIDS reports.* 2010;7(1):28-36.

41. Pandrea I, et al. Coagulation biomarkers predict disease progression in SIV-infected nonhuman primates. *Blood.* 2012;120(1357-66.

42. Deeks SG, et al. Systemic effects of inflammation on health during chronic HIV infection. *Immunity.* 2013;39(4):633-45.

43. Pandrea I, et al. Using the pathogenic and nonpathogenic nonhuman primate model for studying non-AIDS comorbidities. *Current HIV/AIDS reports.* 2015;12(1):54-67.

44. Murphey-Corb M, et al. Isolation of an HTLV-III-related retrovirus from macaques with simian AIDS and its possible origin in asymptomatic mangabeys. *Nature.* 1986;321(6068):435-7.

45. Hirsch VM, et al. Molecular Cloning of SIV From Sooty Mangabey Monkeys. *Journal of medical primatology.* 1989;18(3-4):279-85.

46. Hirsch VM, et al. An African primate lentivirus (SIVsmclosely related to HIV-2. *Nature.* 1989;339(6223):389-92.

47. Hirsch V, et al. A molecularly cloned, pathogenic, neutralization-resistant simian immunodeficiency virus, SIVsmE543-3. *J Virol.* 1997;71(2):1608-20.

48. Hirsch VM, et al. Molecular characterization of SIV in tissues from experimentally infected macaques. *Journal of medical primatology.* 1990;19(3-4):287-94.

49. Hirsch VM, and Johnson PR. Pathogenic diversity of simian immunodeficiency viruses. *Virus Research.* 1994;32(2):183-203.

50. Letvin NL, et al. Immune and Genetic Correlates of Vaccine Protection Against Mucosal Infection by SIV in Monkeys. *Sci Transl Med.* 2011;3(81):81ra36.

51. Wu F, et al. Sequential Evolution and Escape from Neutralization of Simian Immunodeficiency Virus SIVsmE660 Clones in Rhesus Macaques. *J Virol.* 2012;86(16):8835-47.

52. Kirmaier A, et al. TRIM5 Suppresses Cross-Species Transmission of a Primate Immunodeficiency Virus and Selects for Emergence of Resistant Variants in the New Species. *PLOS Biology.* 2010;8(8):e1000462.

53. Lopker Michael J, et al. Derivation and Characterization of Pathogenic Transmitted/Founder Molecular Clones from Simian Immunodeficiency Virus SIVsmE660 and SIVmac251 following Mucosal Infection. *J Virol.* 2016;90(19):8435-53.

54. Brocca-Cofano E, et al. Marginal Effects of Systemic CCR5 Blockade with Maraviroc on Oral Simian Immunodeficiency Virus Transmission to Infant Macaques. *J Virol.* 2018;92(17):e00576-18.

55. Del Prete GQ, et al. Molecularly tagged simian immunodeficiency virus SIVmac239 synthetic swarm for tracking independent infection events. *J Virol.* 2014;88(14):8077-90.

56. Fennessey CM, et al. Genetically-barcoded SIV facilitates enumeration of rebound variants and estimation of reactivation rates in nonhuman primates following interruption of suppressive antiretroviral therapy. *PLoS pathogens.* 2017;13(5):e1006359-e.

57. Khanal S, et al. In Vivo Validation of the Viral Barcoding of Simian Immunodeficiency Virus SIVmac239 and the Development of New Barcoded SIV and Subtype B and C Simian-Human Immunodeficiency Viruses. *J Virol.* 2019;94(1):e01420-19.

58. Diop OM, et al. High levels of viral replication during primary simian immunodeficiency virus SIVagm infection are rapidly and strongly controlled in African green monkeys. *J Virol.* 2000;74(16):7538-47.

59. Gnanadurai CW, et al. Genetic identity and biological phenotype of a transmitted/founder virus representative of nonpathogenic simian immunodeficiency virus infection in African green monkeys. *J Virol.* 2010;84(23):12245-54.

60. Mandell DT, et al. Pathogenic features associated with increased virulence upon Simian immunodeficiency virus cross-species transmission from natural hosts. *J Virol.* 2014;88(12):6778-92.

61. Hatziioannou T, and Bieniasz PD. Antiretroviral restriction factors. *Current Opinion in Virology.* 2011;1(6):526-32.

62. Li J, et al. Infection of cynomolgus monkeys with a chimeric HIV-1/SIVmac virus that expresses the HIV-1 envelope glycoproteins. *Journal of acquired immune deficiency syndromes.* 1992;5(7):639-46.

63. Reimann KA, et al. An env gene derived from a primary human immunodeficiency virus type 1 isolate confers high in vivo replicative capacity to a chimeric simian/human immunodeficiency virus in rhesus monkeys. *J Virol.* 1996;70(5):3198-206.

64. Karlsson GB, et al. Characterization of molecularly cloned simian-human immunodeficiency viruses causing rapid CD4+ lymphocyte depletion in rhesus monkeys. *J Virol.* 1997;71(6):4218-25.

65. Nishimura Y, et al. Highly pathogenic SHIVs and SIVs target different CD4⁺ T cell subsets in rhesus monkeys, explaining their divergent clinical courses. *Proceedings of the National Academy of Sciences of the United States of America.* 2004;101(33):12324-9.

66. Del Prete GQ, et al. Nonhuman primate models for the evaluation of HIV-1 preventive vaccine strategies: model parameter considerations and consequences. *Current Opinion in HIV and AIDS.* 2016;11(6).

67. Sharma A, et al. Development of SHIVs with circulating, transmitted HIV-1 variants. *Journal of medical primatology.* 2015;44(5):296-300.

68. Ndung'u T, et al. Infectious Simian/Human Immunodeficiency Virus with Human Immunodeficiency Virus Type 1 Subtype C from an African Isolate: Rhesus Macaque Model. *J Virol.* 2001;75(23):11417-25.

69. Pal R, et al. Characterization of a simian human immunodeficiency virus encoding the envelope gene from the CCR5-tropic HIV-1 Ba-L. *Journal of acquired immune deficiency syndromes (1999).* 2003;33(3):300-7.

70. Harouse Janet M, et al. Mucosal Transmission and Induction of Simian AIDS by CCR5-Specific Simian/Human Immunodeficiency Virus SHIVSF162P3. *J Virol.* 2001;75(4):1990-5.

71. Chen Z, et al. Enhanced Infectivity of an R5-Tropic Simian/Human Immunodeficiency Virus Carrying Human Immunodeficiency Virus Type 1 Subtype C Envelope after Serial Passages in Pig-Tailed Macaques (Macaca nemestrina). *J Virol.* 2000;74(14):6501-10.

72. Nishimura Y, et al. Generation of the Pathogenic R5-Tropic Simian/Human Immunodeficiency Virus SHIVAD8 by Serial Passaging in Rhesus Macaques. *J Virol.* 2010;84(9):4769-81.

73. Tartaglia LJ, et al. Differential Outcomes following Optimization of Simian-Human Immunodeficiency Viruses from Clades AE, B, and C. *J Virol.* 2020;94(10).

74. Bauer AM, and Bar KJ. Advances in simian--human immunodeficiency viruses for nonhuman primate studies of HIV prevention and cure. *Current Opinion in HIV and AIDS.* 2020;15(5).

75. Gautam R, et al. Pathogenicity and mucosal transmissibility of the R5-tropic simian/human immunodeficiency virus SHIV(AD8) in rhesus macaques: implications for use in vaccine studies. *J Virol.* 2012;86(16):8516-26.

76. Shingai M, et al. Most rhesus macaques infected with the CCR5-tropic SHIV(AD8) generate cross-reactive antibodies that neutralize multiple HIV-1 strains. *Proc Natl Acad Sci U S A.* 2012;109(48):19769-74.

77. Nishimura Y, et al. Prevention and treatment of SHIVAD8 infection in rhesus macaques by a potent d-peptide HIV entry inhibitor. *Proceedings of the National Academy of Sciences.* 2020;117(36):22436-42.

78. Song RJ, et al. Molecularly cloned SHIV-1157ipd3N4: a highly replication- competent, mucosally transmissible R5 simian-human immunodeficiency virus encoding HIV clade C Env. *J Virol.* 2006;80(17):8729-38.

79. Keele BF, and Derdeyn CA. Genetic and antigenic features of the transmitted virus. *Current Opinion in HIV and AIDS.* 2009;4(5).

80. Del Prete GQ, et al. Selection of unadapted, pathogenic SHIVs encoding newly transmitted HIV-1 envelope proteins. *Cell host & microbe.* 2014;16(3):412-8.

81. Li H, et al. Envelope residue 375 substitutions in simian-human immunodeficiency viruses enhance CD4 binding and replication in rhesus macaques. *Proc Natl Acad Sci U S A.* 2016;113(24):E3413-22.

82. O'Brien SP, et al. Rational design and in vivo selection of SHIVs encoding transmitted/founder subtype C HIV-1 envelopes. *PLoS pathogens.* 2019;15(4):e1007632.

83. Bauer AM, et al. Novel Transmitted/Founder Simian-Human Immunodeficiency Viruses for Human Immunodeficiency Virus Latency and Cure Research. *J Virol.* 2020;94(8):e01659-19.

84. Bar Katharine J, et al. Simian-Human Immunodeficiency Virus SHIV.CH505 Infection of Rhesus Macaques Results in Persistent Viral Replication and Induces Intestinal Immunopathology. *J Virol.* 2019;93(18):e00372-19.

85. Zhu P, et al. Distribution and three-dimensional structure of AIDS virus envelope spikes. *Nature.* 2006;441(7095):847-52.

86. Kwong PD, et al. Structure of an HIV gp120 envelope glycoprotein in complex with the CD4 receptor and a neutralizing human antibody. *Nature.* 1998;393(6686):648-59.

87. Buzon V, et al. Crystal structure of HIV-1 gp41 including both fusion peptide and membrane proximal external regions. *PLoS pathogens.* 2010;6(5):e1000880.

88. Weissenhorn W, et al. Atomic structure of the ectodomain from HIV-1 gp41. *Nature.* 1997;387(6631):426-30.

89. Chen Z, et al. Natural infection of a homozygous delta24 CCR5 red-capped mangabey with an R2b-tropic simian immunodeficiency virus. *The Journal of experimental medicine.* 1998;188(11):2057-65.

90. Wetzel KS, et al. CXCR6-Mediated Simian Immunodeficiency Virus SIVagmSab Entry into Sabaeus African Green Monkey Lymphocytes Implicates Widespread Use of Non-CCR5 Pathways in Natural Host Infections. *J Virol.* 2017;91(4).

91. Chan DC, et al. Core structure of gp41 from the HIV envelope glycoprotein. *Cell.* 1997;89(2):263-73.

92. Markosyan RM, et al. HIV-1 envelope proteins complete their folding into six-helix bundles immediately after fusion pore formation. *Molecular biology of the cell.* 2003;14(3):926-38.

93. McDonald D, et al. Visualization of the intracellular behavior of HIV in living cells. *Journal of Cell Biology.* 2002;159(3):441-52.

94. Fernandez J, et al. Microtubule-associated Proteins 1 (MAP1) Promote Human Immunodeficiency Virus Type I (HIV-1) Intracytoplasmic Routing to the Nucleus. *Journal of Biological Chemistry.* 2015;290(8):4631-46.

95. Lukic Z, et al. HIV-1 Uncoating Is Facilitated by Dynein and Kinesin 1. *J Virol.* 2014;88(23):13613-25.

96. Malikov V, et al. HIV-1 capsids bind and exploit the kinesin-1 adaptor FEZ1 for inward movement to the nucleus. *Nature Communications.* 2015;6(1):6660.

97. Dharan A, et al. Bicaudal D2 facilitates the cytoplasmic trafficking and nuclear import of HIV-1 genomes during infection. *Proceedings of the National Academy of Sciences.* 2017;114(50):E10707-E16.

98. Carnes Stephanie K, et al. HIV-1 Engages a Dynein-Dynactin-BICD2 Complex for Infection and Transport to the Nucleus. *J Virol.* 2018;92(20):e00358-18.

99. Burdick RC, et al. HIV-1 uncoats in the nucleus near sites of integration. *Proceedings of the National Academy of Sciences.* 2020;117(10):5486-93.

100. Isel C, et al. Specific initiation and switch to elongation of human immunodeficiency virus type 1 reverse transcription require the post-transcriptional modifications of primer tRNA3Lys. *The EMBO Journal.* 1996;15(4):917-24.

101. Fassati A, and Goff Stephen P. Characterization of Intracellular Reverse Transcription Complexes of Human Immunodeficiency Virus Type 1. *J Virol.* 2001;75(8):3626-35.

102. Boese A, et al. Integrase interactor 1 (Ini1/hSNF5) is a repressor of basal human immunodeficiency virus type 1 promoter activity. *The Journal of general virology.* 2009;90(Pt 10):2503-12.

103. Sorin M, et al. Recruitment of a SAP18-HDAC1 Complex into HIV-1 Virions and Its Requirement for Viral Replication. *PLoS pathogens.* 2009;5(6):e1000463.

104. Warren K, et al. Eukaryotic elongation factor 1 complex subunits are critical HIV-1 reverse transcription cofactors. *Proceedings of the National Academy of Sciences.* 2012;109(24):9587-92.

105. Ramdas P, et al. From Entry to Egress: Strategic Exploitation of the Cellular Processes by HIV-1. *Frontiers in Microbiology.* 2020;11(3021).

106. Debyser Z, et al. Host factors for retroviral integration site selection. *Trends in biochemical sciences.* 2015;40(2):108-16.

107. Hare S, et al. Retroviral intasome assembly and inhibition of DNA strand transfer. *Nature.* 2010;464(7286):232-6.

108. Maertens GN, et al. The mechanism of retroviral integration from X-ray structures of its key intermediates. *Nature.* 2010;468(7321):326-9.

109. Bojja RS, et al. Architecture and Assembly of HIV Integrase Multimers in the Absence of DNA Substrates *. *Journal of Biological Chemistry.* 2013;288(10):7373-86.

110. Wang JY, et al. Structure of a two-domain fragment of HIV-1 integrase: implications for domain organization in the intact protein. *The EMBO journal.* 2001;20(24):7333-43.

111. Schröder AR, et al. HIV-1 integration in the human genome favors active genes and local hotspots. *Cell.* 2002;110(4):521-9.

112. Lewinski MK, et al. Retroviral DNA integration: viral and cellular determinants of target-site selection. *PLoS pathogens.* 2006;2(6):e60.

113. Han Y, et al. Resting CD4+ T cells from human immunodeficiency virus type 1 (HIV-1)-infected individuals carry integrated HIV-1 genomes within actively transcribed host genes. *J Virol.* 2004;78(12):6122-33.

114. Singh PK, et al. LEDGF/p75 interacts with mRNA splicing factors and targets HIV-1 integration to highly spliced genes. *Genes & development.* 2015;29(21):2287-97.

115. Sowd GA, et al. A critical role for alternative polyadenylation factor CPSF6 in targeting HIV-1 integration to transcriptionally active chromatin. *Proc Natl Acad Sci U S A.* 2016;113(8):E1054-63.

116. Lusic M, and Siliciano RF. Nuclear landscape of HIV-1 infection and integration. *Nature Reviews Microbiology.* 2017;15(2):69-82.

117. Chan CN, et al. HIV-1 latency and virus production from unintegrated genomes following direct infection of resting CD4 T cells. *Retrovirology.* 2016;13(1):1.

118. Pereira LA, et al. A compilation of cellular transcription factor interactions with the HIV-1 LTR promoter. *Nucleic Acids Res.* 2000;28(3):663-8.

119. Rosen CA, et al. The location of cis-acting regulatory sequences in the human T cell lymphotropic virus type III (HTLV-III/LAV) long terminal repeat. *Cell.* 1985;41(3):813-23.

120. Cullen BR. Retroviruses as model systems for the study of nuclear RNA export pathways. *Virology.* 1998;249(2):203-10.

121. Sobhian B, et al. HIV-1 Tat assembles a multifunctional transcription elongation complex and stably associates with the 7SK snRNP. *Molecular cell.* 2010;38(3):439-51.

122. Martin Stoltzfus C. *Advances in Virus Research*. Academic Press; 2009:1-40.

123. Mbonye U, and Karn J. Transcriptional control of HIV latency: Cellular signaling pathways, epigenetics, happenstance and the hope for a cure. *Virology.* 2014;454-455(328-39.

124. Kuzembayeva M, et al. Life of psi: How full-length HIV-1 RNAs become packaged genomes in the viral particles. *Virology.* 2014;454-455(362-70.

125. Chen J, et al. Visualizing the translation and packaging of HIV-1 full-length RNA. *Proceedings of the National Academy of Sciences.* 2020;117(11):6145-55.

126. Freed EO. HIV-1 assembly, release and maturation. *Nature Reviews Microbiology.* 2015;13(8):484-96.

127. Chen J, et al. HIV-1 RNA genome dimerizes on the plasma membrane in the presence of Gag protein. *Proceedings of the National Academy of Sciences.* 2016;113(2):E201-E8.

128. Miller CJ, et al. Propagation and dissemination of infection after vaginal transmission of simian immunodeficiency virus. *J Virol.* 2005;79(14):9217-27.

129. Sagar M. HIV-1 transmission biology: selection and characteristics of infecting viruses. *The Journal of infectious diseases.* 2010;202 Suppl 2(Suppl 2):S289-96.

130. Keele BF, et al. Identification and characterization of transmitted and early founder virus envelopes in primary HIV-1 infection. *Proceedings of the National Academy of Sciences.* 2008;105(21):7552-7.

131. Stone M, et al. A Limited Number of Simian Immunodeficiency Virus (SIV) env Variants Are Transmitted to Rhesus Macaques Vaginally Inoculated with SIVmac251. *J Virol.* 2010;84(14):7083-95.

132. Haaland RE, et al. Female genital tract shedding of CXCR4-tropic HIV Type 1 is associated with a majority population of CXCR4-tropic HIV Type 1 in blood and declining CD4(+) cell counts. *AIDS research and human retroviruses.* 2012;28(11):1524-32.

133. Gianella S, et al. Sexual transmission of predicted CXCR4-tropic HIV-1 likely originating from the source partner's seminal cells. *Virology.* 2012;434(1):2-4.

134. Muciaccia B, et al. HIV-1 chemokine co-receptor CCR5 is expressed on the surface of human spermatozoa. *AIDS (London, England).* 2005;19(13):1424-6.

135. Chohan B, et al. Selection for human immunodeficiency virus type 1 envelope glycosylation variants with shorter V1-V2 loop sequences occurs during transmission of certain genetic subtypes and may impact viral RNA levels. *J Virol.* 2005;79(10):6528-31.

136. Gnanakaran S, et al. Recurrent signature patterns in HIV-1 B clade envelope glycoproteins associated with either early or chronic infections. *PLoS pathogens.* 2011;7(9):e1002209.

137. Parrish NF, et al. Phenotypic properties of transmitted founder HIV-1. *Proc Natl Acad Sci U S A.* 2013;110(17):6626-33.

138. Fenton-May AE, et al. Relative resistance of HIV-1 founder viruses to control by interferon-alpha. *Retrovirology.* 2013;10(146.

139. Amerongen HM, et al. Transepithelial transport of HIV-1 by intestinal M cells: a mechanism for transmission of AIDS. *Journal of acquired immune deficiency syndromes.* 1991;4(8):760-5.

140. Fotopoulos G, et al. Transepithelial transport of HIV-1 by M cells is receptor-mediated. *Proceedings of the National Academy of Sciences of the United States of America.* 2002;99(14):9410-4.

141. Spira AI, et al. Cellular targets of infection and route of viral dissemination after an intravaginal inoculation of simian immunodeficiency virus into rhesus macaques. *The Journal of experimental medicine.* 1996;183(1):215-25.

142. Hu J, et al. Simian immunodeficiency virus rapidly penetrates the cervicovaginal mucosa after intravaginal inoculation and infects intraepithelial dendritic cells. *J Virol.* 2000;74(13):6087-95.

143. Kreiss JK, and Hopkins SG. The association between circumcision status and human immunodeficiency virus infection among homosexual men. *The Journal of infectious diseases.* 1993;168(6):1404-8.

144. Veazey Ronald S, et al. Identifying the Target Cell in Primary Simian Immunodeficiency Virus (SIV) Infection: Highly Activated Memory CD4+ T Cells Are Rapidly Eliminated in Early SIV Infection In Vivo. *J Virol.* 2000;74(1):57-64.

145. Mattapallil JJ, et al. Massive infection and loss of memory CD4+ T cells in multiple tissues during acute SIV infection. *Nature.* 2005;434(7037):1093-7.

146. Ribeiro Dos Santos P, et al. Rapid dissemination of SIV follows multisite entry after rectal inoculation. *PLoS One.* 2011;6(5):e19493-e.

147. Miyake A, et al. Rapid dissemination of a pathogenic simian/human immunodeficiency virus to systemic organs and active replication in lymphoid tissues following intrarectal infection. *Journal of General Virology.* 2006;87(5):1311-20.

148. Haase AT. Early events in sexual transmission of HIV and SIV and opportunities for interventions. *Annual review of medicine.* 2011;62(127-39.

149. Li Q, et al. Peak SIV replication in resting memory CD4+ T cells depletes gut lamina propria CD4+ T cells. *Nature.* 2005;434(7037):1148-52.

150. Little SJ, et al. Viral dynamics of acute HIV-1 infection. *The Journal of experimental medicine.* 1999;190(6):841-50.

151. Boirivant M, et al. HIV-1 gp120 Accelerates Fas-Mediated Activation-Induced Human Lamina Propria T Cell Apoptosis. *Journal of Clinical Immunology.* 1998;18(1):39-47.

152. Finkel TH, et al. Apoptosis occurs predominantly in bystander cells and not in productively infected cells of HIV- and SIV-infected lymph nodes. *Nat Med.* 1995;1(2):129-34.

153. Muro-Cacho CA, et al. Analysis of apoptosis in lymph nodes of HIV-infected persons. Intensity of apoptosis correlates with the general state of activation of the lymphoid tissue and not with stage of disease or viral burden. *Journal of immunology (Baltimore, Md : 1950).* 1995;154(10):5555-66.

154. Doitsh G, et al. Cell death by pyroptosis drives CD4 T-cell depletion in HIV-1 infection. *Nature.* 2014;505(7484):509-14.

155. Le Hingrat Q, et al. The Hitchhiker Guide to CD4(+) T-Cell Depletion in Lentiviral Infection. A Critical Review of the Dynamics of the CD4(+) T Cells in SIV and HIV Infection. *Front Immunol.* 2021;12(695674.

156. Brenchley JM, et al. Differential Th17 CD4 T-cell depletion in pathogenic and nonpathogenic lentiviral infections. *Blood.* 2008;112(7):2826-35.

157. Cecchinato V, et al. Altered balance between Th17 and Th1 cells at mucosal sites predicts AIDS progression in simian immunodeficiency virus-infected macaques. *Mucosal Immunology.* 2008;1(4):279-88.

158. Raffatellu M, et al. Simian immunodeficiency virus–induced mucosal interleukin-17 deficiency promotes Salmonella dissemination from the gut. *Nature Medicine.* 2008;14(4):421-8.

159. Schuetz A, et al. Initiation of ART during Early Acute HIV Infection Preserves Mucosal Th17 Function and Reverses HIV-Related Immune Activation. *PLoS pathogens.* 2014;10(12):e1004543.

160. Estes JD, et al. Damaged intestinal epithelial integrity linked to microbial translocation in pathogenic simian immunodeficiency virus infections. *PLoS pathogens.* 2010;6(8):e1001052.

161. Brenchley JM, et al. Microbial translocation is a cause of systemic immune activation in chronic HIV infection. *Nature Medicine.* 2006;12(12):1365-71.

162. Crowell TA, et al. Acute Retroviral Syndrome Is Associated With High Viral Burden, CD4 Depletion, and Immune Activation in Systemic and Tissue Compartments. *Clinical Infectious Diseases.* 2018;66(10):1540-9.

163. McCune JM. The dynamics of CD4+ T-cell depletion in HIV disease. *Nature.* 2001;410(6831):974-9.

164. Sheehy AM, et al. Isolation of a human gene that inhibits HIV-1 infection and is suppressed by the viral Vif protein. *Nature.* 2002;418(6898):646-50.

165. Hrecka K, et al. Vpx relieves inhibition of HIV-1 infection of macrophages mediated by the SAMHD1 protein. *Nature.* 2011;474(7353):658-61.

166. Lahouassa H, et al. SAMHD1 restricts the replication of human immunodeficiency virus type 1 by depleting the intracellular pool of deoxynucleoside triphosphates. *Nature immunology.* 2012;13(3):223-8.

167. Laguette N, et al. SAMHD1 is the dendritic- and myeloid-cell-specific HIV-1 restriction factor counteracted by Vpx. *Nature.* 2011;474(7353):654-7.

168. Neil SJ, et al. Tetherin inhibits retrovirus release and is antagonized by HIV-1 Vpu. *Nature.* 2008;451(7177):425-30.

169. Van Damme N, et al. The interferon-induced protein BST-2 restricts HIV-1 release and is downregulated from the cell surface by the viral Vpu protein. *Cell host & microbe.* 2008;3(4):245-52.

170. Stremlau M, et al. The cytoplasmic body component TRIM5alpha restricts HIV-1 infection in Old World monkeys. *Nature.* 2004;427(6977):848-53.

171. Ghimire D, et al. Novel host restriction factors implicated in HIV-1 replication. *The Journal of general virology.* 2018;99(4):435-46.

172. Yu Q, et al. Single-strand specificity of APOBEC3G accounts for minus-strand deamination of the HIV genome. *Nature structural & molecular biology.* 2004;11(5):435-42.

173. Venkatesh S, and Bieniasz PD. Mechanism of HIV-1 Virion Entrapment by Tetherin. *PLoS pathogens.* 2013;9(7):e1003483.

174. Ganser-Pornillos BK, and Pornillos O. Restriction of HIV-1 and other retroviruses by TRIM5. *Nature Reviews Microbiology.* 2019;17(9):546-56.

175. Campbell EM, et al. TRIM5α-Mediated Ubiquitin Chain Conjugation Is Required for Inhibition of HIV-1 Reverse Transcription and Capsid Destabilization. *J Virol.* 2016;90(4):1849-57.

176. Yu X, et al. Induction of APOBEC3G ubiquitination and degradation by an HIV-1 Vif-Cul5-SCF complex. *Science (New York, NY).* 2003;302(5647):1056-60.

177. Lim ES, et al. The ability of primate lentiviruses to degrade the monocyte restriction factor SAMHD1 preceded the birth of the viral accessory protein Vpx. *Cell host & microbe.* 2012;11(2):194-204.

178. Tristem M, et al. Evolution of the primate lentiviruses: evidence from vpx and vpr. *The EMBO journal.* 1992;11(9):3405-12.

179. Sharp PM, et al. Gene acquisition in HIV and SIV. *Nature.* 1996;383(6601):586-7.

180. Blanco-Melo D, et al. Intrinsic cellular defenses against human immunodeficiency viruses. *Immunity.* 2012;37(3):399-411.

181. Huang X, et al. Cytokine cascade and networks among MSM HIV seroconverters: implications for early immunotherapy. *Scientific Reports.* 2016;6(1):36234.

182. Muema DM, et al. Association between the cytokine storm, immune cell dynamics, and viral replicative capacity in hyperacute HIV infection. *BMC Medicine.* 2020;18(1):81.

183. Roberts L, et al. Plasma cytokine levels during acute HIV-1 infection predict HIV disease progression. *AIDS (London, England).* 2010;24(6):819-31.

184. Stacey AR, et al. Induction of a striking systemic cytokine cascade prior to peak viremia in acute human immunodeficiency virus type 1 infection, in contrast to more modest and delayed responses in acute hepatitis B and C virus infections. *J Virol.* 2009;83(8):3719-33.

185. Beignon AS, et al. Endocytosis of HIV-1 activates plasmacytoid dendritic cells via Toll-like receptor-viral RNA interactions. *The Journal of clinical investigation.* 2005;115(11):3265-75.

186. Sabado RL, et al. Pathways utilized by dendritic cells for binding, uptake, processing and presentation of antigens derived from HIV-1. *European journal of immunology.* 2007;37(7):1752-63.

187. Romagnani C, et al. Activation of human NK cells by plasmacytoid dendritic cells and its modulation by CD4+ T helper cells and CD4+ CD25hi T regulatory cells. *European journal of immunology.* 2005;35(8):2452-8.

188. Flórez-Álvarez L, et al. NK Cells in HIV-1 Infection: From Basic Science to Vaccine Strategies. *Frontiers in Immunology.* 2018;9(2290).

189. Pardo J, et al. Granzymes are essential for natural killer cell-mediated and perf-facilitated tumor control. *European journal of immunology.* 2002;32(10):2881-6.

190. Scott-Algara D, et al. Cutting Edge: Increased NK Cell Activity in HIV-1-Exposed but Uninfected Vietnamese Intravascular Drug Users. *The Journal of Immunology.* 2003;171(11):5663-7.

191. Oliva A, et al. Natural killer cells from human immunodeficiency virus (HIV)-infected individuals are an important source of CC-chemokines and suppress HIV-1 entry and replication in vitro. *The Journal of clinical investigation.* 1998;102(1):223-31.

192. Demers KR, et al. CD8(+) T-cell effector function and transcriptional regulation during HIV pathogenesis. *Immunol Rev.* 2013;254(1):190-206.

193. Ndhlovu ZM, et al. Magnitude and Kinetics of CD8+ T Cell Activation during Hyperacute HIV Infection Impact Viral Set Point. *Immunity.* 2015;43(3):591-604.

194. Bernardin F, et al. Human immunodeficiency virus mutations during the first month of infection are preferentially found in known cytotoxic T-lymphocyte epitopes. *J Virol.* 2005;79(17):11523-8.

195. Goonetilleke N, et al. The first T cell response to transmitted/founder virus contributes to the control of acute viremia in HIV-1 infection. *Journal of Experimental Medicine.* 2009;206(6):1253-72.

196. Tomaras GD, et al. Initial B-cell responses to transmitted human immunodeficiency virus type 1: virion-binding immunoglobulin M (IgM) and IgG antibodies followed by plasma anti-gp41 antibodies with ineffective control of initial viremia. *J Virol.* 2008;82(24):12449-63.

197. Levesque MC, et al. Polyclonal B cell differentiation and loss of gastrointestinal tract germinal centers in the earliest stages of HIV-1 infection. *PLoS Med.* 2009;6(7):e1000107.

198. Lavreys L, et al. Higher Set Point Plasma Viral Load and More-Severe Acute HIV Type 1 (HIV-1) Illness Predict Mortality among High-Risk HIV-1–Infected African Women. *Clinical Infectious Diseases.* 2006;42(9):1333-9.

199. Mellors JW, et al. Prognosis in HIV-1 Infection Predicted by the Quantity of Virus in Plasma. *Science (New York, NY).* 1996;272(5265):1167-70.

200. Deeks SG, et al. Immune activation set point during early HIV infection predicts subsequent CD4+ T-cell changes independent of viral load. *Blood.* 2004;104(4):942-7.

201. Zaunders JJ, et al. Potent antiretroviral therapy of primary human immunodeficiency virus type 1 (HIV-1) infection: partial normalization of T lymphocyte subsets and limited reduction of HIV-1 DNA despite clearance of plasma viremia. *The Journal of infectious diseases.* 1999;180(2):320-9.

202. Tilling R, et al. Parallel decline of CD8+/CD38++ T cells and viraemia in response to quadruple highly active antiretroviral therapy in primary HIV infection. *AIDS (London, England).* 2002;16(4):589-96.

203. Mohri H, et al. Increased turnover of T lymphocytes in HIV-1 infection and its reduction by antiretroviral therapy. *The Journal of experimental medicine.* 2001;194(9):1277-87.

204. Robb ML, et al. Prospective Study of Acute HIV-1 Infection in Adults in East Africa and Thailand. *New England Journal of Medicine.* 2016;374(22):2120-30.

205. Mangkornkanok-Mark M, et al. Immunoperoxidase evaluation of lymph nodes from acquired immune deficiency patients. *Clin Exp Immunol.* 1984;55(3):581-6.

206. Janossy G, et al. An immunohistological approach to persistent lymphadenopathy and its relevance to AIDS. *Clin Exp Immunol.* 1985;59(2):257-66.

207. Veazey RS, et al. Dynamics of CCR5 expression by CD4(+) T cells in lymphoid tissues during simian immunodeficiency virus infection. *J Virol.* 2000;74(23):11001-7.

208. Gottlieb GS, et al. Equal Plasma Viral Loads Predict a Similar Rate of CD4± T Cell Decline in Human Immunodeficiency Virus (HIV) Type 1- and HIV-2-Infected Individuals from Senegal, West Africa. *The Journal of infectious diseases.* 2002;185(7):905-14.

209. Schneider E, et al. Revised surveillance case definitions for HIV infection among adults, adolescents, and children aged <18 months and for HIV infection and AIDS among children aged 18 months to <13 years--United States, 2008. *MMWR Recommendations and reports : Morbidity and mortality weekly report Recommendations and reports.* 2008;57(Rr-10):1-12.

210. Deeks SG, et al. HIV infection. *Nature Reviews Disease Primers.* 2015;1(1):15035.

211. Saravolatz LD, et al. Zidovudine alone or in combination with didanosine or zalcitabine in HIV-infected patients with the acquired immunodeficiency syndrome or fewer than 200 CD4 cells per cubic millimeter. Investigators for the Terry Beirn Community Programs for Clinical Research on AIDS. *The New England journal of medicine.* 1996;335(15):1099-106.

212. DHHS. Panel on Antiretroviral Guidelines for Adults and Adolescents. Guidelines for the Use of Antiretroviral Agents in Adults and Adolescents with HIV. https://clinicalinfo.hiv.gov/sites/default/files/guidelines/documents/AdultandAdolescentGL.pdf. Accessed 09-09-2021.

213. Eisinger RW, et al. HIV Viral Load and Transmissibility of HIV Infection: Undetectable Equals Untransmittable. *JAMA.* 2019;321(5):451-2.

214. Guadalupe M, et al. Severe CD4+ T-Cell Depletion in Gut Lymphoid Tissue during Primary Human Immunodeficiency Virus Type 1 Infection and Substantial Delay in Restoration following Highly Active Antiretroviral Therapy. *J Virol.* 2003;77(21):11708-17.

215. Verhoeven D, et al. Antiviral Therapy during Primary Simian Immunodeficiency Virus Infection Fails To Prevent Acute Loss of CD4+ T Cells in Gut Mucosa but Enhances Their Rapid Restoration through Central Memory T Cells. *J Virol.* 2008;82(8):4016-27.

216. Macal M, et al. Effective CD4+ T-cell restoration in gut-associated lymphoid tissue of HIV-infected patients is associated with enhanced Th17 cells and polyfunctional HIV-specific T-cell responses. *Mucosal Immunology.* 2008;1(6):475-88.

217. Deleage C, et al. Impact of early cART in the gut during acute HIV infection. *JCI Insight.* 2016;1(10).

218. Kelly C, et al. Discordant Immune Response with Antiretroviral Therapy in HIV-1: A Systematic Review of Clinical Outcomes. *PLoS One.* 2016;11(6):e0156099-e.

219. de Paula HHS, et al. Reduction of inflammation and T cell activation after 6 months of cART initiation during acute, but not in early chronic HIV-1 infection. *Retrovirology.* 2018;15(1):76.

220. Ghislain M, et al. Late Antiretroviral Therapy (ART) Initiation Is Associated with Long-Term Persistence of Systemic Inflammation and Metabolic Abnormalities. *PLoS One.* 2015;10(12):e0144317.

221. Marcus JL, et al. Comparison of Overall and Comorbidity-Free Life Expectancy Between Insured Adults With and Without HIV Infection, 2000-2016. *JAMA Network Open.* 2020;3(6):e207954-e.

222. Hirsch VM, et al. Induction of AIDS by simian immunodeficiency virus from an African green monkey: species-specific variation in pathogenicity correlates with the extent of in vivo replication. *J Virol.* 1995;69(2):955-67.

223. Chen Z, et al. Isolation and characterization of the first simian immunodeficiency virus from a feral sooty mangabey (Cercocebus atys) in West Africa. *Journal of medical primatology.* 1995;24(3):108-15.

224. Smith SM, et al. SIVrcm infection of macaques. *Journal of medical primatology.* 1998;27(2-3):94-8.

225. Osterhaus AD, et al. Isolation and partial characterization of a lentivirus from talapoin monkeys (Myopithecus talapoin). *Virology.* 1999;260(1):116-24.

226. Takehisa J, et al. Natural infection of wild-born mandrills (Mandrillus sphinx) with two different types of simian immunodeficiency virus. *AIDS research and human retroviruses.* 2001;17(12):1143-54.

227. Silvestri G, et al. Divergent host responses during primary simian immunodeficiency virus SIVsm infection of natural sooty mangabey and nonnatural rhesus macaque hosts. *J Virol.* 2005;79(7):4043-54.

228. Wagner TA, et al. HIV latency. Proliferation of cells with HIV integrated into cancer genes contributes to persistent infection. *Science (New York, NY).* 2014;345(6196):570-3.

229. Cohn LB, et al. HIV-1 integration landscape during latent and active infection. *Cell.* 2015;160(3):420-32.

230. Ferris AL, et al. Clonal expansion of SIV-infected cells in macaques on antiretroviral therapy is similar to that of HIV-infected cells in humans. *PLoS pathogens.* 2019;15(7):e1007869.

231. Sellier P, et al. Antiretroviral Treatment Start-Time during Primary SIVmac Infection in Macaques Exerts a Different Impact on Early Viral Replication and Dissemination. *PLoS One.* 2010;5(5):e10570.

232. Mannioui A, et al. Dynamics of viral replication in blood and lymphoid tissues during SIVmac251 infection of macaques. *Retrovirology.* 2009;6(1):106.

233. Bourry O, et al. Effect of a short-term HAART on SIV load in macaque tissues is dependent on time of initiation and antiviral diffusion. *Retrovirology.* 2010;7(1):78.

234. Canary LA, et al. Rate of AIDS Progression Is Associated with Gastrointestinal Dysfunction in Simian Immunodeficiency Virus–Infected Pigtail Macaques. *The Journal of Immunology.* 2013;190(6):2959-65.

235. Hao XP, et al. Experimental colitis in SIV-uninfected rhesus macaques recapitulates important features of pathogenic SIV infection. *Nat Commun.* 2015;6(8020.

236. Pandrea I, et al. Coagulation biomarkers predict disease progression in SIV-infected nonhuman primates. *Blood.* 2012;120(7):1357-66.

237. Pandrea I, et al. Antibiotic and Antiinflammatory Therapy Transiently Reduces Inflammation and Hypercoagulation in Acutely SIV-Infected Pigtailed Macaques. *PLoS pathogens.* 2016;12(1):e1005384.

238. Schechter ME, et al. Inflammatory monocytes expressing tissue factor drive SIV and HIV coagulopathy. *Science translational medicine.* 2017;9(405):eaam5441.

239. Zink MC, et al. High viral load in the cerebrospinal fluid and brain correlates with severity of simian immunodeficiency virus encephalitis. *J Virol.* 1999;73(12):10480-8.

240. Gama L, et al. Reactivation of simian immunodeficiency virus reservoirs in the brain of virally suppressed macaques. *AIDS (London, England).* 2017;31(1).

241. Matsuda K, et al. A SIV molecular clone that targets the CNS and induces neuroAIDS in rhesus macaques. *PLoS pathogens.* 2017;13(8):e1006538.

242. Giorgi JV, et al. Shorter survival in advanced human immunodeficiency virus type 1 infection is more closely associated with T lymphocyte activation than with plasma virus burden or virus chemokine coreceptor usage. *The Journal of infectious diseases.* 1999;179(4):859-70.

243. Hazenberg MD, et al. Persistent immune activation in HIV-1 infection is associated with progression to AIDS. *AIDS (London, England).* 2003;17(13):1881-8.

244. Chevalier MF, et al. The Th17/Treg ratio, IL-1RA and sCD14 levels in primary HIV infection predict the T-cell activation set point in the absence of systemic microbial translocation. *PLoS pathogens.* 2013;9(6):e1003453.

245. Brenchley JM, et al. Differential Th17 CD4 T-cell depletion in pathogenic and nonpathogenic lentiviral infections. *Blood.* 2008;112(7):2826-35.

246. Favre D, et al. Critical loss of the balance between Th17 and T regulatory cell populations in pathogenic SIV infection. *PLoS pathogens.* 2009;5(2):e1000295.

247. Brenchley JM, and Douek DC. Microbial translocation across the GI tract. *Annual review of immunology.* 2012;30(149-73.

248. Kristoff J, et al. Early microbial translocation blockade reduces SIV-mediated inflammation and viral replication. *The Journal of clinical investigation.* 2014;124(6):2802-6.

249. Kovacs A, et al. CD8+ T Cell Activation in Women Coinfected with Human Immunodeficiency Virus Type 1 and Hepatitis C Virus. *The Journal of infectious diseases.* 2008;197(10):1402-.

250. Bautista-Amorocho H, et al. Epidemiology, Risk Factors and Genotypes of HBV in HIV-Infected Patients in the Northeast Region of Colombia: High Prevalence of Occult Hepatitis B and F3 Subgenotype Dominance. *PLoS One.* 2014;9(12):e114272.

251. Sheth PM, et al. Coinfection with Herpes Simplex Virus Type 2 Is Associated with Reduced HIV-Specific T Cell Responses and Systemic Immune Activation. *The Journal of infectious diseases.* 2008;197(10):1394-401.

252. Gianella S, et al. Associations between Virologic and Immunologic Dynamics in Blood and in the Male Genital Tract. *J Virol.* 2012;86(3):1307-15.

253. Freeman ML, et al. CD8 T-cell expansion and inflammation linked to CMV coinfection in ART-treated HIV infection. *Clinical infectious diseases : an official publication of the Infectious Diseases Society of America.* 2016;62(3):392-6.

254. Petrara MR, et al. Epstein-Barr Virus load and immune activation in Human Immunodeficiency Virus type 1-infected patients. *Journal of Clinical Virology.* 2012;53(3):195-200.

255. Boulougoura A, and Sereti I. HIV infection and immune activation: the role of coinfections. *Curr Opin HIV AIDS.* 2016;11(2):191-200.

256. Friis-Møller N, et al. Class of antiretroviral drugs and the risk of myocardial infarction. *The New England journal of medicine.* 2007;356(17):1723-35.

257. Contento RL, et al. CXCR4–CCR5: A couple modulating T cell functions. *Proceedings of the National Academy of Sciences.* 2008;105(29):10101-6.

258. Gornalusse GG, et al. Epigenetic mechanisms, T-cell activation, and CCR5 genetics interact to regulate T-cell expression of CCR5, the major HIV-1 coreceptor. *Proc Natl Acad Sci U S A.* 2015;112(34):E4762-71.

259. Kawakami K, et al. Identification and purification of a human immunoglobulin-enhancer-binding protein (NF-kappa B) that activates transcription from a human immunodeficiency virus type 1 promoter in vitro. *Proc Natl Acad Sci U S A.* 1988;85(13):4700-4.

260. Papagno L, et al. Immune Activation and CD8+ T-Cell Differentiation towards Senescence in HIV-1 Infection. *PLOS Biology.* 2004;2(2):e20.

261. Cobos Jiménez V, et al. T-Cell Activation Independently Associates With Immune Senescence in HIV-Infected Recipients of Long-term Antiretroviral Treatment. *The Journal of infectious diseases.* 2016;214(2):216-25.

262. Day CL, et al. PD-1 expression on HIV-specific T cells is associated with T-cell exhaustion and disease progression. *Nature.* 2006;443(7109):350-4.

263. Trautmann L, et al. Upregulation of PD-1 expression on HIV-specific CD8+ T cells leads to reversible immune dysfunction. *Nature Medicine.* 2006;12(10):1198-202.

264. Zhang J-Y, et al. PD-1 up-regulation is correlated with HIV-specific memory CD8+ T-cell exhaustion in typical progressors but not in long-term nonprogressors. *Blood.* 2007;109(11):4671-8.

265. Evans VA, et al. Programmed cell death-1 contributes to the establishment and maintenance of HIV-1 latency. *AIDS (London, England).* 2018;32(11):1491-7.

266. McGary CS, et al. CTLA-4+PD-1- Memory CD4+ T Cells Critically Contribute to Viral Persistence in Antiretroviral Therapy-Suppressed, SIV-Infected Rhesus Macaques. *Immunity*. 2017;47(4):776-88.e5.

267. Schweneker M, et al. HIV-Induced Changes in T Cell Signaling Pathways. *The Journal of Immunology*. 2008;180(10):6490-500.

268. Estes JD, et al. Simian immunodeficiency virus-induced lymphatic tissue fibrosis is mediated by transforming growth factor beta 1-positive regulatory T cells and begins in early infection. *The Journal of infectious diseases*. 2007;195(4):551-61.

269. Estes JD, et al. The role of collagen deposition in depleting CD4+ T cells and limiting reconstitution in HIV-1 and SIV infections through damage to the secondary lymphoid organ niche. *Seminars in immunology*. 2008;20(3):181-6.

270. Zeng M, et al. Cumulative mechanisms of lymphoid tissue fibrosis and T cell depletion in HIV-1 and SIV infections. *The Journal of clinical investigation*. 2011;121(3):998-1008.

271. Estes JD. Pathobiology of HIV/SIV-associated changes in secondary lymphoid tissues. *Immunol Rev*. 2013;254(1):65-77.

272. Schottenfeld D, and Beebe-Dimmer J. Chronic inflammation: a common and important factor in the pathogenesis of neoplasia. *CA: a cancer journal for clinicians*. 2006;56(2):69-83.

273. Dubrow R, et al. HIV infection, aging, and immune function: implications for cancer risk and prevention. *Curr Opin Oncol*. 2012;24(5):506-16.

274. Triant VA, et al. Increased acute myocardial infarction rates and cardiovascular risk factors among patients with human immunodeficiency virus disease. *The Journal of clinical endocrinology and metabolism*. 2007;92(7):2506-12.

275. Hsue PY, et al. Immunologic basis of cardiovascular disease in HIV-infected adults. *The Journal of infectious diseases*. 2012;205 Suppl 3(Suppl 3):S375-82.

276. Levi M, et al. Bidirectional relation between inflammation and coagulation. *Circulation*. 2004;109(22):2698-704.

277. Guaraldi G, et al. Premature age-related comorbidities among HIV-infected persons compared with the general population. *Clinical infectious diseases : an official publication of the Infectious Diseases Society of America*. 2011;53(11):1120-6.

278. Guaraldi G, et al. Aging with HIV vs. HIV seroconversion at older age: a diverse population with distinct comorbidity profiles. *PLoS One*. 2015;10(4):e0118531-e.

279. He T, et al. Modeling aging in HIV infection in nonhuman primates to address an emerging challenge of the post-ART era. *Curr Opin Virol*. 2017;25(66-75.

280. He T, et al. Modeling aging in HIV infection in nonhuman primates to address an emerging challenge of the post-ART era. *Current opinion in virology*. 2017;25(66-75.

281. Dudgeon WD, et al. Counteracting muscle wasting in HIV-infected individuals. *HIV medicine*. 2006;7(5):299-310.

282. Lemoine M, et al. From nonalcoholic fatty liver to nonalcoholic steatohepatitis and cirrhosis in HIV-infected patients: diagnosis and management. *Current opinion in infectious diseases.* 2012;25(1):10-6.

283. Sanmarti M, et al. HIV-associated neurocognitive disorders. *Journal of molecular psychiatry.* 2014;2(1):2.

284. Klatt NR, et al. Microbial translocation, immune activation, and HIV disease. *Trends in Microbiology.* 2013;21(1):6-13.

285. Kim WK, et al. Monocyte heterogeneity underlying phenotypic changes in monocytes according to SIV disease stage. *J Leukoc Biol.* 2010;87(4):557-67.

286. Ziegler-Heitbrock L. The CD14+ CD16+ blood monocytes: their role in infection and inflammation. *J Leukoc Biol.* 2007;81(3):584-92.

287. Dandekar S. Pathogenesis of HIV in the gastrointestinal tract. *Current HIV/AIDS reports.* 2007;4(1):10-5.

288. Brenchley JM, et al. HIV disease: fallout from a mucosal catastrophe? *Nature immunology.* 2006;7(3):235-9.

289. Brenchley JM, and Douek DC. HIV infection and the gastrointestinal immune system. *Mucosal Immunol.* 2008;1(1):23-30.

290. Grossman Z, et al. Pathogenesis of HIV infection: what the virus spares is as important as what it destroys. *Nat Med.* 2006;12(3):289-95.

291. Douek DC, et al. Emerging Concepts in the Immunopathogenesis of AIDS. *Annual review of medicine.* 2008.

292. Veazey RS, et al. The mucosal immune system: primary target for HIV infection and AIDS. *Trends Immunol.* 2001;22(11):626-33.

293. Veazey RS, and Lackner AA. Getting to the guts of HIV pathogenesis. *The Journal of experimental medicine.* 2004;200(6):697-700.

294. Picker LJ, and Watkins DI. HIV pathogenesis: the first cut is the deepest. *Nature immunology.* 2005;6(5):430-2.

295. Steele AK, et al. Microbial exposure alters HIV-1-induced mucosal CD4+ T cell death pathways Ex vivo. *Retrovirology.* 2014;11(14.

296. Paiardini M, et al. Mucosal immune dysfunction in AIDS pathogenesis. *AIDS Rev.* 2008;10(1):36-46.

297. Pandrea I, and Apetrei C. Where the wild things are: Pathogenesis of SIV infection in African nonhuman primate hosts. *Curr HIV/AIDS Reports.* 2010;7(1):28-36.

298. Favre D, et al. Critical loss of the balance between Th17 and T regulatory cell populations in pathogenic SIV infection. *Plos Pathogens.* 2009;5(2):e1000295.

299. Sandler NG, and Douek DC. Microbial translocation in HIV infection: causes, consequences and treatment opportunities. *Nature reviews Microbiology.* 2012;10(9):655-66.

300. Kovacs SB, et al. T-cell depletion in the colonic mucosa of patients with idiopathic CD4 lymphopenia. *The Journal of infectious diseases.* 2015.

301. Sodora DL, and Silvestri G. Immune activation and AIDS pathogenesis. *AIDS (London, England).* 2008;22(4):439-46.

302. Pandrea IV, et al. Acute loss of intestinal CD4+ T cells is not predictive of simian immunodeficiency virus virulence. *Journal of immunology (Baltimore, Md : 1950).* 2007;179(5):3035-46.

303. Pandrea I, et al. Cutting edge: Experimentally induced immune activation in natural hosts of simian immunodeficiency virus induces significant increases in viral replication and CD4+ T cell depletion. *Journal of immunology (Baltimore, Md : 1950).* 2008;181(10):6687-91.

304. Silvestri G, et al. Understanding the benign nature of SIV infection in natural hosts. *The Journal of clinical investigation.* 2007;117(11):3148-54.

305. Apetrei C, et al. Direct inoculation of simian immunodeficiency virus from sooty mangabeys in black mangabeys (Lophocebus aterrimus): first evidence of AIDS in a heterologous African species and different pathologic outcomes of experimental infection. *J Virol.* 2004;78(21):11506-18.

306. Ling B, et al. Classic AIDS in a sooty mangabey after an 18-year natural infection. *J Virol.* 2004;78(16):8902-8.

307. Pandrea I, et al. Chronic SIV infection ultimately causes immunodeficiency in African non-human primates. *AIDS (London, England).* 2001;15(18):2461-2.

308. Pandrea I, et al. Into the wild: simian immunodeficiency virus (SIV) infection in natural hosts. *Trends in immunology.* 2008;29(9):419-28.

309. Apetrei C, et al. Virus Subtype-Specific Features of Natural Simian Immunodeficiency Virus SIV_{smm} Infection in Sooty Mangabeys. *J Virol.* 2007;81(15):7913-23.

310. Broussard SR, et al. Simian immunodeficiency virus replicates to high levels in naturally infected African green monkeys without inducing immunologic or neurologic disease. *J Virol.* 2001;75(5):2262-75.

311. Gueye A, et al. Viral load in tissues during the early and chronic phase of non-pathogenic SIVagm infection. *Journal of medical primatology.* 2004;33(2):83-97.

312. Onanga R, et al. High levels of viral replication contrast with only transient changes in CD4(+) and CD8(+) cell numbers during the early phase of experimental infection with simian immunodeficiency virus SIVmnd-1 in Mandrillus sphinx. *J Virol.* 2002;76(20):10256-63.

313. Pandrea I, et al. Simian immunodeficiency viruses replication dynamics in African non-human primate hosts: common patterns and species-specific differences. *Journal of medical primatology.* 2006;35(4-5):194-201.

314. Souquière S, et al. Simian immunodeficiency virus types 1 and 2 (SIV mnd 1 and 2) have different pathogenic potentials in rhesus macaques upon experimental cross-species transmission. *The Journal of general virology.* 2009;90(Pt 2):488-99.

315. Pandrea I, et al. Simian immunodeficiency virus SIVagm.sab infection of Caribbean African green monkeys: a new model for the study of SIV pathogenesis in natural hosts. *J Virol.* 2006;80(10):4858-67.

316. Pandrea I, et al. Paucity of CD4+CCR5+ T cells is a typical feature of natural SIV hosts. *Blood.* 2006;109(3):1069-76.

317. Pandrea I, et al. Mucosal Simian Immunodeficiency Virus Transmission in African Green Monkeys: Susceptibility to Infection Is Proportional to Target Cell Availability at Mucosal Sites. *J Virol.* 2012;86(8):4158-68.

318. Dunham R, et al. The AIDS resistance of naturally SIV-infected sooty mangabeys is independent of cellular immunity to the virus. *Blood.* 2006;108(1):209-17.

319. Schmitz JE, et al. Inhibition of Adaptive Immune Responses Leads to a Fatal Clinical Outcome in SIV-Infected Pigtailed Macaques but Not Vervet African Green Monkeys. *PLoS pathogens.* 2009;5(12):e1000691.

320. Zahn RC, et al. Suppression of adaptive immune responses during primary SIV infection of sabaeus African green monkeys delays partial containment of viremia but does not induce disease. *Blood.* 2010;115(15):3070-8.

321. Klatt Nichole R, et al. Dynamics of Simian Immunodeficiency Virus SIVmac239 Infection in Pigtail Macaques. *J Virol.* 2012;86(2):1203-13.

322. Compton AA, and Emerman M. Convergence and Divergence in the Evolution of the APOBEC3G-Vif Interaction Reveal Ancient Origins of Simian Immunodeficiency Viruses. *PLoS pathogens.* 2013;9(1):e1003135.

323. Gifford RJ, et al. A transitional endogenous lentivirus from the genome of a basal primate and implications for lentivirus evolution. *Proceedings of the National Academy of Sciences.* 2008;105(51):20362-7.

324. Worobey M, et al. Island Biogeography Reveals the Deep History of SIV. *Science (New York, NY).* 2010;329(5998):1487-.

325. Apetrei C, et al. Pattern of SIVagm Infection in Patas Monkeys Suggests that Host Adaptation to Simian Immunodeficiency Virus Infection May Result in Resistance to Infection and Virus Extinction. *The Journal of infectious diseases.* 2010;202(Supplement_3):S371-S6.

326. Harris Levelle D, et al. Downregulation of Robust Acute Type I Interferon Responses Distinguishes Nonpathogenic Simian Immunodeficiency Virus (SIV) Infection of Natural Hosts from Pathogenic SIV Infection of Rhesus Macaques. *J Virol.* 2010;84(15):7886-91.

327. Palesch D, et al. Sooty mangabey genome sequence provides insight into AIDS resistance in a natural SIV host. *Nature.* 2018;553(7686):77-81.

328. Riddick NE, et al. A Novel CCR5 Mutation Common in Sooty Mangabeys Reveals SIVsmm Infection of CCR5-Null Natural Hosts and Efficient Alternative Coreceptor Use In Vivo. *PLoS pathogens.* 2010;6(8):e1001064.

329. Vinton C, et al. CD4-Like Immunological Function by CD4− T Cells in Multiple Natural Hosts of Simian Immunodeficiency Virus. *J Virol.* 2011;85(17):8702-8.

330. Paiardini M, et al. Low levels of SIV infection in sooty mangabey central memory CD4+ T cells are associated with limited CCR5 expression. *Nature Medicine.* 2011;17(7):830-6.

331. Pandrea I, et al. Paucity of CD4+ CCR5+ T Cells May Prevent Transmission of Simian Immunodeficiency Virus in Natural Nonhuman Primate Hosts by Breast-Feeding. *J Virol.* 2008;82(11):5501-9.

332. Beaumier CM, et al. CD4 downregulation by memory CD4+ T cells in vivo renders African green monkeys resistant to progressive SIVagm infection. *Nature Medicine.* 2009;15(8):879-85.

333. Elliott Sarah TC, et al. Dualtropic CXCR6/CCR5 Simian Immunodeficiency Virus (SIV) Infection of Sooty Mangabey Primary Lymphocytes: Distinct Coreceptor Use in Natural versus Pathogenic Hosts of SIV. *J Virol.* 2015;89(18):9252-61.

334. Marchetti G, et al. Microbial Translocation in the Pathogenesis of HIV Infection and AIDS. *Clinical microbiology reviews.* 2013;26(1):2-18.

335. Lerner AM, et al. Comorbidities in Persons With HIV: The Lingering Challenge. *JAMA.* 2020;323(1):19-20.

336. Morlat P, et al. Causes of death among HIV-infected patients in France in 2010 (national survey): trends since 2000. *AIDS (London, England).* 2014;28(8).

337. Smith CJ, et al. Trends in underlying causes of death in people with HIV from 1999 to 2011 (D:A:D): a multicohort collaboration. *Lancet (London, England).* 2014;384(9939):241-8.

338. Marcus JL, et al. Narrowing the Gap in Life Expectancy Between HIV-Infected and HIV-Uninfected Individuals With Access to Care. *Journal of acquired immune deficiency syndromes (1999).* 2016;73(1):39-46.

339. Schouten J, et al. Cross-sectional Comparison of the Prevalence of Age-Associated Comorbidities and Their Risk Factors Between HIV-Infected and Uninfected Individuals: The AGEhIV Cohort Study. *Clinical Infectious Diseases.* 2014;59(12):1787-97.

340. Evans DT, and Silvestri G. Nonhuman primate models in AIDS research. *Curr Opin HIV AIDS.* 2013;8(4):255-61.

341. Lifson JD, and Haigwood NL. Lessons in nonhuman primate models for AIDS vaccine research: from minefields to milestones. *Cold Spring Harbor perspectives in medicine.* 2012;2(6):a007310.

342. Palella FJ, Jr., and Phair JP. Cardiovascular disease in HIV infection. *Curr Opin HIV AIDS.* 2011;6(4):266-71.

343. Balagopal A, et al. Kupffer cells are depleted with HIV immunodeficiency and partially recovered with antiretroviral immune reconstitution. *AIDS (London, England).* 2009;23(18):2397-404.

344. Tuyama AC, et al. Human immunodeficiency virus (HIV)-1 infects human hepatic stellate cells and promotes collagen I and monocyte chemoattractant protein-1 expression: implications for the pathogenesis of HIV/hepatitis C virus-induced liver fibrosis. *Hepatology (Baltimore, Md).* 2010;52(2):612-22.

345. Justice AC, et al. Does an index composed of clinical data reflect effects of inflammation, coagulation, and monocyte activation on mortality among those aging with HIV? *Clinical infectious diseases : an official publication of the Infectious Diseases Society of America.* 2012;54(7):984-94.

346. Violi F, et al. Association between low-grade disseminated intravascular coagulation and endotoxemia in patients with liver cirrhosis. *Gastroenterology.* 1995;109(2):531-9.

347. Shmagel KV, et al. Systemic inflammation and liver damage in HIV/hepatitis C virus coinfection. *HIV medicine.* 2016;17(8):581-9.

348. Pandrea I, et al. Alcohol's role in HIV transmission and disease progression. *Alcohol Res Health.* 2010;33(3):203-18.

349. Zhang L, et al. The Liver Is a Major Organ for Clearing Simian Immunodeficiency Virus in Rhesus Monkeys. *J Virol.* 2002;76(10):5271-3.

350. Kunisaki KM. Will expanded ART use reduce the burden of HIV-associated chronic lung disease? *Curr Opin HIV AIDS.* 2014;9(1):27-33.

351. Campbell LJ, et al. Spectrum of chronic kidney disease in HIV-infected patients. *HIV medicine.* 2009;10(6):329-36.

352. Kalyesubula R, et al. HIV-Associated Renal and Genitourinary Comorbidities in Africa. *JAIDS Journal of Acquired Immune Deficiency Syndromes.* 2014;67(

353. Ryom L, et al. Antiretroviral therapy, immune suppression and renal impairment in HIV-positive persons. *Curr Opin HIV AIDS.* 2014;9(1):41-7.

354. Stephens EB, et al. Simian-human immunodeficiency virus-associated nephropathy in macaques. *AIDS research and human retroviruses.* 2000;16(13):1295-306.

355. Clarke CL, et al. Peripheral edema with hypoalbuminemia in a nonhuman primate infected with simian-human immunodeficiency virus: a case report. *Journal of the American Association for Laboratory Animal Science : JAALAS.* 2008;47(1):42-8.

356. Saylor D, et al. HIV-associated neurocognitive disorder — pathogenesis and prospects for treatment. *Nature Reviews Neurology.* 2016;12(4):234-48.

357. Holt JL, et al. Neuroimaging studies of the aging HIV-1-infected brain. *Journal of NeuroVirology.* 2012;18(4):291-302.

358. Williams R, et al. Nonhuman primate models of NeuroAIDS. *J Neurovirol.* 2008;14(4):292-300.

359. Beck SE, et al. An SIV/macaque model targeted to study HIV-associated neurocognitive disorders. *Journal of neurovirology.* 2018;24(2):204-12.

360. Finzi D, et al. Latent infection of CD4+ T cells provides a mechanism for lifelong persistence of HIV-1, even in patients on effective combination therapy. *Nat Med.* 1999;5(5):512-7.

361. Pan X, et al. Restrictions to HIV-1 replication in resting CD4+ T lymphocytes. *Cell Research.* 2013;23(7):876-85.

362. Chun T-W, et al. Re-emergence of HIV after stopping therapy. *Nature.* 1999;401(6756):874-5.

363. Chun T-W, et al. Presence of an inducible HIV-1 latent reservoir during highly active antiretroviral therapy. *Proceedings of the National Academy of Sciences.* 1997;94(24):13193-7.

364. Perelson AS, et al. Decay characteristics of HIV-1-infected compartments during combination therapy. *Nature.* 1997;387(6629):188-91.

365. Wong JK, et al. Recovery of replication-competent HIV despite prolonged suppression of plasma viremia. *Science (New York, NY).* 1997;278(5341):1291-5.

366. Chun T-W, et al. Early establishment of a pool of latently infected, resting CD4⁺ T cells during primary HIV-1 infection. *Proceedings of the National Academy of Sciences.* 1998;95(15):8869-73.

367. Archin NM, et al. Interval dosing with the HDAC inhibitor vorinostat effectively reverses HIV latency. *The Journal of clinical investigation.* 2017;127(8):3126-35.

368. Wei DG, et al. Histone deacetylase inhibitor romidepsin induces HIV expression in CD4 T cells from patients on suppressive antiretroviral therapy at concentrations achieved by clinical dosing. *PLoS pathogens.* 2014;10(4):e1004071.

369. Mousseau G, et al. The Tat Inhibitor Didehydro-Cortistatin A Prevents HIV-1 Reactivation from Latency. *mBio.* 2015;6(4).

370. Donahue DA, et al. The Viral Protein Tat Can Inhibit the Establishment of HIV-1 Latency. *J Virol.* 2012;86(6):3253-63.

371. Borducchi EN, et al. Ad26/MVA therapeutic vaccination with TLR7 stimulation in SIV-infected rhesus monkeys. *Nature.* 2016;540(284.

372. Tsai A, et al. Toll-Like Receptor 7 Agonist GS-9620 Induces HIV Expression and HIV-Specific Immunity in Cells from HIV-Infected Individuals on Suppressive Antiretroviral Therapy. *J Virol.* 2017.

373. Murray SM, et al. Reduction of Immune Activation with Chloroquine Therapy during Chronic HIV Infection. *J Virol.* 2010;84(22):12082-6.

374. Josefsson L, et al. The HIV-1 reservoir in eight patients on long-term suppressive antiretroviral therapy is stable with few genetic changes over time. *Proceedings of the National Academy of Sciences.* 2013;110(51):E4987-E96.

375. Porichis F, et al. Differential impact of PD-1 and/or interleukin-10 blockade on HIV-1-specific CD4 T cell and antigen-presenting cell functions. *J Virol.* 2014;88(5):2508-18.

376. Palmer BE, et al. In vivo blockade of the PD-1 receptor suppresses HIV-1 viral loads and improves CD4+ T cell levels in humanized mice. *Journal of immunology (Baltimore, Md : 1950).* 2013;190(1):211-9.

377. Jones RB, et al. Tim-3 expression defines a novel population of dysfunctional T cells with highly elevated frequencies in progressive HIV-1 infection. *The Journal of experimental medicine.* 2008;205(12):2763-79.

378. Zhang Z-N, et al. Elevation of Tim-3 and PD-1 Expression on T Cells Appears Early in HIV Infection, and Differential Tim-3 and PD-1 Expression Patterns Can Be Induced by Common γ-Chain Cytokines. *BioMed Research International.* 2015;2015(916936.

379. Peretz Y, et al. CD160 and PD-1 Co-Expression on HIV-Specific CD8 T Cells Defines a Subset with Advanced Dysfunction. *PLoS pathogens.* 2012;8(8):e1002840.

380. Vandergeeten C, et al. Interleukin-7 promotes HIV persistence during antiretroviral therapy. *Blood.* 2013;121(21):4321-9.

381. Seay K, et al. In Vivo Activation of Human NK Cells by Treatment with an Interleukin-15 Superagonist Potently Inhibits Acute In Vivo HIV-1 Infection in Humanized Mice. *J Virol.* 2015;89(12):6264-74.

382. Younes SA, et al. IL-15 promotes activation and expansion of CD8+ T cells in HIV-1 infection. *The Journal of clinical investigation.* 2016;126(7):2745-56.

383. Mendez-Lagares G, et al. IL-21 Therapy Controls Immune Activation and Maintains Antiviral CD8(+) T Cell Responses in Acute Simian Immunodeficiency Virus Infection. *AIDS research and human retroviruses.* 2017;33(S1):S81-s92.

384. Hale M, et al. Engineering HIV-Resistant, Anti-HIV Chimeric Antigen Receptor T Cells. *Molecular therapy : the journal of the American Society of Gene Therapy.* 2017;25(3):570-9.

385. Hütter G, et al. CCR5 Targeted Cell Therapy for HIV and Prevention of Viral Escape. *Viruses.* 2015;7(8):4186-203.

386. Allers K, et al. Evidence for the cure of HIV infection by CCR5Δ32/Δ32 stem cell transplantation. *Blood.* 2011;117(10):2791-9.

387. Gupta RK, et al. HIV-1 remission following CCR5Δ32/Δ32 haematopoietic stem-cell transplantation. *Nature.* 2019;568(7751):244-8.

388. Eberhard JM, et al. Vulnerability to reservoir reseeding due to high immune activation after allogeneic hematopoietic stem cell transplantation in individuals with HIV-1. *Sci Transl Med.* 2020;12(542).

389. Saez-Cirion A, and Muller-Trutwin M. The Yellow Brick Road towards HIV Eradication. *Trends Immunol.* 2019;40(6):465-7.

390. Dufour C, et al. The multifaceted nature of HIV latency. *The Journal of clinical investigation.* 2020;130(7):3381-90.

391. Margolis DM, et al. Curing HIV: Seeking to Target and Clear Persistent Infection. *Cell.* 2020;181(1):189-206.

392. Massanella M, et al. Residual inflammation and viral reservoirs: alliance against an HIV cure. *Curr Opin HIV AIDS.* 2016;11(2):234-41.

393. Passaes CP, and Saez-Cirion A. HIV cure research: advances and prospects. *Virology.* 2014;454-455(340-52.

394. Rabezanahary H, et al. Despite early antiretroviral therapy effector memory and follicular helper CD4 T cells are major reservoirs in visceral lymphoid tissues of SIV-infected macaques. *Mucosal Immunology.* 2020;13(1):149-60.

395. Finzi D, et al. Identification of a Reservoir for HIV-1 in Patients on Highly Active Antiretroviral Therapy. *Science (New York, NY).* 1997;278(5341):1295-300.

396. Finzi D, et al. Latent infection of CD4+ T cells provides a mechanism for lifelong persistence of HIV-1, even in patients on effective combination therapy. *Nat Med.* 1999;5(5):512-7.

397. Jordan A, et al. HIV reproducibly establishes a latent infection after acute infection of T cells in vitro. *EMBO J.* 2003;22(

398. Siliciano JD, et al. Long-term follow-up studies confirm the stability of the latent reservoir for HIV-1 in resting CD4+ T cells. *Nat Med.* 2003;9(6):727-8.

399. Delobel P, et al. Persistence of distinct HIV-1 populations in blood monocytes and naive and memory CD4 T cells during prolonged suppressive HAART. *AIDS (London, England).* 2005;19(16):1739-50.

400. Chomont N, et al. HIV reservoir size and persistence are driven by T cell survival and homeostatic proliferation. *Nat Med.* 2009;15(8):893-900.

401. Buzon MJ, et al. HIV-1 persistence in CD4+ T cells with stem cell-like properties. *Nat Med.* 2014;20(2):139-42.

402. Kleinman AJ, et al. Regulatory T Cells As Potential Targets for HIV Cure Research. *Front Immunol.* 2018;9(734):734.

403. Pallikkuth S, et al. Peripheral T Follicular Helper Cells Are the Major HIV Reservoir within Central Memory CD4 T Cells in Peripheral Blood from Chronically HIV-Infected Individuals on Combination Antiretroviral Therapy. *J Virol.* 2016;90(6):2718-28.

404. Wong ME, et al. The HIV Reservoir in Monocytes and Macrophages. *Frontiers in immunology.* 2019;10(1435-.

405. Spiegel H, et al. Follicular dendritic cells are a major reservoir for human immunodeficiency virus type 1 in lymphoid tissues facilitating infection of CD4+ T-helper cells. *Am J Pathol.* 1992;140(1):15-22.

406. Badia R, et al. CD32 expression is associated to T-cell activation and is not a marker of the HIV-1 reservoir. *Nature Communications.* 2018;9(1):2739.

407. Hütter G, et al. Long-Term Control of HIV by CCR5 Delta32/Delta32 Stem-Cell Transplantation. *New England Journal of Medicine.* 2009;360(7):692-8.

408. Henrich TJ, et al. Antiretroviral-free hiv-1 remission and viral rebound after allogeneic stem cell transplantation: Report of 2 cases. *Annals of Internal Medicine.* 2014;161(5):319-27.

409. Persaud D, et al. Absence of Detectable HIV-1 Viremia after Treatment Cessation in an Infant. *New England Journal of Medicine.* 2013;369(19):1828-35.

410. Luzuriaga K, et al. Viremic Relapse after HIV-1 Remission in a Perinatally Infected Child. *New England Journal of Medicine.* 2015;372(8):786-8.

411. Sáez-Cirión A, et al. Post-Treatment HIV-1 Controllers with a Long-Term Virological Remission after the Interruption of Early Initiated Antiretroviral Therapy ANRS VISCONTI Study. *PLoS pathogens.* 2013;9(3):e1003211.

412. Violari A, et al. *International AIDS Society 2017*. Paris, France; 2017.

413. Cummins NW, et al. Extensive virologic and immunologic characterization in an HIV-infected individual following allogeneic stem cell transplant and analytic cessation of antiretroviral therapy: A case study. *PLoS medicine.* 2017;14(11):e1002461-e.

414. Folks T, et al. Induction of HTLV-III/LAV from a nonvirus-producing T-cell line: implications for latency. *Science (New York, NY).* 1986;231(4738):600-2.

415. Nabel G, and Baltimore D. An inducible transcription factor activates expression of human immunodeficiency virus in T cells. *Nature.* 1987;326(6114):711-3.

416. Siekevitz M, et al. Activation of the HIV-1 LTR by T cell mitogens and the trans-activator protein of HTLV-I. *Science (New York, NY).* 1987;238(4833):1575-8.

417. Duh EJ, et al. Tumor necrosis factor alpha activates human immunodeficiency virus type 1 through induction of nuclear factor binding to the NF-kappa B sites in the long terminal repeat. *Proceedings of the National Academy of Sciences.* 1989;86(15):5974-8.

418. Zack JA, et al. HIV-1 entry into quiescent primary lymphocytes: Molecular analysis reveals a labile, latent viral structure. *Cell.* 1990;61(2):213-22.

419. Bukrinsky MI, et al. Quiescent T Lymphocytes as an Inducible Virus Reservoir in HIV-1 Infection. *Science (New York, NY).* 1991;254(5030):423-7.

420. Chun T-W, et al. In vivo fate of HIV-1-infected T cells: Quantitative analysis of the transition to stable latency. *Nature Medicine.* 1995;1(12):1284-90.

421. Sahu GK, et al. A novel in vitro system to generate and study latently HIV-infected long-lived normal CD4+ T-lymphocytes. *Virology.* 2006;355(2):127-37.

422. Bosque A, and Planelles V. Induction of HIV-1 latency and reactivation in primary memory CD4+ T cells. *Blood.* 2009;113(1):58-65.

423. Burke B, et al. Primary cell model for activation-inducible human immunodeficiency virus. *J Virol.* 2007;81(14):7424-34.

424. Marini A, et al. An in vitro system to model the establishment and reactivation of HIV-1 latency. *Journal of immunology (Baltimore, Md : 1950).* 2008;181(11):7713-20.

425. Tyagi M, et al. Establishment of HIV Latency in Primary CD4+ Cells Is due to Epigenetic Transcriptional Silencing and P-TEFb Restriction. *J Virol.* 2010;84(13):6425-37.

426. Yang HC, et al. Small-molecule screening using a human primary cell model of HIV latency identifies compounds that reverse latency without cellular activation. *The Journal of clinical investigation.* 2009;119(11):3473-86.

427. Yang H-C. Primary cell models of HIV latency. *Current Opinion in HIV and AIDS.* 2011;6(1).

428. Verdin E, et al. Chromatin disruption in the promoter of human immunodeficiency virus type 1 during transcriptional activation. *The EMBO Journal.* 1993;12(8):3249-59.

429. Keedy Kara S, et al. A Limited Group of Class I Histone Deacetylases Acts To Repress Human Immunodeficiency Virus Type 1 Expression. *J Virol.* 2009;83(10):4749-56.

430. Van Lint C, et al. Transcriptional activation and chromatin remodeling of the HIV-1 promoter in response to histone acetylation. *The EMBO Journal.* 1996;15(5):1112-20.

431. Lusic M, et al. Regulation of HIV-1 gene expression by histone acetylation and factor recruitment at the LTR promoter. *The EMBO Journal.* 2003;22(24):6550-61.

432. Friedman J, et al. Epigenetic Silencing of HIV-1 by the Histone H3 Lysine 27 Methyltransferase Enhancer of Zeste 2. *J Virol.* 2011;85(17):9078-89.

433. Boehm D, et al. SMYD2-Mediated Histone Methylation Contributes to HIV-1 Latency. *Cell host & microbe.* 2017;21(5):569-79.e6.

434. Imai K, et al. Involvement of Histone H3 Lysine 9 (H3K9) Methyltransferase G9a in the Maintenance of HIV-1 Latency and Its Reactivation by BIX01294 *. *Journal of Biological Chemistry.* 2010;285(22):16538-45.

435. Chéné Id, et al. Suv39H1 and HP1γ are responsible for chromatin-mediated HIV-1 transcriptional silencing and post-integration latency. *The EMBO Journal.* 2007;26(2):424-35.

436. He G, and Margolis David M. Counterregulation of Chromatin Deacetylation and Histone Deacetylase Occupancy at the Integrated Promoter of Human Immunodeficiency Virus Type 1 (HIV-1) by the HIV-1 Repressor YY1 and HIV-1 Activator Tat. *Molecular and Cellular Biology.* 2002;22(9):2965-73.

437. Williams SA, et al. NF-κB p50 promotes HIV latency through HDAC recruitment and repression of transcriptional initiation. *The EMBO Journal.* 2006;25(1):139-49.

438. Tyagi M, and Karn J. CBF-1 promotes transcriptional silencing during the establishment of HIV-1 latency. *The EMBO Journal.* 2007;26(24):4985-95.

439. Greger IH, et al. Transcriptional interference perturbs the binding of Sp1 to the HIV-1 promoter. *Nucleic Acids Res.* 1998;26(5):1294-301.

440. Lenasi T, et al. Transcriptional Interference Antagonizes Proviral Gene Expression to Promote HIV Latency. *Cell host & microbe.* 2008;4(2):123-33.

441. Han Y, et al. Orientation-Dependent Regulation of Integrated HIV-1 Expression by Host Gene Transcriptional Readthrough. *Cell host & microbe.* 2008;4(2):134-46.

442. Sedore SC, et al. Manipulation of P-TEFb control machinery by HIV: recruitment of P-TEFb from the large form by Tat and binding of HEXIM1 to TAR. *Nucleic Acids Res.* 2007;35(13):4347-58.

443. Muniz L, et al. Controlling Cellular P-TEFb Activity by the HIV-1 Transcriptional Transactivator Tat. *PLoS pathogens.* 2010;6(10):e1001152.

444. Parada CA, and Roeder RG. Enhanced processivity of RNA polymerase II triggered by Tat-induced phosphorylation of its carboxy-terminal domain. *Nature.* 1996;384(6607):375-8.

445. Kim Young K, et al. Phosphorylation of the RNA Polymerase II Carboxyl-Terminal Domain by CDK9 Is Directly Responsible for Human Immunodeficiency Virus Type 1 Tat-Activated Transcriptional Elongation. *Molecular and Cellular Biology.* 2002;22(13):4622-37.

446. Bourgeois Cyril F, et al. Spt5 Cooperates with Human Immunodeficiency Virus Type 1 Tat by Preventing Premature RNA Release at Terminator Sequences. *Molecular and Cellular Biology.* 2002;22(4):1079-93.

447. Jang MK, et al. The Bromodomain Protein Brd4 Is a Positive Regulatory Component of P-TEFb and Stimulates RNA Polymerase II-Dependent Transcription. *Molecular cell.* 2005;19(4):523-34.

448. Yang Z, et al. Recruitment of P-TEFb for Stimulation of Transcriptional Elongation by the Bromodomain Protein Brd4. *Molecular cell.* 2005;19(4):535-45.

449. Li Z, et al. The BET bromodomain inhibitor JQ1 activates HIV latency through antagonizing Brd4 inhibition of Tat-transactivation. *Nucleic Acids Res.* 2013;41(1):277-87.

450. Boehm D, et al. BET bromodomain-targeting compounds reactivate HIV from latency via a Tat-independent mechanism. *Cell Cycle.* 2013;12(3):452-62.

451. Chun T-W, et al. Decay of the HIV Reservoir in Patients Receiving Antiretroviral Therapy for Extended Periods: Implications for Eradication of Virus. *The Journal of infectious diseases.* 2007;195(12):1762-4.

452. Gandhi RT, et al. Selective Decay of Intact HIV-1 Proviral DNA on Antiretroviral Therapy. *The Journal of infectious diseases.* 2021;223(2):225-33.

453. Chun TW, et al. Quantification of latent tissue reservoirs and total body viral load in HIV-1 infection. *Nature.* 1997;387(6629):183-8.

454. Bruner KM, et al. Defective proviruses rapidly accumulate during acute HIV-1 infection. *Nature Medicine.* 2016;22(9):1043-9.

455. Bullen CK, et al. New ex vivo approaches distinguish effective and ineffective single agents for reversing HIV-1 latency in vivo. *Nat Med.* 2014;20(4):425-9.

456. Kuzmichev YV, et al. A CD3/CD28 microbead-based HIV-1 viral outgrowth assay. *Journal of virus eradication.* 2017;3(2):85-9.

457. Patel SS, et al. Phenotypic and functional characterization of human T cell clones. *Journal of immunology (Baltimore, Md : 1950).* 1988;141(11):3726-36.

458. Beliakova-Bethell N, et al. Relative efficacy of T cell stimuli as inducers of productive HIV-1 replication in latently infected CD4 lymphocytes from patients on suppressive cART. *Virology.* 2017;508(127-33.

459. Laird GM, et al. Rapid quantification of the latent reservoir for HIV-1 using a viral outgrowth assay. *PLoS pathogens.* 2013;9(5):e1003398.

460. Pollack RA, et al. Defective HIV-1 Proviruses Are Expressed and Can Be Recognized by Cytotoxic T Lymphocytes, which Shape the Proviral Landscape. *Cell host & microbe.* 2017;21(4):494-506.e4.

461. Ho Y-C, et al. Replication-Competent Noninduced Proviruses in the Latent Reservoir Increase Barrier to HIV-1 Cure. *Cell.* 2013;155(3):540-51.

462. Hosmane NN, et al. Proliferation of latently infected CD4(+) T cells carrying replication-competent HIV-1: Potential role in latent reservoir dynamics. *The Journal of experimental medicine.* 2017;214(4):959-72.

463. Bui JK, et al. Proviruses with identical sequences comprise a large fraction of the replication-competent HIV reservoir. *PLoS pathogens.* 2017;13(3):e1006283.

464. Li B, et al. Rapid reversion of sequence polymorphisms dominates early human immunodeficiency virus type 1 evolution. *J Virol.* 2007;81(1):193-201.

465. Wang Z, et al. Measuring replication competent HIV-1: advances and challenges in defining the latent reservoir. *Retrovirology.* 2018;15(1):21.

466. Hiener B, et al. Identification of Genetically Intact HIV-1 Proviruses in Specific CD4(+) T Cells from Effectively Treated Participants. *Cell reports.* 2017;21(3):813-22.

467. Lee GQ, et al. Clonal expansion of genome-intact HIV-1 in functionally polarized Th1 CD4+ T cells. *The Journal of clinical investigation.* 2017;127(7):2689-96.

468. Kijak GH, et al. Next-generation sequencing of HIV-1 single genome amplicons. *Biomol Detect Quantif.* 2019;17(100080-.

469. Arias A, et al. Sanger and Next Generation Sequencing Approaches to Evaluate HIV-1 Virus in Blood Compartments. *Int J Environ Res Public Health.* 2018;15(8):1697.

470. Bruner KM, et al. A quantitative approach for measuring the reservoir of latent HIV-1 proviruses. *Nature.* 2019;566(7742):120-5.

471. Kinloch NN, et al. HIV-1 diversity considerations in the application of the Intact Proviral DNA Assay (IPDA). *Nature Communications.* 2021;12(1):165.

472. Gaebler C, et al. Combination of quadruplex qPCR and next-generation sequencing for qualitative and quantitative analysis of the HIV-1 latent reservoir. *Journal of Experimental Medicine.* 2019;216(10):2253-64.

473. Eriksson S, et al. Comparative Analysis of Measures of Viral Reservoirs in HIV-1 Eradication Studies. *PLoS pathogens.* 2013;9(2):e1003174.

474. Imamichi H, et al. Defective HIV-1 proviruses produce novel protein-coding RNA species in HIV-infected patients on combination antiretroviral therapy. *Proc Natl Acad Sci U S A.* 2016;113(31):8783-8.

475. Imamichi H, et al. Defective HIV-1 proviruses produce viral proteins. *Proceedings of the National Academy of Sciences.* 2020;117(7):3704-10.

476. Policicchio BB, et al. Animal Models for HIV Cure Research. *Frontiers in immunology.* 2016;7(12.

477. Apetrei C, et al. Nonhuman primate models for HIV cure research. *PLoS pathogens.* 2012;8(8):e1002892.

478. Choudhary SK, et al. Latent HIV-1 infection of resting CD4(+) T cells in the humanized Rag2(-)/(-) gammac(-)/(-) mouse. *J Virol.* 2012;86(1):114-20.

479. Denton PW, et al. Generation of HIV latency in humanized BLT mice. *J Virol.* 2012;86(1):630-4.

480. Honeycutt JB, et al. Macrophages sustain HIV replication in vivo independently of T cells. *The Journal of clinical investigation.* 2016;126(4):1353-66.

481. Olesen R, et al. ART influences HIV persistence in the female reproductive tract and cervicovaginal secretions. *The Journal of clinical investigation.* 2016;126(3):892-904.

482. Garcia JV. In vivo platforms for analysis of HIV persistence and eradication. *The Journal of clinical investigation.* 2016;126(2):424-31.

483. Nishimura Y, et al. High frequencies of resting CD4+ T cells containing integrated viral DNA are found in rhesus macaques during acute lentivirus infections. *Proc Natl Acad Sci U S A.* 2009;106(19):8015-20.

484. Shen A, et al. Resting CD4+ T lymphocytes but not thymocytes provide a latent viral reservoir in a simian immunodeficiency virus-Macaca nemestrina model of human immunodeficiency virus type 1-infected patients on highly active antiretroviral therapy. *J Virol.* 2003;77(8):4938-49.

485. Crise B, et al. Simian immunodeficiency virus integration preference is similar to that of human immunodeficiency virus type 1. *J Virol.* 2005;79(19):12199-204.

486. Barber SA, et al. Mechanism for the establishment of transcriptional HIV latency in the brain in a simian immunodeficiency virus-macaque model. *The Journal of infectious diseases.* 2006;193(7):963-70.

487. Shen A, et al. Novel pathway for induction of latent virus from resting CD4(+) T cells in the simian immunodeficiency virus/macaque model of human immunodeficiency virus type 1 latency. *J Virol.* 2007;81(4):1660-70.

488. Bourry O, et al. Effect of a short-term HAART on SIV load in macaque tissues is dependent on time of initiation and antiviral diffusion. *Retrovirology.* 2010;7(78.

489. Mannioui A, et al. Dynamics of viral replication in blood and lymphoid tissues during SIVmac251 infection of macaques. *Retrovirology.* 2009;6(106.

490. Shytaj IL, et al. A highly intensified ART regimen induces long-term viral suppression and restriction of the viral reservoir in a simian AIDS model. *PLoS pathogens.* 2012;8(6):e1002774.

491. Del Prete GQ, et al. Short Communication: Comparative Evaluation of Coformulated Injectable Combination Antiretroviral Therapy Regimens in Simian Immunodeficiency Virus-Infected Rhesus Macaques. *AIDS research and human retroviruses.* 2016;32(2):163-8.

492. Dinoso JB, et al. Treatment intensification does not reduce residual HIV-1 viremia in patients on highly active antiretroviral therapy. *Proc Natl Acad Sci U S A.* 2009;106(23):9403-8.

493. Gandhi RT, et al. No Evidence for Decay of the Latent Reservoir in HIV-1–Infected Patients Receiving Intensive Enfuvirtide-Containing Antiretroviral Therapy. *The Journal of infectious diseases.* 2010;201(2):293-6.

494. Gandhi RT, et al. The Effect of Raltegravir Intensification on Low-level Residual Viremia in HIV-Infected Patients on Antiretroviral Therapy: A Randomized Controlled Trial. *PLOS Medicine.* 2010;7(8):e1000321.

495. Hammer SM, et al. A randomized, placebo-controlled trial of abacavir intensification in HIV-1-infected adults with virologic suppression on a protease inhibitor-containing regimen. *HIV clinical trials.* 2010;11(6):312-24.

496. Mousseau G, et al. Targeting HIV Transcription: The Quest for a Functional Cure. *Current topics in microbiology and immunology.* 2015;389(121-45.

497. Tebas P, et al. Gene editing of CCR5 in autologous CD4 T cells of persons infected with HIV. *The New England journal of medicine.* 2014;370(10):901-10.

498. Deeks SG, et al. A Phase II Randomized Study of HIV-Specific T-Cell Gene Therapy in Subjects with Undetectable Plasma Viremia on Combination Antiretroviral Therapy. *Molecular Therapy.* 2002;5(6):788-97.

499. Zhen A, et al. Long-term persistence and function of hematopoietic stem cell-derived chimeric antigen receptor T cells in a nonhuman primate model of HIV/AIDS. *PLoS pathogens.* 2017;13(12):e1006753.

500. Cummins NW, et al. Prime, Shock, and Kill: Priming CD4 T Cells from HIV Patients with a BCL-2 Antagonist before HIV Reactivation Reduces HIV Reservoir Size. *J Virol.* 2016;90(8):4032-48.

501. Cummins NW, et al. Maintenance of the HIV reservoir is antagonized by selective BCL2 inhibition. *J Virol.* 2017.

502. Liu J, et al. Antibody-mediated protection against SHIV challenge includes systemic clearance of distal virus. *Science (New York, NY).* 2016;353(6303):1045-9.

503. Xu L, et al. Trispecific broadly neutralizing HIV antibodies mediate potent SHIV protection in macaques. *Science (New York, NY).* 2017;358(6359):85-90.

504. Ng'uni T, et al. Major Scientific Hurdles in HIV Vaccine Development: Historical Perspective and Future Directions. *Frontiers in Immunology.* 2020;11(2761).

505. Sivanandham R, et al. Nonhuman Primate Testing of the Impact of Different Treg Depletion Strategies on Reactivation and Clearance of Latent Simian Immunodeficiency Virus. *J Virol.* 2020:JVI.00533-20.

506. Wightman F, et al. Effect of ipilimumab on the HIV reservoir in an HIV-infected individual with metastatic melanoma. *AIDS (London, England).* 2015;29(4):504-6.

507. Hryniewicz A, et al. CTLA-4 blockade decreases TGF-β, IDO, and viral RNA expression in tissues of SIVmac251-infected macaques. *Blood.* 2006;108(12):3834-42.

508. Petrovas C, et al. PD-1 is a regulator of virus-specific CD8+ T cell survival in HIV infection. *The Journal of experimental medicine.* 2006;203(10):2281-92.

509. Velu V, et al. Elevated expression levels of inhibitory receptor programmed death 1 on simian immunodeficiency virus-specific CD8 T cells during chronic infection but not after vaccination. *J Virol.* 2007;81(11):5819-28.

510. Margolis DM. Eradication Therapies for HIV Infection: Time to Begin Again. *AIDS research and human retroviruses.* 2011;27(4):347-53.

511. Shan L, et al. Stimulation of HIV-1-Specific Cytolytic T Lymphocytes Facilitates Elimination of Latent Viral Reservoir after Virus Reactivation. *Immunity.* 2012;36(3):491-501.

512. Deeks SG. HIV: Shock and kill. *Nature.* 2012;487(7408):439-40.

513. Blazkova J, et al. Effect of Histone Deacetylase Inhibitors on HIV Production in Latently Infected, Resting CD4+ T Cells From Infected Individuals Receiving Effective Antiretroviral Therapy. *The Journal of infectious diseases.* 2012;206(5):765-9.

514. Bullen CK, et al. New ex vivo approaches distinguish effective and ineffective single agents for reversing HIV-1 latency in vivo. *Nat Med.* 2014;20(4):425-9.

515. Cillo AR, et al. Quantification of HIV-1 latency reversal in resting CD4+ T cells from patients on suppressive antiretroviral therapy. *Proceedings of the National Academy of Sciences.* 2014;111(19):7078-83.

516. Gutierrez C, et al. Bryostatin-1 for latent virus reactivation in HIV-infected patients on antiretroviral therapy. *AIDS (London, England).* 2016;30(9):1385-92.

517. Prins JM, et al. Immuno-activation with anti-CD3 and recombinant human IL-2 in HIV-1-infected patients on potent antiretroviral therapy. *AIDS (London, England).* 1999;13(17):2405-10.

518. Jones RB, et al. Histone Deacetylase Inhibitors Impair the Elimination of HIV-Infected Cells by Cytotoxic T-Lymphocytes. *PLoS pathogens.* 2014;10(8):e1004287.

519. Policicchio BB, et al. Multi-dose Romidepsin Reactivates Replication Competent SIV in Post-antiretroviral Rhesus Macaque Controllers. *PLoS pathogens.* 2016;12(9):e1005879.

520. Migueles SA, et al. Defective human immunodeficiency virus-specific CD8+ T-cell polyfunctionality, proliferation, and cytotoxicity are not restored by antiretroviral therapy. *J Virol.* 2009;83(22):11876-89.

521. Ananworanich J, et al. Markers of HIV reservoir size and immune activation after treatment in acute HIV infection with and without raltegravir and maraviroc intensification. *Journal of virus eradication.* 2015;1(2):116-22.

522. Cohen YZ, and Caskey M. Broadly neutralizing antibodies for treatment and prevention of HIV-1 infection. *Curr Opin HIV AIDS.* 2018;13(4):366-73.

523. Wang CX, and Cannon PM. The clinical applications of genome editing in HIV. *Blood.* 2016;127(21):2546-52.

524. Duarte R, et al. *Allogeneic Transplantation in Patients with HIV-Infection: A Pair Matched Cohort Study by the European Society for Blood and Marrow Transplantation.* 2015.

525. Dornadula G, et al. Residual HIV-1 RNA in Blood Plasma of Patients Taking Suppressive Highly Active Antiretroviral Therapy. *JAMA.* 1999;282(17):1627-32.

526. Palmer S, et al. Low-level viremia persists for at least 7 years in patients on suppressive antiretroviral therapy. *Proceedings of the National Academy of Sciences.* 2008;105(10):3879-84.

527. Dinoso JB, et al. Treatment intensification does not reduce residual HIV-1 viremia in patients on highly active antiretroviral therapy. *Proceedings of the National Academy of Sciences.* 2009;106(23):9403-8.

528. Gandhi RT, et al. No effect of raltegravir intensification on viral replication markers in the blood of HIV-1-infected patients receiving antiretroviral therapy. *Journal of acquired immune deficiency syndromes (1999).* 2012;59(3):229-35.

529. Rasmussen TA, et al. The effect of antiretroviral intensification with dolutegravir on residual virus replication in HIV-infected individuals: a randomised, placebo-controlled, double-blind trial. *The lancet HIV.* 2018;5(5):e221-e30.

530. Chaillon A, et al. Size, Composition, and Evolution of HIV DNA Populations during Early Antiretroviral Therapy and Intensification with Maraviroc. *J Virol.* 2018;92(3):e01589-17.

531. Kim CJ, et al. Impact of intensified antiretroviral therapy during early HIV infection on gut immunology and inflammatory blood biomarkers. *AIDS (London, England).* 2017;31(11).

532. Kao SY, et al. Anti-termination of transcription within the long terminal repeat of HIV-1 by tat gene product. *Nature.* 1987;330(6147):489-93.

533. Feng S, and Holland EC. HIV-1 tat trans-activation requires the loop sequence within tar. *Nature.* 1988;334(6178):165-7.

534. Ahlenstiel CL, et al. Block and Lock HIV Cure Strategies to Control the Latent Reservoir. *Frontiers in Cellular and Infection Microbiology.* 2020;10(424).

535. Meredith LW, et al. Potent inhibition of HIV-1 replication by a Tat mutant. *PLoS One.* 2009;4(11):e7769-e.

536. Jin H, et al. Shutdown of HIV-1 Transcription in T Cells by Nullbasic, a Mutant Tat Protein. *mBio.* 2016;7(4):e00518-16.

537. Mousseau G, et al. An analog of the natural steroidal alkaloid cortistatin A potently suppresses Tat-dependent HIV transcription. *Cell host & microbe.* 2012;12(1):97-108.

538. Kessing CF, et al. In Vivo Suppression of HIV Rebound by Didehydro-Cortistatin A, a "Block-and-Lock" Strategy for HIV-1 Treatment. *Cell reports.* 2017;21(3):600-11.

539. Vansant G, et al. Block-And-Lock Strategies to Cure HIV Infection. *Viruses.* 2020;12(1):84.

540. Vargas B, et al. Inhibitors of Signaling Pathways That Block Reversal of HIV-1 Latency. *Antimicrobial Agents and Chemotherapy.* 2019;63(2):e01744-18.

541. Ebina H, et al. Harnessing the CRISPR/Cas9 system to disrupt latent HIV-1 provirus. *Sci Rep.* 2013;3(2510.

542. Zhu W, et al. The CRISPR/Cas9 system inactivates latent HIV-1 proviral DNA. *Retrovirology.* 2015;12(1):22.

543. Yin C, et al. In Vivo Excision of HIV-1 Provirus by saCas9 and Multiplex Single-Guide RNAs in Animal Models. *Molecular Therapy.* 2017;25(5):1168-86.

544. Mout R, et al. In Vivo Delivery of CRISPR/Cas9 for Therapeutic Gene Editing: Progress and Challenges. *Bioconjugate Chemistry.* 2017;28(4):880-4.

545. Hale M, et al. Engineering HIV-Resistant, Anti-HIV Chimeric Antigen Receptor T Cells. *Molecular Therapy.* 2017;25(3):570-9.

546. Leslie GJ, et al. Potent and Broad Inhibition of HIV-1 by a Peptide from the gp41 Heptad Repeat-2 Domain Conjugated to the CXCR4 Amino Terminus. *PLoS pathogens.* 2016;12(11):e1005983.

547. Maldini CR, et al. Dual CD4-based CAR T cells with distinct costimulatory domains mitigate HIV pathogenesis in vivo. *Nature Medicine.* 2020;26(11):1776-87.

548. Ventoso I, et al. Involvement of HIV-1 protease in virus-induced cell killing. *Antiviral research.* 2005;66(1):47-55.

549. Algeciras-Schimnich A, et al. Analysis of HIV Protease Killing Through Caspase 8 Reveals a Novel Interaction Between Caspase 8 and Mitochondria. *The Open Virology Journal.* 2007;1(39-46.

550. Sainski AM, et al. The HIV-1-Specific Protein Casp8p41 Induces Death of Infected Cells through Bax/Bak. *J Virol.* 2011;85(16):7965-75.

551. Sainski AM, et al. Casp8p41 generated by HIV protease kills CD4 T cells through direct Bak activation. *The Journal of Cell Biology.* 2014;206(7):867-76.

552. Natesampillai S, et al. HIV Protease-Generated Casp8p41, When Bound and Inactivated by Bcl2, Is Degraded by the Proteasome. *J Virol.* 2018;92(13):e00037-18.

553. Alto A, et al. The Combination of Venetoclax and Ixazomib Selectively and Efficiently Kills HIV-Infected Cell Lines but Has Unacceptable Toxicity in Primary Cell Models. *J Virol.* 2021;95(12):e00138-21.

554. Ren Y, et al. BCL-2 antagonism sensitizes cytotoxic T cell–resistant HIV reservoirs to elimination ex vivo. *The Journal of clinical investigation.* 2020;130(5):2542-59.

555. Suntharalingam G, et al. Cytokine Storm in a Phase 1 Trial of the Anti-CD28 Monoclonal Antibody TGN1412. *New England Journal of Medicine.* 2006;355(10):1018-28.

556. Alegre ML, et al. Cytokine release syndrome induced by the 145-2C11 anti-CD3 monoclonal antibody in mice: prevention by high doses of methylprednisolone. *Journal of immunology (Baltimore, Md : 1950).* 1991;146(4):1184-91.

557. Hütter G. Stem cell transplantation in strategies for curing HIV/AIDS. *AIDS Research and Therapy.* 2016;13(1):31.

558. Kordelas L, et al. Shift of HIV tropism in stem-cell transplantation with CCR5 Delta32 mutation. *The New England journal of medicine.* 2014;371(9):880-2.

559. Koelsch KK, et al. Impact of Allogeneic Hematopoietic Stem Cell Transplantation on the HIV Reservoir and Immune Response in 3 HIV-Infected Individuals. *Journal of acquired immune deficiency syndromes (1999).* 2017;75(3):328-37.

560. Burton DR, et al. A large array of human monoclonal antibodies to type 1 human immunodeficiency virus from combinatorial libraries of asymptomatic seropositive individuals. *Proceedings of the National Academy of Sciences.* 1991;88(22):10134-7.

561. Klasse PJ. Neutralization of Virus Infectivity by Antibodies: Old Problems in New Perspectives. *Advances in Biology.* 2014;2014(157895.

562. Mallery DL, et al. Antibodies mediate intracellular immunity through tripartite motif-containing 21 (TRIM21). *Proc Natl Acad Sci U S A.* 2010;107(46):19985-90.

563. Forthal D, et al. New paradigms for functional HIV-specific nonneutralizing antibodies. *Current opinion in HIV and AIDS.* 2013;8(5):393-401.

564. Wu X, et al. Rational Design of Envelope Identifies Broadly Neutralizing Human Monoclonal Antibodies to HIV-1. *Science (New York, NY).* 2010;329(5993):856-61.

565. McCoy LE. The expanding array of HIV broadly neutralizing antibodies. *Retrovirology.* 2018;15(1):70.

566. Moldt B, et al. Highly potent HIV-specific antibody neutralization in vitro translates into effective protection against mucosal SHIV challenge in vivo. *Proceedings of the National Academy of Sciences.* 2012;109(46):18921-5.

567. Shingai M, et al. Passive transfer of modest titers of potent and broadly neutralizing anti-HIV monoclonal antibodies block SHIV infection in macaques. *Journal of Experimental Medicine.* 2014;211(10):2061-74.

568. Saunders KO, et al. Broadly Neutralizing Human Immunodeficiency Virus Type 1 Antibody Gene Transfer Protects Nonhuman Primates from Mucosal Simian-Human Immunodeficiency Virus Infection. *J Virol.* 2015;89(16):8334-45.

569. Gautam R, et al. A single injection of anti-HIV-1 antibodies protects against repeated SHIV challenges. *Nature.* 2016;533(7601):105-9.

570. Julg B, et al. Protective Efficacy of Broadly Neutralizing Antibodies with Incomplete Neutralization Activity against Simian-Human Immunodeficiency Virus in Rhesus Monkeys. *J Virol.* 2017;91(20):e01187-17.

571. Ledgerwood JE, et al. Safety, pharmacokinetics and neutralization of the broadly neutralizing HIV-1 human monoclonal antibody VRC01 in healthy adults. *Clin Exp Immunol.* 2015;182(3):289-301.

572. Gaudinski MR, et al. Safety and pharmacokinetics of the Fc-modified HIV-1 human monoclonal antibody VRC01LS: A Phase 1 open-label clinical trial in healthy adults. *PLOS Medicine.* 2018;15(1):e1002493.

573. Huang Y, et al. Population pharmacokinetics analysis of VRC01, an HIV-1 broadly neutralizing monoclonal antibody, in healthy adults. *mAbs.* 2017;9(5):792-800.

574. Niessl J, et al. Combination anti-HIV-1 antibody therapy is associated with increased virus-specific T cell immunity. *Nature Medicine.* 2020;26(2):222-7.

575. Caskey M, et al. Viraemia suppressed in HIV-1-infected humans by broadly neutralizing antibody 3BNC117. *Nature.* 2015;522(7557):487-91.

576. Caskey M, et al. Antibody 10-1074 suppresses viremia in HIV-1-infected individuals. *Nature Medicine.* 2017;23(2):185-91.

577. Crowell TA, et al. Safety and efficacy of VRC01 broadly neutralising antibodies in adults with acutely treated HIV (RV397): a phase 2, randomised, double-blind, placebo-controlled trial. *The lancet HIV.* 2019;6(5):e297-e306.

578. Reh L, et al. Capacity of Broadly Neutralizing Antibodies to Inhibit HIV-1 Cell-Cell Transmission Is Strain- and Epitope-Dependent. *PLoS pathogens.* 2015;11(7):e1004966.

579. Li H, et al. Reduced Potency and Incomplete Neutralization of Broadly Neutralizing Antibodies against Cell-to-Cell Transmission of HIV-1 with Transmitted Founder Envs. *J Virol.* 2017;91(9).

580. Parsons MS, et al. Partial efficacy of a broadly neutralizing antibody against cell-associated SHIV infection. *Sci Transl Med.* 2017;9(402).

581. Walker LM, et al. Broad neutralization coverage of HIV by multiple highly potent antibodies. *Nature.* 2011;477(7365):466-70.

582. Kong R, et al. Improving Neutralization Potency and Breadth by Combining Broadly Reactive HIV-1 Antibodies Targeting Major Neutralization Epitopes. *J Virol.* 2015;89(5):2659-71.

583. Wagh K, et al. Potential of conventional & bispecific broadly neutralizing antibodies for prevention of HIV-1 subtype A, C & D infections. *PLoS pathogens.* 2018;14(3):e1006860.

584. Nishimura Y, et al. Early antibody therapy can induce long-lasting immunity to SHIV. *Nature.* 2017;543(7646):559-63.

585. Nishimura Y, et al. Immunotherapy during the acute SHIV infection of macaques confers long-term suppression of viremia. *Journal of Experimental Medicine.* 2020;218(1).

586. Borducchi EN, et al. Antibody and TLR7 agonist delay viral rebound in SHIV-infected monkeys. *Nature.* 2018;563(7731):360-4.

587. Hsu DC, et al. TLR7 agonist, N6-LS and PGT121 delayed viral rebound in SHIV-infected macaques after antiretroviral therapy interruption. *PLoS pathogens.* 2021;17(2):e1009339.

588. Lim S-Y, et al. *Conference on Retroviruses and Opportunistic Infections*. Boston, Massachusettes; 2020.

589. Gebara NY, et al. HIV-1 elite controllers: an immunovirological review and clinical perspectives. *Journal of virus eradication.* 2019;5(3):163-6.

590. Gray G, et al. Overview of STEP and Phambili trial results: two phase IIb test-of-concept studies investigating the efficacy of MRK adenovirus type 5 gag/pol/nef subtype B HIV vaccine. *Current opinion in HIV and AIDS.* 2010;5(5):357-61.

591. Bekker L-G, et al. Subtype C ALVAC-HIV and bivalent subtype C gp120/MF59 HIV-1 vaccine in low-risk, HIV-uninfected, South African adults: a phase 1/2 trial. *The lancet HIV.* 2018;5(7):e366-e78.

592. Laher F, et al. Safety and immune responses after a 12-month booster in healthy HIV-uninfected adults in HVTN 100 in South Africa: A randomized double-blind placebo-controlled trial of ALVAC-HIV (vCP2438) and bivalent subtype C gp120/MF59 vaccines. *PLoS medicine.* 2020;17(2):e1003038-e.

593. Gray GE, et al. Vaccine Efficacy of ALVAC-HIV and Bivalent Subtype C gp120–MF59 in Adults. *New England Journal of Medicine.* 2021;384(12):1089-100.

594. Abdul-Jawad S, et al. Increased Valency of Conserved-mosaic Vaccines Enhances the Breadth and Depth of Epitope Recognition. *Molecular therapy : the journal of the American Society of Gene Therapy.* 2016;24(2):375-84.

595. Barouch DH, et al. Evaluation of a mosaic HIV-1 vaccine in a multicentre, randomised, double-blind, placebo-controlled, phase 1/2a clinical trial (APPROACH) and in rhesus monkeys (NHP 13-19). *Lancet (London, England).* 2018;392(10143):232-43.

596. Fischer W, et al. Polyvalent vaccines for optimal coverage of potential T-cell epitopes in global HIV-1 variants. *Nat Med.* 2007;13(1):100-6.

597. . Johnson & Johnson and Global Partners Announce Results from Phase 2b Imbokodo HIV Vaccine Clinical Trial in Young Women in Sub-Saharan Africa. https://www.jnj.com/johnson-johnson-and-global-partners-announce-results-from-phase-2b-imbokodo-hiv-vaccine-clinical-trial-in-young-women-in-sub-saharan-africa. Accessed 9-13, 2021.

598. Mothe B, et al. Safety and immunogenicity of a modified vaccinia Ankara-based HIV-1 vaccine (MVA-B) in HIV-1-infected patients alone or in combination with a drug to reactivate latent HIV-1. *The Journal of antimicrobial chemotherapy.* 2015;70(6):1833-42.

599. Hansen SG, et al. Effector memory T cell responses are associated with protection of rhesus monkeys from mucosal simian immunodeficiency virus challenge. *Nat Med.* 2009;15(3):293-9.

600. Hansen SG, et al. Immune clearance of highly pathogenic SIV infection. *Nature.* 2013;502(7469):100-4.

601. Murray SE, et al. Fibroblast-adapted human CMV vaccines elicit predominantly conventional CD8 T cell responses in humans. *The Journal of experimental medicine.* 2017;214(7):1889-99.

602. Combadière B, et al. Peptide-Based Vaccination for Antibody Responses Against HIV. *Vaccines (Basel).* 2019;7(3):105.

603. Belyakov IM, et al. Mucosal immunization with HIV-1 peptide vaccine induces mucosal and systemic cytotoxic T lymphocytes and protective immunity in mice against intrarectal recombinant HIV-vaccinia challenge. *Proceedings of the National Academy of Sciences.* 1998;95(4):1709-14.

604. Kelleher AD, et al. Safety and immunogenicity of UBI HIV-1MN octameric V3 peptide vaccine administered by subcutaneous injection. *AIDS research and human retroviruses.* 1997;13(1):29-32.

605. Gorse GJ, et al. A dose-ranging study of a prototype synthetic HIV-1MN V3 branched peptide vaccine. The National Institute of Allergy and Infectious Diseases AIDS Vaccine Evaluation Group. *The Journal of infectious diseases.* 1996;173(2):330-9.

606. Flynn NM, et al. Placebo-controlled phase 3 trial of a recombinant glycoprotein 120 vaccine to prevent HIV-1 infection. *The Journal of infectious diseases.* 2005;191(5):654-65.

607. Vieillard V, et al. HIV therapeutic vaccine enhances non-exhausted CD4+ T cells in a randomised phase 2 trial. *npj Vaccines.* 2019;4(1):25.

608. Pollard RB, et al. Safety and efficacy of the peptide-based therapeutic vaccine for HIV-1, Vacc-4x: a phase 2 randomised, double-blind, placebo-controlled trial. *The Lancet Infectious diseases.* 2014;14(4):291-300.

609. Rockstroh JK, et al. Re-boost immunizations with the peptide-based therapeutic HIV vaccine, Vacc-4x, restores geometric mean viral load set-point during treatment interruption. *PLoS One.* 2019;14(1):e0210965.

610. Chupradit K, et al. Current Peptide and Protein Candidates Challenging HIV Therapy beyond the Vaccine Era. *Viruses.* 2017;9(10):281.

611. Dando TM, and Perry CM. Enfuvirtide. *Drugs.* 2003;63(24):2755-66; discussion 67-8.

612. Dorr P, et al. Maraviroc (UK-427,857), a potent, orally bioavailable, and selective small-molecule inhibitor of chemokine receptor CCR5 with broad-spectrum anti-human immunodeficiency virus type 1 activity. *Antimicrobial agents and chemotherapy.* 2005;49(11):4721-32.

613. Bi W, et al. IgG Fc-binding motif-conjugated HIV-1 fusion inhibitor exhibits improved potency and in vivo half-life: Potential application in combination with broad neutralizing antibodies. *PLoS pathogens.* 2019;15(12):e1008082.

614. Martins MA, et al. Vaccine protection against SIVmac239 acquisition. *Proceedings of the National Academy of Sciences of the United States of America.* 2019;116(5):1739-44.

615. Martins MA, et al. Rectal Acquisition of Simian Immunodeficiency Virus (SIV) SIVmac239 Infection despite Vaccine-Induced Immune Responses against the Entire SIV Proteome. *J Virol.* 2020;94(24):e00979-20.

616. Moreno-Fernandez ME, et al. Homeostasis and function of regulatory T cells in HIV/SIV infection. *J Virol.* 2012;86(19):10262-9.

617. Tran TA, et al. Resting regulatory CD4 T cells: a site of HIV persistence in patients on long-term effective antiretroviral therapy. *PLoS One.* 2008;3(10):e3305.

618. Allers K, et al. Gut mucosal FOXP3+ regulatory CD4+ T cells and Nonregulatory CD4+ T cells are differentially affected by simian immunodeficiency virus infection in rhesus macaques. *J Virol.* 2010;84(7):3259-69.

619. Bi X, et al. High frequency and proliferation of CD4+ FOXP3+ Treg in HIV-1-infected patients with low CD4 counts. *European journal of immunology.* 2009;39(1):301-9.

620. Weiss L, et al. Human immunodeficiency virus-driven expansion of CD4+CD25+ regulatory T cells, which suppress HIV-specific CD4 T-cell responses in HIV-infected patients. *Blood.* 2004;104(10):3249-56.

621. Nikolova M, et al. Regulatory T cells differentially modulate the maturation and apoptosis of human CD8+ T-cell subsets. *Blood.* 2009;113(19):4556-65.

622. Nilsson J, et al. HIV-1-driven regulatory T-cell accumulation in lymphoid tissues is associated with disease progression in HIV/AIDS. *Blood.* 2006;108(12):3808-17.

623. Elahi S, et al. Protective HIV-specific CD8+ T cells evade Treg cell suppression. *Nat Med.* 2011;17(8):989-95.

624. Queen C, et al. A humanized antibody that binds to the interleukin 2 receptor. *Proc Natl Acad Sci U S A.* 1989;86(24):10029-33.

625. Williams DP, et al. Diphtheria toxin receptor binding domain substitution with interleukin-2: genetic construction and properties of a diphtheria toxin-related interleukin-2 fusion protein. *Protein engineering.* 1987;1(6):493-8.

626. Collier RJ. Diphtheria toxin: mode of action and structure. *Bacteriological Reviews.* 1975;39(1):54-85.

627. Atchison E, et al. A pilot study of denileukin diftitox (DD) in combination with high-dose interleukin-2 (IL-2) for patients with metastatic renal cell carcinoma (RCC). *Journal of immunotherapy (Hagerstown, Md : 1997).* 2010;33(7):716-22.

628. Kaminetzky D, and Hymes KB. Denileukin diftitox for the treatment of cutaneous T-cell lymphoma. *Biologics : Targets & Therapy.* 2008;2(4):717-24.

629. Baur AS, et al. Denileukin diftitox (ONTAK) induces a tolerogenic phenotype in dendritic cells and stimulates survival of resting T_{reg}. *Blood.* 2013;122(13):2185-94.

630. Foss FM, et al. A multicenter phase II trial to determine the safety and efficacy of combination therapy with denileukin diftitox and cyclophosphamide, doxorubicin, vincristine and prednisone in untreated peripheral T-cell lymphoma: the CONCEPT study. *Leukemia & lymphoma.* 2013;54(7):1373-9.

631. Telang S, et al. Phase II trial of the regulatory T cell-depleting agent, denileukin diftitox, in patients with unresectable stage IV melanoma. *BMC cancer.* 2011;11(515.

632. Ma D, et al. Simian Immunodeficiency Virus SIVsab Infection of Rhesus Macaques as a Model of Complete Immunological Suppression with Persistent Reservoirs of Replication-Competent Virus: Implications for Cure Research. *J Virol.* 2015;89(11):6155-60.

633. Pandrea I, et al. Functional cure of SIVagm infection in rhesus macaques results in complete recovery of CD4+ T cells and is reverted by CD8+ cell depletion. *PLoS pathogens.* 2011;7(8):e1002170.

634. He T, et al. Cutting Edge: T Regulatory Cell Depletion Reactivates Latent Simian Immunodeficiency Virus (SIV) in Controller Macaques While Boosting SIV-Specific T Lymphocytes. *J Immunol.* 2016;197(12):4535-9.

635. Wang Z, et al. Ontak-like human IL-2 fusion toxin. *J Immunol Methods.* 2017;448(51-8.

636. Peraino JS, et al. Diphtheria toxin-based bivalent human IL-2 fusion toxin with improved efficacy for targeting human CD25(+) cells. *J Immunol Methods.* 2014;405(57-66.

637. Ishida T, and Ueda R. CCR4 as a novel molecular target for immunotherapy of cancer. *Cancer science.* 2006;97(11):1139-46.

638. Nishikawa H, and Sakaguchi S. Regulatory T cells in tumor immunity. *International journal of cancer.* 2010;127(4):759-67.

639. Iellem A, et al. Unique chemotactic response profile and specific expression of chemokine receptors CCR4 and CCR8 by CD4(+)CD25(+) regulatory T cells. *The Journal of experimental medicine.* 2001;194(6):847-53.

640. Agrawal L, et al. Multiple determinants are involved in HIV coreceptor use as demonstrated by CCR4/CCL22 interaction in peripheral blood mononuclear cells (PBMCs). *J Leukoc Biol.* 2002;72(5):1063-74.

641. Wang Z, et al. Treg depletion in non-human primates using a novel diphtheria toxin-based anti-human CCR4 immunotoxin. *Molecular oncology.* 2016;10(4):553-65.

642. Ni X, et al. Reduction of regulatory T cells by Mogamulizumab, a defucosylated anti-CC chemokine receptor 4 antibody, in patients with aggressive/refractory mycosis fungoides and Sezary syndrome. *Clinical cancer research : an official journal of the American Association for Cancer Research.* 2015;21(2):274-85.

643. Ogura M, et al. Multicenter phase II study of mogamulizumab (KW-0761), a defucosylated anti-cc chemokine receptor 4 antibody, in patients with relapsed peripheral T-cell lymphoma and cutaneous T-cell lymphoma. *Journal of clinical oncology : official journal of the American Society of Clinical Oncology.* 2014;32(11):1157-63.

644. Appelbaum FR, et al. Treatment of malignant lymphoma in 100 patients with chemotherapy, total body irradiation, and marrow transplantation. *Journal of Clinical Oncology.* 1987;5(9):1340-7.

645. McCune WJ, et al. Clinical and Immunologic Effects of Monthly Administration of Intravenous Cyclophosphamide in Severe Systemic Lupus Erythematosus. *New England Journal of Medicine.* 1988;318(22):1423-31.

646. Gladstone DE, et al. High-dose cyclophosphamide for severe systemic lupus erythematosus. *Lupus.* 2002;11(7):405-10.

647. Petri M, et al. High Dose Cyclophosphamide versus Monthly Intravenous Cyclophosphamide for Systemic Lupus Erythematosus. *Arthritis and rheumatism.* 2010;62(5):1487-93.

648. Glode LM, et al. Metronomic therapy with cyclophosphamide and dexamethasone for prostate carcinoma. *Cancer.* 2003;98(8):1643-8.

649. Lutsiak MEC, et al. Inhibition of $CD4^{+}25^{+}$ T regulatory cell function implicated in enhanced immune response by low-dose cyclophosphamide. *Blood.* 2005;105(7):2862-8.

650. Ikezawa Y, et al. Cyclophosphamide decreases the number, percentage and the function of CD25+ CD4+ regulatory T cells, which suppress induction of contact hypersensitivity. *Journal of Dermatological Science.* 2005;39(2):105-12.

651. Heylmann D, et al. Human CD4+CD25+ Regulatory T Cells Are Sensitive to Low Dose Cyclophosphamide: Implications for the Immune Response. *PLoS One.* 2013;8(12):e83384.

652. Zhao J, et al. Selective Depletion of $CD4^{+}CD25^{+}Foxp3^{+}$ Regulatory T Cells by Low-Dose Cyclophosphamide Is Explained by Reduced Intracellular ATP Levels. *Cancer Research.* 2010;70(12):4850-8.

653. Loyher PL, et al. CCR2 Influences T Regulatory Cell Migration to Tumors and Serves as a Biomarker of Cyclophosphamide Sensitivity. *Cancer Res.* 2016;76(22):6483-94.

654. Walter S, et al. Multipeptide immune response to cancer vaccine IMA901 after single-dose cyclophosphamide associates with longer patient survival. *Nat Med.* 2012;18(8):1254-61.

655. Ghiringhelli F, et al. Metronomic cyclophosphamide regimen selectively depletes CD4+CD25+ regulatory T cells and restores T and NK effector functions in end stage cancer patients. *Cancer Immunology, Immunotherapy.* 2007;56(5):641-8.

656. Nakahara T, et al. Cyclophosphamide enhances immunity by modulating the balance of dendritic cell subsets in lymphoid organs. *Blood.* 2010;115(22):4384-92.

657. Alonso CM, and Lozada CJ. Effects of IV cyclophosphamide on HIV viral replication in a patient with systemic lupus erythematosus. *Clinical and experimental rheumatology.* 2000;18(4):510-2.

658. Bartlett JA, et al. Addition of cyclophosphamide to antiretroviral therapy does not diminish the cellular reservoir in HIV-infected persons. *AIDS research and human retroviruses.* 2002;18(8):535-43.

659. Zajac AJ, et al. Viral Immune Evasion Due to Persistence of Activated T Cells Without Effector Function. *Journal of Experimental Medicine.* 1998;188(12):2205-13.

660. Chew GM, et al. TIGIT Marks Exhausted T Cells, Correlates with Disease Progression, and Serves as a Target for Immune Restoration in HIV and SIV Infection. *PLoS pathogens.* 2016;12(1):e1005349.

661. Fromentin R, et al. CD4+ T Cells Expressing PD-1, TIGIT and LAG-3 Contribute to HIV Persistence during ART. *PLoS pathogens.* 2016;12(7):e1005761.

662. Jones RB, et al. Tim-3 expression defines a novel population of dysfunctional T cells with highly elevated frequencies in progressive HIV-1 infection. *Journal of Experimental Medicine.* 2008;205(12):2763-79.

663. Vali B, et al. HCV-specific T cells in HCV/HIV co-infection show elevated frequencies of dual Tim-3/PD-1 expression that correlate with liver disease progression. *European journal of immunology.* 2010;40(9):2493-505.

664. Hurst J, et al. Immunological biomarkers predict HIV-1 viral rebound after treatment interruption. *Nature Communications.* 2015;6(1):8495.

665. Kaufmann DE, et al. Upregulation of CTLA-4 by HIV-specific CD4+ T cells correlates with disease progression and defines a reversible immune dysfunction. *Nature immunology.* 2007;8(11):1246-54.

666. Elrefaei M, et al. HIV-Specific TGF-β-Positive CD4(+) T Cells Do Not Express Regulatory Surface Markers and Are Regulated by CTLA-4. *AIDS research and human retroviruses.* 2010;26(3):329-37.

667. Cecchinato V, et al. Immune Activation Driven by CTLA-4 Blockade Augments Viral Replication at Mucosal Sites in Simian Immunodeficiency Virus Infection. *The Journal of Immunology.* 2008;180(8):5439-47.

668. Le Garff G, et al. Transient HIV-specific T cells increase and inflammation in an HIV-infected patient treated with nivolumab. *AIDS (London, England).* 2017;31(7).

669. Guihot A, et al. Drastic decrease of the HIV reservoir in a patient treated with nivolumab for lung cancer. *Annals of Oncology.* 2018;29(2):517-8.

670. Scully EP, et al. Inconsistent HIV reservoir dynamics and immune responses following anti-PD-1 therapy in cancer patients with HIV infection. *Ann Oncol.* 2018;29(10):2141-2.

671. Fromentin R, et al. PD-1 blockade potentiates HIV latency reversal ex vivo in CD4+ T cells from ART-suppressed individuals. *Nature Communications.* 2019;10(1):814.

672. Antonioli L, et al. CD39 and CD73 in immunity and inflammation. *Trends in Molecular Medicine.* 2013;19(6):355-67.

673. Gupta PK, et al. CD39 Expression Identifies Terminally Exhausted CD8+ T Cells. *PLoS pathogens.* 2015;11(10):e1005177.

674. Li J, et al. Reversal of the CD8+ T-Cell Exhaustion Induced by Chronic HIV-1 Infection Through Combined Blockade of the Adenosine and PD-1 Pathways. *Frontiers in Immunology.* 2021;12(2128).

675. Zhang X, et al. Potent and Selective Stimulation of Memory-Phenotype CD8⁺ T Cells In Vivo by IL-15. *Immunity.* 1998;8(5):591-9.

676. Lodolce JP, et al. IL-15 Receptor Maintains Lymphoid Homeostasis by Supporting Lymphocyte Homing and Proliferation. *Immunity.* 1998;9(5):669-76.

677. Mueller YM, et al. IL-15 enhances survival and function of HIV-specific CD8+ T cells. *Blood.* 2003;101(3):1024-9.

678. Garrido C, et al. Interleukin-15-Stimulated Natural Killer Cells Clear HIV-1-Infected Cells following Latency Reversal Ex Vivo. *J Virol.* 2018;92(12):e00235-18.

679. Lugli E, et al. IL-15 delays suppression and fails to promote immune reconstitution in virally suppressed chronically SIV-infected macaques. *Blood.* 2011;118(9):2520-9.

680. Mueller Yvonne M, et al. Interleukin-15 Increases Effector Memory CD8+ T Cells and NK Cells in Simian Immunodeficiency Virus-Infected Macaques. *J Virol.* 2005;79(8):4877-85.

681. Harwood O, and O'Connor S. Therapeutic Potential of IL-15 and N-803 in HIV/SIV Infection. *Viruses.* 2021;13(9).

682. Watson DC, et al. Treatment with native heterodimeric IL-15 increases cytotoxic lymphocytes and reduces SHIV RNA in lymph nodes. *PLoS pathogens.* 2018;14(2):e1006902.

683. Zhu X, et al. Novel Human Interleukin-15 Agonists. *The Journal of Immunology.* 2009;183(6):3598-607.

684. Jones RB, et al. A Subset of Latency-Reversing Agents Expose HIV-Infected Resting CD4+ T-Cells to Recognition by Cytotoxic T-Lymphocytes. *PLoS pathogens.* 2016;12(4):e1005545.

685. Ellis-Connell Amy L, et al. ALT-803 Transiently Reduces Simian Immunodeficiency Virus Replication in the Absence of Antiretroviral Treatment. *J Virol.* 2018;92(3):e01748-17.

686. McBrien JB, et al. Robust and persistent reactivation of SIV and HIV by N-803 and depletion of CD8+ cells. *Nature.* 2020;578(7793):154-9.

687. McBrien Julia B, et al. Combination of CD8β Depletion and Interleukin-15 Superagonist N-803 Induces Virus Reactivation in Simian-Human Immunodeficiency Virus-Infected, Long-Term ART-Treated Rhesus Macaques. *J Virol.* 2020;94(19):e00755-20.

688. Webb GM, et al. The human IL-15 superagonist N-803 promotes migration of virus-specific CD8+ T and NK cells to B cell follicles but does not reverse latency in ART-suppressed, SHIV-infected macaques. *PLoS pathogens.* 2020;16(3):e1008339.

689. Pallikkuth S, et al. The role of interleukin-21 in HIV infection. *Cytokine Growth Factor Rev.* 2012;23(4-5):173-80.

690. White L, et al. Differential effects of IL-21 and IL-15 on perforin expression, lysosomal degranulation, and proliferation in CD8 T cells of patients with human immunodeficiency virus-1 (HIV). *Blood.* 2007;109(9):3873-80.

691. Strbo N, et al. IL-21 augments natural killer effector functions in chronically HIV-infected individuals. *AIDS (London, England).* 2008;22(13):1551-60.

692. Pallikkuth S, et al. Interleukin-21 administration to rhesus macaques chronically infected with simian immunodeficiency virus increases cytotoxic effector molecules in T cells and NK cells and enhances B cell function without increasing immune activation or viral replication. *Vaccine.* 2011;29(49):9229-38.

693. Micci L, et al. Interleukin-21 combined with ART reduces inflammation and viral reservoir in SIV-infected macaques. *The Journal of clinical investigation.* 2015;125(12):4497-513.

694. Harper J, et al. IL-21 and IFNα therapy rescues terminally differentiated NK cells and limits SIV reservoir in ART-treated macaques. *Nature Communications.* 2021;12(1):2866.

695. Ylisastigui L, et al. Coaxing HIV-1 from resting CD4 T cells: histone deacetylase inhibition allows latent viral expression. *AIDS (London, England).* 2004;18(8):1101-8.

696. Archin NM, et al. Expression of Latent HIV Induced by the Potent HDAC Inhibitor Suberoylanilide Hydroxamic Acid. *AIDS research and human retroviruses.* 2009;25(2):207-12.

697. Elliott JH, et al. Activation of HIV transcription with short-course vorinostat in HIV-infected patients on suppressive antiretroviral therapy. *PLoS pathogens.* 2014;10(10):e1004473.

698. Kulkosky J, et al. Prostratin: activation of latent HIV-1 expression suggests a potential inductive adjuvant therapy for HAART. *Blood.* 2001;98(10):3006-15.

699. Korin YD, et al. Effects of Prostratin on T-Cell Activation and Human Immunodeficiency Virus Latency. *J Virol.* 2002;76(16):8118-23.

700. Banerjee C, et al. BET bromodomain inhibition as a novel strategy for reactivation of HIV-1. *Journal of leukocyte biology.* 2012;92(6):1147-54.

701. Sampey GC, et al. The SMAC Mimetic AZD5582 is a Potent HIV Latency Reversing Agent. *bioRxiv.* 2018:312447.

702. Yamamoto T, et al. STING agonists activate latently infected cells and enhance SIV-specific responses ex vivo in naturally SIV controlled cynomolgus macaques. *Scientific Reports.* 2019;9(1):5917.

703. Thibault S, et al. TLR5 stimulation is sufficient to trigger reactivation of latent HIV-1 provirus in T lymphoid cells and activate virus gene expression in central memory CD4+ T cells. *Virology.* 2009;389(1):20-5.

704. Novis CL, et al. Reactivation of latent HIV-1 in central memory CD4+T cells through TLR-1/2 stimulation. *Retrovirology.* 2013;10(1):119.

705. Li P, et al. Stimulating the RIG-I pathway to kill cells in the latent HIV reservoir following viral reactivation. *Nature Medicine.* 2016;22(807.

706. Bam RA, et al. TLR7 Agonist GS-9620 Is a Potent Inhibitor of Acute HIV-1 Infection in Human Peripheral Blood Mononuclear Cells. *Antimicrobial Agents and Chemotherapy.* 2017;61(1):e01369-16.

707. Tsai A, et al. Toll-Like Receptor 7 Agonist GS-9620 Induces HIV Expression and HIV-Specific Immunity in Cells from HIV-Infected Individuals on Suppressive Antiretroviral Therapy. *Journal of Virology.* 2017;91(8):e02166-16.

708. Macedo AB, et al. Dual TLR2 and TLR7 agonists as HIV latency-reversing agents. *JCI insight.* 2018;3(19):e122673.

709. Spivak AM, et al. Ex Vivo Bioactivity and HIV-1 Latency Reversal by Ingenol Dibenzoate and Panobinostat in Resting CD4(+) T Cells from Aviremic Patients. *Antimicrob Agents Chemother.* 2015;59(10):5984-91.

710. Jiang G, et al. Synergistic Reactivation of Latent HIV Expression by Ingenol-3-Angelate, PEP005, Targeted NF-kB Signaling in Combination with JQ1 Induced p-TEFb Activation. *PLoS pathogens.* 2015;11(7):e1005066.

711. Wang P, et al. Reactivation of HIV-1 from Latency by an Ingenol Derivative from Euphorbia Kansui. *Scientific Reports.* 2017;7(1):9451.

712. Yang H, et al. Dual effects of the novel ingenol derivatives on the acute and latent HIV-1 infections. *Antiviral research.* 2019;169(104555.

713. Darcis G, et al. An In-Depth Comparison of Latency-Reversing Agent Combinations in Various In Vitro and Ex Vivo HIV-1 Latency Models Identified Bryostatin-1+JQ1 and Ingenol-B+JQ1 to Potently Reactivate Viral Gene Expression. *PLoS pathogens.* 2015;11(7):e1005063.

714. Martínez-Bonet M, et al. Synergistic Activation of Latent HIV-1 Expression by Novel Histone Deacetylase Inhibitors and Bryostatin-1. 2015;5(16445.

715. Grunstein M. Histone acetylation in chromatin structure and transcription. *Nature.* 1997;389(6649):349-52.

716. McGhee JD, and Felsenfeld G. Nucleosome structure. *Annual review of biochemistry.* 1980;49(1):1115-56.

717. Norton VG, et al. Nucleosome linking number change controlled by acetylation of histones H3 and H4. *Journal of Biological Chemistry.* 1990;265(32):19848-52.

718. Lee DY, et al. A positive role for histone acetylation in transcription factor access to nucleosomal DNA. *Cell.* 1993;72(1):73-84.

719. Van Lint C, et al. Transcriptional activation and chromatin remodeling of the HIV-1 promoter in response to histone acetylation. *Embo j.* 1996;15(5):1112-20.

720. Coull JJ, et al. The Human Factors YY1 and LSF Repress the Human Immunodeficiency Virus Type 1 Long Terminal Repeat via Recruitment of Histone Deacetylase 1. *J Virol.* 2000;74(15):6790-9.

721. Lu HK, et al. Ex vivo response to histone deacetylase (HDAC) inhibitors of the HIV long terminal repeat (LTR) derived from HIV-infected patients on antiretroviral therapy. *PLoS One.* 2014;9(11):e113341.

722. Kim H-J, and Bae S-C. Histone deacetylase inhibitors: molecular mechanisms of action and clinical trials as anti-cancer drugs. *American Journal of Translational Research.* 2011;3(2):166-79.

723. Archin NM, et al. Administration of vorinostat disrupts HIV-1 latency in patients on antiretroviral therapy. *Nature.* 2012;487(7408):482-5.

724. Kroon EDMB, et al. A randomized trial of vorinostat with treatment interruption after initiating antiretroviral therapy during acute HIV-1 infection. *Journal of virus eradication.* 2020;6(3):100004.

725. Tsai P, et al. In vivo analysis of the effect of panobinostat on cell-associated HIV RNA and DNA levels and latent HIV infection. *Retrovirology.* 2016;13(1):36.

726. Rasmussen TA, et al. Panobinostat, a histone deacetylase inhibitor, for latent-virus reactivation in HIV-infected patients on suppressive antiretroviral therapy: a phase 1/2, single group, clinical trial. *The Lancet HIV.* 2014;1(1):e13-e21.

727. Søgaard OS, et al. The Depsipeptide Romidepsin Reverses HIV-1 Latency In Vivo. *PLoS pathogens.* 2015;11(9):e1005142.

728. Nakajima H, et al. FR901228, a Potent Antitumor Antibiotic, Is a Novel Histone Deacetylase Inhibitor. *Experimental Cell Research.* 1998;241(1):126-33.

729. Furumai R, et al. FK228 (Depsipeptide) as a Natural Prodrug That Inhibits Class I Histone Deacetylases. *Cancer Research.* 2002;62(17):4916-21.

730. Grant C, et al. Romidepsin: a new therapy for cutaneous T-cell lymphoma and a potential therapy for solid tumors. *Expert Rev Anticancer Ther.* 2010;10(7):997-1008.

731. Bertino EM, and Otterson GA. Romidepsin: a novel histone deacetylase inhibitor for cancer. *Expert Opinion on Investigational Drugs.* 2011;20(8):1151-8.

732. Ueda H, et al. FR901228, a novel antitumor bicyclic depsipeptide produced by Chromobacterium violaceum No. 968. III. Antitumor activities on experimental tumors in mice. *The Journal of antibiotics.* 1994;47(3):315-23.

733. Ueda H, et al. FR901228, a novel antitumor bicyclic depsipeptide produced by Chromobacterium violaceum No. 968. I. Taxonomy, fermentation, isolation, physico-chemical and biological properties, and antitumor activity. *The Journal of antibiotics.* 1994;47(3):301-10.

734. Ueda H, et al. Action of FR901228, a novel antitumor bicyclic depsipeptide produced by Chromobacterium violaceum no. 968, on Ha-ras transformed NIH3T3 cells. *Bioscience, biotechnology, and biochemistry.* 1994;58(9):1579-83.

735. Zhang L, et al. Zinc binding groups for histone deacetylase inhibitors. *J Enzyme Inhib Med Chem.* 2018;33(1):714-21.

736. Valdez BC, et al. Romidepsin targets multiple survival signaling pathways in malignant T cells. *Blood Cancer Journal.* 2015;5(10):e357-e.

737. Mizutani H, et al. Romidepsin (FK228), a potent histone deacetylase inhibitor, induces apoptosis through the generation of hydrogen peroxide. *Cancer science.* 2010;101(10):2214-9.

738. Radhakrishnan V, et al. Romidepsin (depsipeptide) induced cell cycle arrest, apoptosis and histone hyperacetylation in lung carcinoma cells (A549) are associated with increase in p21 and hypophosphorylated retinoblastoma proteins expression. *Biomedicine & Pharmacotherapy.* 2008;62(2):85-93.

739. Doi S, et al. The histone deacetylase inhibitor FR901228 induces caspase-dependent apoptosis via the mitochondrial pathway in small cell lung cancer cells. *Molecular Cancer Therapeutics.* 2004;3(11):1397-402.

740. Aron JL, et al. Depsipeptide (FR901228) induces histone acetylation and inhibition of histone deacetylase in chronic lymphocytic leukemia cells concurrent with activation of caspase 8–mediated apoptosis and down-regulation of c-FLIP protein. *Blood.* 2003;102(2):652-8.

741. Kodani M, et al. Suppression of phosphatidylinositol 3-kinase/Akt signaling pathway is a determinant of the sensitivity to a novel histone deacetylase inhibitor, FK228, in lung adenocarcinoma cells. *Oncol Rep.* 2005;13(3):477-83.

742. Saijo K, et al. Romidepsin (FK228) and its analogs directly inhibit phosphatidylinositol 3-kinase activity and potently induce apoptosis as histone deacetylase/phosphatidylinositol 3-kinase dual inhibitors. *Cancer science.* 2012;103(11):1994-2001.

743. Marshall JL, et al. A phase I trial of Depsipeptide (FR901228) in patients with advanced cancer. *Journal of Experimental Therapeutics and Oncology.* 2002;2(6):325-32.

744. Sandor V, et al. Phase I Trial of the Histone Deacetylase Inhibitor, Depsipeptide (FR901228, NSC 630176), in Patients with Refractory Neoplasms. *Clinical Cancer Research.* 2002;8(3):718-28.

745. Mothe B, et al. HIVconsv Vaccines and Romidepsin in Early-Treated HIV-1-Infected Individuals: Safety, Immunogenicity and Effect on the Viral Reservoir (Study BCN02). *Front Immunol.* 2020;11(823.

746. Rosás-Umbert M, et al. In vivo Effects of Romidepsin on T-Cell Activation, Apoptosis and Function in the BCN02 HIV-1 Kick&Kill Clinical Trial. *Frontiers in Immunology.* 2020;11(418).

747. Del Prete GQ, et al. Elevated plasma viral loads in romidepsin treated SIV-infected rhesus macaques on suppressive combination antiretroviral therapy. *Antimicrobial Agents and Chemotherapy.* 2015.

748. Jønsson Kasper L, et al. Histone Deacetylase Inhibitor Romidepsin Inhibits De Novo HIV-1 Infections. *Antimicrobial Agents and Chemotherapy.* 2015;59(7):3984-94.

749. Williams SA, et al. Prostratin antagonizes HIV latency by activating NF-kappaB. *J Biol Chem.* 2004;279(40):42008-17.

750. Chowdhury IH, et al. The phorbol ester TPA strongly inhibits HIV-1-induced syncytia formation but enhances virus production: possible involvement of protein kinase C pathway. *Virology.* 1990;176(1):126-32.

751. Kulkosky J, et al. Prostratin: activation of latent HIV-1 expression suggests a potential inductive adjuvant therapy for HAART. *Blood.* 2001;98(10):3006-15.

752. Bögi K, et al. Differential selectivity of ligands for the C1a and C1b phorbol ester binding domains of protein kinase Cdelta: possible correlation with tumor-promoting activity. *Cancer Res.* 1998;58(7):1423-8.

753. DeChristopher BA, et al. Designed, synthetically accessible bryostatin analogues potently induce activation of latent HIV reservoirs in vitro. *Nature chemistry.* 2012;4(9):705-10.

754. Marsden MD, et al. Characterization of designed, synthetically accessible bryostatin analog HIV latency reversing agents. *Virology.* 2018;520(83-93.

755. Brogdon J, et al. In vitro effects of the small-molecule protein kinase C agonists on HIV latency reactivation. *Scientific Reports.* 2016;6(1):39032.

756. McKernan LN, et al. Protein Kinase C: One Pathway towards the Eradication of Latent HIV-1 Reservoirs. *Advances in Virology.* 2012;2012(805347.

757. Albert BJ, et al. Combinations of isoform-targeted histone deacetylase inhibitors and bryostatin analogues display remarkable potency to activate latent HIV without global T-cell activation. *Scientific Reports.* 2017;7(1):7456.

758. Laird GM, et al. Ex vivo analysis identifies effective HIV-1 latency–reversing drug combinations. *The Journal of clinical investigation.* 2015;125(5):1901-12.

759. Sloane JL, et al. Prodrugs of PKC modulators show enhanced HIV latency reversal and an expanded therapeutic window. *Proceedings of the National Academy of Sciences.* 2020;117(20):10688-98.

760. Adolf W, et al. 3-0-angeloylingenol, the toxic and skin irritant factor from latex of euphorbia anitiquorum l.(euphorbiaceae) and from a derived thai purgative and anthelimintic (vermifuge) drug. *ScienceAsia.* 1983;9(081-8.

761. Kedei N, et al. Characterization of the Interaction of Ingenol 3-Angelate with Protein Kinase C. *Cancer Research.* 2004;64(9):3243-55.

762. Jiang G, et al. Reactivation of HIV latency by a newly modified Ingenol derivative via protein kinase Cδ–NF-κB signaling. *AIDS (London, England).* 2014;28(11).

763. Abreu CM, et al. Dual role of novel ingenol derivatives from Euphorbia tirucalli in HIV replication: inhibition of de novo infection and activation of viral LTR. *PLoS One.* 2014;9(5):e97257.

764. Fujiwara M, et al. Ingenol Derivatives are Highly Potent and Selective Inhibitors of HIV Replication in Vitro. *Antiviral Chemistry and Chemotherapy.* 1996;7(5):230-6.

765. Ersvaer E, et al. The Protein Kinase C Agonist PEP005 (Ingenol 3-Angelate) in the Treatment of Human Cancer: A Balance between Efficacy and Toxicity. *Toxins.* 2010;2(1).

766. Pandeló José D, et al. Reactivation of latent HIV-1 by new semi-synthetic ingenol esters. *Virology.* 2014;462-463(328-39.

767. Jiang G, et al. Disruption of latent HIV in vivo during the clearance of actinic keratosis by ingenol mebutate. *JCI Insight.* 2019;4(7).

768. Filippakopoulos P, et al. Selective inhibition of BET bromodomains. *Nature.* 2010;468(7327):1067-73.

769. Bisgrove DA, et al. Conserved P-TEFb-interacting domain of BRD4 inhibits HIV transcription. *Proc Natl Acad Sci U S A.* 2007;104(34):13690-5.

770. Lu P, et al. The BET inhibitor OTX015 reactivates latent HIV-1 through P-TEFb. *Scientific reports.* 2016;6(24100-.

771. Huang H, et al. A Novel Bromodomain Inhibitor Reverses HIV-1 Latency through Specific Binding with BRD4 to Promote Tat and P-TEFb Association. *Frontiers in Microbiology.* 2017;8(1035).

772. Zhang X-x, et al. The BET bromodomain inhibitor apabetalone induces apoptosis of latent HIV-1 reservoir cells following viral reactivation. *Acta Pharmacologica Sinica.* 2019;40(1):98-110.

773. Liang T, et al. A novel bromodomain inhibitor, CPI-203, serves as an HIV-1 latency-reversing agent by activating positive transcription elongation factor b. *Biochemical Pharmacology.* 2019;164(237-51.

774. Gallastegui E, et al. Combination of Biological Screening in a Cellular Model of Viral Latency and Virtual Screening Identifies Novel Compounds That Reactivate HIV-1. *J Virol.* 2012;86(7):3795-808.

775. Abner E, et al. A New Quinoline BRD4 Inhibitor Targets a Distinct Latent HIV-1 Reservoir for Reactivation from Other "Shock" Drugs. *J Virol.* 2018;92(10):e02056-17.

776. Vamos M, et al. Expedient Synthesis of Highly Potent Antagonists of Inhibitor of Apoptosis Proteins (IAPs) with Unique Selectivity for ML-IAP. *ACS Chemical Biology.* 2013;8(4):725-32.

777. Finlay D, et al. Small-Molecule IAP Antagonists Sensitize Cancer Cells to TRAIL-Induced Apoptosis: Roles of XIAP and cIAPs. *Molecular Cancer Therapeutics.* 2014;13(1):5-15.

778. Sun S-C. The noncanonical NF-κB pathway. *Immunol Rev.* 2012;246(1):125-40.

779. Pache L, et al. BIRC2/cIAP1 Is a Negative Regulator of HIV-1 Transcription and Can Be Targeted by Smac Mimetics to Promote Reversal of Viral Latency. *Cell host & microbe.* 2015;18(3):345-53.

780. Hattori S-i, et al. Combination of a Latency-Reversing Agent With a Smac Mimetic Minimizes Secondary HIV-1 Infection in vitro. *Frontiers in Microbiology.* 2018;9(2022).

781. Nixon CC, et al. Systemic HIV and SIV latency reversal via non-canonical NF-κB signalling in vivo. *Nature.* 2020;578(7793):160-5.

782. Mavigner M, et al. CD8 Lymphocyte Depletion Enhances the Latency Reversal Activity of the SMAC Mimetic AZD5582 in ART-Suppressed Simian Immunodeficiency Virus-Infected Rhesus Macaques. *J Virol.* 2021;95(8):e01429-20.

783. Pache L, et al. Pharmacological Activation of Non-canonical NF-κB Signaling Activates Latent HIV-1 Reservoirs In Vivo. *Cell reports Medicine.* 2020;1(3):100037.

784. Takahama S, and Yamamoto T. Pattern Recognition Receptor Ligands as an Emerging Therapeutic Agent for Latent HIV-1 Infection. *Frontiers in Cellular and Infection Microbiology.* 2020;10(216).

785. Kuse N, et al. Priming of HIV-1-specific CD8⁺ T cells with strong functional properties from naïve T cells. *EBioMedicine.* 2019;42(109-19.

786. Aroh C, et al. Innate Immune Activation by cGMP-AMP Nanoparticles Leads to Potent and Long-Acting Antiretroviral Response against HIV-1. *Journal of immunology (Baltimore, Md : 1950).* 2017;199(11):3840-8.

787. Palermo E, et al. Activation of Latent HIV-1 T Cell Reservoirs with a Combination of Innate Immune and Epigenetic Regulators. *J Virol.* 2019;93(21):e01194-19.

788. Mavigner M, et al. 26 - Sting agonist as a kick and kill agent to target the HIV reservoir. *Journal of virus eradication.* 2019;5(14-5.

789. Lisziewicz J, et al. Antisense oligodeoxynucleotide phosphorothioate complementary to Gag mRNA blocks replication of human immunodeficiency virus type 1 in human peripheral blood cells. *Proc Natl Acad Sci U S A.* 1994;91(17):7942-6.

790. Martinsen JT, et al. The Use of Toll-Like Receptor Agonists in HIV-1 Cure Strategies. *Frontiers in immunology.* 2020;11(1112-.

791. Equils O, et al. Toll-like receptor 2 (TLR2) and TLR9 signaling results in HIV-long terminal repeat trans-activation and HIV replication in HIV-1 transgenic mouse spleen cells: implications of simultaneous activation of TLRs on HIV replication. *Journal of immunology (Baltimore, Md : 1950).* 2003;170(10):5159-64.

792. Séréni D, et al. Pharmacokinetics and Tolerability of Intravenous Trecovirsen (GEM®91), an Antisense Phosphorothioate Oligonucleotide, in HIV-Positive Subjects. *The Journal of Clinical Pharmacology.* 1999;39(1):47-54.

793. Agrawal S, and Martin RR. Was Induction of HIV-1 Through TLR9? *The Journal of Immunology.* 2003;171(4):1621-2.

794. Winckelmann AA, et al. Administration of a Toll-Like Receptor 9 Agonist Decreases the Proviral Reservoir in Virologically Suppressed HIV-Infected Patients. *PLoS One.* 2013;8(4):e62074.

795. Schmidt M, et al. Design and Structural Requirements of the Potent and Safe TLR-9 Agonistic Immunomodulator MGN1703. *Nucleic Acid Therapeutics.* 2015;25(3):130-40.

796. Offersen R, et al. A Novel Toll-Like Receptor 9 Agonist, MGN1703, Enhances HIV-1 Transcription and NK Cell-Mediated Inhibition of HIV-1-Infected Autologous CD4+ T Cells. *J Virol.* 2016;90(9):4441-53.

797. Vibholm L, et al. Short-Course Toll-Like Receptor 9 Agonist Treatment Impacts Innate Immunity and Plasma Viremia in Individuals With Human Immunodeficiency Virus Infection. *Clinical Infectious Diseases.* 2017;64(12):1686-95.

798. Vibholm LK, et al. Effects of 24-week Toll-like receptor 9 agonist treatment in HIV type 1+ individuals. *AIDS (London, England).* 2019;33(8).

799. Del Prete GQ, et al. TLR7 agonist administration to SIV-infected macaques receiving early initiated cART does not induce plasma viremia. *JCI Insight.* 2019;4(11).

800. Riddler S, et al. Vesatolimod (GS-9620) is safe and pharmacodynamically active in HIV-infected individuals. *Journal of the International AIDS Society.* 2019;22(43.

801. O'Neill LAJ, et al. A guide to immunometabolism for immunologists. *Nat Rev Immunol.* 2016;16(9):553-65.

802. MacIver NJ, et al. Metabolic regulation of T lymphocytes. *Annual review of immunology.* 2013;31(259-83.

803. Liu Y, et al. mTOR Signaling in T Cell Immunity and Autoimmunity. *International Reviews of Immunology.* 2015;34(1):50-66.

804. Trautmann L, et al. Profound metabolic, functional, and cytolytic differences characterize HIV-specific CD8 T cells in primary and chronic HIV infection. *Blood.* 2012;120(17):3466-77.

805. Patsoukis N, et al. PD-1 alters T-cell metabolic reprogramming by inhibiting glycolysis and promoting lipolysis and fatty acid oxidation. *Nature communications.* 2015;6(6692-.

806. Staron MM, et al. The transcription factor FoxO1 sustains expression of the inhibitory receptor PD-1 and survival of antiviral CD8(+) T cells during chronic infection. *Immunity.* 2014;41(5):802-14.

807. Bengsch B, et al. Bioenergetic Insufficiencies Due to Metabolic Alterations Regulated by the Inhibitory Receptor PD-1 Are an Early Driver of CD8(+) T Cell Exhaustion. *Immunity.* 2016;45(2):358-73.

808. Schurich A, et al. Distinct Metabolic Requirements of Exhausted and Functional Virus-Specific CD8 T Cells in the Same Host. *Cell reports.* 2016;16(5):1243-52.

809. Angin M, et al. Metabolic plasticity of HIV-specific CD8+ T cells is associated with enhanced antiviral potential and natural control of HIV-1 infection. *Nature Metabolism.* 2019;1(7):704-16.

810. Valle-Casuso JC, et al. Cellular Metabolism Is a Major Determinant of HIV-1 Reservoir Seeding in CD4+ T Cells and Offers an Opportunity to Tackle Infection. *Cell Metabolism.* 2019;29(3):611-26.e5.

811. van der Windt GJ, and Pearce EL. Metabolic switching and fuel choice during T-cell differentiation and memory development. *Immunol Rev.* 2012;249(1):27-42.

812. Igarashi T, et al. Emergence of a highly pathogenic simian/human immunodeficiency virus in a rhesus macaque treated with anti-CD8 mAb during a primary infection with a nonpathogenic virus. *Proc Natl Acad Sci U S A.* 1999;96(24):14049-54.

813. Igarashi T, et al. Macrophage are the principal reservoir and sustain high virus loads in rhesus macaques after the depletion of CD4+ T cells by a highly pathogenic simian immunodeficiency virus/HIV type 1 chimera (SHIV): Implications for HIV-1 infections of humans. *Proc Natl Acad Sci U S A.* 2001;98(2):658-63.

814. Orenstein JM, et al. Macrophages as a Source of HIV During Opportunistic Infections. *Science (New York, NY).* 1997;276(5320):1857-61.

815. Clements JE, et al. The central nervous system as a reservoir for simian immunodeficiency virus (SIV): steady-state levels of SIV DNA in brain from acute through asymptomatic infection. *The Journal of infectious diseases.* 2002;186(7):905-13.

816. Zalar A, et al. Macrophage HIV-1 infection in duodenal tissue of patients on long term HAART. *Antiviral research.* 2010;87(2):269-71.

817. Yukl SA, et al. A comparison of methods for measuring rectal HIV levels suggests that HIV DNA resides in cells other than CD4+ T cells, including myeloid cells. *AIDS (London, England).* 2014;28(3):439-42.

818. Honeycutt JB, et al. HIV persistence in tissue macrophages of humanized myeloid-only mice during antiretroviral therapy. *Nat Med.* 2017;23(5):638-43.

819. Busca A, et al. Critical role for antiapoptotic Bcl-xL and Mcl-1 in human macrophage survival and cellular IAP1/2 (cIAP1/2) in resistance to HIV-Vpr-induced apoptosis. *J Biol Chem.* 2012;287(18):15118-33.

820. Rappaport J, and Volsky DJ. Role of the macrophage in HIV-associated neurocognitive disorders and other comorbidities in patients on effective antiretroviral treatment. *J Neurovirol.* 2015;21(3):235-41.

821. Vojnov L, et al. The majority of freshly sorted simian immunodeficiency virus (SIV)-specific CD8(+) T cells cannot suppress viral replication in SIV-infected macrophages. *J Virol.* 2012;86(8):4682-7.

822. Clayton KL, et al. Resistance of HIV-infected macrophages to CD8(+) T lymphocyte-mediated killing drives activation of the immune system. *Nature immunology.* 2018;19(5):475-86.

823. Mailliard RB, et al. Selective Induction of CTL Helper Rather Than Killer Activity by Natural Epitope Variants Promotes Dendritic Cell–Mediated HIV-1 Dissemination. *The Journal of Immunology.* 2013;191(5):2570-80.

824. Smith KN, et al. Effective Cytotoxic T Lymphocyte Targeting of Persistent HIV-1 during Antiretroviral Therapy Requires Priming of Naive CD8⁺ T Cells. *mBio.* 2016;7(3):e00473-16.

825. Smith KN, et al. Programming T cell Killers for an HIV Cure: Teach the New Dogs New Tricks and Let the Sleeping Dogs Lie. *Forum on immunopathological diseases and therapeutics.* 2015;6(1-2):67-77.

826. Campbell GR, et al. SMAC mimetics induce autophagy-dependent apoptosis of HIV-1-infected macrophages. *Cell Death & Disease.* 2020;11(7):590.

827. Bobardt M, et al. The inhibitor apoptosis protein antagonist Debio 1143 Is an attractive HIV-1 latency reversal candidate. *PLoS One.* 2019;14(2):e0211746.

828. He T, et al. Cutting Edge: T Regulatory Cell Depletion Reactivates Latent Simian Immunodeficiency Virus (SIV) in Controller Macaques While Boosting SIV-Specific T Lymphocytes. *J Immunol.* 2016;197(12):4535-9.

829. Kersten MJ, et al. Treatment of AIDS-related non-Hodgkin's lymphoma with chemotherapy (CNOP) and r-hu-G-CSF: clinical outcome and effect on HIV-1 viral load. *Ann Oncol.* 1998;9(10):1135-8.

830. Kleinman AJ, et al. Pharmacokinetics and Immunological Effects of Romidepsin in Rhesus Macaques. *Frontiers in Immunology.* 2020;11(3118).

831. Policicchio BB, et al. Dynamics of Simian Immunodeficiency Virus Two-Long-Terminal-Repeat Circles in the Presence and Absence of CD8(+) Cells. *J Virol.* 2018;92(13):e02100-17.

832. Pandrea I, et al. Functional Cure of SIVagm Infection in Rhesus Macaques Results in Complete Recovery of CD4+ T Cells and Is Reverted by CD8+ Cell Depletion. *PLoS pathogens.* 2011;7(8):e1002170.

833. Ma D, et al. Simian Immunodeficiency Virus SIVsab Infection of Rhesus Macaques as a Model of Complete Immunological Suppression with Persistent Reservoirs of Replication-Competent Virus: Implications for Cure Research. *J Virol.* 2015;89(11):6155-60.

834. Chen Y, et al. Reference values of clinical chemistry and hematology parameters in rhesus monkeys (Macaca mulatta). *Xenotransplantation.* 2009;16(6):496-501.

835. Koo B-S, et al. Reference values of hematological and biochemical parameters in young-adult cynomolgus monkey (Macaca fascicularis) and rhesus monkey (Macaca mulatta) anesthetized with ketamine hydrochloride. *Laboratory Animal Research.* 2019;35(1):7.

836. Fennessey CM, et al. Genetically-barcoded SIV facilitates enumeration of rebound variants and estimation of reactivation rates in nonhuman primates following interruption of suppressive antiretroviral therapy. *PLOS Pathogens.* 2017;13(5):e1006359.

837. Johnson LF, et al. Life Expectancies of South African Adults Starting Antiretroviral Treatment: Collaborative Analysis of Cohort Studies. *PLoS Med.* 2013;10(4):e1001418.

838. Jessen H, et al. How a single patient influenced HIV research--15-year follow-up. *The New England journal of medicine.* 2014;370(7):682-3.

839. Davey RT, Jr., et al. HIV-1 and T cell dynamics after interruption of highly active antiretroviral therapy (HAART) in patients with a history of sustained viral suppression. *Proc Natl Acad Sci U S A.* 1999;96(26):15109-14.

840. Furtado MR, et al. Persistence of HIV-1 Transcription in Peripheral-Blood Mononuclear Cells in Patients Receiving Potent Antiretroviral Therapy. *New England Journal of Medicine.* 1999;340(21):1614-22.

841. Chun T-W, et al. AIDS: Re-emergence of HIV after stopping therapy. *Nature.* 1999;401(6756):874-5.

842. Pierson T, et al. Reservoirs for HIV-1: mechanisms for viral persistence in the presence of antiviral immune responses and antiretroviral therapy. *Annual review of immunology.* 2000;18(665-708.

843. Winckelmann A, et al. Romidepsin-induced HIV-1 Viremia during Effective ART Contains Identical Viral Sequences with Few Deleterious Mutations. *AIDS (London, England).* 2017:10.1097/QAD.0000000000001400.

844. Gonder JC, and Laber K. A Renewed Look at Laboratory Rodent Housing and Management. *ILAR Journal.* 2007;48(1):29-36.

845. Brocca-Cofano E, et al. Marginal effects of systemic CCR5 blockade with maraviroc on oral simian immunodeficiency virus transmission to infant macaques. *J Virol.* 2018;92(17).

846. He T, et al. High-fat diet exacerbates SIV pathogenesis and accelerates disease progression. *The Journal of clinical investigation.* 2019;129(12):5474-88.

847. Brocca-Cofano E, et al. Pathogenic correlates of simian immunodeficiency virus-associated B cell dysfunction. *J Virol.* 2017;91(23).

848. Sivanandham R, et al. Neutrophil extracellular trap production contributes to pathogenesis in SIV-infected nonhuman primates. *The Journal of clinical investigation.* 2018;128(11):5178-83.

849. Schindelin J, et al. Fiji: an open-source platform for biological-image analysis. *Nature Methods.* 2012;9(676.

850. Schneider CA, et al. NIH Image to ImageJ: 25 years of image analysis. *Nature Methods.* 2012;9(671.

851. Hendrix CW, et al. MTN-001: randomized pharmacokinetic cross-over study comparing tenofovir vaginal gel and oral tablets in vaginal tissue and other compartments. *PloS one.* 2013;8(1):e55013-e.

852. Patterson KB, et al. Penetration of tenofovir and emtricitabine in mucosal tissues: implications for prevention of HIV-1 transmission. *Sci Transl Med.* 2011;3(112):112re4.

853. Mardirossian G, et al. A new rectal model for dosimetry applications. *Journal of nuclear medicine : official publication, Society of Nuclear Medicine.* 1999;40(9):1524-31.

854. Stein JV, et al. CCR7-mediated physiological lymphocyte homing involves activation of a tyrosine kinase pathway. *Blood.* 2003;101(1):38-44.

855. Uehara S, et al. A role for CCR9 in T lymphocyte development and migration. *Journal of immunology (Baltimore, Md : 1950).* 2002;168(6):2811-9.

856. Jones RB, et al. Histone deacetylase inhibitors impair the elimination of HIV-infected cells by cytotoxic T-lymphocytes. *PLoS Pathog.* 2014;10(8):e1004287.

857. Piekarz RL, et al. Phase II multi-institutional trial of the histone deacetylase inhibitor romidepsin as monotherapy for patients with cutaneous T-cell lymphoma. *Journal of clinical oncology : official journal of the American Society of Clinical Oncology.* 2009;27(32):5410-7.

858. Woo S, et al. Population pharmacokinetics of romidepsin in patients with cutaneous T-cell lymphoma and relapsed peripheral T-cell lymphoma. *Clinical cancer research : an official journal of the American Association for Cancer Research.* 2009;15(4):1496-503.

859. Berg SL, et al. Plasma and cerebrospinal fluid pharmacokinetics of depsipeptide (FR901228) in nonhuman primates. *Cancer Chemotherapy and Pharmacology.* 2004;54(1):85-8.

860. Chun TW, et al. Persistence of HIV in gut-associated lymphoid tissue despite long-term antiretroviral therapy. *The Journal of infectious diseases.* 2008;197(5):714-20.

861. Rothenberger MK, et al. Large number of rebounding/founder HIV variants emerge from multifocal infection in lymphatic tissues after treatment interruption. *Proceedings of the National Academy of Sciences.* 2015;112(10):E1126-E34.

862. Avalos CR, et al. Brain Macrophages in Simian Immunodeficiency Virus-Infected, Antiretroviral-Suppressed Macaques: a Functional Latent Reservoir. *mBio.* 2017;8(4):e01186-17.

863. Takahashi K, et al. Localization of HIV-1 in human brain using polymerase chain reaction/in situ hybridization and immunocytochemistry. *Annals of Neurology.* 1996;39(6):705-11.

864. Wiley CA, et al. Cellular localization of human immunodeficiency virus infection within the brains of acquired immune deficiency syndrome patients. *Proceedings of the National Academy of Sciences of the United States of America.* 1986;83(18):7089-93.

865. Nagaya Y, et al. Utility of Cerebrospinal Fluid Drug Concentration as a Surrogate for Unbound Brain Concentration in Nonhuman Primates. *Drug Metabolism and Pharmacokinetics.* 2014;29(5):419-26.

866. Gray LR, et al. CNS-specific regulatory elements in brain-derived HIV-1 strains affect responses to latency-reversing agents with implications for cure strategies. *Molecular Psychiatry.* 2016;21(4):574-84.

867. Naughton CA. Drug-induced nephrotoxicity. *American family physician.* 2008;78(6):743-50.

868. Kudoh A, et al. Increase in serum creatine phosphokinase concentrations after suxamethonium during sevoflurane or isoflurane anaesthesia in children. *British journal of anaesthesia.* 1997;78(4):372-4.

869. Ohta Y, et al. Involvement of oxidative stress in increases in the serum levels of various enzymes and components in rats with water-immersion restraint stress. *J Clin Biochem Nutr.* 2009;45(3):347-54.

870. Janossy G, et al. T lymphocyte regeneration after transplantation of T cell depleted allogeneic bone marrow. *Clin Exp Immunol.* 1986;63(3):577-86.

871. Inada T, et al. Effect of propofol and isoflurane anaesthesia on the immune response to surgery*. *Anaesthesia.* 2004;59(10):954-9.

872. Tomihari M, et al. A comparison of the immunological effects of propofol and isoflurane for maintenance of anesthesia in healthy dogs. *J Vet Med Sci.* 2015;77(10):1227-33.

873. Petersen CM, et al. Internalization, lysosomal degradation and new synthesis of surface membrane CD4 in phorbol ester-activated T-lymphocytes and U-937 cells. *Experimental Cell Research.* 1992;201(1):160-73.

874. Mackay LK, et al. Cutting Edge: CD69 Interference with Sphingosine-1-Phosphate Receptor Function Regulates Peripheral T Cell Retention. *The Journal of Immunology.* 2015;194(5):2059-63.

875. Verheyen J, et al. Rapid Rebound of a Preexisting CXCR4-tropic Human Immunodeficiency Virus Variant After Allogeneic Transplantation With CCR5 Δ32 Homozygous Stem Cells. *Clinical Infectious Diseases.* 2019;68(4):684-7.

876. Veazey RS, et al. Characterization of gut-associated lymphoid tissue (GALT) of normal rhesus macaques. *Clinical immunology and immunopathology.* 1997;82(3):230-42.

877. Policicchio BB, et al. Multi-dose romidepsin reactivates replication competent SIV in post-antiretroviral rhesus macaque controllers. *PLoS Pathog.* 2016;12(9):e1005879-e.

878. Kikukawa R, et al. Differential susceptibility to the acquired immunodeficiency syndrome retrovirus in cloned cells of human leukemic T-cell line Molt-4. *J Virol.* 1986;57(3):1159-62.

879. Fukazawa Y, et al. B cell follicle sanctuary permits persistent productive simian immunodeficiency virus infection in elite controllers. *Nature Medicine.* 2015;21(2):132-9.

880. Fukazawa Y, et al. Lymph node T cell responses predict the efficacy of live attenuated SIV vaccines. *Nature Medicine.* 2012;18(11):1673-81.

881. Kleinman AJ, et al. Pharmacokinetics and Immunological Effects of Romidepsin in Rhesus Macaques. *Front Immunol.* 2020;11(579158.

882. Gaufin T, et al. Experimental depletion of CD8+ cells in acutely SIVagm-Infected African Green Monkeys results in increased viral replication. *Retrovirology.* 2010;7(1):42.

883. Jacobson JM, et al. Evidence that intermittent structured treatment interruption, but not immunization with ALVAC-HIV vCP1452, promotes host control of HIV replication: the results of AIDS Clinical Trials Group 5068. *The Journal of infectious diseases.* 2006;194(5):623-32.

884. Ho HN, et al. Circulating HIV-specific CD8+ cytotoxic T cells express CD38 and HLA-DR antigens. *The Journal of Immunology.* 1993;150(7):3070-9.

885. Cartwright EK, et al. CD8(+) Lymphocytes Are Required for Maintaining Viral Suppression in SIV-Infected Macaques Treated with Short-Term Antiretroviral Therapy. *Immunity.* 2016;45(3):656-68.

886. Schmitz JE, et al. Effect of CD8+ lymphocyte depletion on virus containment after simian immunodeficiency virus SIVmac251 challenge of live attenuated SIVmac239delta3-vaccinated rhesus macaques. *J Virol.* 2005;79(13):8131-41.

887. Khan S, et al. Differentiating Immune Cell Targets in Gut-Associated Lymphoid Tissue for HIV Cure. *AIDS research and human retroviruses.* 2017;33(S1):S-40-S-58.

888. Mowat AM, and Viney JL. The anatomical basis of intestinal immunity. *Immunol Rev.* 1997;156(145-66.

889. Mehandru S, et al. Mechanisms of gastrointestinal CD4+ T-cell depletion during acute and early human immunodeficiency virus type 1 infection. *J Virol.* 2007;81(2):599-612.

890. d'Ettorre G, et al. HIV persistence in the gut mucosa of HIV-infected subjects undergoing antiretroviral therapy correlates with immune activation and increased levels of LPS. *Current HIV research.* 2011;9(3):148-53.

891. Yukl SA, et al. Differences in HIV Burden and Immune Activation within the Gut of HIV-Positive Patients Receiving Suppressive Antiretroviral Therapy. *The Journal of infectious diseases.* 2010;202(10):1553-61.

892. Kim EJ, et al. Clinically significant responses achieved with romidepsin across disease compartments in patients with cutaneous T-cell lymphoma. *Leukemia & lymphoma.* 2015;56(10):2847-54.

893. Giacomet V, et al. No cure of HIV infection in a child despite early treatment and apparent viral clearance. *Lancet (London, England).* 2014;384(9950):1320.

894. Kuhn L, et al. Early antiretroviral treatment of infants to attain HIV remission. *EClinicalMedicine.* 2020;18(

895. Chun T-W, et al. Rebound of plasma viremia following cessation of antiretroviral therapy despite profoundly low levels of HIV reservoir: implications for eradication. *AIDS (London, England).* 2010;24(18):2803-8.

896. Sanyal A, et al. Novel assay reveals a large, inducible, replication-competent HIV-1 reservoir in resting CD4(+) T cells. *Nat Med.* 2017;23(7):885-9.

897. Battivelli E, et al. Distinct chromatin functional states correlate with HIV latency reactivation in infected primary CD4(+) T cells. *Elife.* 2018;7(e34655.

898. McMahon DK, et al. A phase I/II randomized, placebo-controlled trial of romidepsin in persons with HIV-1 on suppressive antiretroviral therapy to assess safety and activation of HIV-1 expression (A5315). *The Journal of infectious diseases.* 2020.

899. Díaz-Carballo D, et al. Enhanced antitumoral activity of TLR7 agonists via activation of human endogenous retroviruses by HDAC inhibitors. *Communications Biology.* 2021;4(1):276.

900. Zeng R, et al. Synergy of IL-21 and IL-15 in regulating CD8+ T cell expansion and function. *The Journal of experimental medicine.* 2005;201(1):139-48.

901. Strengell M, et al. IL-21 in Synergy with IL-15 or IL-18 Enhances IFN-γ Production in Human NK and T Cells. *The Journal of Immunology.* 2003;170(11):5464-9.

902. Pouw N, et al. Combination of IL-21 and IL-15 enhances tumour-specific cytotoxicity and cytokine production of TCR-transduced primary T cells. *Cancer immunology, immunotherapy : CII.* 2010;59(6):921-31.

903. Kinter AL, et al. The Common γ-Chain Cytokines IL-2, IL-7, IL-15, and IL-21 Induce the Expression of Programmed Death-1 and Its Ligands. *The Journal of Immunology.* 2008;181(10):6738-46.

904. Wrangle JM, et al. ALT-803, an IL-15 superagonist, in combination with nivolumab in patients with metastatic non-small cell lung cancer: a non-randomised, open-label, phase 1b trial. *The Lancet Oncology.* 2018;19(5):694-704.

905. Drusbosky L, et al. Complete response to avelumab and IL-15 superagonist N-803 with Abraxane in Merkel cell carcinoma: a case study. *Journal for ImmunoTherapy of Cancer.* 2020;8(2):e001098.

906. Knudson KM, et al. Mechanisms involved in IL-15 superagonist enhancement of anti-PD-L1 therapy. *Journal for ImmunoTherapy of Cancer.* 2019;7(1):82.

907. Jochems C, et al. The multi-functionality of N-809, a novel fusion protein encompassing anti-PD-L1 and the IL-15 superagonist fusion complex. *OncoImmunology.* 2019;8(2):e1532764.

908. Li Y, et al. Targeting IL-21 to tumor-reactive T cells enhances memory T cell responses and anti-PD-1 antibody therapy. *Nature Communications.* 2021;12(1):951.